

1983

TORSIONAL OSCILLATIONS IN A GEARED SYSTEM WITH CLEARANCES.

SUBHASH CHANDRA. JASUJA

University of Windsor

Follow this and additional works at: <http://scholar.uwindsor.ca/etd>

Recommended Citation

JASUJA, SUBHASH CHANDRA., "TORSIONAL OSCILLATIONS IN A GEARED SYSTEM WITH CLEARANCES." (1983).
Electronic Theses and Dissertations. Paper 4401.

This online database contains the full-text of PhD dissertations and Masters' theses of University of Windsor students from 1954 forward. These documents are made available for personal study and research purposes only, in accordance with the Canadian Copyright Act and the Creative Commons license—CC BY-NC-ND (Attribution, Non-Commercial, No Derivative Works). Under this license, works must always be attributed to the copyright holder (original author), cannot be used for any commercial purposes, and may not be altered. Any other use would require the permission of the copyright holder. Students may inquire about withdrawing their dissertation and/or thesis from this database. For additional inquiries, please contact the repository administrator via email (scholarship@uwindsor.ca) or by telephone at 519-253-3000ext. 3208.

CANADIAN THESES ON MICROFICHE

I.S.B.N.

THESES CANADIENNES SUR MICROFICHE



National Library of Canada
Collections Development Branch

Canadian Theses on
Microfiche Service

Ottawa, Canada
K1A 0N4

Bibliothèque nationale du Canada
Direction du développement des collections

Service des thèses canadiennes
sur microfiche

NOTICE

The quality of this microfiche is heavily dependent upon the quality of the original thesis submitted for microfilming. Every effort has been made to ensure the highest quality of reproduction possible.

If pages are missing, contact the university which granted the degree.

Some pages may have indistinct print especially if the original pages were typed with a poor typewriter ribbon or if the university sent us a poor photocopy.

Previously copyrighted materials (journal articles, published tests, etc.) are not filmed.

Reproduction in full or in part of this film is governed by the Canadian Copyright Act, R.S.C. 1970, c. C-30. Please read the authorization forms which accompany this thesis.

THIS DISSERTATION
HAS BEEN MICROFILMED
EXACTLY AS RECEIVED

AVIS

La qualité de cette microfiche dépend grandement de la qualité de la thèse soumise au microfilmage. Nous avons tout fait pour assurer une qualité supérieure de reproduction.

S'il manque des pages, veuillez communiquer avec l'université qui a conféré le grade.

La qualité d'impression de certaines pages peut laisser à désirer, surtout si les pages originales ont été dactylographiées à l'aide d'un ruban usé ou si l'université nous a fait parvenir une photocopie de mauvaise qualité.

Les documents qui font déjà l'objet d'un droit d'auteur (articles de revue, examens publiés, etc.) ne sont pas microfilmés.

La reproduction, même partielle, de ce microfilm est soumise à la Loi canadienne sur le droit d'auteur, SRC 1970, c. C-30. Veuillez prendre connaissance des formules d'autorisation qui accompagnent cette thèse.

LA THÈSE A ÉTÉ
MICROFILMÉE TELLE QUE
NOUS L'AVONS REÇUE

TORSIONAL OSCILLATIONS IN A GEARED
SYSTEM WITH CLEARANCES

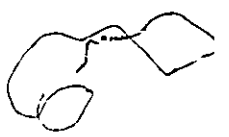
A Dissertation
Submitted to the Faculty of Graduate Studies Through the
Department of Mechanical Engineering in Partial Fulfillment
of the Requirements for the Degree of
Doctor of Philosophy at the
University of Windsor

by

Subhash C. Jasuja

Windsor, Ontario

1983



Subhash C. Jasuja 1983

793037

ABSTRACT

The torsional vibration characteristics of a geared system with clearance are investigated in this study. The clearance results in a bilinear restoring force characteristic which is non-linear in nature. This particular type of non-linearity causes the generation of ultraharmonic, harmonic and subharmonic resonances.

Analytical solutions are derived for ultraharmonic, harmonic and subharmonic resonances by the application of the Ritz averaging method with two or three term approximations for forcing functions of the type $T \cos \omega t$ and $C \omega^2 \cos \omega t$. T and C are constants and ω is the forcing frequency. The accuracy of this approximate method is verified by means of analog computer simulation. The analytical solutions agree quite closely with analog computer results. The analytical solutions are also compared with experimental results obtained from a mechanical model with a bilinear restoring force characteristic. The mechanical model exhibits ultraharmonic and harmonic resonances, but fails to develop distinct subharmonic resonances owing to inadequate power capacity of the vibrator system used. With the analog computer however, the subharmonic resonance is excited over a limited frequency range. Although the experimental results are lower in magnitude than predicted, they distinctly show the nature of non-linear response. The theory of limiting conditions for the generation of subharmonic resonances is developed in Appendix IV.

ACKNOWLEDGEMENT

I would like to express my sincere thanks to Dr. Z.F. Reif for his encouragement and guidance during this investigation. The major portion of the research work was conducted during the period of 1970 through 1975. I am indebted to Professor W.G. Colborne, who was the Head of the Department of Mechanical Engineering during that period, for permitting me to pursue this research and to utilize the research facilities extensively.

The constant inspiration and understanding of my wife, Veena are deeply appreciated.

This research was supported by the National Research Council of Canada Grant #A7439 and financial assistance provided by the University of Windsor in the form of teaching assistantships and Postgraduate Scholarship.

I would like to express my gratitude to the Central Research Shop of the University of Windsor for fabricating the experimental equipment and to Mr. W. Beck, engineering technologist, for providing assistance during the course of this project. My fellow graduate students and the faculty members are also acknowledged for their valuable discussions and suggestions.

TABLE OF CONTENTS

	Page
ABSTRACT	iii
ACKNOWLEDGEMENT	iv
TABLE OF CONTENTS	v
LIST OF FIGURES	viii
NOMENCLATURE	xv
1. INTRODUCTION	
1.1 Characteristics of Non-Linear Systems	1
1.2 Subject of investigation	2
1.3 Analytical Methods for the Solution of Non-linear Vibration Problems	3
1.3.1 Ritz Averaging Method	5
1.4 Simulation of Physical Systems	7
1.4.1 Analog Computer	7
1.4.2 Digital Computer	9
2. LITERATURE SURVEY	
2.1 Literature Related to Basic Non- linear Vibration Studies	10
2.2 Approximate Methods of the Solution of Non-linear Vibration Problems	11
2.3 Study of Piecewise Linear Systems	14
3. ANALYTICAL SOLUTIONS	
3.1 The Development of the Governing Differential Equations of Motion	20
3.1.a Forcing Input of Type $T \cos \omega t$	20
3.1.b Forcing Input of Type $C\omega^2 \cos \omega t$	21
3.2 Analytical Solutions of the Equation of Motion	21

	Page
4. EXPERIMENTAL STUDY	
4.1 Simulation Techniques	24
4.1.1 Analog Computer Simulation	24
4.1.2 Digital Computer Simulation	25
4.2 Mechanical Model Technique	
4.2.1 Design of the Model of the Bilinear Non-linear System	26
4.2.2 Instrumentation	
4.2.2.1 Vibration Excitation System	28
4.2.2.2 Vibration Read out/ Processing System	28
4.2.3 Experimental Procedure	28
4.2.4 Measurement and Analysis of Experimental Data	29
5. DISCUSSION OF RESULTS	
5.1.a Harmonic Resonance	31
5.1.b 3rd Order Ultraharmonic Resonance	37
5.1.c 1/3rd Order Subharmonic Resonance	42
5.1.d Overall View of the Resonance Phenomena	47
5.2 Review of Results Obtained by Mechanical Model Technique	48
5.3 Estimate of Experimental Errors	50
5.4 Remarks on the Application of the Results	51
6. CONCLUSIONS AND SCOPE OF FUTURE WORK	
6.1 Conclusions	53
6.2 Scope of Future Work	54

	Page
BIBLIOGRAPHY	56
FIGURES	69
APPENDIX	
I. ANALYTICAL SOLUTION DEVELOPMENT	145
II. ITERATIVE PROCEDURE FOR THE SOLUTION OF SIMULTANEOUS EQUATIONS	160
III.1 RELATIONSHIP BETWEEN SHAKER PIN MOTION AND INPUT TORQUE TO THE SHAFT	163
III.2. CALCULATION OF THE NON-DIMENSIONAL AMPLITUDES OF MOTION	165
IV. LIMITING CONDITIONS FOR THE GENERATION OF THE HIGHER ORDER RESONANCES	167
V. EXPERIMENTAL ERROR ANALYSIS (ANALYTICAL APPROACH)	170
VITA	173

LIST OF FIGURES

Figure	Page	
3.1.1.1.a	Representation of a Bilinear System	69
3.1.1.1.b	Restoring Force Characteristics of a Bilinear System (Asymmetrical)	70
3.1.1.1.c	Restoring Force Characteristics of a Symmetrical Bilinear System	71
3.1.1.2	Amplitude Versus Angular Displacement Plot (Asymmetrical System). Harmonic Resonance	72
3.1.2.1	Amplitude Versus Angular Displacement Plot (Asymmetrical System). 3rd Order Ultraharmonic Resonance	73
3.1.3.1	Amplitude Versus Angular Displacement Plot (Asymmetrical System). 1/3rd Order Subharmonic Resonance	74
3.2.1.2	Amplitude Versus Angular Displacement Plot (Symmetrical System) Harmonic Resonance	75
3.2.2.1	Amplitude Versus Angular Displacement Plot (Symmetrical System). 3rd Order Ultraharmonic Resonance	76
3.2.3.1	Amplitude Versus Angular Displacement Plot (Symmetrical System). 1/3 Order Subharmonic Resonance	77
4.1.1.1	Generalized Analog Computer Circuit Diagram	78
4.1.1.2	Circuit Diagram for the Bilinear Restoring Force Characteristics	79
4.1.1.3	Generation of $T \cos \omega t$	80
4.1.1.4	Generation of $C \omega^2 \cos \omega t$	81
4.1.2.1	Block Diagram and Structural Statements for a Bilinear System	82

Figure		Page
4.1.2.2	Function Generation Capabilities in CSMP Technique	83
4.2.1.1	Design Details of the Mechanical Model	84
4.2.1.2	Tooth Block Assembly	85
4.2.1.3	Overall View of the Experimental Set Up	86
4.2.2.1	Schematic Diagram of Experimental Set Up	87
4.2.3.1	View Showing Shaker Pin Attachment to the Vibrating Arm 'A' and Control Accelerometer	88
5.1.1	Harmonic Resonance Response for the Symmetrical System ($\bar{\theta}_1 = 0$) Disturbing Torque = $T \cos \omega t$. Plot \bar{Q}_1 Vs η	89
5.1.2	Harmonic Resonance Response for the Asymmetrical System ($\bar{\theta}_1 = 0.05, \bar{S} = 2.0$) Disturbing Torque = $T \cos \omega t$. Plot \bar{Q}_1 Vs η	90
5.1.3	Harmonic Resonance Response for Asymmetrical System ($\bar{\theta}_1 = 0.05, \bar{S} = 1.0$). Disturbing Torque = $T \cos \omega t$. Plot \bar{Q}_1 Vs η	91
5.1.4	Harmonic Resonance Response for Asymmetrical System ($\bar{\theta}_1 = 0.05, \bar{S} = 1.0$). Disturbing Torque = $T \cos \omega t$. Plot \bar{M} Vs η	92
5.1.5	Harmonic Resonance Response for Symmetrical System. Disturbing Torque = $C \omega^2 \cos \omega t$. Plot \bar{Q}_1 Vs η	93
5.1.6	Analog Computer Output, Free Vibration Response ($\bar{S} = 0$). Disturbing Torque = $T \cos \omega t$	94
5.1.7	Analog Computer Output, Forced Vibration Response ($\eta = 0.7$). In-Phase Motion. Disturbing Torque = $T \cos \omega t, \bar{S} = 2.0$	95
5.1.8	Analog Computer Output, Forced Vibration Response ($\eta = 1.1$). Out of Phase Motion. Disturbing Torque = $T \cos \omega t, \bar{S} = 2.0$	96

Figure		Page
5.1.9	Digital Computer CSMP Output. Free Vibration Response ($\bar{S} = 0$). Disturbing Torque = $T \cos \omega t$	97
5.1.10	3rd Order Ultraharmonic Resonance Response for Symmetrical System ($\bar{\theta}_1 = 0$). Disturbing Torque = $T \cos \omega t$, Plot \bar{Q}_3 Vs η	98
5.1.11	3rd Order Ultraharmonic Resonance Response for Symmetrical System ($\bar{\theta}_1 = 0$). Disturbing Torque = $T \cos \omega t$. Plot \bar{Q}_1 Vs η	99
5.1.12	3rd Order Ultraharmonic Resonance Reponse for Asymmetrical System ($\bar{\theta}_1 = 0.05$). Disturbing Torque = $T \cos \omega t$ ($\bar{S} = 2.0$). Plot \bar{Q}_3 Vs η	100
5.1.13	3rd Order Ultraharmonic Resonance Response for Asymmetrical System ($\bar{\theta}_1 = 0.05$). Disturbing Torque = $T \cos \omega t$ ($\bar{S} = 2.0$). Plot \bar{Q}_1 Vs η	101
5.1.14	3rd Order Ultraharmonic Resonance Response for Asymmetrical System ($\bar{\theta}_1 = 0.05$). Disturbing Torque = $T \cos \omega t$ ($\bar{S} = 2.0$). Plot \bar{M} Vs η	102
5.1.15	3rd Order Ultraharmonic Resonance Response for Asymmetrical System ($\bar{\theta}_1 = 0.05$). Disturbing Torque = $T \cos \omega t$ ($\bar{S} = 1.0$). Plot \bar{Q}_3 Vs η	103
5.1.16	3rd Order Ultraharmonic Resonance Response for Asymmetrical System ($\bar{\theta}_1 = 0.05$). Disturbing Torque = $T \cos \omega t$ ($\bar{S} = 1.0$). Plot \bar{Q}_1 Vs η	104
5.1.17	3rd Order Ultraharmonic Resonance Reponse for Asymmetrical System ($\bar{\theta}_1 = 0.05$). Disturbing Torque = $T \cos \omega t$ ($\bar{S} = 1.0$). Plot \bar{M} Vs η	105

Figure		Page
5.1.18	3rd Order Ultraharmonic Resonance Response for Symmetrical System. Disturbing Torque = $C \omega^2 \cos \omega t$ ($Z' = 10.0$). Plot \bar{Q}_3 Vs η	106
5.1.19	3rd Order Ultraharmonic Resonance Response for Symmetrical System. Disturbing Torque = $C \omega^2 \cos \omega t$ ($Z' = 10.0$). Plot \bar{Q}_1 Vs η	107
5.1.20	Analog Computer Output. 3rd Order Ultraharmonic Resonance Response ($\eta = 0.24$). Disturbing Torque = $T \cos \omega t$, $\bar{S} = 2.0$	108
5.1.21	Digital Computer CSMP Output. 3rd Order Ultraharmonic Resonance Response ($\eta = 0.24$). Disturbing Torque = $T \cos \omega t$ ($\bar{S} = 2.0$)	109
5.1.22	Analog Computer Output. 3rd Order Ultraharmonic Resonance Response for Symmetrical System ($\bar{\theta}_1 = 0$, $\eta = 0.22$). Disturbing Torque = $C \omega^2 \cos \omega t$ ($Z' = 10.0$)	110
5.1.23	Digital Computer CSMP Output. 3rd Order Ultraharmonic Resonance Response for Symmetrical System ($\bar{\theta}_1 = 0$, $\eta = 0.22$). Disturbing Torque = $C \omega^2 \cos \omega t$ ($Z' = 10.0$)	111
5.1.24	1/3rd Order Subharmonic Resonance Response for Symmetrical System ($\bar{\theta}_1 = 0$, $\bar{S} = 2.0$). Disturbing Torque = $T \cos \omega t$. Plot $\bar{Q}_{1/3}$ Vs η	112
5.1.25	1/3rd Order Subharmonic Resonance Response for Symmetrical System ($\bar{\theta}_1 = 0$, $\bar{S} = 2.0$). Disturbing Torque = $T \cos \omega t$. Plot \bar{Q}_1 Vs η	113
5.1.26	1/3rd Order Subharmonic Resonance Response for Symmetrical System ($\bar{\theta}_1 = 0$, $\bar{S} = 2.0$). Disturbing Torque = $T \cos \omega t$. Plot \bar{M} Vs η	114

Figure		Page
5.1.27	Locus of Cut Off Frequency, 1/3rd Order Subharmonic Resonance. Disturbing Torque = $T \cos \omega t$	115
5.1.28.	1/3rd Order Subharmonic Resonance Response for Symmetrical System. Disturbing Torque = $C \omega^2 \cos \omega t$ ($Z' = 2.0$). Plot $\bar{Q}_{1/3}$ Vs η	116
5.1.29	1/3 Order Subharmonic Resonance Response for Symmetrical System. Disturbing Torque = $C \omega^2 \cos \omega t$, ($Z' = 2.0$). Plot \bar{Q}_1 Vs η	117
5.1.30	Analog Computer Output. 1/3rd Order Subharmonic Resonance Response for Symmetrical System ($\bar{\theta}_1 = 0$, $\eta = 1.6$). Disturbing Torque = $T \cos \omega t$ ($\bar{S} = 2.0$)	118
5.1.31	Digital Computer CSMP Output. 1/3 Order Subharmonic Resonance Response for Symmetrical System ($\bar{\theta}_1 = 0$, $\eta = 1.6$). Disturbing Torque = $T \cos \omega t$, $\bar{S} = 2.0$	119
5.1.32	Analog Computer Output. 1/3rd Order Subharmonic Resonance Response for Symmetrical System ($\bar{\theta}_1 = 0$, $\eta = 2.4$). Disturbing Torque = $C \omega^2 \cos \omega t$, $Z' = 2.0$	120
5.1.33	Digital Computer CSMP Output. 1/3rd Order Subharmonic Resonance Response for Symmetrical System ($\bar{\theta}_1 = 0$, $\eta = 2.4$). Disturbing Torque = $C \omega^2 \cos \omega t$, $Z' = 2.0$	121
5.1.34	Resonance Spectrum for Theoretical Values of Main Components of Motion. Disturbing Torque = $T \cos \omega t$ ($\bar{S} = 2.0$)	122
5.2.1	Acceleration Waveform Display. $f = 9.6$ Hz, $p = 26.0$ Hz, $\eta = 0.37$, $\bar{S} = 2.0$	123

Figure		Page
5.2.2	Acceleration Waveform Display. $f = 13.8$ Hz, $p = 26.0$ Hz, $\eta = 0.53$, $\bar{S} = 2.0$	123
5.2.3	Acceleration Waveform Display. $f = 19.9$ Hz, $p = 26.0$ Hz, $\eta = 0.76$, $\bar{S} = 2.0$	124
5.2.4	Acceleration Waveform Display. $f = 33.3$ Hz, $p = 26.0$ Hz, $\eta = 1.28$, $\bar{S} = 2.0$	124
5.2.5	Frequency Spectrum of Acceleration at Point 'P' at $f = 9.6$ Hz, $\eta = 0.37$, $\bar{S} = 2.0$	125
5.2.6	Frequency Spectrum of Acceleration at Point 'P' at $f = 13.8$ Hz, $\eta = 0.53$, $\bar{S} = 2.0$	126
5.2.7	Frequency Spectrum Acceleration at Point 'P' at $f = 19.9$ Hz, $\eta = 0.76$, $\bar{S} = 2.0$	127
5.2.8	Frequency Spectrum of Acceleration at Point 'P' at $f = 33.3$ Hz, $\eta = 1.28$, $\bar{S} = 2.0$	128
5.2.9	Experimental Results, Plot \bar{Q}_1 Vs η , $\bar{S} = 2.0$	129
5.2.10	Experimental Results, Plot \bar{Q}_2 Vs η , $\bar{S} = 2.0$	130
5.2.11	Experimental Results, Plot \bar{Q}_3 Vs η , $\bar{S} = 2.0$	131
5.2.12	Experimental Results, Plot \bar{Q}_4 Vs η , $\bar{S} = 2.0$	132
5.2.13	Experimental Results, Plot \bar{Q}_1 Vs η , $\bar{S} = 1.5$	133
5.2.14	Experimental Results, Plot \bar{Q}_2 Vs η , $\bar{S} = 1.5$	134
5.2.15	Experimental Results, Plot \bar{Q}_3 Vs η , $\bar{S} = 1.5$	135
5.2.16	Experimental Results, Plot \bar{Q}_4 Vs η , $\bar{S} = 1.5$	136
5.2.17	Experimental Results, Plot \bar{Q}_1 Vs η , $\bar{S} = 2.5$	137
5.2.18	Experimental Results, Plot \bar{Q}_2 Vs η , $\bar{S} = 2.5$	138
5.2.19	Experimental Results, Plot \bar{Q}_3 Vs η , $\bar{S} = 2.5$	139
5.2.20	Experimental Results, Plot \bar{Q}_4 Vs η , $\bar{S} = 2.5$	140
5.2.21	Experimental Results, Plot \bar{Q}_1 Vs η , $\bar{S} = 1.0,$ 1.5, 2.0, 2.5	141

Figure		Page
5.2.22	Experimental Results, Plot \bar{Q}_2 Vs η , $\bar{S} = 1.0$, 1.5, 2.0, 2.5	142
5.2.23	Experimental Results, Plot \bar{Q}_3 Vs η , $\bar{S} = 1.0$, 1.5, 2.0, 2.5	143
5.2.24	Experimental Results, Plot \bar{Q}_4 Vs η , $\bar{S} = 1.0$, 1.5, 2.0, 2.5	144

NOMENCLATURE

C	Rotating torque.
C'	Damping coefficient.
$C_c = 2p.J$	Critical damping coefficient.
$E(\theta)$	Error function or differential equation of motion.
f_3	Forcing function.
J	Polar moment of inertia of oscillating mass.
K	Linear torsional stiffness.
M	Mean dynamic displacement from the static equilibrium position.
$\bar{M} = \frac{M}{\theta_0}$	Non-dimensional mean displacement.
$p = \sqrt{\frac{K}{J}}$	Equivalent linear natural frequency.
Q_1	Amplitude of fundamental component of motion.
Q_2	Amplitude of the second harmonic component of motion.
Q_3	Amplitude of the third harmonic or of the ultra-harmonic of 3rd order.
Q_4	Amplitude of the fourth harmonic component of motion.
$Q_{1/3}$	Amplitude of the 1/3 harmonic or of the subharmonic of 1/3rd order.
$\bar{Q}_1 = \frac{Q_1}{\theta_0}$	} Non-dimensional amplitudes.
$\bar{Q}_3 = \frac{Q_3}{\theta_0}$	
$\bar{Q}_{1/3} = \frac{Q_{1/3}}{\theta_0}$	
G_1, G_2, G_3, G_4 etc.	Amplitudes of harmonic components of acceleration.

n_1, n_2, n_3, n_4 etc. Magnitudes of harmonic components of acceleration in terms of the acceleration due to gravity.

r Distance of the accelerometer axis from the center of the shaft.

r_1 Radial distance of the contact line on tooth from the center of the shaft.

$\bar{S} = \frac{T}{K\theta_0}$ Non-dimensional forcing amplitude.

t Period of oscillation of motion, period of disturbing force.

T Periodic torque.

T_0 Static torque.

W_r, W_{r_1} Uncertainties involved in the measurements of r and r_1 respectively.

W_{n_1}, W_{n_2}, \dots Uncertainties involved in measurement of acceleration harmonics.

W_t Uncertainty involved in the measurements of the period of the disturbing force.

W_{θ_0} Uncertainty involved in gap clearance measurements.

$Z = \frac{C}{J}$ Disturbing torque constant.

$Z' = \frac{Z}{\theta_0} = \frac{C}{J\theta_0}$ Non-dimensional forcing amplitude.

$\eta = \frac{\omega}{p}$ Frequency ratio.

μ Coefficient of non-linearity (L^{-2}).

ω Non-linear frequency, frequency of disturbing force.

τ_1, τ_2	Angular displacements at the beginning and the end of angular clearance.
θ	Angular displacement from the static equilibrium position.
$2\theta_0$	Angular clearance (backlash).
θ_1	Angular position of beginning of angular clearance measured from 0.
$\bar{\theta} = \frac{\theta}{\theta_0}$	Non-dimensional displacement from the static equilibrium position.
$\zeta = \frac{C'}{C_c}$	Damping ratio.

1. INTRODUCTION

1.1 CHARACTERISTICS OF NON-LINEAR SYSTEMS

Vibrating systems have generally non-linear restoring force characteristics. In most cases the magnitude of nonlinearity is sufficiently small to provide acceptable results with a linear approximation. Non-linearities are of two types; continuous and discontinuous. Continuous non-linear restoring forces are produced by imperfect elasticity of materials, such as rubber used for flexible couplings and vibration isolation suspensions, geometric configurations of linear springs and by large amplitudes of angular motion. There are specially designed springs, such as Belleville, sine and wire mesh, which have continuous non-linear characteristics. Discontinuous non-linearities are exhibited by systems with restoring force characteristics represented by simple combinations of straight lines. In practice, they often result from the discontinuous contact with elastic restraints due to clearances and backlash.

The vibration of systems with non-linear restoring forces is periodic, but contains harmonics of the fundamental oscillation. As a result three distinct types of forced vibration can occur, which are the harmonic, ultraharmonic and subharmonic resonances. The harmonic resonance is equivalent to a linear resonance. An ultraharmonic is the resonance of one of the higher harmonics of motion when

it reaches the region of the natural frequency of the system. Similarly a subharmonic is the resonance of one of the harmonics whose frequency is $1/n$ times the forcing frequency, where n is an integer. The type of resonance and its order are defined by the ratio of the frequency of the predominant component of the motion to the frequency of the disturbing force.

The ultraharmonic and subharmonic resonances are the general characteristics of a non-linear system. Their order and magnitude are typical for a specific system. For example a non-linear system with symmetrical restoring force characteristics may exhibit odd orders of resonances only. Asymmetrical restoring force characteristic, on the other hand, may produce both even and odd order resonances.

1.2 SUBJECT OF INVESTIGATION

In this study, the vibration response of a torsional system with bilinear type torsional stiffness has been investigated. This non-linear restoring force characteristic results from a clearance in a geared system vibrating torsionally. The restoring force is zero within the clearance and acts linearly when contact is made. This type of restoring force characteristic is found in actual power transmission systems with angular clearances. These clearances are caused by the backlash in gear teeth, wear of tooth flanks etc. In torsional vibrations, excessive

shocks and cyclic stresses may result from such nonlinearities causing premature failures. In a particular case a failure due to such a condition has been observed in the drive of a Krupp-Renn revolving kiln (12).*

The aim of this investigation is to study this nonlinear phenomenon qualitatively and quantitatively.

1.3 ANALYTICAL METHODS FOR THE SOLUTION OF NONLINEAR VIBRATION EQUATIONS

In most cases it is not possible to obtain exact solutions for the differential equations representing nonlinear vibration. Approximate solutions of such equations to the first degree, are not difficult or laborious. These are often preferred over exact solutions for the sake of simplicity. The latter, if at all possible, often require tedious calculations. On the other hand, one of the difficulties with approximate solutions is the selection of the most suitable method from the many which are in existence. The factors which have to be considered when the choice is made, are the magnitude of non-linearity and the accuracy of the solution, the laboriousness of the procedure and the type of vibration or resonance represented by the equation.

There are several methods which produce solutions in the closed form. These are:

* Numbers in parentheses denote publications listed in the bibliography, pages 56 through 68.

1. Ritz Averaging Method
2. Krylov-Bogoliubov and Mitropolski Method
3. Perturbation Method
4. Substitution Method

The Ritz averaging method provides sufficiently accurate solutions. The effectiveness of the method improves with the magnitude of non-linearity. Non-autonomous systems and asymmetrical restoring force characteristics do not present any undue difficulties. Higher orders of approximations yield better accuracy, but the complexity of the problem increases. However, the difficulties are of a purely algebraic nature. There is no impediment to the application of the Ritz averaging method to systems of more than one degree of freedom, where the majority of other methods become extremely complicated or fail altogether.

The substitution method closely follows the Ritz averaging method in terms of accuracy which increases with the order of approximation. There is no difference in the laboriousness of the two methods, but the simplicity of the mathematical basis for the substitution method may be an advantage in some applications.

The perturbation method is very laborious and perhaps its only advantage is that the form of the solution need not be assumed before application. The Krylov-Bogoliubov method is very useful in the analysis of self excited oscillations and non-linear damping. The perturbation and Krylov-Bogoliubov methods are suitable only for quasilinear systems with symmetrical

restoring force characteristics. In case of forced vibration, the amplitude of the disturbing force is restricted to small values within the limits imposed by the magnitude of non-linearity.

There are also graphical procedures available, such as the Phase-Plane method and numerical integration techniques. Their range of application is generally restricted to point solutions. Furthermore, they are unsuitable for the analysis of the more complex types of non-linear effects such as sub-harmonic and ultraharmonic resonances.

1.3.1 RITZ AVERAGING METHOD

After careful evaluation, the Ritz averaging method was selected for the problem under study. Its application is described below:

Consider the non-linear differential equation

$$J\ddot{\theta} + C'\dot{f}_1(\dot{\theta}) + K f_2(\theta) = f_3(t) \quad (1.3.1.1)$$

in which the restoring force $f_2(\theta)$ and the damping force $f_1(\dot{\theta})$ are non-linear odd functions of the displacement and velocity respectively. In other words $-f_2(\theta) = f_2(-\theta)$ and $-f_1(\dot{\theta}) = f_1(-\dot{\theta})$. If we divide through by the constant moment of mass inertia J and place $\frac{K}{J} = p^2$ and $\frac{C'}{J} = 2 \zeta p$, the differential equation $E(\theta)$ becomes:

$$E(\theta) = \ddot{\theta} + 2 \zeta p \dot{f}_1(\dot{\theta}) + p^2 f_2(\theta) - \frac{1}{J} f_3(t) = 0 \quad (1.3.1.1a)$$

We then assume our approximate solution of equation (1.3.1.1a) consisting of n terms and denote it by $\tilde{\theta}$, so that

$$\tilde{\theta} = a_1 \phi_1(t) + a_2 \phi_2(t) + \dots + a_n \phi_n(t) \quad (1.3.1.2)$$

Upon substitution of the approximate solution $\tilde{\theta}$, the differential equation becomes $E(\tilde{\theta})$ and $E(\tilde{\theta}) \neq 0$. This equation deficiency $E(\tilde{\theta})$ will vary from instant to instant, but over an arbitrary duration of time T it will be possible to demand that each of the n weighted averages of the deficiency must vanish. In calculating the weighted averages of $E(\tilde{\theta})$, we postulate the existence of n weight functions and denote them by $\omega_1(t)$, $\omega_2(t)$, ... $\omega_n(t)$. The Ritz averaging criterion then states that if $\omega_1(t)$ is placed equal to $\phi_1(t)$, $\omega_2(t)$ placed equal to $\phi_2(t)$, etc. and finally $\omega_n(t)$ placed equal to $\phi_n(t)$, the resulting n averaging integrals, each placed equal to zero will yield n algebraic equations from which the coefficients a_1, a_2, \dots, a_n can be found. Under these circumstances the approximate solution for $\tilde{\theta}$ will be the best obtainable in the n terms chosen.

The Ritz averaging integrals are given by:

$$\int_0^T \{E(\tilde{\theta}) \phi_1(t)\} dt = 0$$

$$\int_0^T \{E(\tilde{\theta}) \phi_2(t)\} dt = 0$$

and similarly

$$\int_0^T \{E(\tilde{\theta}) \phi_n(t)\} dt = 0 \quad (1.3.1.3)$$

For a steady state vibration of a non-linear system acted upon by a sinusoidal excitation, the Ritz criterion (1.3.1.3) may be expressed for the duration $T = \frac{2\pi}{\omega}$ or alternatively for the angle of 2π radians as follows:

$$\int_0^{2\pi} \{E(\tilde{\theta}) \phi_1(\omega t)\} d(\omega t) = 0$$

$$\int_0^{2\pi} \{E(\tilde{\theta}) \phi_2(\omega t)\} d(\omega t) = 0$$

and

$$\int_0^{2\pi} \{E(\tilde{\theta}) \phi_n(\omega t)\} d(\omega t) = 0 \quad (1.3.1.3a)$$

1.3.2 OTHER METHODS

Application of remaining methods has been explained in various textbooks (83), (38), (15), (84), (68), (38) and various publications (76).

1.4 SIMULATION OF THE PHYSICAL SYSTEM

1.4.1 ANALOG COMPUTER

In practice, physical systems can in most cases be represented by mathematical equations or sets of equations. Their solutions are often difficult or practically impossible to obtain by the classic approach. The analog computer provides rapid solutions of linear or non-linear equations and makes possible qualitative surveys of the behavior of the simulated system.

The analog computer performs the required mathematical operations in a parallel manner on continuous variables. In electronic analog computers, the continuous variables are

d.c. voltages. The electronic analog computer makes it possible to build an electrical model of a physical system, where the voltages on the computer represent the dependent variables of the physical system. Except for a constant of proportionality or a scale factor, each voltage will behave with time in a manner similar to the physical system variable. The actual behavior is thus simulated because of the equivalence of operation of the electrical model. This capability of the analog computer is of great value in performing scientific research or engineering design because it permits an insight into the relationship between the mathematical equations and the response of the physical system. Once the electrical model is completed, well controlled experiments can be performed quickly, inexpensively, and with great flexibility to predict the behavior of the physical system.

The analog computer is basically a set of mathematical building blocks, each able to perform specific mathematical operations on voltages. By appropriately interconnecting these building blocks, an electrical model is produced, in which the voltages at the outputs of the blocks obey the relation given in the mathematical description of a physical system. The standard components of an analog computer perform the following operations: inversion, algebraic summation, integration with respect to time, multiplication and division, and function generation.

1.4.2 DIGITAL COMPUTER

Non-linear differential equations are difficult to compute even with the help of a digital computer (53). Recently, the availability of the Continuous System Modelling Program (CSMP) has simplified the numerical solutions of non-linear ordinary differential equations (22).

The Continuous System Modelling Program is designed to facilitate the digital simulation of continuous processes, whose behavior follows a set of ordinary differential equations. This program provides an application oriented language that allows these problems to be prepared directly and simply from either a block diagram representation or a set of ordinary differential equations. This program includes a basic set of functional blocks, with which the components of a continuous system may be represented. It accepts application oriented statements for defining the connections between these functional blocks. CSMP also accepts FORTRAN statements to deal with non-linear and time variant problems of considerable complexity. The application of CSMP allows the user to concentrate upon the phenomenon being studied rather than upon the detailed technique for numerical computation.

2. LITERATURE SURVEY

2.1 LITERATURE RELATED WITH BASIC NON-LINEAR VIBRATION STUDIES

Several books are exclusively devoted to non-linear vibrations, such as Stoker (83), Minorsky (68) and Hayashi (32).

Some chapters deal with this subject in Timoshenko (84), Jacobson and Ayre (38) and DenHartog (15). In general these books describe non-linear systems and methods of obtaining analytical solutions. An interesting publication (14) presents a broad overview of non-linear systems and their characteristics as compared to linear systems.

Most of the past work is based on non-linear systems represented by the well known Duffing equation, which is

$$\ddot{x} + C \dot{x} + K(x \pm \mu x^n) = P \cos \omega t$$

where n is an integer.

Klotter and Pinney (48) have studied forced vibrations in systems represented by a Duffing Equation with a hardening type restoring force characteristic. They also have established a stability criterion for vibrations of their system.

Similarly, Caughey (10) has studied conditions for the existence and the stability of ultraharmonics and sub-harmonics in forced oscillations of systems having a small cubic non-linearity represented by the Duffing equation.

Burgess (9) has published a report on the harmonic,

superharmonic and subharmonic response of a single degree of freedom system of the Duffing type. Atkinson (2) has obtained ultraharmonic oscillations as solutions to the Duffing equation using an electronic differential analyzer and verified results obtained earlier by Burgess.

Raganti (79) has obtained the subharmonic solutions of order $1/3$ of the damped Duffing equation with large non-linearity in a suitable parametric form. The solutions are compared with the results obtained by direct numerical integration of the same equation, using the Runge-Kutta method.

Hayashi (35) has investigated the stability criteria of non-linear periodic oscillations and has studied subharmonic oscillations in non-linear systems (33). He has shown that the order of subharmonics has a close relationship with the form of the non-linear characteristics e.g. subharmonic oscillations of order $1/3$ are related with the non-linear characteristic expressed by cubic and quintic functions.

2.2 APPROXIMATE METHODS FOR THE SOLUTION OF NON-LINEAR VIBRATION PROBLEMS

The literature was reviewed for the most suitable approximate method available for obtaining analytical solutions for the bilinear type restoring force characteristics. Special attention was given to the methods in which an approximate solution is assumed. In the search along these lines several possible approaches were observed. For instance,

Mahalingam (63) has proposed an approximate solution for forced vibration. In this method, the problem of free vibration is first solved and the response to forced vibration is then found using a frequency function in place of the actual restoring force characteristics. The author claims that this method is powerful when the restoring force characteristic is made up of a number of straight lines. Similarly Schweisinger and Manmuth (81) have proposed a one term approximation method based on the Ritz procedure. DenHartog (16) has introduced approximate graphical solutions for the problem of forced vibration of an undamped single degree of freedom vibrating system with a non-linear spring, whose characteristic is given in the form of a curve. His approach is based on the quarter cycle energy method. As a follow up of DenHartog's publication, Silverman (82) came up with an application of Hamilton's principle to obtain forced vibration displacement in the form of a Fourier Series.

Brock (6) has proposed an iterative procedure employing numerical integrations for the analysis of free and forced vibrations of undamped systems having non-linear elasticity. There are few publications suggesting graphical solution for solving transient vibration problems. Lemon (50) has given a procedure for adopting the phase plane method to the solution of a single degree of freedom system with a non-linear restoring force characteristic. Bruce (7) has shown application of the graphical method to a simple case of free vibrations of a non-linear system, with a restoring force characteristic

composed of linear segments. Bishop (5) has again applied the graphical method to the free and forced vibrations of a bilinear system. He has also suggested the approximation of any spring characteristic by a series of straight lines. Evaldson, Ayre and Jacobsen (25) have obtained the response of a non-linear system, with spring characteristics composed of straight lines, to transient disturbances, using the graphical solution technique.

There are several references (83), (45), (46) and (47) on the application of the Ritz averaging method for solving non-linear vibration problems. A technical report by Klotter (45) is of particular interest. In this publication, the author has introduced the Ritz averaging method and has applied it to cases for which exact solutions were possible. The first case studied was the undamped vibration of systems with restoring forces of the polynomial type. Exact solutions were compared with results obtained by means of the Ritz method using a single term approximation and good agreement was shown to exist.

The second case relates to free or forced vibrations of systems with several types of piecewise linear restoring force characteristics. The author has again compared the exact values with the averaging method using a single term solution and has shown that the single term approximate solutions are very close to the exact solutions when the driving frequency is not close to any type of non-linear resonance other than harmonic. Reif (77), (78) has applied the Ritz averaging method to obtain


solutions of the ultraharmonic resonance of order 2 and the subharmonic resonance of order $1/2$ for a non-linear system with an asymmetrical restoring force characteristic. He has also verified these results by means of an analog computer. Reif (76) has also solved the Duffing equation using the Ritz averaging, Krylov-Bogoliubov, perturbation and substitution methods and has compared the accuracy and relative advantages of these methods on the basis of an analog computer simulation.

Levenson (51) derived a numerical solution of subharmonic response for the Duffing equation.

Ashwell and Chauhan (1) have applied the method of harmonic balance to a study of subharmonic oscillations of order $1/2$ with single degree of freedom systems having non-linear spring characteristics of skew symmetrical form.

2.3 STUDY OF PIECEWISE LINEAR SYSTEMS

DenHartog and Mikina (16) and DenHartog and Heiles (17) have studied forced vibration in non-linear systems with various combinations of linear springs. The authors have obtained the exact solutions for the steady state motion of these systems under the influence of a harmonic external force. The results have been plotted for stiffness ratios $K_1/K_2 = 0, 0.5, 2$ and ∞ in the non-dimensional form. In these solutions the presence of higher order harmonics in the motion has been ignored. They however form a basis for approximate solutions that may be analytically simpler.



Klotter (45) has obtained approximate solutions for forced vibration in non-linear systems with various combinations of linear springs, using the Ritz averaging method. This method is much simpler than the exact solution (18) and provides an acceptable degree of accuracy for practical applications.

Atkinson and Heflinger (3) have studied a bilinear system by means of an electronic analog. They have shown the existence of ultraharmonic and subharmonic components in the system response. This publication provides a basic understanding of the bilinear system.

Chaloupka (12) has given a case study of the drive of a Krupp-Renn revolving kiln, in which excessive wear of the gears was observed after several years of operation. The study indicates that the failure was caused by a subharmonic resonance of order $1/2$, which resulted from the non-linear character of the torsional stiffness of the drive due to excessive backlash in the gear teeth. The author has studied this problem experimentally and analytically.

Bruevich (8) has investigated the action of harmonic oscillations on a piecewise linear system. An equation is obtained for the periods of a piecewise linear system of any order in the case when the characteristic of the non-linear element is continuous and consists of segments of two intersecting lines, and the external perturbation is harmonic.

Maezawa (55) has introduced an analytical method to

obtain steady state solutions for forced vibration of asymmetric piecewise linear systems using a method utilizing appropriate perfect Fourier series expansion. This method consists of 1. Linearizing the original non-linear equation of motion by expanding the non-linear part of the restoring and damping force into a Fourier series with the same period as the given exciting force; 2. Obtaining the formal solution of the linearized equation by taking the non-linear part to be an exciting force from without. The solution contains certain unknown coefficients of the Fourier expansion; 3. Determining these unknown coefficients from the conditions that the formal solution satisfies the given piecewise linear characteristics of the system. These requirements result in an infinite set of simultaneous linear equations for the non-dimensionalized coefficients of this Fourier expansion as an infinite number of unknowns. The author has given a method utilizing the appropriate series transformation for the improvement of convergence. Numerical computations were performed and response curves for two typical cases were shown to illustrate this method. The theory was also verified by means of an analog computer.

Maezawa (56), (57), (58), (61), has also shown the application of the Fourier series method for obtaining subharmonic and superharmonic resonance solutions in a piecewise linear system. He (62) has also discussed forced vibrations in an unsymmetrical piecewise linear system excited by general

periodic force functions. The superharmonic resonances up to the second order, are analyzed by means of a perfect Fourier series.

Tsuda (90) has obtained solutions for harmonic, sub-harmonic and ultraharmonic resonances of a one dimensional power transmission system having an angular clearance. The author has discussed stability discrimination and has solved approximately the maximum amplitude state of the system under velocity proportional damping and collision damping, which takes place at the clearance. The author has presented a series of numerical diagrams to determine maximum amplitude states of the system. He has also verified experimentally his theory on the approximation of collision damping.

Yeh and Yao (93) have obtained the response of bilinear structure systems to earthquake loads using the continuous system modelling program (CSMP) (95). The results of their study show that the bilinear system is more effective in resisting earthquake loads than the corresponding linear system with either spring component of the bilinear system.

Karasudhi, Tan and Lee (40) have analyzed the vibration of a single storey frame with bilinear hysteresis, supporting a rotating machine. The excitation force, caused by the rotating unbalanced mass of the machine, was sinusoidal with a frequency dependent amplitude. It was shown that the system exhibits unbounded resonance when the product of the machine unbalanced mass and its eccentricity exceeds a critical value.

Masri (65) has obtained an exact solution for the steady state motion of a sinusoidally excited single-degree-of-freedom system with bilinear hysteresis and viscous damping.

Dubowsky and Freudenstein (22) have presented the dynamic behavior of an elastic mechanical joint with clearances. The authors have formulated a mechanical model and have obtained the dynamic response analytically and numerically. The results include the frequency response, displacements, force amplification and vibrational characteristics of the system under various operating conditions. The authors have shown the application of the describing function technique (well known in control engineering) to obtain approximate solutions of the system.

OVERALL REVIEW OF ANALYTICAL METHODS SUITABLE FOR THE SOLUTION OF THE PIECEWISE LINEAR SYSTEM

The exact analytical solutions for piecewise linear systems obtained by DenHartog and Mikina (16), and DenHartog and Heiles (17), provide a basis for the comparison of solutions obtained by other approximate methods. The exact solution, discussed in the above mentioned references, does not make allowance for higher order harmonics and thus is unsuitable for ultraharmonic and subharmonic resonance solutions. Moreover the exact solution is tedious to obtain.

Graphical methods appear to be predominantly suitable for free vibrations and cannot be applied to ultraharmonic

and subharmonic resonances.

There are several publications suggesting one term approximation methods (81), (63), (82) and (5) for obtaining solutions for forced vibrations of non-linear systems with piecewise linear restoring forces. However, these methods can be applied to the harmonic resonance, but cannot be extended to the ultraharmonic and subharmonic resonances.

Several authors have used the Ritz averaging method with various non-linear problems, for which either exact solutions or experimental results, such as analog computer, were known. They have shown that the method provided very satisfactory accuracy and has greater scope of applicability. Burgess (9) has obtained solutions for harmonic, ultraharmonic and subharmonic responses of a system of the Duffing type, using the Ritz averaging method. Klotter (45) has applied this method to free and forced vibrations of systems with several types of piecewise linear restoring force characteristics and has shown good agreement between exact solutions and the Ritz averaging method with a single term approximation.

Based on these considerations, the Ritz averaging method was selected for the theoretical analysis of the system under study.

3. ANALYTICAL SOLUTIONS

3.1 THE DEVELOPMENT OF THE GOVERNING DIFFERENTIAL EQUATIONS OF MOTION

3.1.a. FORCING INPUT OF THE TYPE $T \cos \omega t$

Figure 3.1.1.1b shows the restoring force characteristics of an asymmetrical bilinear system. The asymmetry is caused by the action of a constant torque T_0 . The mean position of the vibration is shifted to 0, which is now used as the origin. The angular displacement θ_1 represents the shift due to the constant torque T_0 . The range of displacement is divided into three regions. Within regions I and III, the stiffness is linear and the tooth contact is made with the restrainer walls. Region II represents motion within the clearance where the stiffness is zero. The equation of motion in region I is given by:

$$J\ddot{\theta} + K\theta = T_0 + T \cos \omega t \quad \text{for } \theta \geq -\theta_1 \quad (3.1.A.1)$$

The equation of motion in region II is given by:

$$J\ddot{\theta} = T_0 + T \cos \omega t \quad \text{for } -(2\theta_0 + \theta_1) \leq \theta \leq -\theta_1 \quad (3.1.A.2)$$

and the equation of motion in region III is given by:

$$J\ddot{\theta} + K[\theta - \{-(2\theta_0 + \theta_1)\}] = T_0 + T \cos \omega t \\ \text{for } \theta < -(2\theta_0 + \theta_1) \quad (3.1.A.3)$$

For the special case of a symmetrical bilinear restoring force characteristic, the mean torque $T_0 = 0$ and thus the asymmetry factor, $\theta_1 = 0$.

3.1.b FORCING INPUT OF THE TYPE $C \omega^2 \text{Cos } \omega t$

The equations of motion are derived for a system with a symmetrical restoring force characteristic. Figure 3.1.1.1C shows the restoring force characteristic.

The equation of motion in region I is given by:

$$J\ddot{\theta} + K(\theta - \theta_0) = C \omega^2 \text{Cos } \omega t$$

or

$$\ddot{\theta} + p^2(\theta - \theta_0) = Z \omega^2 \text{Cos } \omega t \quad \text{for } \theta \geq \theta_0 \quad (3.1.B.1)$$

where

$$Z = \frac{C}{J} \quad \text{and} \quad p^2 = \frac{K}{J} .$$

The equation of motion in region II is given by:

$$J\ddot{\theta} = C \omega^2 \text{Cos } \omega t$$

or

$$\ddot{\theta} = Z \omega^2 \text{Cos } \omega t \quad \text{for} \quad -\theta_0 \leq \theta \leq \theta_0 \quad (3.1.B.2)$$

The equation of motion in region III is given by:

$$J\ddot{\theta} + K[\theta - (-\theta_0)] = C \omega^2 \text{Cos } \omega t$$

or

$$\ddot{\theta} + p^2[\theta - (-\theta_0)] = Z \omega^2 \text{Cos } \omega t \quad \text{for } \theta \leq -\theta_0 \quad (3.1.B.3)$$

3.2 ANALYTICAL SOLUTIONS OF THE EQUATIONS OF MOTION

The equations of motion are solved by using the Ritz averaging method. To apply the Ritz averaging method a solution for the displacement must be assumed in the form of a series.

The series is truncated in accordance with the degree of accuracy required. The assumed approximation must satisfy the boundary conditions corresponding to a periodic

solution. It must also be consistent with the physical restraints of the system. The general form of the solution can be expressed as:

$$\begin{aligned} \tilde{\theta} = M + Q_1 \cos \omega t + Q_2 \cos 2\omega t + Q_3 \cos 3\omega t \\ + Q_4 \cos 4\omega t + \dots \end{aligned} \quad (3.2.1)$$

The constant term M results from the asymmetry of the restoring force. The term $Q_1 \cos \omega t$ represents the fundamental harmonic component of the motion and the other terms represent higher harmonic components. The fundamental harmonic of the same frequency as the disturbing force must be included to allow for the transfer of energy to the vibrating system. The other harmonics become predominant components of motion at their corresponding orders of ultraharmonic resonances, e.g. Q_2 , Q_3 and Q_4 peak out at 2nd, 3rd and 4th order ultraharmonic resonances..

For the harmonic resonance, a two term solution of the following form is assumed:

$$\tilde{\theta} = M + Q_1 \cos \omega t \quad (3.2.2)$$

The above is the simplest approximation which can be used with an asymmetrical restoring force. The term M represents the shift of the mean value, the term $Q_1 \cos \omega t$ is necessary to allow transfer of energy from the forcing function. The analytical solutions are fully developed in Appendix I.

For 3rd order ultraharmonic resonance, the simplest form of the solution must consist of the following three terms:

$$\tilde{\theta} = M + Q_1 \cos \omega t + Q_3 \cos 3\omega t \quad (3.2.3)$$

In the above, the additional term $Q_3 \cos 3\omega t$ is included to represent the predominant component of the ultraharmonic resonance. The analytical solutions are obtained in Appendix I.

For the 1/3rd order subharmonic resonance, a three term solution of the following form must be used:

$$\tilde{\theta} = M + Q_1 \cos \omega t + Q_{1/3} \cos \frac{\omega t}{3} \quad (3.2.4)$$

The term $Q_{1/3} \cos \frac{\omega t}{3}$ represents the predominant component of the 1/3rd order subharmonic resonance. The analytical solutions are presented in Appendix I.

4. EXPERIMENTAL STUDY

4.1 SIMULATION TECHNIQUES

4.1.1 ANALOG COMPUTER SIMULATION

An EAI model TR-20 analog computer was used for this study. This computer has twenty operational amplifiers, twenty coefficient potentiometers, six integrator modules, non-linear computing components and function generators.

ANALOG COMPUTATION

The dynamic equation of motion of a bilinear system is given by:

$$\ddot{\theta} + p^2 f(\theta) = T(t) \quad (4.1.1.1)$$

Where $f(\theta)$ represents the bilinear restoring force characteristics.

$$\text{and } T(t) = T \cos \omega t \text{ or } C \omega^2 \cos \omega t$$

p = circular linear natural frequency.

Generalized circuits for the solution of equation (4.1.1.1) are given in figures 4.1.1.1 to 4.1.1.4. In order to maintain reasonable machine accuracy and to reduce the effect of transient vibration, separate computing sequences of short duration were used for each frequency. Corresponding values of total amplitude and phase angle were set as initial conditions for the forced vibration. A small amount of damping was introduced at the start of computation and was then gradually reduced to zero before the output was recorded by means of a two channel pen recorder. This

technique was used to remove the transient free vibration which was excited by the start of computation. For each set of results, one cycle of vibration was divided into several parts and ordinates were scaled off, and a harmonic analysis was carried out by means of a digital computer.

4.1.2 DIGITAL COMPUTER SIMULATION

The Continuous System Modeling Program (CSMP) was used to simulate the bilinear vibrating system. The block diagram and the corresponding structural statements are shown in Figure 4.1.2.1. Two function generators were used to produce the bilinear effect and the periodic disturbing force input. The general forms of the generators are shown in Figure 4.1.2.2.

At each frequency, initial values were set for the amplitude and numerical integrations were performed from $t = 0$ to $t = 150$ secs. Results were printed and plotted at an interval of 0.1 sec. A small amount of damping was introduced in the system to damp out the transient component. However, the system response seemed to be influenced by damping. This was evident by the presence of a small phase difference between the periodic disturbing input and the vibration output. The vibration output was steady after $t = 100$ seconds. A cycle of steady state vibration was divided into several parts and ordinates were recorded. These values of ordinates were fed to another digital computer program for harmonic analysis.

4.2 MECHANICAL MODEL TECHNIQUE

4.2.1 DESIGN OF THE MODEL OF THE BILINEAR NON-LINEAR SYSTEM

The design details of the experimental model are shown in Figure 4.2.1.1. It consists of a shaft with a circular cross section 'S', a rectangular vibrating arm 'A', four bush bearing 'B', a tooth block 'D' and a rigid restrainer 'E'.

The system has a natural frequency of 26 Hz. The shaft diameter is $5/8$ " and the length between the vibrating arm and the tooth block is 32". The dimensions of the vibrating arm are $8" \times 2 \frac{1}{4}" \times 1 \frac{1}{4}"$. The fixed end consists of a case hardened restrainer with a cavity to accommodate the tooth block. The tooth block is clamped on the shaft. The tooth block is made in two halves. The upper half contains a rectangular tooth and is case hardened. The tooth block assembly slides into the restrainer cavity. A slot is cut in the restrainer to accommodate the tooth block and a fixed clearance ($0.0015"$) is maintained between the tooth and outer restrainer slot walls. The tooth block assembly is shown in Figure 4.2.1.2.

The shaft is supported by four bush bearings. Each bearing consists of a phosphor bronze bushing contained in a mild steel housing. A slot is cut in the bush and a screw is provided to adjust pressure on the shaft. A hole is also provided for lubrication.

The bearing housings and restrainer are mounted on the base plate 'C'. Three $3/4$ " holes are provided on the base

plate to clamp it on a vibration isolated table. The overall view of the set up is shown in Figure 4.2.1.3.

The vibration excitation system is also shown in Figure 4.2.1.3. The electro dynamic shaker is mounted upside down on a specially fabricated structure. The shaker pin is connected to the vibrating arm through a soft helical spring. A counter weight is attached on the vibrating arm to bring the shaker pin to its mechanical center as shown in Figure 4.2.1.3.

REMARKS ON THE DEVELOPMENT OF THE EXPERIMENTAL MODEL

The described apparatus was developed through several stages of improvement. Initially the vibrator was suspended by means of springs but it was not possible to maintain its stability under all operating conditions. The shaker pin was also connected to the vibrating arm by a piano wire. It was, however, observed that the motion of the vibrating arm was interacting with the shaker pin movement, which could not be kept sinusoidal. The results were not repeatable. Hence this scheme was abandoned and a fixed suspension system for the shaker was designed with a spring coupling to the model. This arrangement proved satisfactory in operation.

Several tooth gap clearances ($2\theta_0$) of magnitudes 0.01", 0.005" and 0.003" were tried. The vibration excitation system could not maintain constant shaker pin displacement within this range at higher frequencies. Thus the subharmonic resonance could not be excited. Consequently, the experiments were restricted to the 0.003" clearance only.

4.2.2 INSTRUMENTATION

A schematic diagram of the experimental set-up is shown in Figure 4.2.2.1. The arm 'A' is excited sinusoidally at point 'Q' and the system response is picked up by an accelerometer mounted at location 'P'. The accelerometer output is amplified and fed to a real time analyzer to obtain frequency analyses.

4.2.2.1 VIBRATION EXCITATION SYSTEM

The vibration excitation system consists of an automatic vibration exciter control (B&K 1025), excitation amplifier (GM, 5535), electrodynamic shaker (PR 7270) and accelerometer preamplifier (B&K 2622).

4.2.2.2 VIBRATION PICK-UP SYSTEM

The vibration pick-up system consists of an accelerometer (B&K 4343) and accelerometer preamplifier (B&K 2623).

4.2.2.3 VIBRATION READOUT/PROCESSING SYSTEM

The vibration readout system consists of a measuring amplifier (B&K 2607), oscilloscope (Tetronix type 564), X-Y display (SD 13116-2A) and X-Y recorder (Hewlett-Packard).

The vibration processing system consists of a frequency analyzer such as B&K 2107 or 2113 and a real time analyzer (SD 301).

4.2.3 EXPERIMENTAL PROCEDURE

Firstly, the vibration test system was set up to control the shaker motion. To achieve shaker control an accelerometer 'R' (B&K 4333) was installed on the shaker pin. The output of this accelerometer was fed back to the

automatic vibration exciter control via the accelerometer preamplifier. This forms a control feedback loop for the shaker and the exciter. Figure 4.2.3.1 shows a control accelerometer mounted on the shaker pin attachment. The automatic vibration exciter control was then set up for a constant displacement mode by selecting a compressor regulation speed and adjusting the output voltage for a required vibration level. Subsequently the frequency was swept through the desired range and the system response was monitored.

4.2.4 MEASUREMENT AND ANALYSIS OF EXPERIMENTAL DATA

An accelerometer 'P' was installed on the vibration arm 'A' at a distance 3.5" from the shaft axis to monitor the system vibration response. The accelerometer was connected to the measuring amplifier through an accelerometer preamplifier and an associated power supply unit (ZR 0024). The measuring amplifier was calibrated using an accelerometer calibrator (B&K 4291).

The measuring amplifier output was connected to a Spectral Dynamics real time analyzer unit, which consisted of a real time analyzer, ensemble average (SD 309), X-Y display and an X-Y recorder. The real time analyzer was also calibrated in conjunction with the measuring amplifier. The X-axis of the X-Y display represented frequency on a linear scale and its range was selected on the real time analyzer. The Y-axis represented component amplitudes and was set to a logarithmic (dB) scale.

The shaker pin displacement was preset to 0.1 in. peak-to-peak and the frequency was scanned to observe the harmonic resonance and thus obtain the natural frequency of the mechanical model. Using this technique, the natural frequency of the system was found to be 26 Hz. The same procedure was repeated with several other shaker pin displacements to verify the results.

The shaker pin displacement was preset to 0.056 in., 0.07 in., 0.105 in., 0.140 in., and 0.175 in. peak-to-peak to correspond with values of $\bar{S} = 0.8, 1.0, 1.5, 2.0$ and 2.5 . The relationship between the shaker pin displacement and \bar{S} is shown in Appendix III. The frequency of the shaker pin was adjusted manually. At each frequency setting the output of the accelerometer mounted at 'P' (figure 4.2.2.1) was observed on the storage oscilloscope and a frequency analysis was carried out using the real time analyzer. The acceleration components were converted into non-dimensional amplitudes \bar{Q}_1, \bar{Q}_2 etc. (shown in Appendix III). Several frequency settings were taken to observe the ultraharmonic, harmonic and subharmonic resonance phenomena.

5. DISCUSSION OF RESULTS

5.1 GENERAL DISCUSSION

The analytical solutions are firstly developed for a system with an asymmetrical restoring force characteristic. The asymmetrical solutions can be simplified for symmetrical restoring force characteristics by assuming $\bar{\theta}_1 = 0$.

The main contribution of this study is the development of the analytical solutions by means of the Ritz averaging method for the ultraharmonic, harmonic and subharmonic resonances of a system with a bilinear asymmetrical restoring force characteristic. It is believed that the obtained results, in terms of the asymmetry factor $\bar{\theta}_1$, are in the simplest form for adequate definition of the behavior of the system.

It should be noted that in the graphs analytical results are represented by solid lines and experimental results by points.

5.1.a HARMONIC RESONANCE:

The harmonic resonance phenomenon in a non-linear system corresponds basically to the linear resonance and takes place at the natural frequency of the system. The expressions are developed in Appendix I. Section I.1.1 deals with the disturbing torque of type $T \cos \omega t$. The general expressions for the analytical solutions with the asymmetrical restoring force characteristic are obtained by assuming a two term solution and applying the Ritz averaging method. Two simultaneous equations, (I.1.1.6)

and (I.1.1.7), are produced.

The equations (I.1.1.6) through (I.1.1.9) are solved for selected values of the parameters \bar{S} and $\bar{\theta}_1$. Corresponding values of \bar{M} and \bar{n} are calculated for set magnitudes of \bar{Q}_1 . The analytical results are computed for the asymmetry factor, $\bar{\theta}_1 = 0$ and 0.05 . The value $\bar{\theta}_1 = 0$ represents the special case of the symmetrical restoring force characteristic. The other value $\bar{\theta}_1 = 0.05$, represents weak symmetry and thus corresponds best to the restoring force characteristic of the mechanical model. The analytical results for the symmetrical restoring force characteristic for different values of excitation amplitude \bar{S} are shown in figure 5.1.1. The backbone curve ($\bar{S} = 0$) represents the free vibration response of the system. The response curve has positive and negative branches. The motion is stable due to the absence of the jump phenomenon.

The analog computer results are superimposed on the analytical results, shown in figure 5.1.1. The analog computer results are in close agreement with the analytical solutions and thus verify the accuracy of the Ritz averaging method. It also indicates that a two term solution is a very good approximation.

It should be noted, however, that the two term solution is not valid in regions of low or high values of η , where ultraharmonic and subharmonic resonances occur and corresponding approximate solutions must have additional terms. The

results are shown by dotted lines for $\eta < 0.4$ where ultraharmonic resonances develop.

Solutions for the asymmetrical restoring force characteristic, with an asymmetry factor $\bar{\theta}_1 = 0.05$, are shown in figures 5.1.2 through 5.1.4. The response curve of the amplitude \bar{Q}_1 is shown in figures 5.1.2 & 5.1.3 for $\bar{S} = 2.0$ and 1.0 respectively. While the analog computer results agree very well with the analytical solution, indicating again that the Ritz method with a two term approximation yields very good results, the experimental values are generally lower in magnitude and there is a shift to the right. One possible explanation is that the experimental value for the natural frequency of the mechanical model was measured too low, which resulted in higher values of the frequency ratio η . The natural frequency of the mechanical model was determined by running a forced vibration test. This procedure is discussed in section 4.2.4. Thus some error in determining the natural frequency is possible due to the influence of damping and the difficulty in locating exactly the peak of resonance. As an estimation of the influence of this error in determining the natural frequency, referring to figure 5.1.2, the point $\bar{Q}_1 = 9.4049$, $\eta = 0.9111$ will shift to $\eta = 0.87$ for an error of 1 Hz in the experimental value of the natural frequency and to $\eta = 0.85$ and $\eta = 0.81$ for errors of 2 Hz and 3 Hz respectively. Similarly a point $\bar{Q}_1 = 3.9143$, $\eta = 0.7023$ will shift to $\eta = 0.68$ for an error of 1 Hz and $\eta = 0.65$ and $\eta = 0.63$ for errors of 2 Hz and 3 Hz respectively.

In the analytical and analog computer models damping was absent, but in the mechanical model a damping ratio $\zeta = 0.07$ was determined experimentally. The experimental points show a typical influence of damping, which reduces the amplitude of vibration. Some additional energy dissipation is also caused by the collision of the teeth with the clearance walls. Although the experimental results are consequently lower, the general trend is maintained.

In the mechanical model, the vibration output was monitored by an accelerometer mounted on the vibrating arm at point 'P' (shown in figure 4.2.2.1). The accelerometer outputs at different forcing frequencies are shown in figures 5.2.1 through 5.2.4 and their frequency spectra are shown in figures 5.2.5 through 5.2.8. The forcing frequencies are selected to show typical acceleration patterns in the low frequency region, where the ultraharmonic resonances develop, and in the harmonic resonance region. Figure 5.2.7 shows an acceleration spectrum at a forcing frequency, $f = 19.9$ Hz ($n = 0.76$), which is away from the ultraharmonic resonance region and near the harmonic resonance. The odd order harmonics are predominant. The 1st order harmonic, which is the main component of the motion, has the maximum amplitude. Figure 5.2.8 presents the acceleration spectrum at the forcing frequency $f = 33.3$ Hz ($n = 1.28$), which is just beyond the harmonic resonance peak. Odd order harmonics predominate. Figures 5.2.5 and 5.2.6 show the frequency contents of the acceleration at forcing frequencies $f = 9.6$ Hz

($\eta = 0.37$) and 13.8 Hz ($\eta = 0.53$) respectively. The development of the 3rd and 2nd ultraharmonic resonances can be clearly seen.

The vibration energy is spread over the harmonic components of the actual vibration motion. In the approximate analytical solution all the energy is represented by a single term, which consequently will be greater in magnitude than the corresponding single experimental term.

The existence of the constant term M in the analytical solutions of the symmetrical restoring force characteristics is not clearly evident in the first instance. In general, M should not be there with the symmetrical system but it must be used because the origin for the definition of stiffness has been chosen at the point 'O' (shown in figure 3.1.1.1b). When $\bar{\theta}_1 = 0$, the point 'O' moves to the end of the clearance. The natural mean position of the motion remains off-set by an amount $-\theta_0$ from this new origin, hence the mean shift \bar{M} is equal to -1. The plot of \bar{M} versus η is shown in figure 5.1.4.

The analog and digital computer outputs are shown in figures 5.1.6 through 5.1.9. The free vibration response obtained on the analog computer for $\bar{\theta} = 2.0, 3.0, 4.0$ is shown in figure 5.1.6. Digital computer simulation results for $\bar{\theta} = 2.0$ are shown in figure 5.1.9. Several runs were made on the digital computer to obtain free vibration responses for $\bar{\theta} = 2.0, 3.0$ and 4.0. In both simulation

techniques identical results were obtained. Similarly, forced vibration responses were obtained on the analog computer for different forcing amplitudes $\bar{S} = 1.0$ and 2.0. Typical analog computer outputs are shown in figures 5.1.7 and 5.1.8. From these plots the phase shift of the amplitude $\bar{\theta}$ before and after the harmonic resonance is evident.

The harmonic resonance of the system, with a symmetrical bilinear restoring force characteristic, to the centrifugal type input $C \omega^2 \cos \omega t$ is obtained by solving two simultaneous equations (I.2.1.5) and (I.2.1.6), which are developed in section I.2.1 (Appendix I). Both equations are solved for set values of parameters \bar{Q}_1 and Z' and corresponding values of η are calculated. Analytical results for a particular value of $Z' = 2.0$ are shown in figure 5.1.5. The backbone curve ($Z' = 0$) is also drawn in this figure. There are two distinct branches for a particular value of Z' . The negative branch becomes asymptotic to $|\bar{Q}_1| = Z'$ at high values of η , but the single term solution is not valid in this region due to the presence of the subharmonic resonance. The single term solution is also not valid in the $\eta = 1/3$ region, where the 3rd order ultraharmonic resonance takes place. The analog computer results are superimposed on the analytical results. There is good agreement with analytical solutions, which supports the suitability of the single term approximation for this case and the

accuracy of the Ritz method.

5.1.b 3RD ORDER ULTRAHARMONIC RESONANCE:

Ultraharmonic resonances take place when frequencies of the higher harmonics of motion coincide with the natural frequency of the system.

The general form of the displacement is expressed in series form as:

$$\tilde{\theta} = M + Q_1 \cos \omega t + Q_3 \cos 3\omega t + Q_5 \cos 5\omega t + \dots \text{ etc.}$$

In the above expression normally Q_3 and Q_5 etc. are negligibly small, unless $3\omega = p$ or nearly so, then $n = 1/3$ and Q_3 is magnified producing the ultraharmonic resonance of order 3.

This condition is evident in the spectrum shown in figure 5.2.5. Similarly at or near $5\omega = p$, Q_5 is magnified. The order of the ultraharmonic resonance is defined by the ratio $\frac{p}{\omega}$. The term Q_1 must be included in the corresponding approximation solution for the transfer of energy to all vibration components, which can take place only at the frequency of the disturbing effect. Hence the simplest approximate solution for the 3rd order ultraharmonic resonance must have the first three terms. Thus,

$$\tilde{\theta} = M + Q_1 \cos \omega t + Q_3 \cos 3\omega t$$

The analytical solutions are developed in Appendix I. Section I.1.2 corresponds to the input of type $T \cos \omega t$ and

section I.2.2 covers the input of the type $C \omega^2 \text{Cos } \omega t$.

The application of the Ritz method with the disturbing torque $T \text{Cos } \omega t$ results in five simultaneous equations (I.1.2.5) through (I.1.2.9). Similar expressions are developed for an input of the type $C \omega^2 \text{Cos } \omega t$, by assuming a two term solution. The application of the Ritz averaging method results in three simultaneous equations (I.2.2.7) through (I.2.2.9). The equations (I.1.2.5) through (I.1.2.9) are solved for selected values of the parameters \bar{S} and $\bar{\theta}_1$. For set magnitudes of \bar{Q}_3 corresponding values of \bar{M} , \bar{Q}_1 and η are calculated. The analytical results are obtained for $\bar{\theta}_1 = 0$ and 0.05 . The analytical results for the symmetrical restoring force characteristic are shown in figure 5.1.10 and 5.1.11. Figure 5.1.10 shows the response curve of the 3rd harmonic component \bar{Q}_3 and the harmonic component \bar{Q}_1 is shown in figure 5.1.11. The curve of \bar{Q}_3 has both positive and negative branches and the motion appears to be stable since conditions for a jump are not present. The component \bar{Q}_3 has a well defined resonance near $\eta = 1/3$. The component \bar{Q}_1 has two positive branches, which correspond to the positive and negative branches of \bar{Q}_3 . \bar{Q}_1 does not depart significantly from the harmonic resonance curve developed in the previous section. \bar{Q}_3 becomes dominant only in the ultraharmonic resonance region. The relative magnitudes of the 3rd order ultraharmonic resonance are compared to the harmonic resonance in figure 5.1.34. Analytical and analog computer results show

good agreement. Therefore, the validity of the three term approximation and the accuracy of the Ritz method are verified.

The analytical results for the asymmetrical restoring force characteristics with an asymmetry factor, $\bar{\theta}_1 = 0.05$ and $\bar{S} = 2.0$ and 1.0 are shown in figures 5.1.12 through 5.1.17. The experimental results were obtained for the mechanical model for $\bar{S} = 0.8, 1.0, 1.5, 2.0$ and 2.5 and are shown in figures 5.2.9 through 5.2.20. The experimental data reduction technique is discussed in detail in section 5.2. Figures 5.1.12 and 5.1.13 show analytical and experimental results of \bar{Q}_3 and \bar{Q}_1 for a particular value of $\bar{S} = 2.0$. Referring to figure 5.1.12, experimental values of \bar{Q}_3 indicate a valley and a peak. The peak corresponds to the 3rd order ultraharmonic resonance and it is shifted towards the right. The explanations for this shift are the same as for the harmonic resonance. An additional factor, which is of greater influence here than in the harmonic resonance region, is the presence in the actual motion of significant higher harmonics, as shown in figure 5.2.5. Since these are neglected in the theoretical solution, experimental values of Q_3 must be lower due to the spread of energy over a greater number of components. The experimental results dip down between $\eta = 0.2$ and 0.4 with a minimum at approximately $\eta = 0.25$. This is possibly due to the formation of the 4th order ultraharmonic. Under these conditions

the 4th order harmonic would absorb the major portion of the vibration energy at the expense of the 3rd order component. Similar conditions appear to prevail near $\eta = 0.5$ where the 2nd order ultraharmonic resonance may be initiated. Referring to figure 5.2.11 and 5.2.12, it is observed that the component \bar{Q}_4 peaks out at $\eta = 0.25$, then \bar{Q}_3 starts developing and reaches maximum value at about $\eta = 0.36$. Referring to figures 5.2.10 and 5.2.11, it is observed that the component \bar{Q}_2 peaks at about $\eta = 0.53$ and \bar{Q}_3 bottoms out. The experimental values of \bar{Q}_1 are consistently lower than the analytical results and they are also shifted towards the right (figure 5.1.13). As in the case of harmonic resonance the contributing factor for lowering of experimental results are damping, error in determination of the natural frequency of the mechanical model, collision and approximation in the solution. Although the experimental results are lower in magnitude, yet they show well defined 2nd, 3rd and 4th order ultraharmonic resonances. Experimental results for $\bar{S} = 1.0$ & 1.5 are shown in figure 5.1.15 through 5.1.17 and 5.2.13 through 5.2.16. The results indicate the same trends as for $\bar{S} = 2.0$, as discussed before.

The ultraharmonic resonance, produced by the forcing input of the type $C \omega^2 \cos \omega t$, is obtained by solving the three simultaneous equations (I.2.2.7) through (I.2.2.9). For set magnitudes of \bar{Q}_3 corresponding values of \bar{Q}_1 and η are calculated for selected values of the parameter Z' .

Analytical results, for a particular value $Z' = 10.0$, are shown in figures 5.1.18 and 5.1.19. Figure 5.1.18 shows the curve of the 3rd harmonic component \bar{Q}_3 and that of the fundamental component \bar{Q}_1 is shown in figure 5.1.19. The curve of \bar{Q}_3 has positive and negative branches and the motion will be stable since the conditions for a jump are not present. The component \bar{Q}_1 has two positive branches corresponding to both branches of \bar{Q}_3 .

The analog and digital computer simulation results are superimposed on the analytical solutions, shown in figures 5.1.18 and 5.1.19. On the analog computer it was observed that the 3rd order ultraharmonic resonance could only be generated at comparatively high values of Z' .

An expression for the limiting value of Z' , below which non-linear conditions do not exist, is developed in Appendix IV. With this criterion it can be shown that the system has a non-linear restoring force characteristic only when $Z' \geq 1$. Hence, the ultraharmonic resonance can be excited only with values of Z' greater than 1. However, the 3rd order ultraharmonic resonance could not be produced on the analog computer for magnitudes of Z' lower than 6.0. It appears that this is due to inherent damping present in the electronic components of the analog computer, the introduction of damping at the beginning of computation and the weak nature of the ultraharmonic resonance itself.

The analog and digital outputs are shown in figures

5.1.20 through 5.1.23. In figures 5.1.20 and 5.1.21 the existence of the 3rd order ultraharmonic resonance is clearly evident. Similarly the analog and digital computer outputs for the forcing function $C \omega^2 \cos \omega t$ and values of $Z' = 10.0$ and $\eta = 0.22$ are shown in figures 5.1.22 and 5.1.23.

5.1.c 1/3RD ORDER SUBHARMONIC RESONANCE:

When the frequency ω of the disturbing torque rises well above p , the natural frequency of the system, new and additional components appear in the motion with frequencies of $\frac{\omega}{3}$ and $\frac{\omega}{5}$ etc. The original harmonics of frequencies 2ω , 3ω , etc. become now negligibly small. The displacement function is:

$$\begin{aligned} \tilde{\theta} = M + Q_1 \cos \omega t + Q_{1/3} \cos \frac{\omega t}{3} + Q_{1/5} \cos \frac{\omega t}{5} + \dots \\ + Q_3 \cos 3\omega t + Q_5 \cos 5\omega t + \dots \text{ etc.} \end{aligned}$$

In the above expression $Q_{1/3}$ and $Q_{1/5}$ are small in comparison with Q_1 , unless $\frac{\omega}{3} = p$ or nearly so, when $Q_{1/3}$ is magnified and the subharmonic resonance of order 1/3 takes place. Similarly at $\frac{\omega}{5} = p$, $Q_{1/5}$ is magnified and subharmonic resonance of order 1/5 is generated. The term Q_1 must be included in the assumed solution to allow for the transfer of vibratory energy at the frequency of the disturbing force. The simplest approximate solution for the 1/3rd order subharmonic resonance will thus have the following terms:

$$\bar{\theta} = M + Q_1 \text{Cos } \omega t + Q_{1/3} \cdot \text{Cos } \frac{\omega t}{3}$$

The analytical solutions are derived in Appendix I. Sections I.1.3 and I.2.3 correspond to the inputs of the type $T \text{ Cos } \omega t$ and $C \omega^2 \text{ Cos } \omega t$ respectively.

The application of the Ritz method to the asymmetrical case results in five simultaneous equations, (I.1.3.5) to (I.1.3.9). Similar expressions are developed for the symmetrical restoring force characteristic and an input of the type $C \omega^2 \text{ Cos } \omega t$ by assuming a two term solution. Three simultaneous equations (I.2.3.7) to (I.2.3.9) are then produced. The solutions are shown in Appendix I. The equations (I.1.3.5) through (I.1.3.9) are solved for selected values of the parameter \bar{S} and $\bar{\theta}_1$. For set magnitudes of $\bar{Q}_{1/3}$ corresponding values of \bar{M} , \bar{Q}_1 and η are calculated. The analytical results are obtained for the symmetrical restoring force characteristic ($\bar{\theta}_1 = 0$) and are shown in figures 5.1.24 through 5.1.26. The figure 5.1.24 shows the response curve of the 1/3rd harmonic component $\bar{Q}_{1/3}$. The harmonic component \bar{Q}_1 is shown in figure 5.1.25. Both are drawn for $\bar{S} = 2.0$. The curve of $\bar{Q}_{1/3}$ has both positive and negative branches and the motion is stable since conditions for a jump are not present. In the analytical results the component $\bar{Q}_{1/3}$ has a well defined resonance at $\eta = 3.0$. The component \bar{Q}_1 has two negative branches corresponding to both branches of $\bar{Q}_{1/3}$. The comparison of relative mag-

nitudes of $\bar{Q}_{1/3}$ and Q_1 indicates that in the subharmonic resonance region, $\bar{Q}_{1/3}$ develops very rapidly whereas \bar{Q}_1 drops down slowly. For instance, while $\bar{Q}_{1/3}$ increases from 2.0 to 14.0, \bar{Q}_1 drops down from 0.8 to 0.2, for a variation of $\eta = 1.8$ to 2.8. A plot of \bar{M} versus η is shown in figure 5.1.26.

The physical system was simulated on the analog and digital computers for a symmetrical bilinear restoring force characteristic. Both types of inputs were used. With $T \cos \omega t$ and $\bar{S} = 2.0$, the system produced 1/3rd order subharmonic resonance over a narrow frequency range, $\eta = 1.6$ to 2.0, with the right initial conditions. As the frequency increased beyond $\eta = 2.0$, the overall amplitude of the vibration became less than the clearance, thus the tooth lost contact with the retainer walls and the system reverted to a linear restoring force characteristic. These results indicate that the excitation of this type of resonance depends upon the magnitude of the disturbing effect. It was expected that a disturbing force amplitude-frequency boundary was present, beyond which the subharmonic resonance cannot exist. The mathematical development of the equation of this boundary is shown in Appendix IV. This criterion establishes a relationship between cut-off frequencies and forcing amplitudes. The cut-off frequency is the highest value, above which a forcing function cannot excite the subharmonic resonance.

Although for $\bar{S} = 2.0$ the theoretical cut-off frequency is $\eta = 1.45$, the analog computer results show the possible presence of the subharmonic resonance for values of η up to 2.0. The application of a larger amplitude of motion as the initial condition, will result in a wider frequency range of tooth contact, thus extending correspondingly the subharmonic resonance limit.

The sample wave forms for $\bar{S} = 2.0$ and $\eta = 1.6$ are shown in figure 5.1.30. The digital computer simulation response is shown in figure 5.1.31. This technique also verifies analytical and analog computer results as shown in figure 5.1.24.

To generate the 1/3rd order subharmonic resonance in the mechanical model, a stepped shaft of natural frequency 12 Hz was used in place of the 5/8" diameter shaft with 26 Hz natural frequency. The purpose of this change was to be able to vibrate the system at higher frequencies and still maintain constant displacement output within the power limitations of the shaker.

In the testing procedure the system was vibrated through a wide range of frequencies with a maximum value of $\bar{S} = 2.5$. It was not possible to generate a subharmonic resonance, at higher frequencies the system just followed the harmonic resonance response. As indicated by the cut off frequency equation, at higher frequencies, the tooth lost contact with the walls of the clearance space and reverted to a linear restoring force. Owing to the inherent damping produced

primarily by the four bush bearings, the maximum output power of the shaker was insufficient to increase the amplitude for maintaining tooth contact and hence also the non-linear restoring force in the subharmonic resonance region. Moreover, the dissipation of energy is proportional to the square of the frequency of vibration, and hence the subharmonic components are more sensitive to damping. It is expected that if a shaker with sufficient power had been available, the subharmonic resonance would have been generated.

The analytical results which are independent of damping, indicate with sufficiently large disturbing force amplitudes the presence of a strong 1/3rd order subharmonic resonance, as shown in figure 5.1.24. It could only be verified with a limited success by means of simulation techniques utilizing analog and digital computers.

The subharmonic resonance response to the forcing input of the type $C \omega^2 \cos \omega t$ is shown in figures 5.1.28 and 5.1.29. Figure 5.1.28 presents the curve of the 1/3rd harmonic component $\bar{Q}_{1/3}$. Similarly, the harmonic component \bar{Q}_1 is shown in figure 5.1.29. The curve of $\bar{Q}_{1/3}$ has positive and negative branches and the motion will be stable due to the absence of the jump phenomenon. The component \bar{Q}_1 has two negative branches corresponding to both branches of $\bar{Q}_{1/3}$. There is close agreement between simulation and analytical results for $\bar{Q}_{1/3}$. But the analog computer values for \bar{Q}_1 are more scattered and generally are lower in magnitude. The dif-

ference is caused by damping introduced in the simulation technique. Typical analog and digital computer wave forms are given in figures 5.1.32 and 5.1.33.

With this type of disturbing effect it is also possible for the system to revert to linear restoring force conditions. The appropriate analysis is shown in Appendix IV. It establishes the limiting value of Z' below which non-linear conditions do not exist and hence the subharmonic resonance cannot be excited. Using this criterion the limiting value of Z' is 1. Therefore with $Z' \geq 1$, the subharmonic resonance can take place.

5.1.d OVERALL VIEW OF THE RESONANCE PHENOMENA

The analytical solutions for the 3rd order ultraharmonic, harmonic and 1/3rd order subharmonic resonances with the excitation torque of the type $T \cos \omega t$ are grouped together in figure 5.1.34 for comparison. In the absence of damping, the amplitudes become asymptotic or indefinite near the resonance. Hence their peak values are indeterminate. The development of typical non-linear resonance is clearly observed. In comparison with the harmonic resonance, it is evident that the intensity of the 1/3rd order subharmonic resonance is at least as great. Although because of equipment limitations, a quantitative experimental verification was not possible, there is sufficient evidence to indicate that in ^{lightly} damped systems subharmonic resonances can be destructive. The amplitudes of the 3rd order ultraharmonic resonance are relatively smaller and should not,

in general, cause serious problems. Vibration with a symmetrical bilinear restoring force characteristic contains predominantly odd order ultraharmonic and subharmonic resonances, as shown for example by Atkinson (3).

5.2 REVIEW OF RESULTS OBTAINED BY THE MECHANICAL MODEL TECHNIQUE

Acceleration wave forms and their frequency composition at several frequency settings for $\bar{S} = 2.0$ are shown in figures 5.2.1 through 5.2.8. The frequency spectra at these forcing frequencies indicate the presence of several higher harmonic components. For comparison of magnitudes of individual harmonic components, one should bear in mind that the amplitude of the first acceleration harmonic component is equal to $\omega^2 Q_1$ and similarly the second, third and fourth components are $4\omega^2 Q_2$, $9\omega^2 Q_3$ and $16\omega^2 Q_4$ respectively, where Q_1 , Q_2 , Q_3 and Q_4 are the displacement amplitudes. At each frequency setting, the first four harmonics were read from the real time analyzer output and were converted into non-dimensional amplitudes \bar{Q}_1 , \bar{Q}_2 , \bar{Q}_3 and \bar{Q}_4 (as shown in Appendix III.2). The plots of \bar{Q}_1 , \bar{Q}_2 , \bar{Q}_3 and \bar{Q}_4 versus n are presented in figures 5.2.9 through 5.2.12. A careful study of these results indicates the existence of 2nd, 3rd and 4th order ultraharmonic resonances. The even order ultraharmonic resonances are present because of effective asymmetry in the restoring force characteristic, which results from the inability to obtain perfect balance of the driving arm. The asymmetry is specified by the para-

meter $\bar{\theta}_1$, which has been defined before. Figure 5.2.9 shows, for $\bar{\theta}_1 = 0.05$, the variation of \bar{Q}_1 . In figure 5.2.10 the magnification of \bar{Q}_2 in the neighbourhood of $n = 0.5$ indicates the 2nd order ultraharmonic resonance. A subsidiary energy transfer from the 4th order resonance is also evident in the vicinity of $n = 0.25$. Similar conditions are evident in Figures 5.2.11 and 5.2.12 and are repeated for other values of \bar{S} in Figures 5.2.13 to 5.2.20.

In summary the mechanical model showed a well defined harmonic resonance and 2nd, 3rd and 4th order ultraharmonic resonances. The comparison of amplitudes indicates that the strength of resonance decreases inversely with the order magnitude.

Subharmonic resonances, as discussed previously, could not be generated on the mechanical model because of the inadequate power of the vibrator.

For quantitative evaluation, spectra of experimental values of \bar{Q}_1 , \bar{Q}_2 , \bar{Q}_3 and \bar{Q}_4 at different values of n , for $\bar{S} = 1.0, 1.5, 2.0$ and 2.5 are shown in figures 5.2.21 through 5.2.24. Referring to figure 5.2.21, before the harmonic resonance, the \bar{Q}_1 component develops in proportion with the forcing amplitude \bar{S} . But beyond it decreases rapidly, hence the accuracy of the measured values in that region is in question. A greater dependence of the higher order components upon \bar{S} in the range of their respective resonances is evident

from Figures 5.2.22 to 5.2.24.

5.3 ESTIMATE OF EXPERIMENTAL ERRORS

The errors are considered in two parts:

1. Transducer and readout equipment.
2. Data reduction.

Transducer and Readout Errors:

Accelerometers, including cables, are individually calibrated by the manufacturer to a suggested accuracy of $\pm 2\%$, with flat frequency response within 2% from 1 Hz to 12000 Hz and with stability better than 2% per year. The mass of the accelerometer is quite small in comparison with the vibrating arm. Hence the mass loading effect of the accelerometer is negligible.

The accuracy of the accelerometer calibrator is stated to be better than $\pm 2\%$ by the manufacturer.

The digital counter, which was used to determine frequency of the shaker pin, measured the period of the oscillation in milli seconds. The instrument error on frequency values was within $\pm 0.1\%$.

Data Reduction:

The real time analyzer was calibrated for 1 'g' peak which corresponded with 50 dB on the Y-axis. During frequency analyses of the accelerometer output, the acceleration harmonics were read within ± 1 dB or 12.23% accuracy. The acceleration harmonics were converted into non-dimensional amplitudes as shown in Appendix III.2. Evaluation of equation

III.2.2 indicates that the non-dimensional amplitude of motion (\bar{Q}_1) depends primarily upon the magnitude of the acceleration harmonic (n_1) and the angular clearance (θ_0). The accuracy in the calculation of \bar{Q}_1 is a function of accuracy involved in acceleration measurements, which are within ± 1 dB and clearance measurements, which can be within $\pm 16.66\%$. The period 't' can be measured within 0.1% accuracy. Hence it is not considered a source of errors.

The error involved in natural frequency measurements would influence the values of the frequency ratio n . As a rough estimate, an overall reading error of 2 Hz would result in an error of 7% in the value of n . An analytical approach of the experimental error analysis is presented in Appendix V.

5.4 REMARKS ON THE APPLICATION OF THE RESULTS

The piecewise linear restoring force characteristic is caused by discontinuous contact with elastic restraints due to clearances. The example of such phenomenon is a geared system in which torsional oscillations are generally present when transmitting power. Such a system will exhibit the harmonic, ultraharmonic and subharmonic resonances. Chaloupka (12) has shown the existence of a 1/2 order subharmonic resonance in a torsional system with gears. In this particular publication, the author has studied the behavior of a system having piecewise linear restoring force characteristics caused by backlash in gear teeth.

The results obtained suggest that ultraharmonic resonances

can be easily excited, but because of the relatively small amplitudes they are not likely to cause serious problems in real systems. Subharmonic resonances, on the other hand, will only be excited with large disturbing forces in strongly non-linear systems with relatively low damping. Although this may not occur often in practice, when it does it is likely to be very destructive.

The relatively simple method developed in this project, of calculating the limiting frequency above which the subharmonic resonances cannot be excited, should be very useful in practical applications.

Although the study dealt with torsional vibration, the results obtained can be easily applied to the vibration of any system with clearances, by replacing appropriately angular parameters and variables.

6. CONCLUSIONS AND SCOPE OF FUTURE WORK

6.1 CONCLUSIONS

The following conclusions are drawn from the investigation undertaken:

1. The Ritz averaging method with two or three term approximation provides satisfactory results.
2. The mechanical model with slight asymmetrical restoring force characteristics develops even and odd order ultraharmonic resonances.
3. A system with symmetrical restoring force characteristics develops only odd order ultraharmonic and subharmonic resonances.
4. The ultraharmonic resonances can be easily generated, but their intensities are much smaller in comparison with the harmonic resonance.
5. Analytical solutions without damping indicate the possibility of large amplitude subharmonic resonances in the case of a forcing input of the type $T \cos \omega t$. Experiments with the mechanical model and the analog computer show that it is difficult to generate this resonance in actual systems at low excitation amplitudes. The subharmonic resonance appears also to be proportionately more susceptible to damping. It must be therefore concluded that such a resonance is likely to occur only in systems with large non-linearity, very low damping and high excitation forces. If it is excited, however,

it is at least as destructive to the vibrating system as the harmonic resonance.

6. The analytical solutions indicate also the possibility of large amplitude ultraharmonic resonance with excitation of the type $C \omega^2 \cos \omega t$. The system failed to show this resonance at low magnitudes of Z' . Experimental results however, suggest again that such a resonance can only be excited in system with very low damping and high excitation forces. On the other hand, as indicated by analog computer testing, this type of excitation appears to have a higher potential for generating subharmonic resonances. The magnitude of this resonance is significant and it is comparable with the harmonic resonance.

6.2 SCOPE OF FUTURE WORK

The most important consequence of non-linear vibration, caused by clearances, is the possibility of exciting subharmonic resonances. It is recommended that an improved mechanical model with a sufficiently powerful vibrator, be used to verify the theoretical results obtained in that frequency domain.

In geared systems there are additional sources of non-linearity, which were not considered in this study. Since their combined effect may be greater than that due to clearances, it is also recommended to investigate the following:

1. Stiffness variations due to the number of teeth simul-

taneously in contact.

2. Stiffness variations due to the sliding of the point of contact along the tooth profile.

BIBLIOGRAPHY

1. Ashwell, G.J. and Chauhan, A.P., "A Study of $1/2$ Subharmonic Oscillations by the Harmonic Balance", Journal of Sound and Vibration, 27, 3, April 1973, pp 313-324.
2. Atkinson, C.P., "Superharmonic Oscillations as a Solution to Duffing Equation as Solved by an Electronic Differential Analyzer", Journal of Applied Mechanics, December 1957.
3. Atkinson, C.P. and Heflinger, L.O., "Subharmonic and Superharmonic Oscillations of a Bilinear Vibrating System", Journal of Franklin Institute, Vol. 262, No. 3, September 1956, pp 185-190.
4. Bennett, J.A. and Rinkel, R.L., "Ultraharmonic Vibrations of Nonlinear Beams", A.I.A.A. Journal 10, 5, May 1972, pp 715-716.
5. Bishop, R.E.D., "On the Graphical Solution of Transient Vibration Problems", Institute of Mechanical Engineers (London), Vol. 168, No. 10, 1954, pp 299-322.
6. Brock, J.E., "An Iterative Numerical Method for Nonlinear Vibrations", Journal of Applied Mechanics, March 1951, pp 1-11.
7. Bruce, V.G., "A Graphical Method for Solving Vibration Problems of a Single Degree of Freedom", Bull. of Siesmological Society of America, 1951, pp 101-109.

8. Bruevich, A.N. "Action of Harmonic Oscillations On a Piecewise-Linear System", Autom Remote Control, Vol. 35, No. 7, July 1974, pp 1195-1200.
9. Burgess, J.C., "Harmonic, Superharmonic and Subharmonic Response of a Single Degree of Freedom System of the Duffing Type", Tech. Report No. 27, 1954, Standford University.
10. Caughey, T.K., "The Existence and Stability of Ultraharmonic and Subharmonics in Forced Nonlinear Oscillations", Journal of Applied Mechanics 1954, pp 327-335.
11. Cakiroglu, Adnan and Ozmen Gunaj, "Numerical Integration of Forced-Vibration Equations", Journal of the Engineering Mechanics Div. A.S.C.E., Vol. 94, No. EM3, Proc. Paper 5968, June 1968, pp 711-729.
12. Chaloupka, V., "On the Initiation of Subharmonic Resonance in a Torsional System with Gears", Nonlinear Vibration Problems, Warsaw, 5, 1963.
13. Cheshankov, B.I., "On Subharmonic Oscillations of a Pendulum", PMM Journal of Applied Mathematics and Mechanics, 35, 2, 1971, pp 301-306.
14. Clauser, F.H., "The Behavior of Nonlinear Systems", Journal of Aero. Science, 1956, Vol. 23, pp 411.
15. DenHartog, J.P., "Mechanical Vibrations", McGraw Hill, New York.
16. DenHartog, J.P., "The Amplitude of Nonharmonic Vibrations", Journal of Franklin Institute, Vol. 216, 1933.

17. DenHartog, J.P. and Mikina, J., "Forced Vibrations with Nonlinear Spring Constants", Journal of Applied Mechanics, Vol. 54, 1932.
18. DenHartog, J.P. and Heiles, R.M., "Forced Vibrations in Nonlinear Systems with Various Combinations of Linear Springs", Journal of Applied Mechanics, Vol. 58, 1936.
19. Dokainish, M.A. and Kumar R., "Transverse Beam Vibrations", Journal of Engineering Mechanics, Proc. of the American Society of Civil Engineers, 98, EM6, 1972, pp 1381-1395.
20. Dokainish, M.A. and Kumar, R., "Experimental and Theoretical Analysis of the Transverse Vibrations of a Beam Having Bilinar Support", Experimental Mechanics, June 1971, pp 263-270.
21. Douglas, F., "Vibrations of Systems Having Variable Elasticity Characteristics", Part I and II-Free Vibrations of Two-Rate System. Bull. of Mech. Eng. Educ., Vol. 6, No. 2, 1967, pp 103-111. Part III Forced Vibrations, pp 333-344.
22. Dubowsky, S. and Freudenstein, F., "Dynamic Analysis of Mechanical Systems with Clearances", Journal of Engineering for Industry, Trans. of A.S.M.E., 1971, pp 305-316.
23. Duffing, G., "Erzwungene Schwingungen bei veranderlicher Eigen frequenz", F. Vieweg u. Sohn, Braunschweig, 1918.

24. Eller, Antony, "Fractional Harmonic Frequency Pairs in Nonlinear Systems", Acoustical Society of America, Vol. 53, No. 3, March 1973, pp 758-765.
25. Evaldson, Ayre and Jacobson, "Response of an Elastic-ally Nonlinear System to Transient Distrubances", Journal of Franklin Institute, 1949, pp 473-494.
26. Farshad, M. and Shahinpoor, M., "Beam on Bilinear Elastic Foundations", Int. Journal of Mech. Sciences, Vol. 14, No. 7, 1972, pp 441-445.
27. Fleishman, B.A., "Harmonic and Subharmonic Response of an On-Off Control System to Sinusoidal Inputs", Journal of Franklin Institute.
28. Freidrichs, K.O. and Stoker, J.J., "Forced Vibrations of Systems with Nonlinear Restoring Force", Quart. App. Maths, Vol. 1, 1943, pp 97-115.
29. Freidrichs, K.O., "On Non-Linear Vibrations of Third Order", from Studies in Non-Linear Vibration Theory, Inst. for Math. and Mech., New York University, 1946.
30. Fu, C.C., "Stable Harmonic and Subharmonic Oscillations of a System with Piecewise Linear Restoring Forces", Journal of Applied Mechanics, 1974, pp 273-277.
31. Gen Hokkaido, Yamada, "Vibration Damping Effect of the Impact Damper on a Piecewise Linear Mass Spring System", Bull. J.S.M.E., Vol. 17, No. 104, 1974, pp 210-217.

32. Hayashi, C., "Nonlinear Oscillations in Physical Systems", McGraw Hill Book Company, 1964.
33. Hayashi, C., "Subharmonic Oscillations in Nonlinear Systems", Journal of Applied Physics, Vol. 24, 1953, pp 521-529.
34. Hayashi, C., "Stability Investigation of the Nonlinear Periodic Oscillations", Journal of Applied Physics, 1953, pp 344-348.
35. Hayashi, C., "Stability Investigation of the Nonlinear-Periodic Oscillations", Journal of Applied Physics, Vol. 24, No. 3, 1953, pp 344-348.
36. Holman, J.P., "Experimental Methods for Engineers", 1971, McGraw-Hill, New York.
37. Huskey, H.D. and Korn, G.A., Edited by, "Computer Handbook", McGraw Hill, New York.
38. Jacobson, S.J. and Ayre, R.S., "Engineering Vibrations", 1958, McGraw Hill, New York and London.
39. Johnson, C.L., "Analog Computer Techniques", 1956, McGraw-Hill, New York.
40. Karasudhi, P., Tan, G., Lee, S.L., "Vibration of Frame Foundation with Bilinear Hysteresis for Rotating Machinery", Journal of Engineering for Industry, Trans. A.S.M.E., Vol. 96, Ser B n3, Aug. 1974, pp 1010-1014.
41. Kido, M. and Inagaki, Y., "An Experimental Study of Subharmonic Oscillations in a Nonlinear System", Bull. of Osaka Prefecture Series A, 18, 1, 67-79, 1969.

42. Kirsten Peter Bergakad, Freigakad, "Theoretische Untersuchung Der Erzeugenen Schwingungen Von Systemen Mit Unsymmetrishchen Stueckweis-Linearen Kennlinien (Theoretical Study of Forced Vibrations In Systems with Unsymmetric Piecewise Linear Characteristics)", E. Ger Pol Acad-Sc Inst. Fundam Tech Res Nonlinear Vib. Probl, Vol. 14, 1973, pp 159-167.
43. Kline, S.J. and McClintock, F.A., "Describing Uncertainties in Single-Sample Experiments", A.S.M.E. Mechanical Engineering, Vol. 75, January 1953, pp 3-8.
44. Klotter, K., "Nonlinear Vibrations Treated by the Averaging Method of W. Ritz", Stanford University.
45. Klotter, K. "Nonlinear Vibration Problems Treated by the Averaging Method of W. Ritz", N6-Onr-251, Task Order 2, Technical Report No. 17, Part I, Part II, Stanford University.
46. Klotter, K., and Cobb, P.R., "Nonlinear Vibration Problems Treated by the Ritz Averaging Method", Technical Report 109, Division of the Engineering Mechanics, Stanford University, 1957.
47. Klotter, K. and Cobb, P.R., "On Use of Non-Sinusoidal Approximating Functions for the Nonlinear Oscillations Problems", A.S.M.E., Trans. Journal of Applied Mechanics, Vol. 27, Series E, n 3 , September 1960.
48. Klotter and Pinney, "A Comprehensive Stability Criterion for Forced Vibrations in Nonlinear Systems", Journal of Applied Mechanics, March 1953.

49. Korn, G.A. and Korn, T.M., "Electronic Analog Computers", 1956, McGraw Hill, New York,.
50. Lemon, J., "Etude Graphique des vibrations de systems a unseul degre de liberte", Revue Universalle de Mines, Liege 8 series T, XI no. 7 (mai 1935)",
Surla Sollicitation dynamique des edifices elances parelevent", Proc. Roy. Acad. de Belge, T. XII (1932),
51. Levenson, M.E., "A Numerical Determination of Subharmonic Response for the Duffing Equation", Quart. of App. Maths., 25; April 1957, pp 11-17.
52. Levenson, M.E. "Harmonic and Subharmonic Response for the Duffing Equation", Thesis, New York University, 1948.
53. Loud, W.S., "Branching Phenomena for Periodic Solution of Non-Antononomous Piecewise Linear System", Int. Journal of Nonlinear Mechanics, Vol. 3, 1968, pp 273-293.
54. Ludeke, C.A., "Predominantly Subharmonic Oscillations", Journal of Applied Physics, Vol. 22, 1951, pp 1321-1326.
55. Maezawa, S., "Steady Forced Vibrations of Unsymmetrical Piecewise Linear Systems", 1st Report, Explanation of Analytical Procedure, Bull. of J.S.M.E., Vol. 4, No. 14, 1961, pp 201-229. 2nd Report, Comparison with Analog Computer Experiments. 3rd Report, Application to the Ultrasonic Carving Machine.

56. Maezawa, S., "Perfect Fourier Series Solution for Subharmonic Vibration of Piecewise Linear System", Polaska Akadema Nauk Instytut Podstawowych-Problenow Techniki-Zaklad Badania Dragon, No. 5, 1963, pp 156-164.
57. Mawzawa, S., "Superharmonic Resonance in Piecewise Linear System (Effect of Damping and Stability Problem)", Bull. of J.S.M.E., Vol. 16, No. 96, June 1973.
58. Maezawa, S., "Superharmonic Resonance in a Piecewise Linear System", Acta Technica CSAV, 12, 1, 1967, pp 1-12.
59. Maezawa, S., "Steady Impact Vibrations in Mechanical Systems, with Brokenline Collision Characteristics", Yamanashi Univ. Kofu, Japan; Watanabe Takashi Pol Acad. Sci.; Inst. Fundam Tech Res. Nonlinear Vib. Probl, Vol. 14, 1973, pp 473-500.
60. Maezawa, S., "Stability of Forced Vibration in Unsymmetrical Piecewise Linear System", Macanica Technica.
61. Maezawa, S., "Subharmonic Resonance of Mechanical System with a Brokenline Characteristic", Report of the Institute of Thermomechanics CSAV, Prague, 1969.
62. Maezawa, S. and Kumano, H., "Forced Vibration in an Unsymmetric Piecewise-Linear System Excited by General Periodic Force Functions", Bulletin of the J.S.M.E., Vol. 23, No. 175, January 1980.
63. Mahalingam, S., "Forced Vibration of Systems with Non-symmetrical Characteristics", Journal of Applied Mechanics, Sept. 1957.

64. Mamaev, K.M., "Investigation of the Dynamics of Toothed Transmission, using an Electronic Model", Mashinovedenie, No. 6, pp 54-58, 1966, RZM No. 4, 1967, Rev. 4A 206.
65. Masri, S.F., "Forced Vibration of the Damped Bilinear Hysteretic Oscillator"; J. Acous. Soc. Am., Vol. 57, No. 1, Jan. 1975.
66. Masri, S.F., "Electric-analog Study of Impact Dampers", Experimental Mechanics, Feb. 1967, pp 49-55.
67. Matkowsky, B.J., Rogers, E.H. and Rubenfield, L.A., "Generation and Stability of Subharmonic and Modulated Subharmonic Oscillations in Nonlinear Systems", Quart. of App. Maths., Vol. xxx, October 1972, No. 3.
68. Minorsky, N., "Nonlinear Oscillations", Van Nostrand, 1962.
69. Mitropolsky, U.A., "Averaging Method in Nonlinear Mechanics", Institute of Nonlinear Mechanics, Vol. 2, 1967, pp 69-96.
70. Nguyen Van Das, "Interaction of Subharmonic Oscillations", J. Tech Phys., Vol. 6, No. 2, 1975, pp 227-237.
71. Paslay, P.R., and Gurtin, N.E., "The Vibration Response of a Linear Undamped System Resting on a Nonlinear Spring", Journal of App. Mechanics, Trans. A.S.M.E. 1960, pp 272-274.
72. Pipes, L.A., "Applied Mathematics for Engineers and Physicists", McGraw-Hill, 1958.

73. Porter, B., and Billett, R.A., "Harmonic and Subharmonic Vibrations of Continuous System Having Nonlinear Constraints", Int. Journal of Mech. Sciences, Vol 7, No. 6, 1965, pp 431-439.
74. Pust, L., "Subharmonic Vibrations of Strongly Nonlinear Mechanical Systems", Revue Roumaine des Sciences Techniques Seriede Mechnique Applique, 16, 1, 1971, pp 91-100.
75. Rauser, M., "Steady Oscillations of Systems with Nonlinear and Unsymmetrical Elasticity", Journal of Applied Mechanics, Vol. 60, 1938, pp A 169-A 177.
76. Reif, Z.F., "Approximate Methods for the Solution of Non-linear Vibration Equations", Bull. Mech. Eng. Educ., Vol. 9, 1970, pp 231-234.
77. Reif, Z.F., "Subharmonic Response of Order $1/2$ with an Asymmetrical Restoring Force", Aeronautical Journal, February 1973, pp 98-101.
78. Reif, Z.F., and Carnegie, W., "Ultraharmonic Resonance of a System with an Asymmetrical Restoring Force Characteristics", Journal of Mechanical Engineering Science, Vol. 11, No. 6, 1969, pp 592-597.
79. Riganti, R., "Subharmonic Solutions of the Duffing Equation with Large Non-linearity", Int. J. Non-linear Mechanics, Vol. 13, 1978, pp 21-31.
80. Rosenberg, R.M., "On the Periodic Solutions of the Forced Oscillator Equation", Quart. of App. Maths, Vol. XV, No. 4, January 1958, pp 341-354.

81. Schweisinger, G. and Manmouh, F., "On One Term Approximations of Forced Non-harmonic Vibrations", Journal of Applied Mechanics, June 1950, pp 202-208.
82. Silverman, S.M., "On Forced Pseudo Harmonic Vibrations", Journal of Franklin Institute, Vol. 217, 1934.
83. Stoker, J.J., "Nonlinear Vibrations in Mechanical and Electrical Systems", 1950. Interscience Publishers, New York and London.
84. Timoshenko, S., "Vibration Problems in Engineering", D. Van Nostrand, Co., 3rd Edition, New York, 1955.
85. Thomas J. and Tondl, A., "On the Existence of Subultra-harmonic Resonance of a Single Mass Non-linear System Excited by Periodic Force", Nonlinear Vibration Problems, Warsaw, Vol. 8, 00 11-22.
- 86.. Thrasher, L.W. and Binder, R.C., "A Practical Application of Uncertainty Calculations to Measured Data", Trans. of the A.S.M.E., February 1957, pp 373-376.
87. Tomas, J. "Ultra Subharmonic Resonance in a Duffing System", Int. Journal of Nonlinear Mechanics, Oct. 1971, pp 625, 631.
88. Tondl, A., "Notes on the Identification of Subharmonic Resonances of Rotors", Journal of Sound & Vibration 31, 1, Nov. 1973, pp 119-127.

89. Tseng, W.Y. and Dugundji, J., "Nonlinear Vibrations of a Beam Under Harmonic Excitation", A.S.M.E. Paper 70-WA/APM-13.
90. Tsuda, K., "On the Vibration of a Power Transmission System Having Angular Clearances", Part I, II, III and IV. Bull. of J.S.M.E., Vol. 2, No. 6, 1959, pp 324-348.
91. Vajtasek, S., "Some Non-Autonomous Systems with Piecewise Linear Characteristics", Acta Technica CSAV, 18, 7, 1973, pp 103-110.
92. Wilie, C.R., "On the Forced Vibrations of Nonlinear Springs", Journal of Franklin Institute, Vol 236, 1943, pp 273-281.
93. Yeh, H.Y. and Yao, J.T.P., "Response of Bilinear System to Earthquake Loads", A.S.M.E., 69-VIBR-20.
94. Zahradka, J., "Torsional Vibrations of a Nonlinear Driving System with Cardan Shafts", Journal of Sound and Vibration, 26, 4, February 1973, pp 533-550.
95. System/360 Continuous System Modeling Program (360-CS-16X) Users Manual", (H20-0367-3) I.B.M. Corp., White Plains, New York 1967.

96. E.A.I. Handbook of Analog Computation.

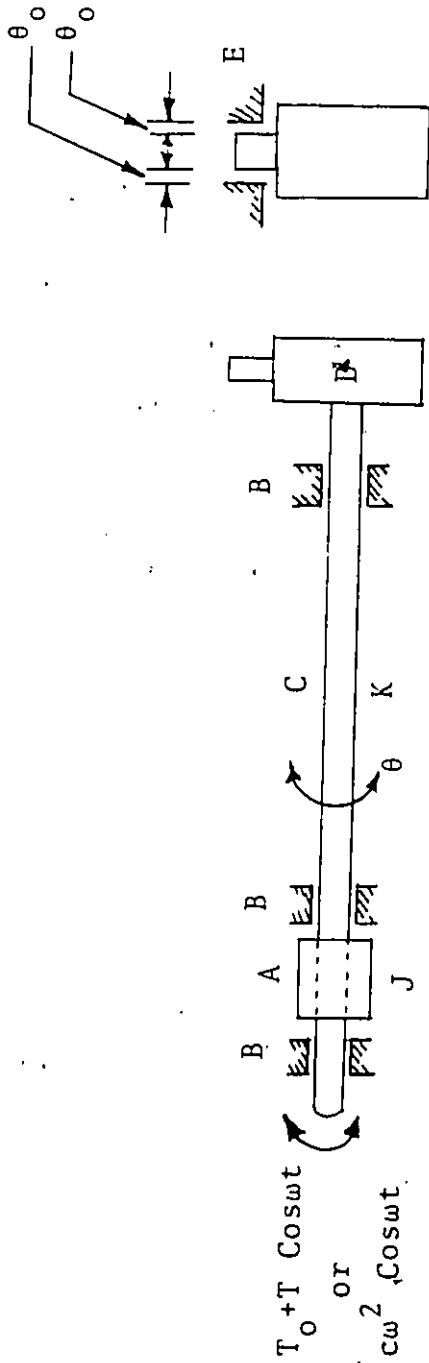


Figure 3.1.1.1a. Representation of a Bilinear System

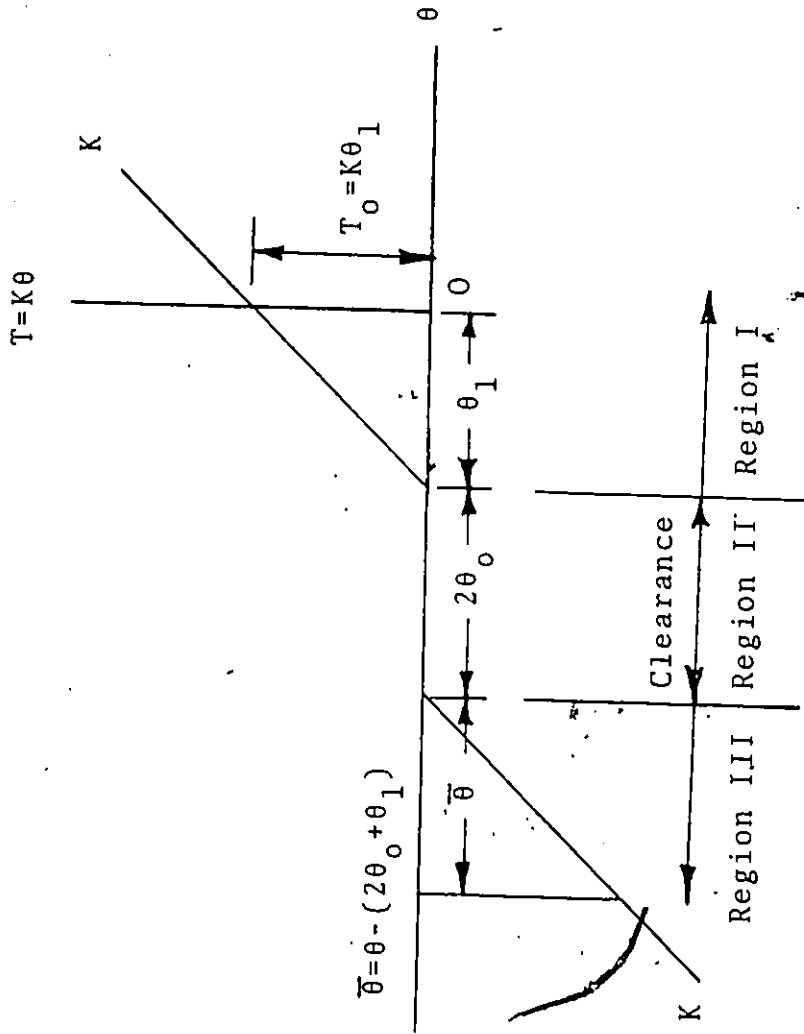


Figure 3.1.1.1b Restoring Force Characteristics of a Bilinear System (Asymmetrical)

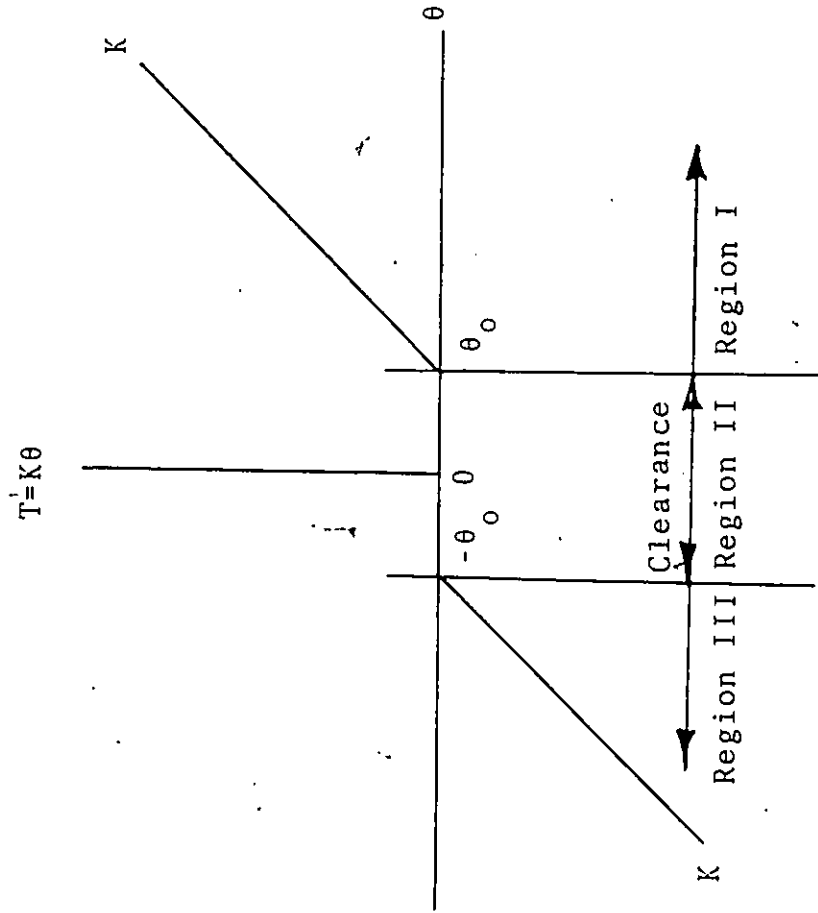


Figure 3.1.1.1.c Restoring Force Characteristics of a Symmetrical Bilinear System

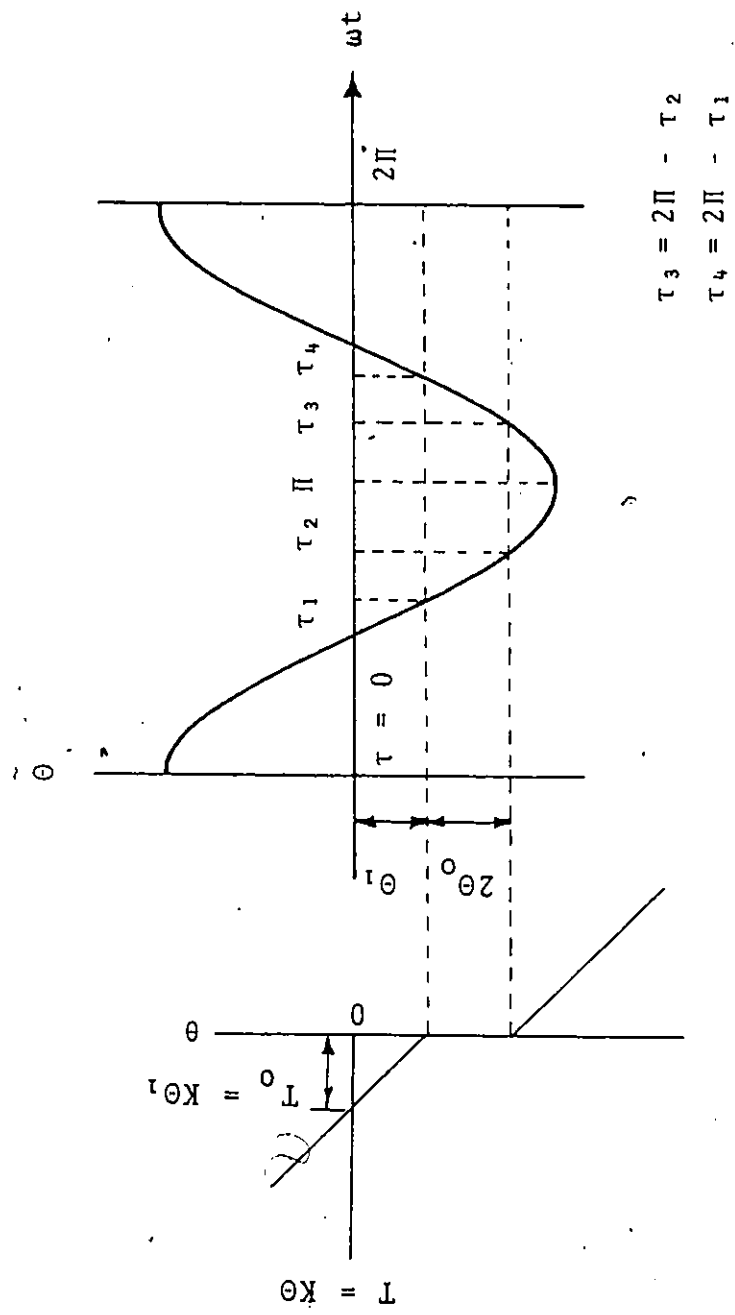


Figure 3.1.1.2 Amplitude Versus Angular Displacement Plot (Asymmetrical System). Harmonic Resonance.

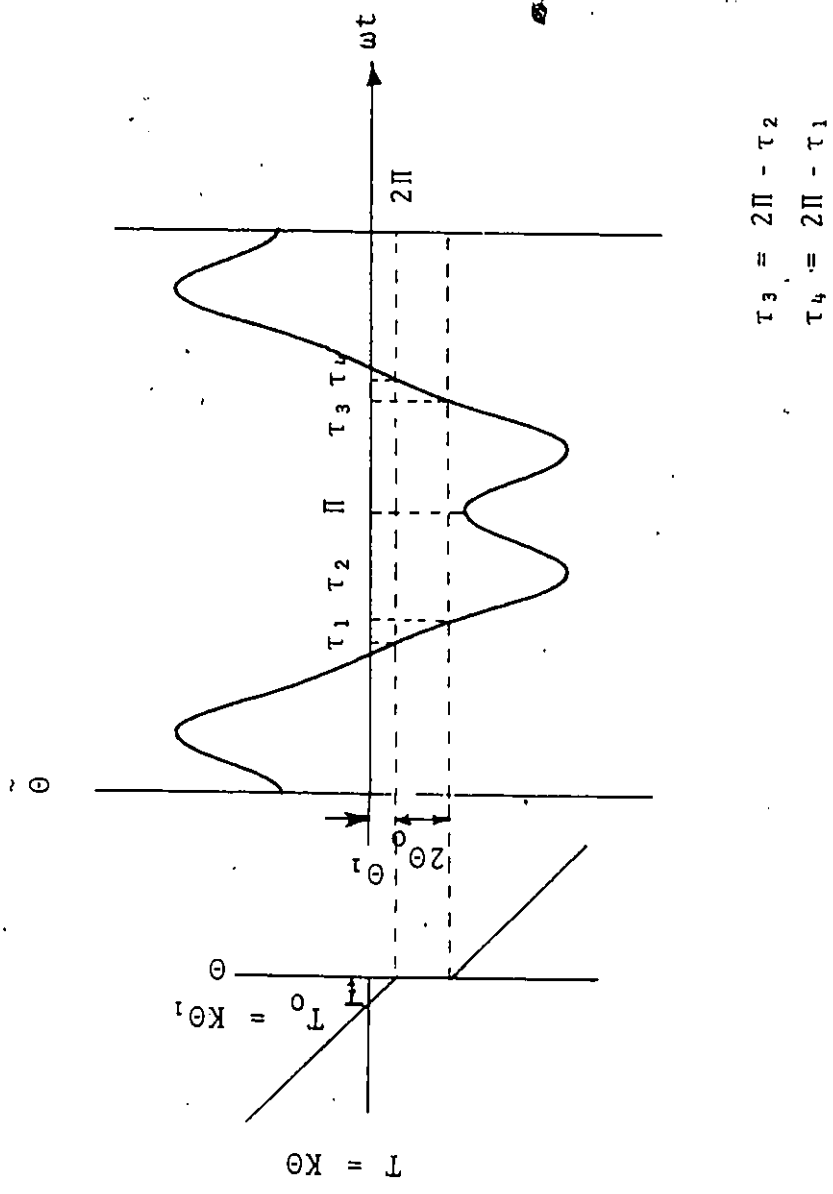


Figure 3.1.2.1 Amplitude Versus Angular Displacement Plot (Asymmetrical System). 3rd Order Ultraharmonic Resonance.

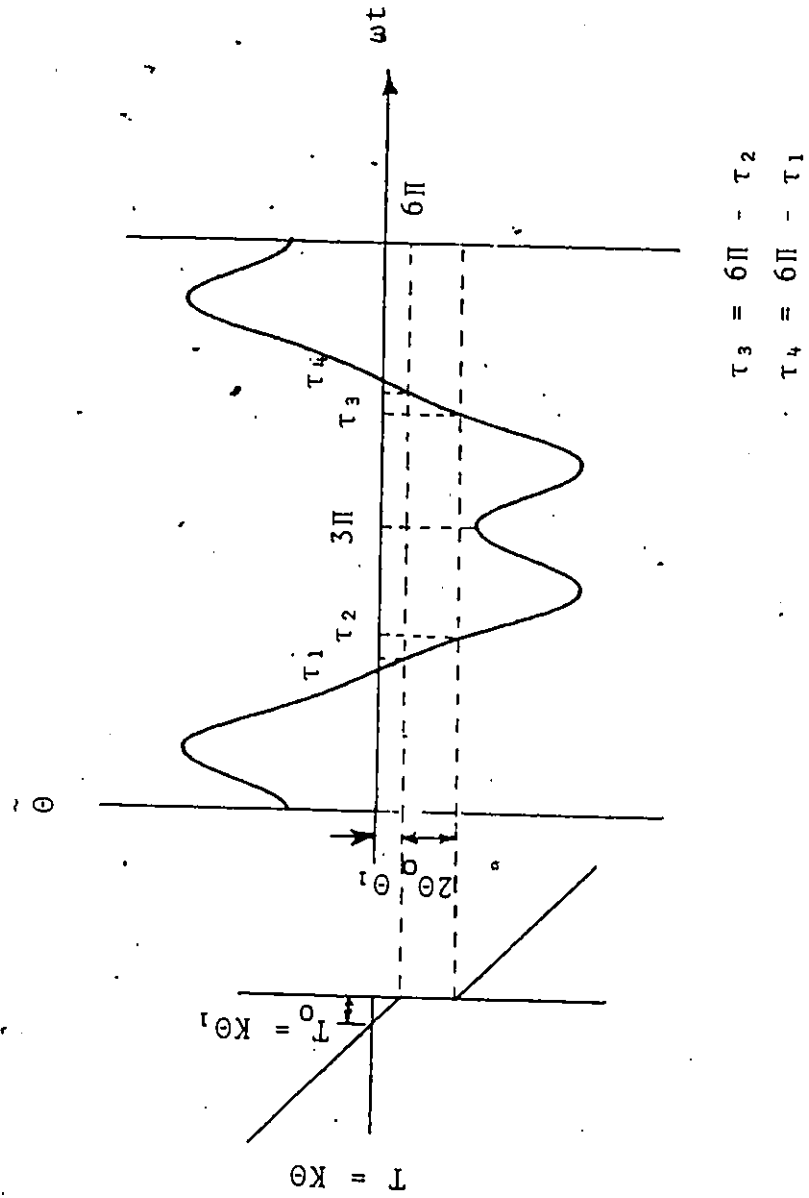


Figure 3.1.1.3.1. Amplitude Versus Angular Displacement Plot (Asymmetrical System). 1/3rd Order Subharmonic Resonance.

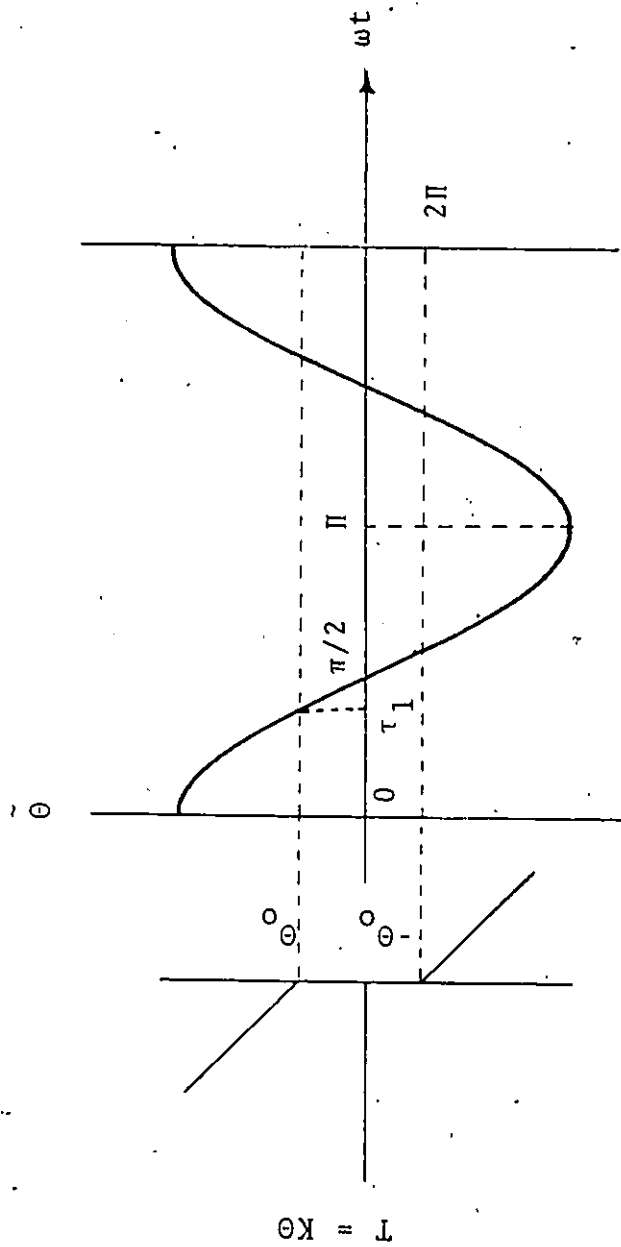


Figure 3.2.1.1.2 Amplitude Versus Angular Displacement Plot (Symmetrical System). Harmonic Resonance.

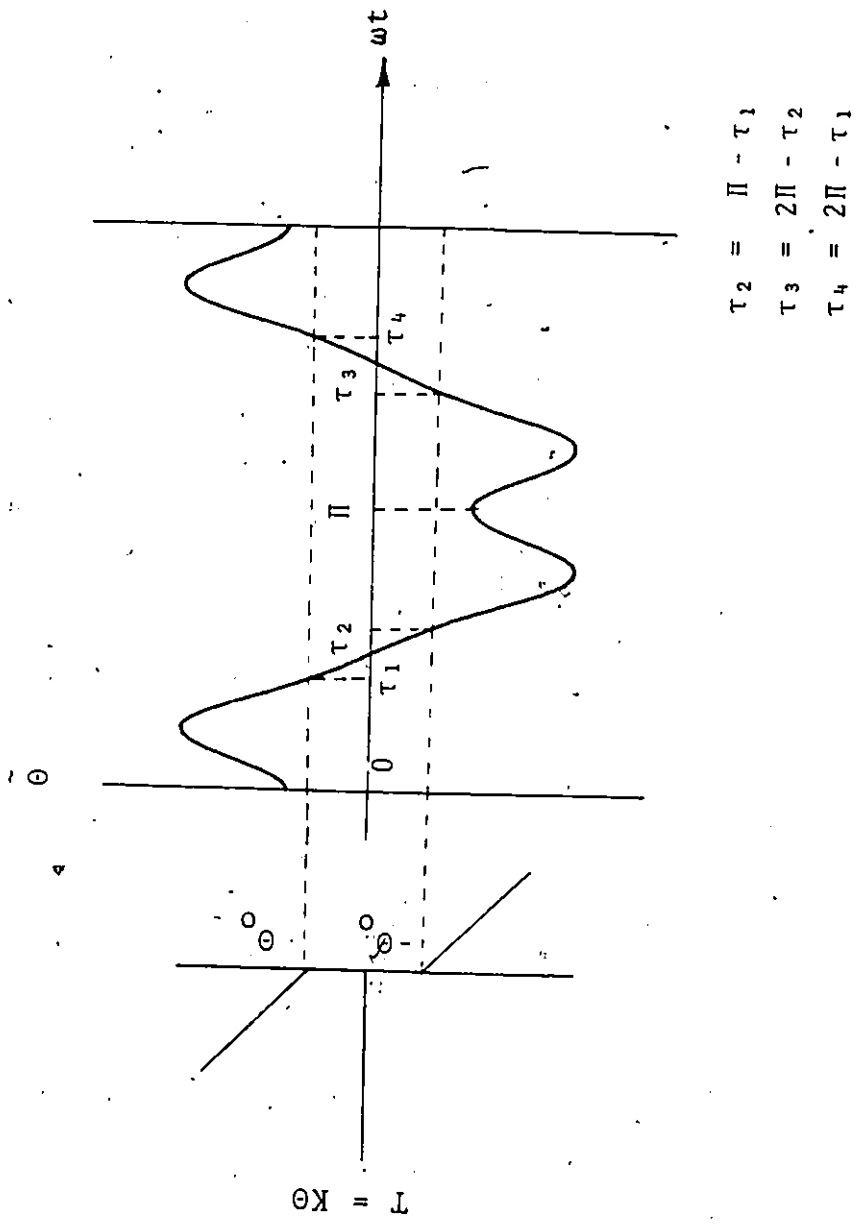


Figure 3.2.2.1 Amplitude Versus Angular Displacement Plot (Symmetrical System). 3rd Order Ultraharmonic Resonance.

Machine Equation $\ddot{\theta} + p^2 f(\theta) = T(t)$ or $\ddot{\theta} = -p^2 f(\theta) + T(t)$

$T(t) = T_0 + T \cos \omega t$

$f(\theta) = C \omega^2 \cos \omega t$
 Bilinear restoring force characteristics

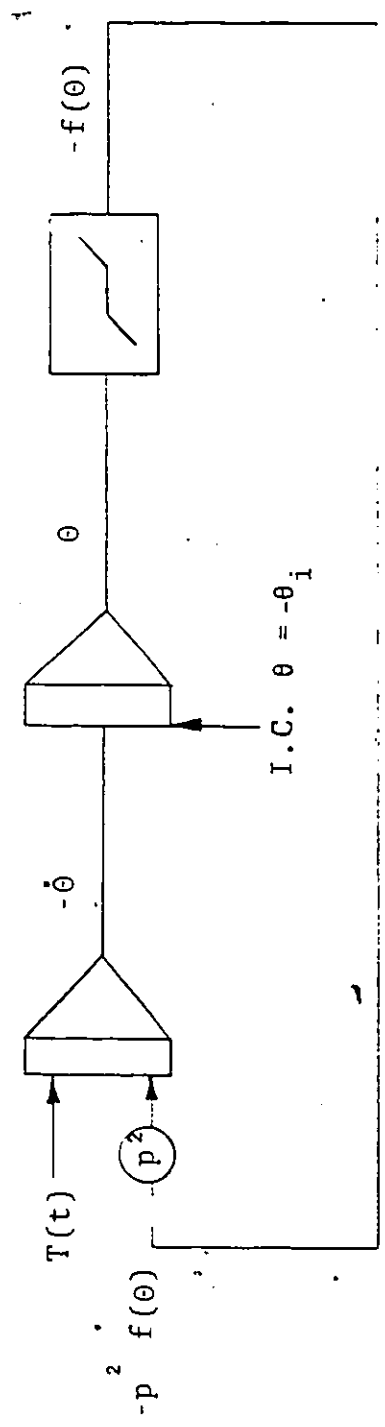


Figure 4.1.1.1 Generalized Analog Computer Circuit Diagram

Symbols Definition

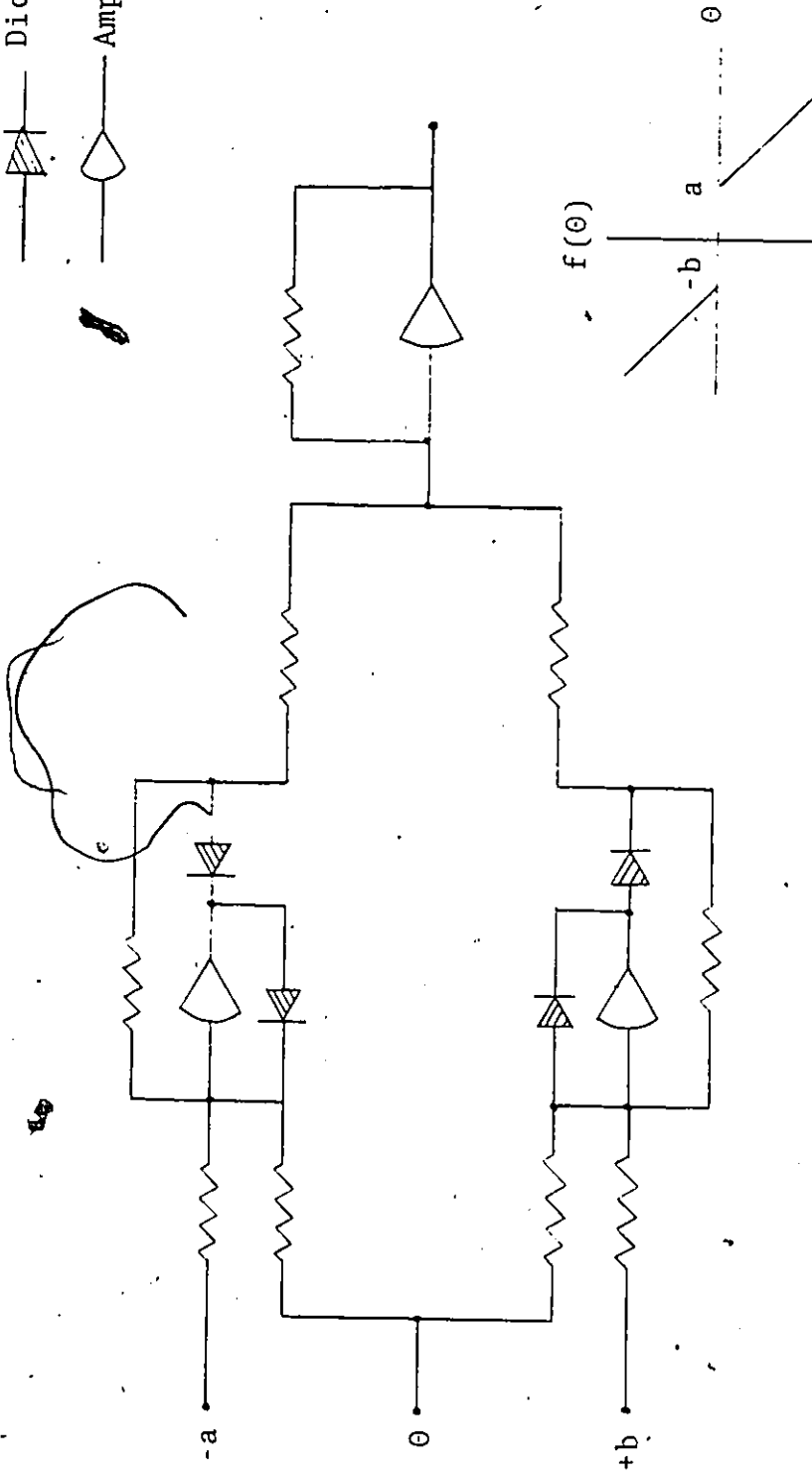
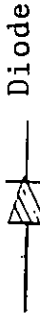


Figure 4.1.1.2 Circuit Diagram for the Bilinear Restoring Force Characteristics

Equation of undamped free vibrations is given by --

$$\ddot{z} + \omega^2 z = 0$$

Solution of above equation is given by --

$$z = A \cos \omega t + B \sin \omega t \quad t = 0, \dot{z} = 0, z = z_0$$

$$z = z_0 \cos \omega t$$

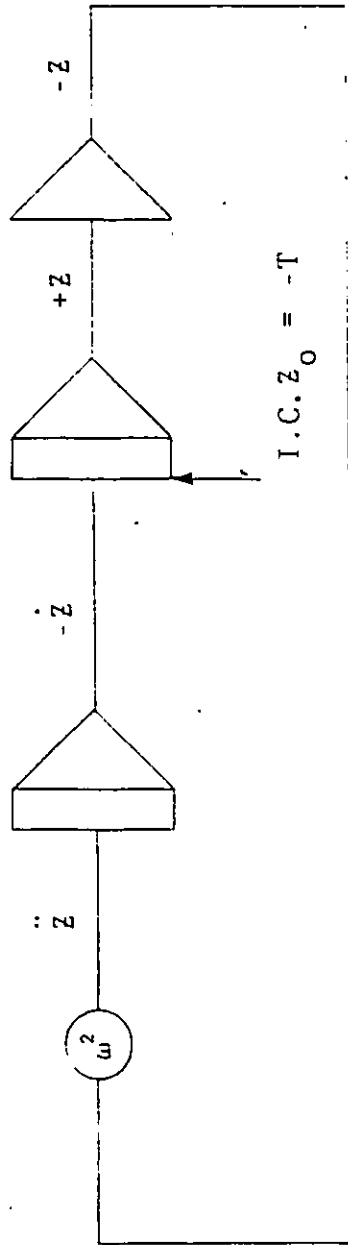


Figure 4.1.1.3 Generation of $T \cos \omega t$

$$\ddot{Z} + \omega^2 Z = 0$$

$\ddot{Z} = -\omega^2 Z$ Machine Equation

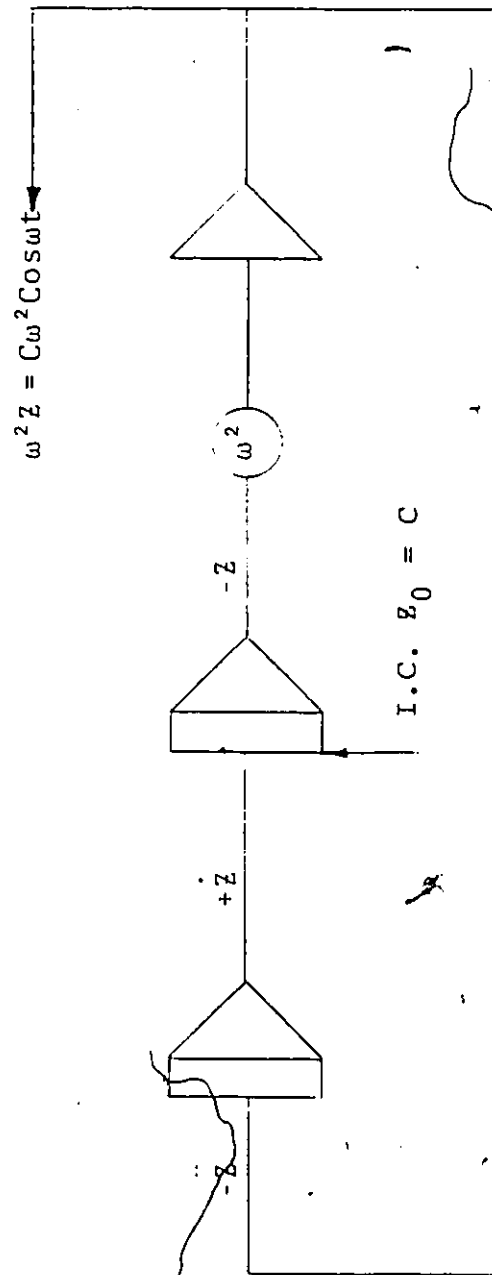
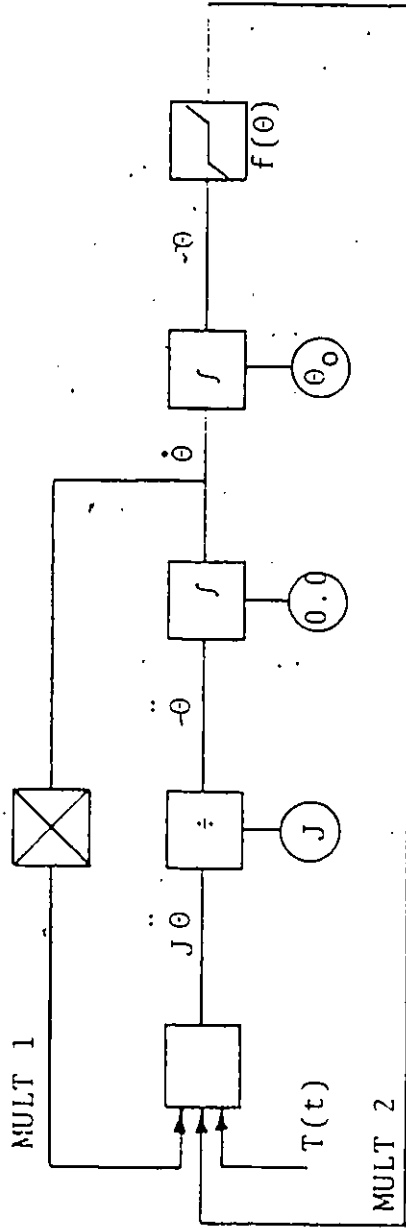


Figure 4.1.1.4 Generation of $C\omega^2 \cos \omega t$



STRUCTURAL STATEMENTS

$$TH2DOT = (MULT1 + MULT2 = T(t))/J$$

$$THDOT = INTGRL (IC1, TH2DOT)$$

$$MULT1 = -C * THDOT$$

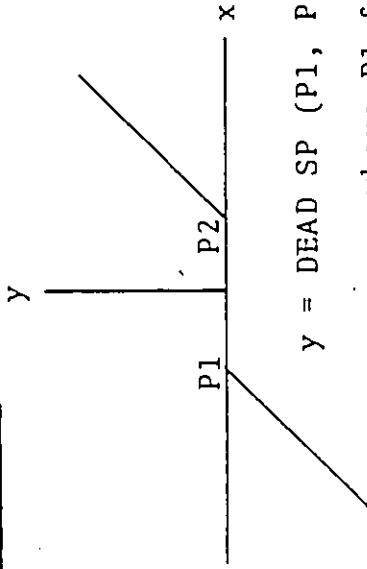
$$THETA = INTGRL (IC2, THDOT)$$

$$MULT2 = -DEADSP (p1, P2, THETA)$$

$$T(t) = T * SINE (0, \omega, PI/2)$$

Figure 4.1.2.1 Block Diagram and Structural Statements for a Bilinear System

a. Generation of Deadspace



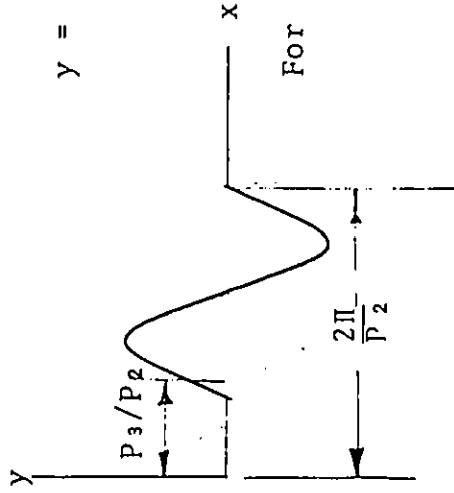
$y = \text{DEAD SP (P1, P2, x)}$

where P1 & P2 are dead spaces

x - Input

y - Output

b. Generation of Sinusoidal Function



$y = \text{SINE (P1, P2, P3)}$ where P1 = Delay

P2 = Frequency

P3 = Phase shift in radians.

For cosine function, P3 = $\pi/2$, P1 = 0

Figure 4.1.2.2 Function Generation Capabilities in CSMP Technique

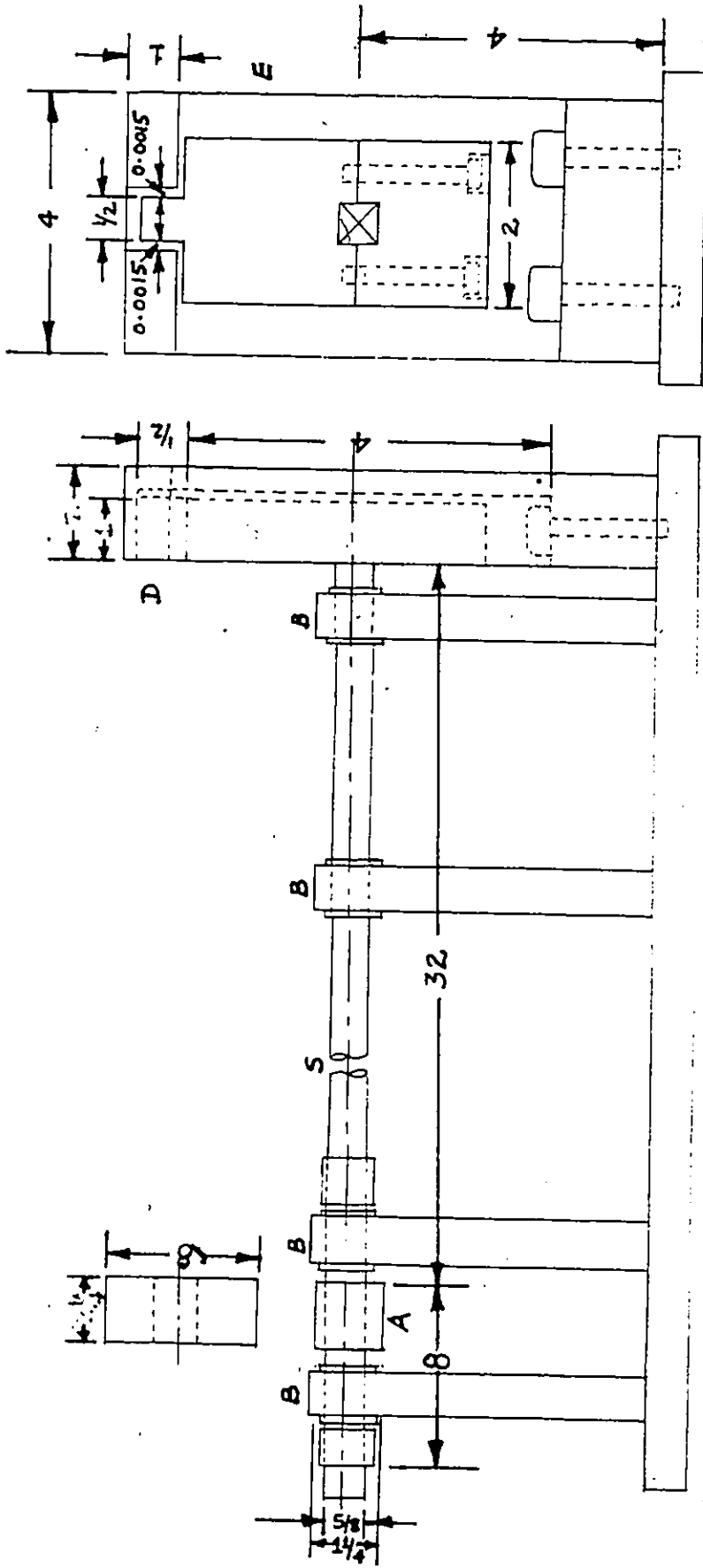


Figure 4.2.1.1 Design Details of the Mechanical Model

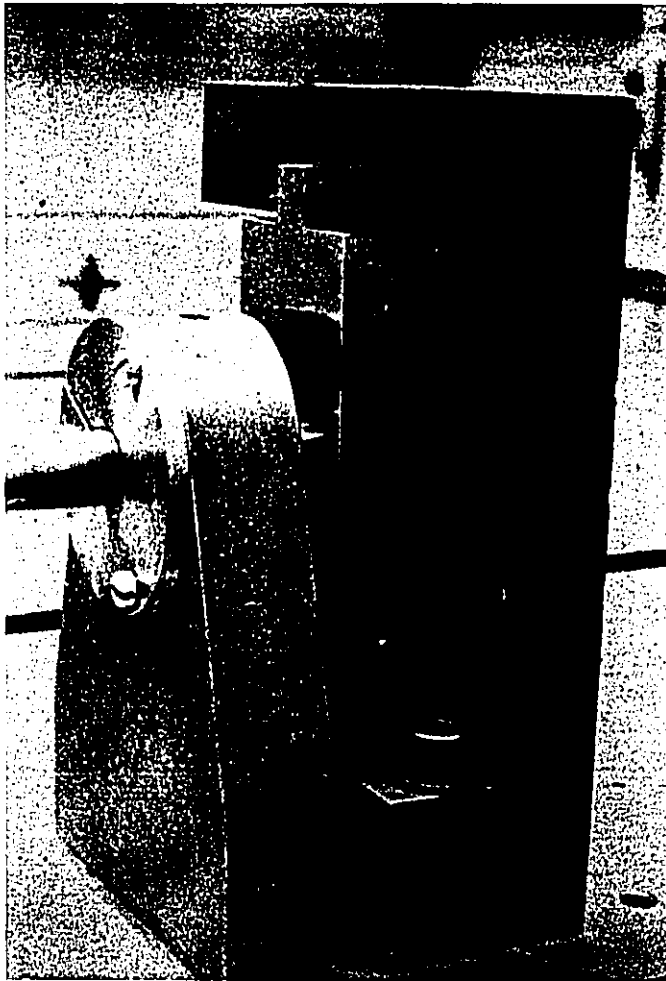


Figure 4.2.1.2 Tooth Block Assembly

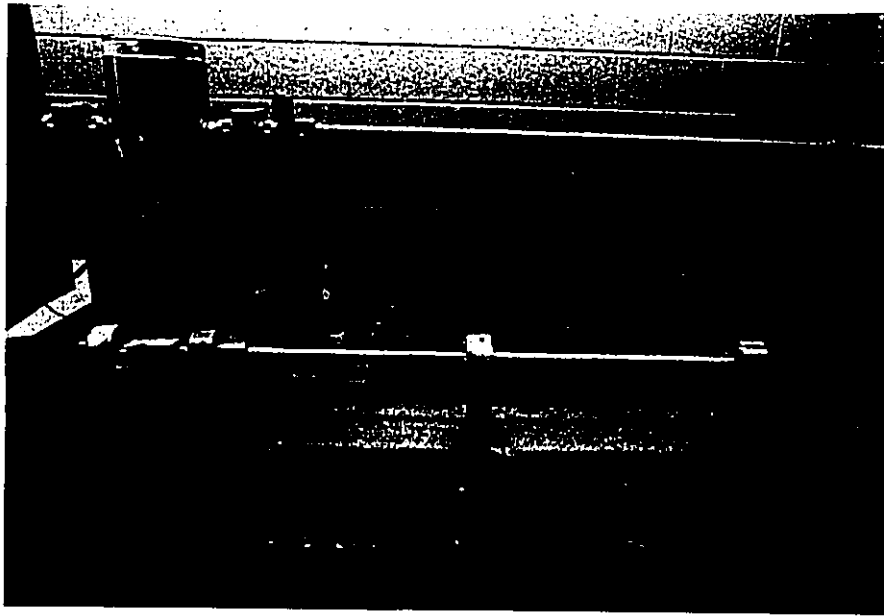


Figure 4.2.1.3 Overall View of the Experimental Set Up

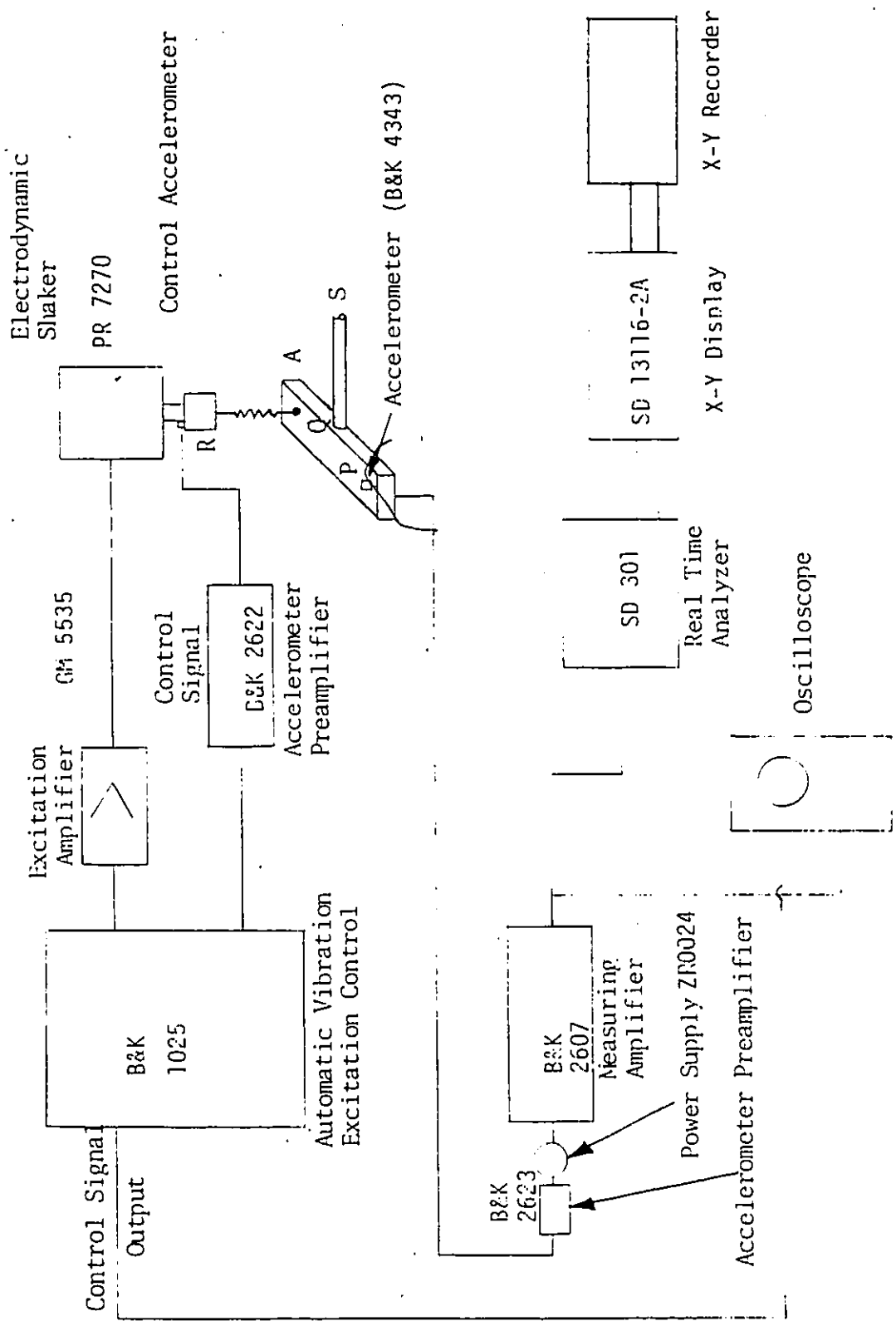


Figure 4.2.2.1 Schematic Diagram of Experimental Set Up

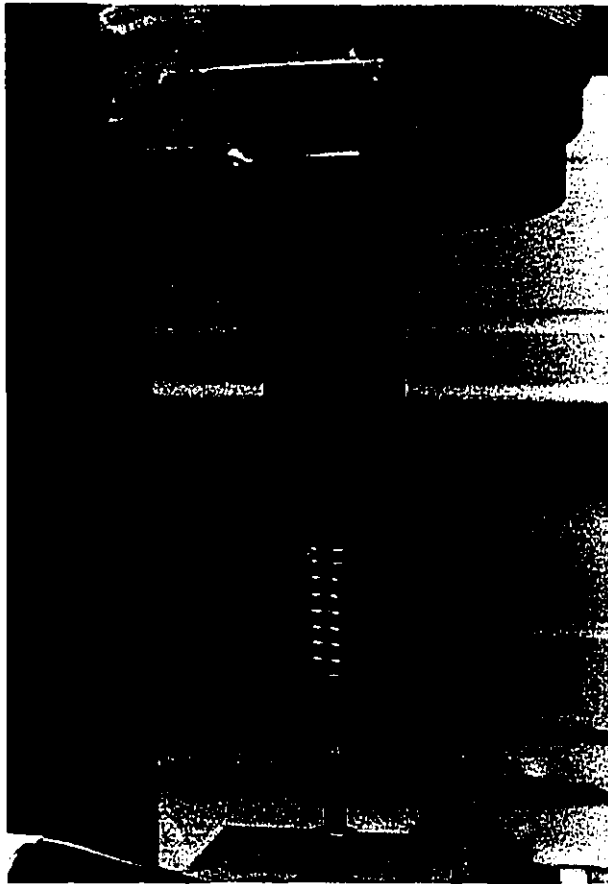


Figure 4.2.3.1 View Showing Shaker Pin
Attachment to the Vibrating
Arm 'A' and Control Acceler-
ometer

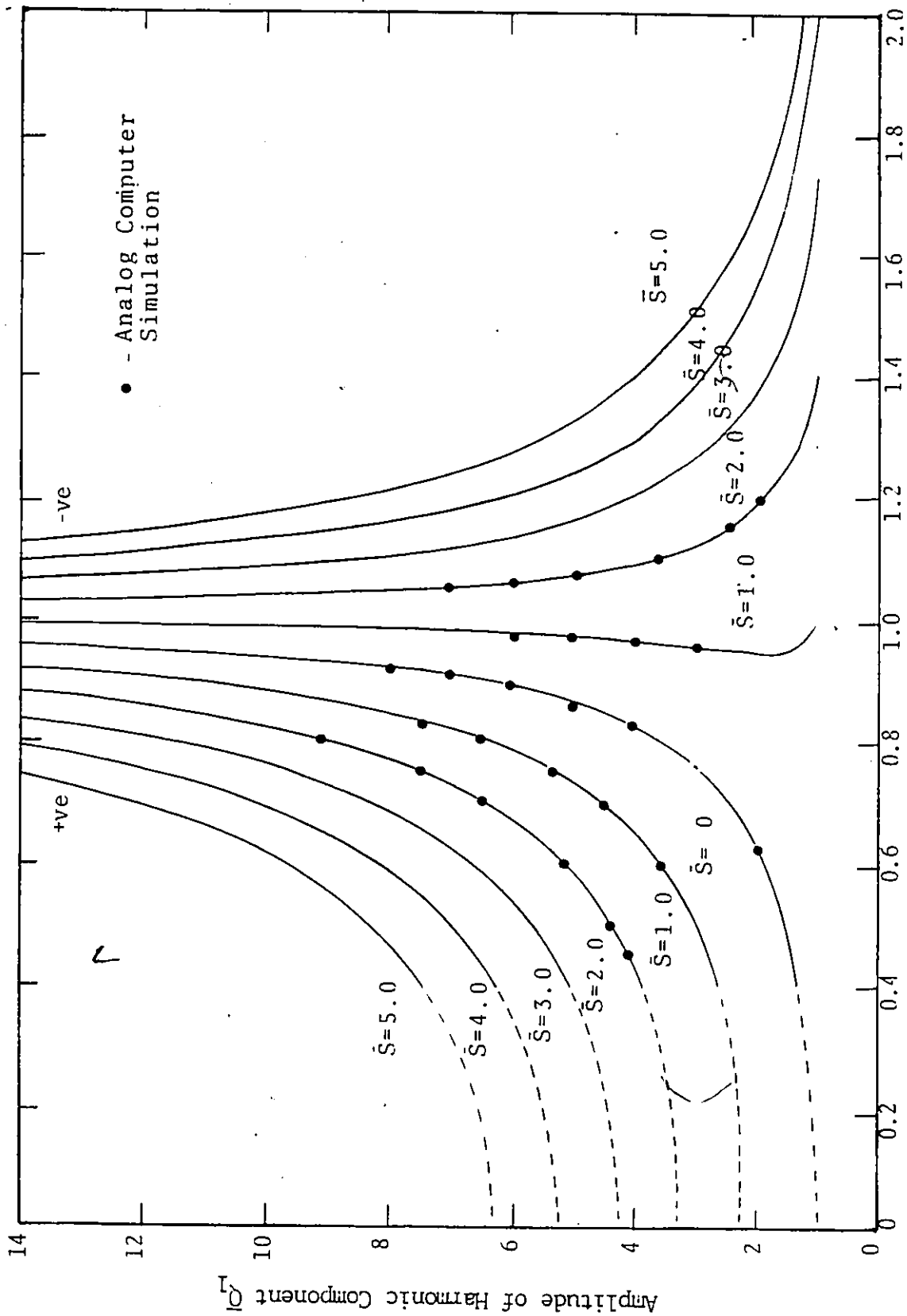


Figure 5.1.1 Harmonic Resonance Response for the Symmetrical System ($\phi_1=0$) Disturbing Torque = $T \cos \omega t$. Plot Q_1 Vs n .

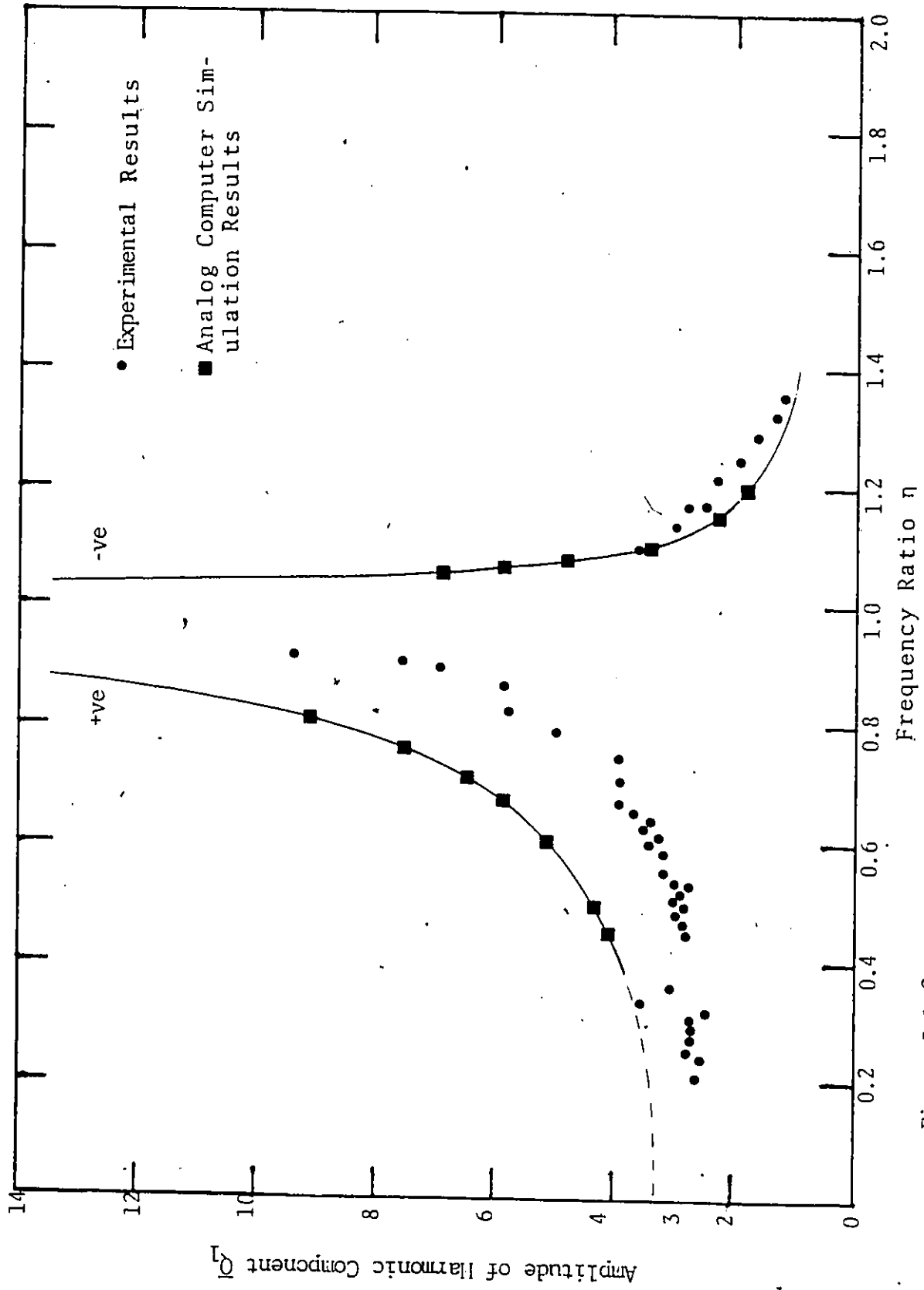


Figure 5.1.1.2 Harmonic Resonance Response for Asymmetrical System ($\theta_1 = 0.05, S = 2.0$)
Disturbing Torque = $T \cos \omega t$. Plot Q_1 Vs. η .

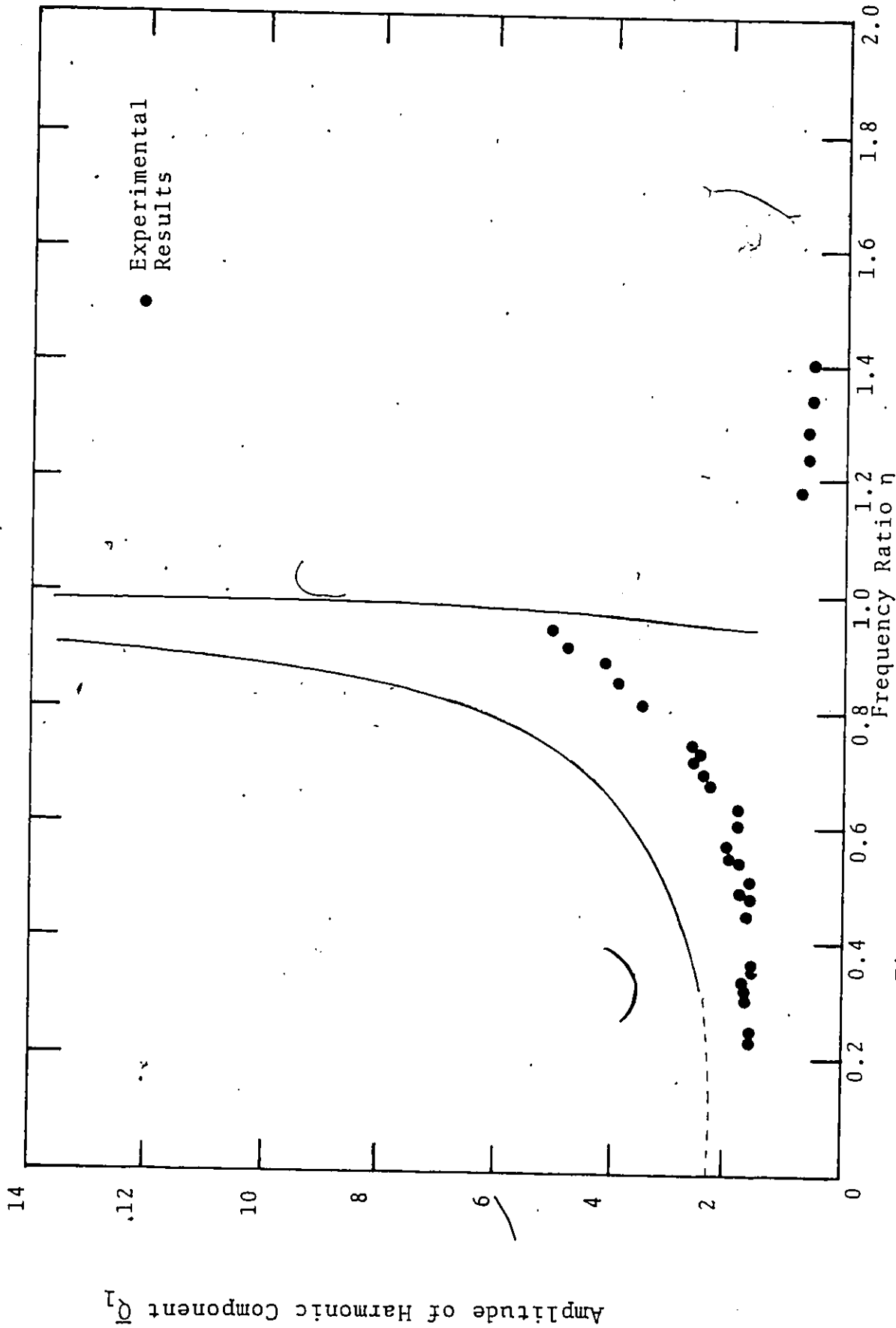


Figure 5.1.3 Harmonic Resonance Response for Asymmetrical System ($\bar{\theta}_1=0.05, \bar{S}=1.0$) Disturbing Torque = $T \cos \omega t$. Plot Q_1 Vs η .

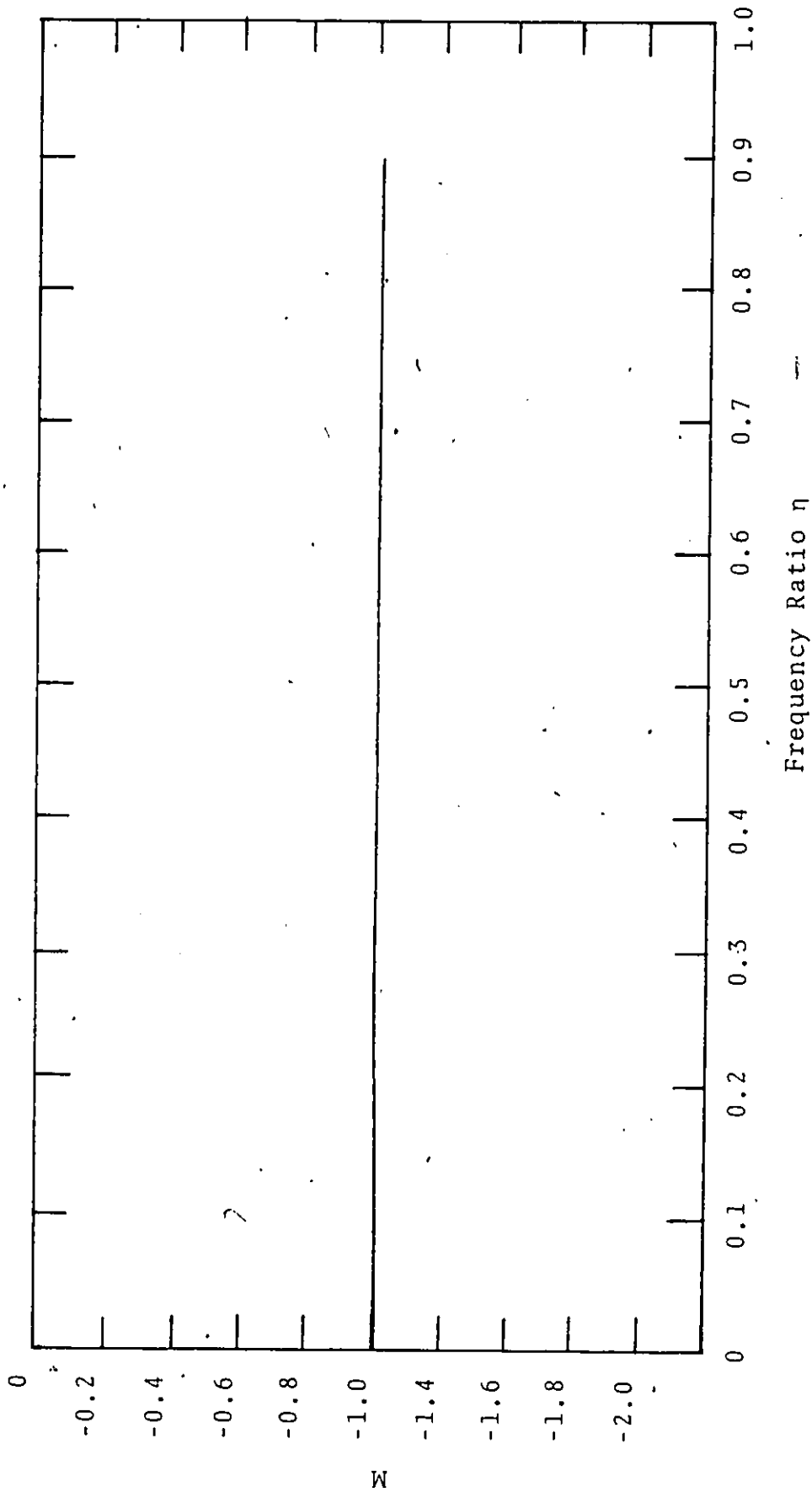


Figure 5.1.4 Harmonic Resonance Response for Asymmetrical System ($\bar{\theta}_1=0.05, \bar{S}=1.0$)
 Disturbing Torque = $T \cos \omega t$, Plot M Vs η .

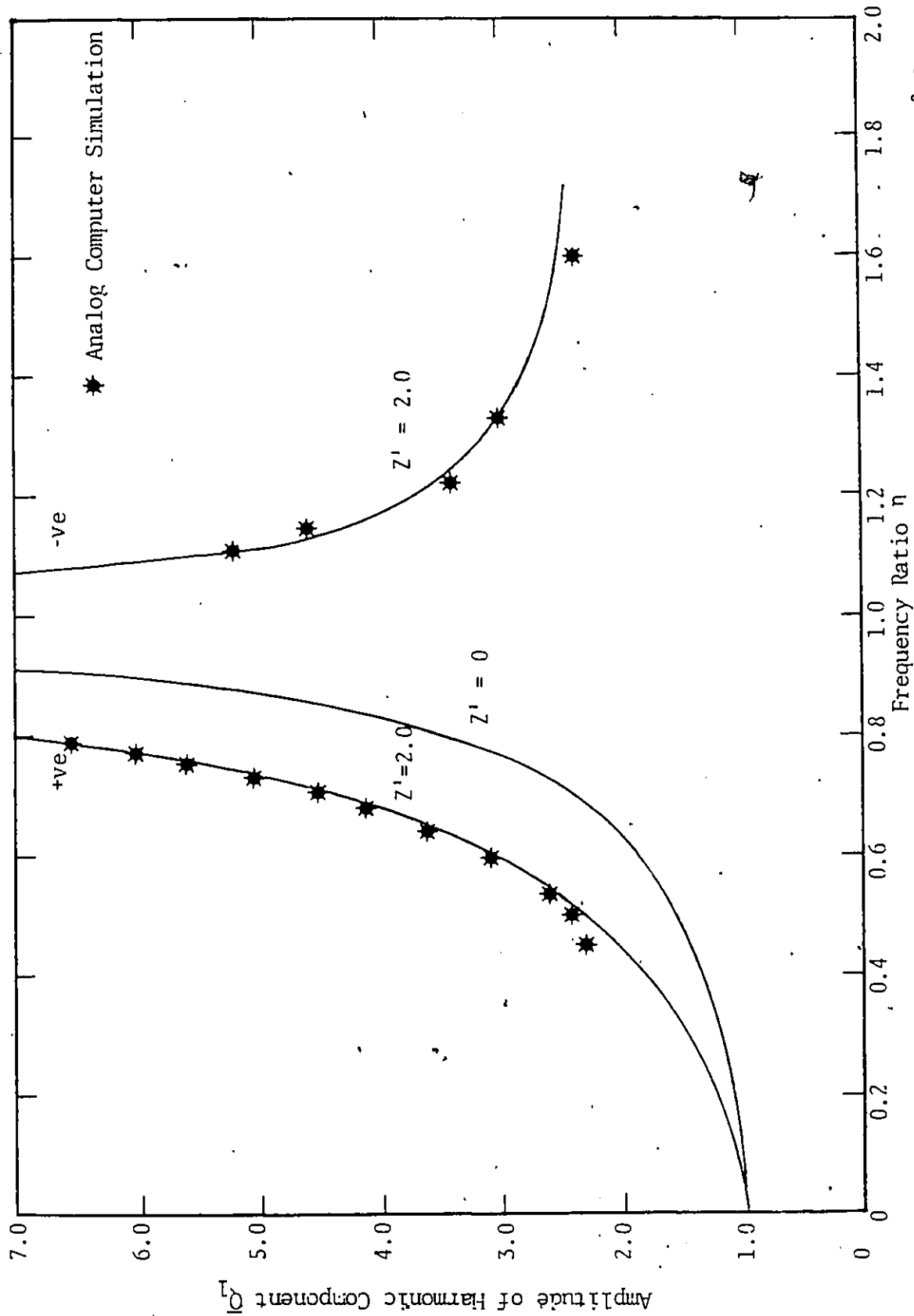


Figure 5.1.5 Harmonic Resonance Response for Symmetrical System. Disturbing Torque = $C \omega^2 \cos \omega t$. Plot Q_1 Vs η .

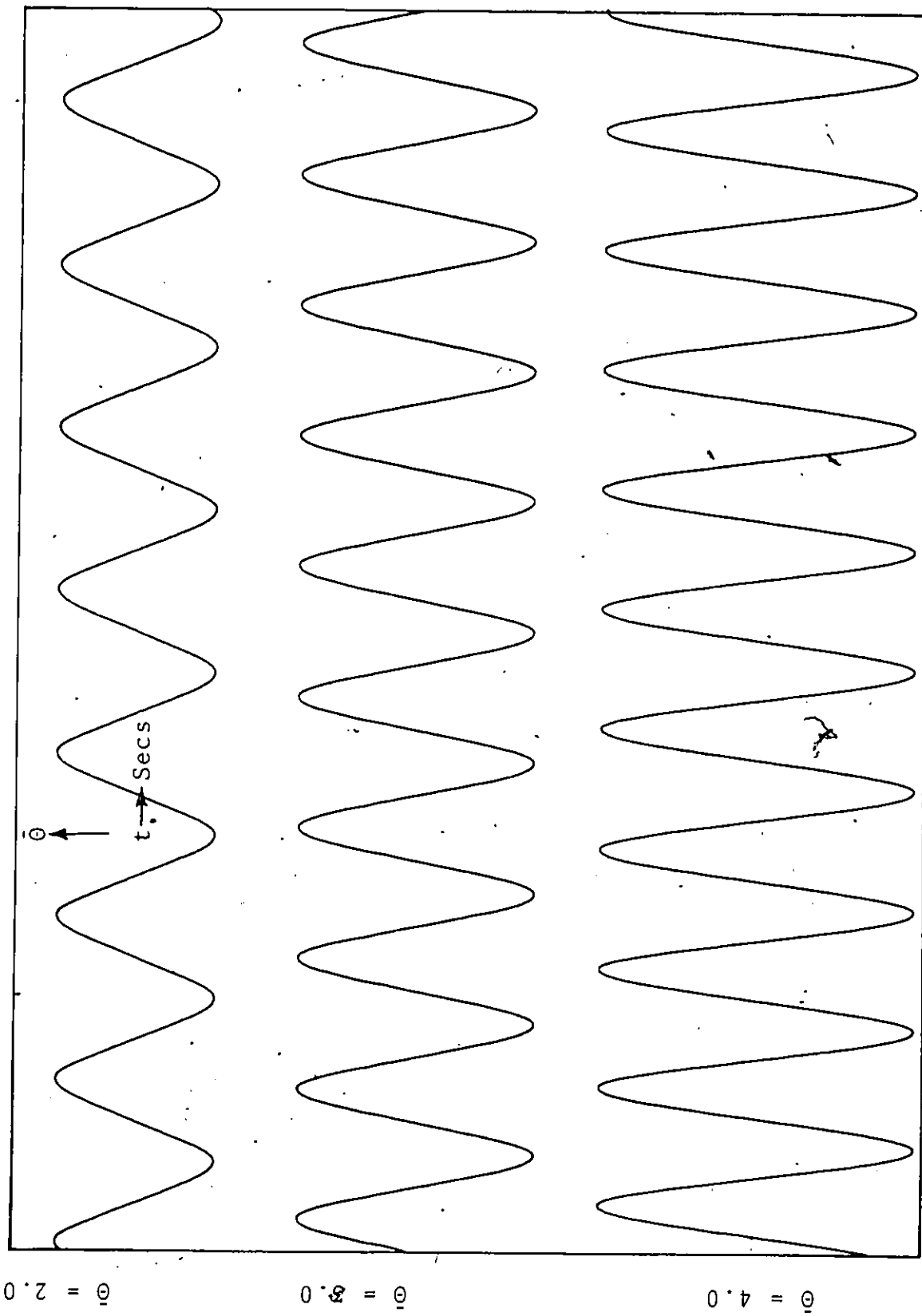


Figure 5.1.6 Analog Computer Output, Free Vibration Response ($\bar{S}=0$)
 Disturbing Torque = $\bar{T} \cos \omega t$

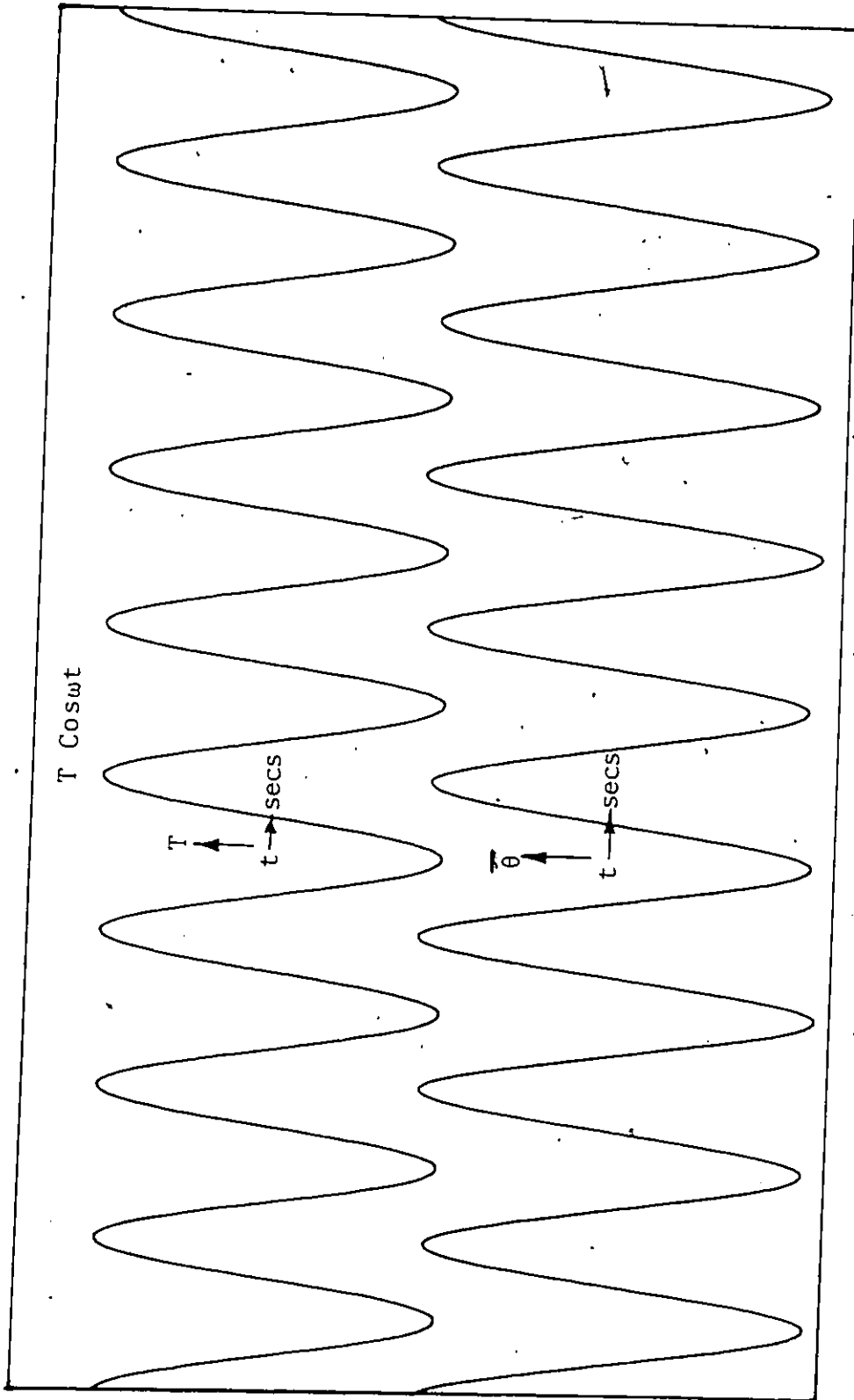
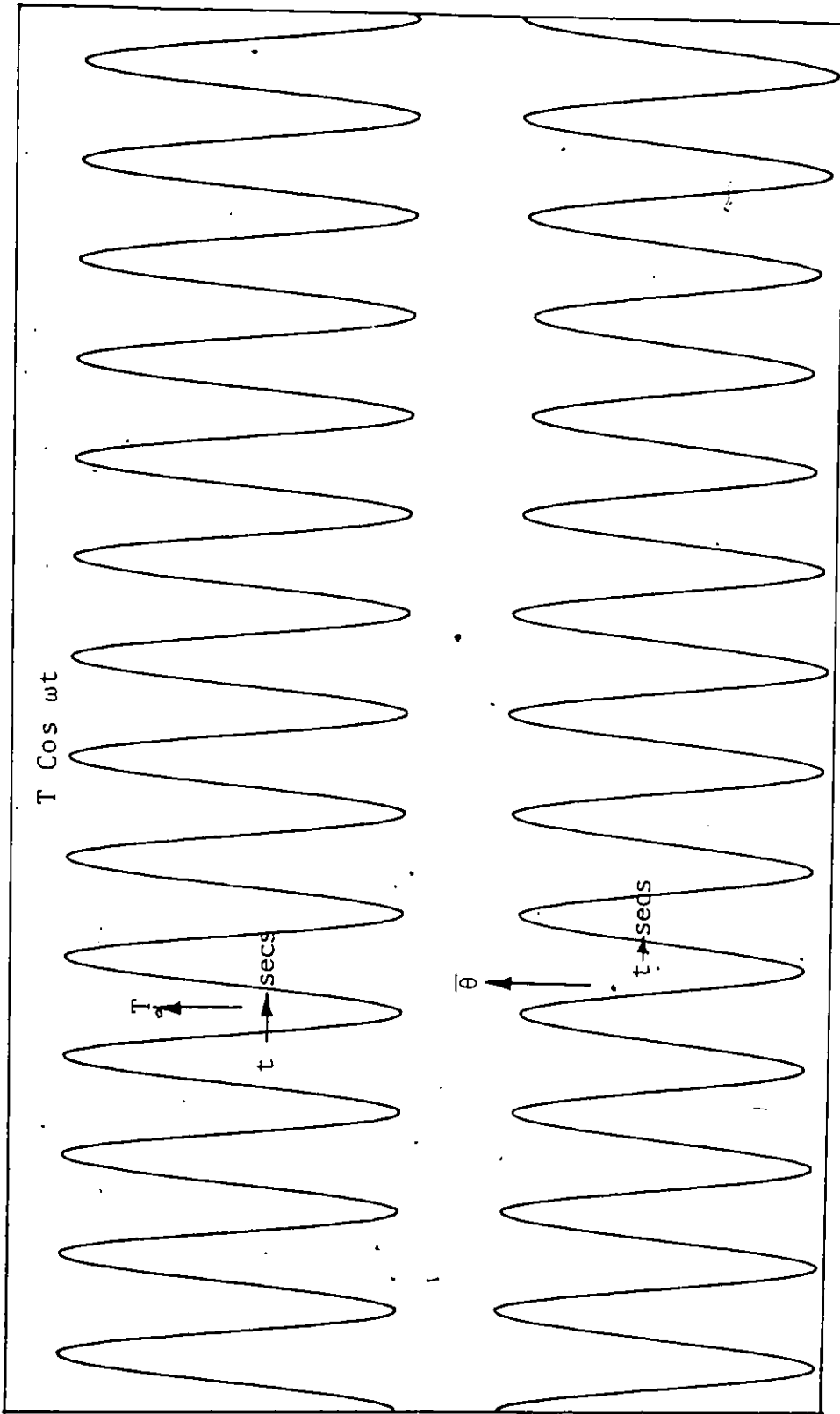


Figure 5.1.7 Analog Computer Output, Forced Vibration Response ($\eta=0.7$)
 In-Phase Motion
 Disturbing Torque = $T \cos \omega t$, $\dot{S} = 2.0$



$\eta = 1.1$ Out of Phase

Figure 5.1.8 Analog Computer Output, Forced Vibration Response ($\eta = 1.1$)
 Out of Phase Motion
 Disturbing Torque = $T \cos wt$, $\dot{S} = 2.0$

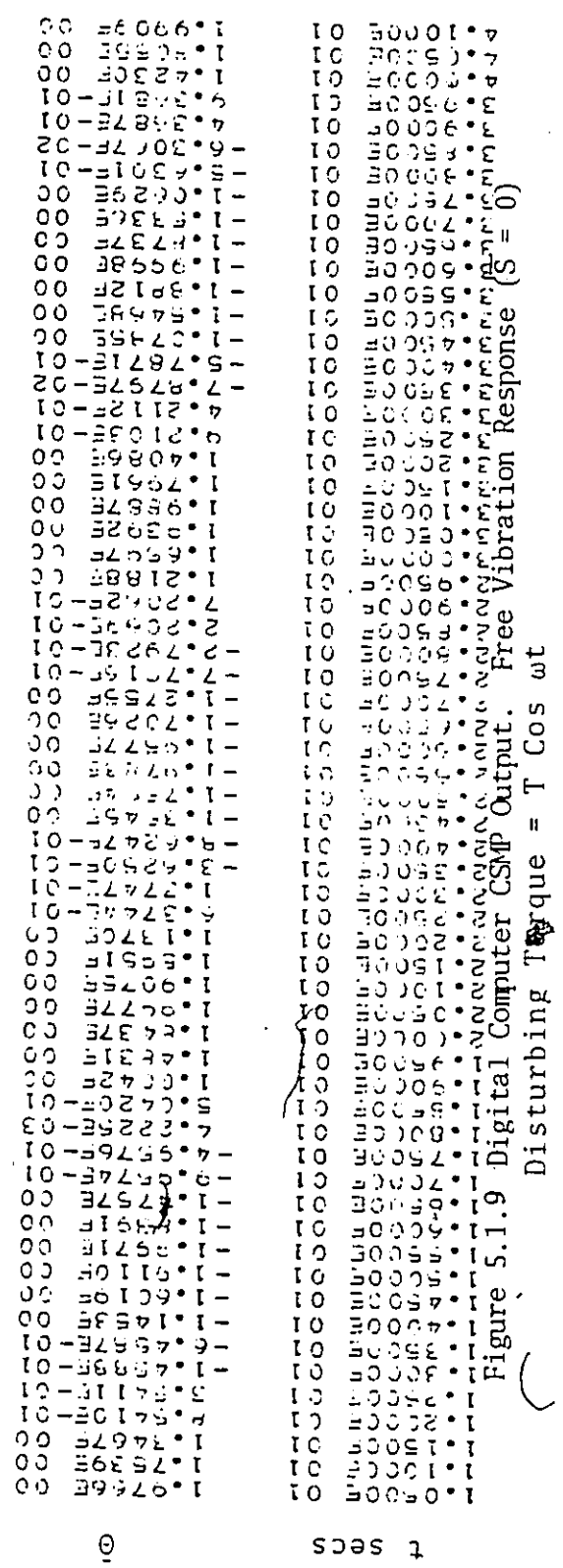
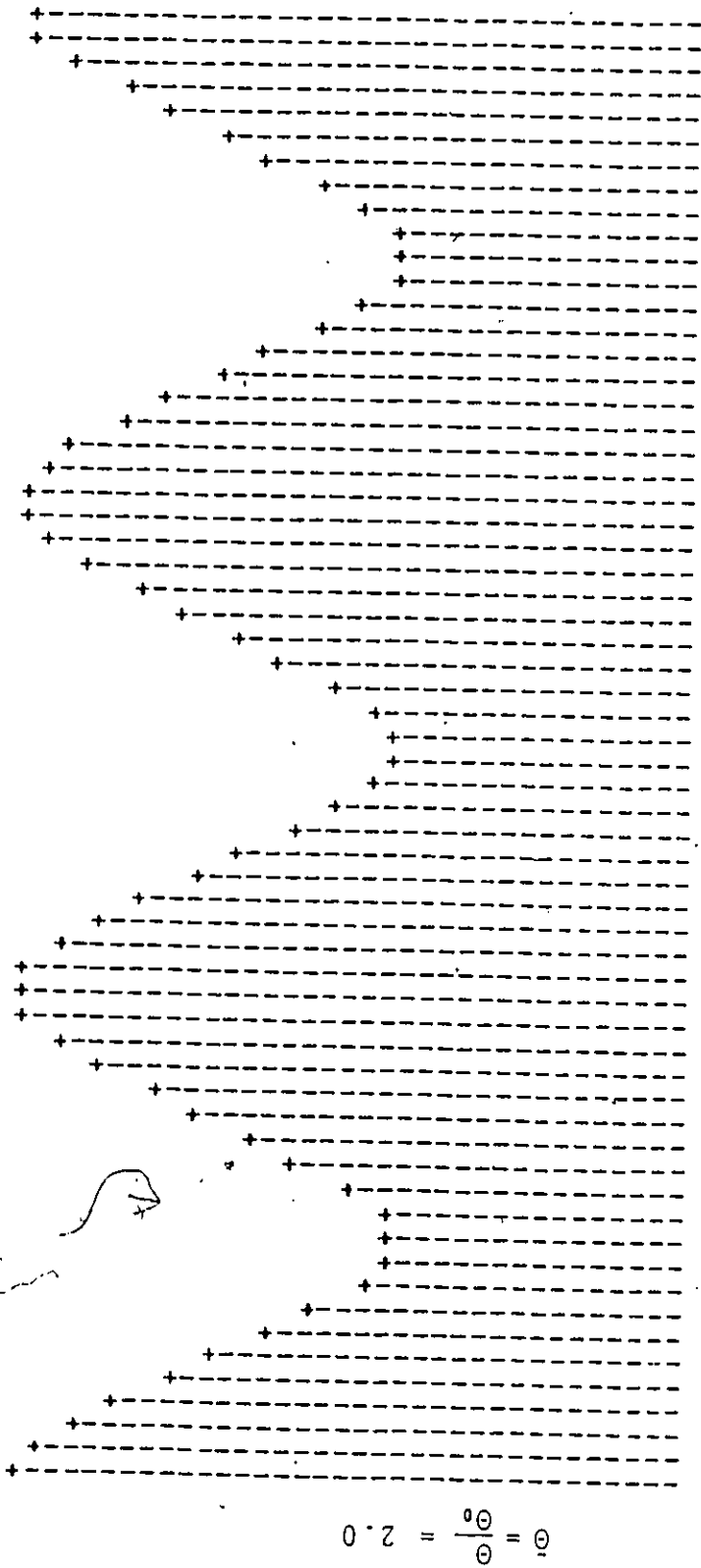


Figure 5.1.9 Digital Computer CSMP Output. Free Vibration Response ($S = 0$) Disturbing Torque = $T \cos \omega t$

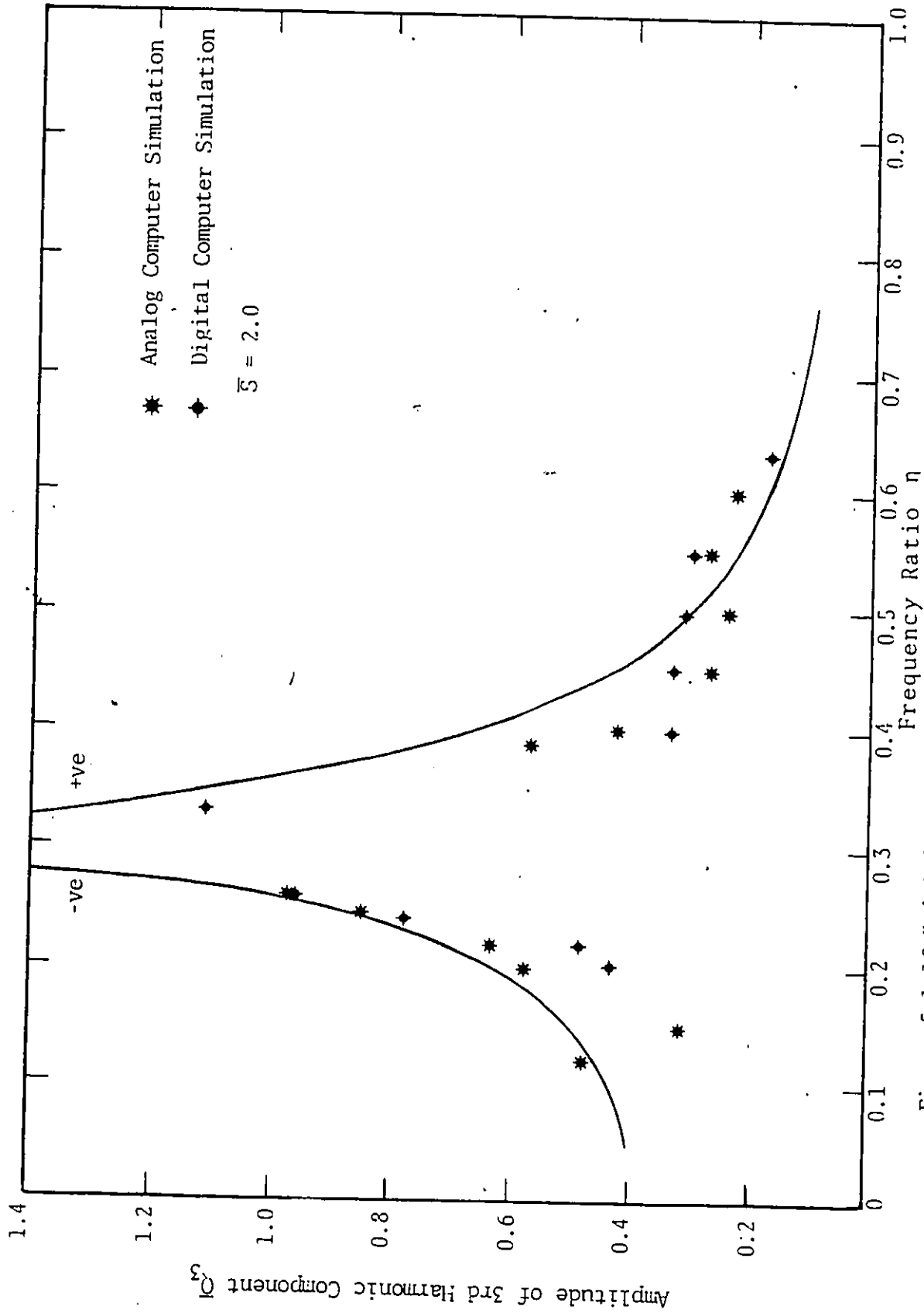


Figure 5.1.10 3rd Order Ultraharmonic Resonance Response for Symmetrical System ($\theta_1 = 0$). Disturbing Torque = $T \cos \omega t$. Plot \bar{Q}_3 Vs η .

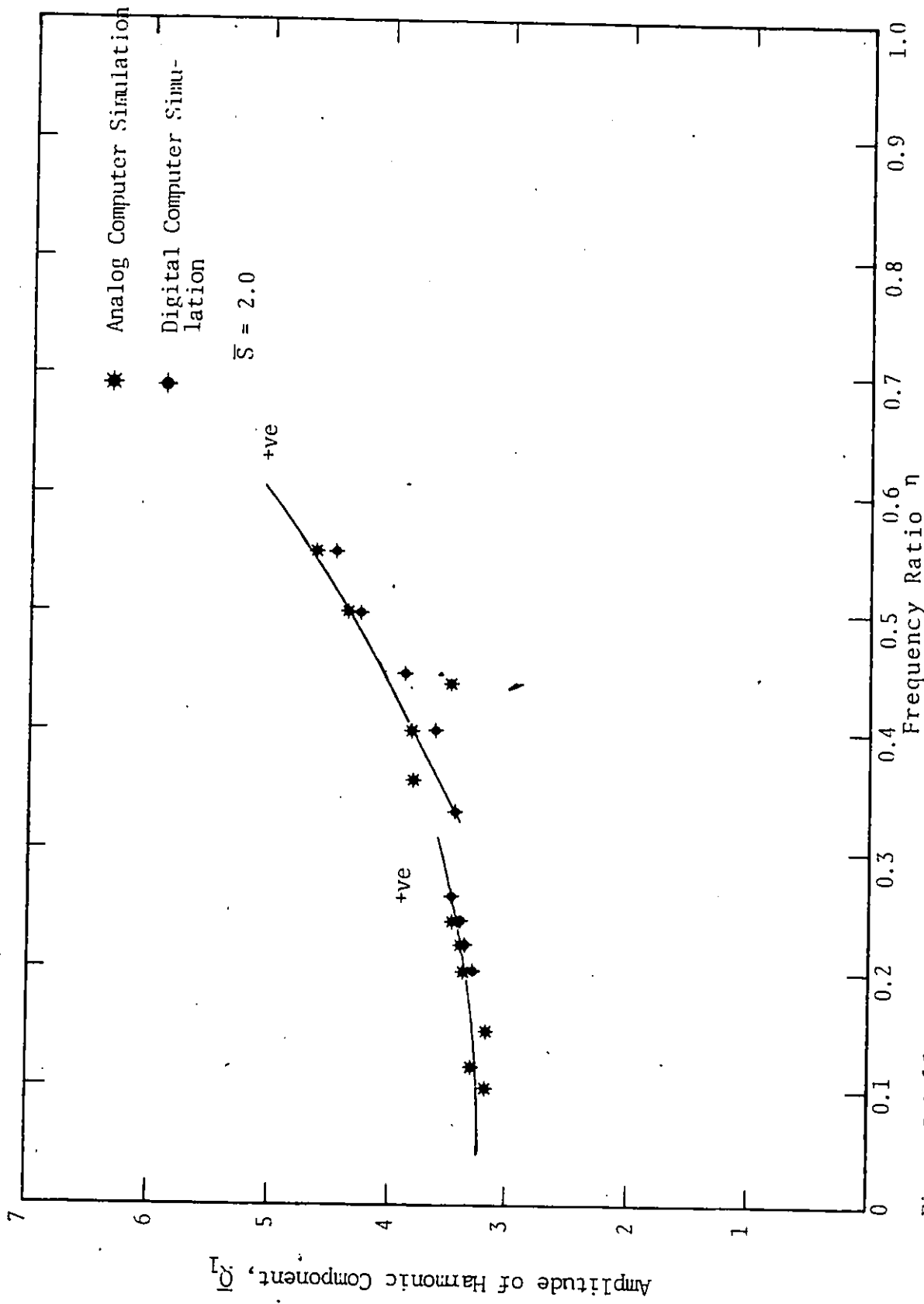


Figure 5.1.11 3rd Order Ultraharmonic Resonance Response for Symmetrical System ($\bar{\theta}_1 = 0$)
 Disturbing Torque = $T \cos \omega t$ Plot Q_1 Vs η .

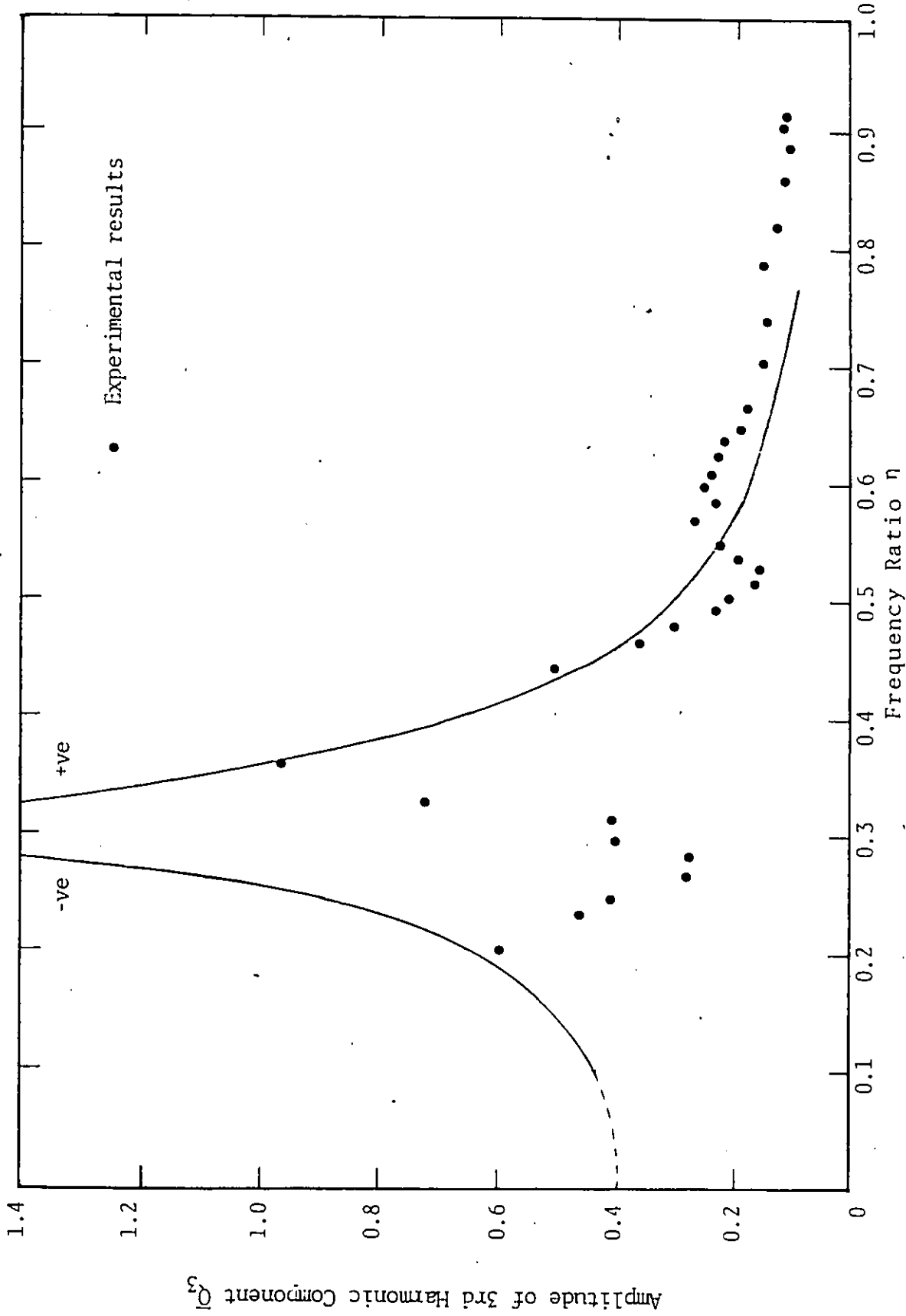


Figure 5.1.12 3rd Order Ultraharmonic Resonance Response for Asymmetrical System ($\hat{\theta}_1 = 0.05$)
Disturbing Torque = $T \cos \omega t$ ($S = 2.0$). Plot \bar{Q}_3 Vs η .

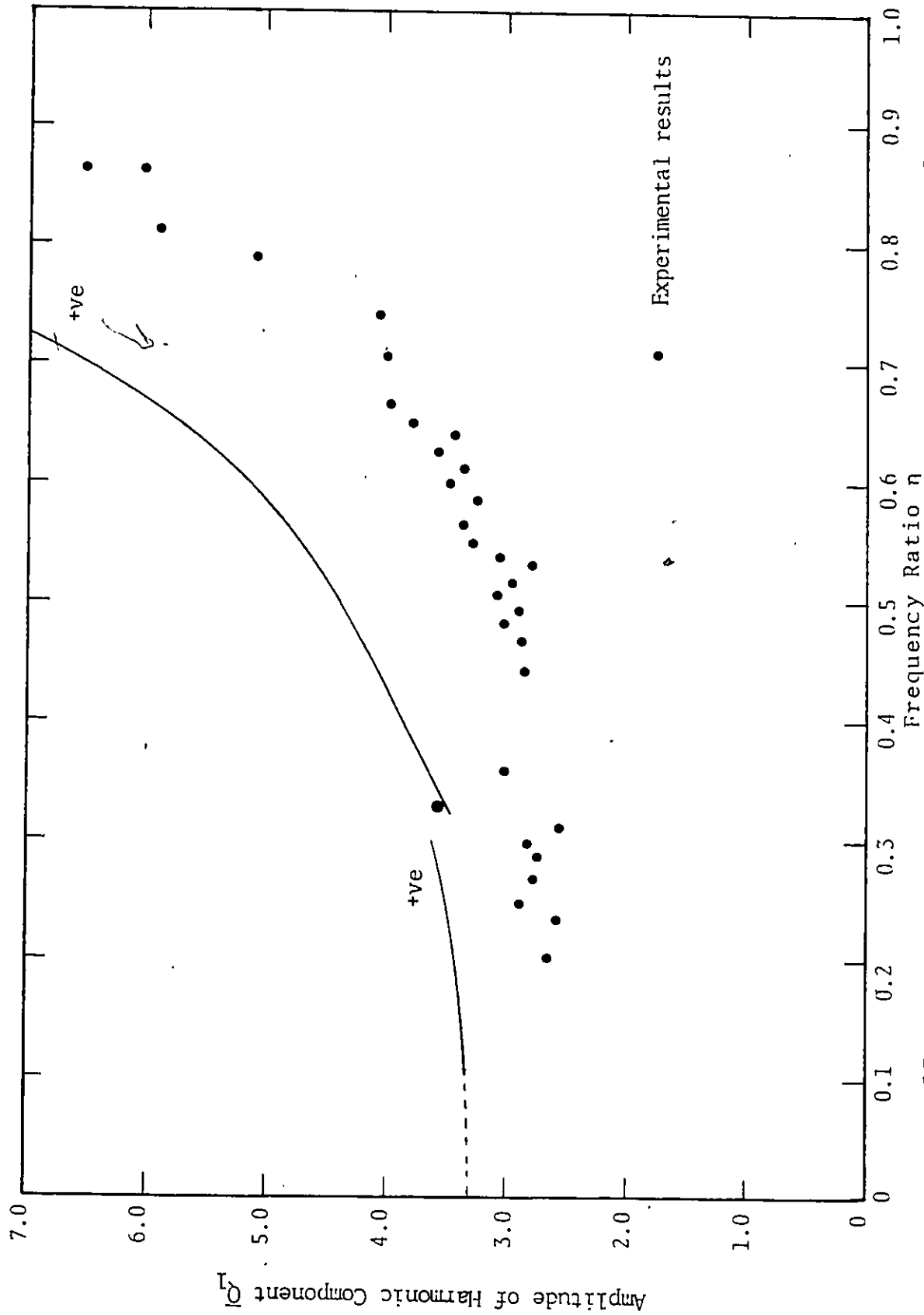


Figure 5.1.13 3rd Order Ultraharmonic Resonance Response for Asymmetrical System ($\bar{\theta}_1 = 0.05$)
Disturbing Torque = $T \cos \omega t$ ($S = 2.0$). Plot Q_1 Vs n .

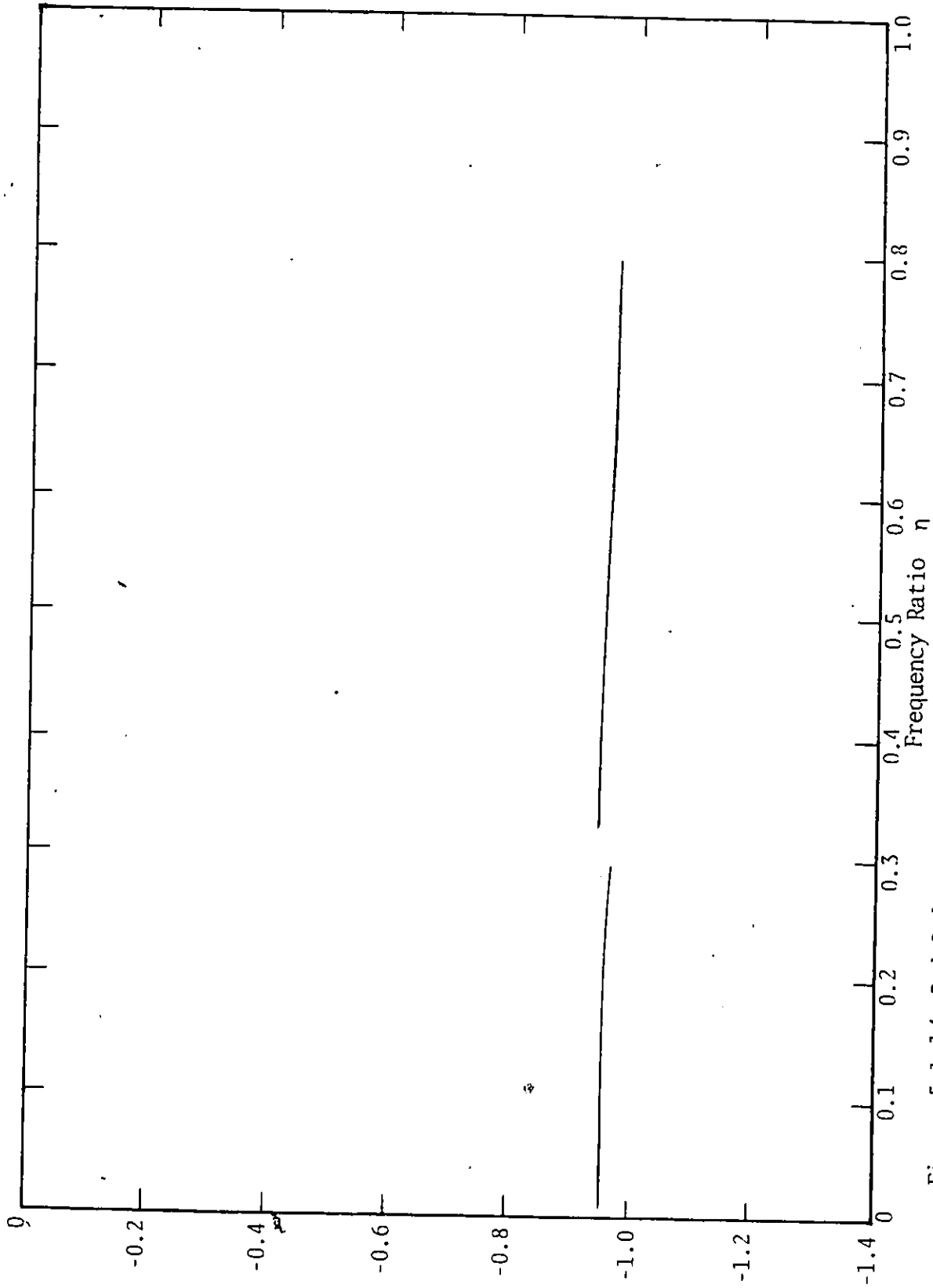


Figure 5.1.14 3rd Order Ultraharmonic Resonance Response for Asymmetrical System
($\hat{\theta}_1 = 0.05$) Disturbing Torque = $T \cos \omega t$ ($\hat{S} = 2.0$). Plot M Vs η .

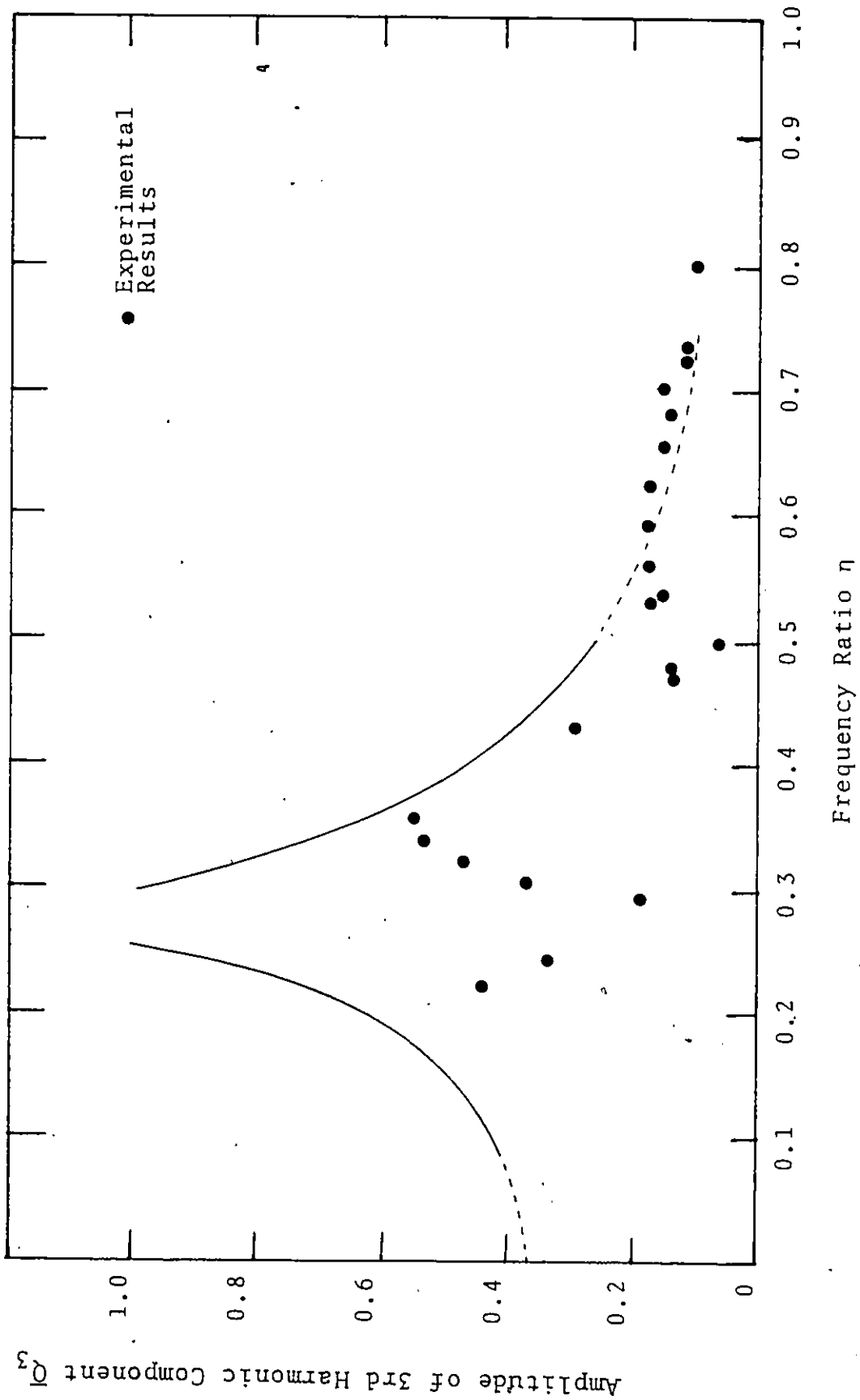


Figure 5.1.15 3rd Order Ultraharmonic Resonance Response for Asymmetrical System ($\bar{\theta}_1=0.05$) Disturbing Torque = $T \cos \omega t$ ($\bar{S}=1.0$). Plot \bar{Q}_3 Vs η .

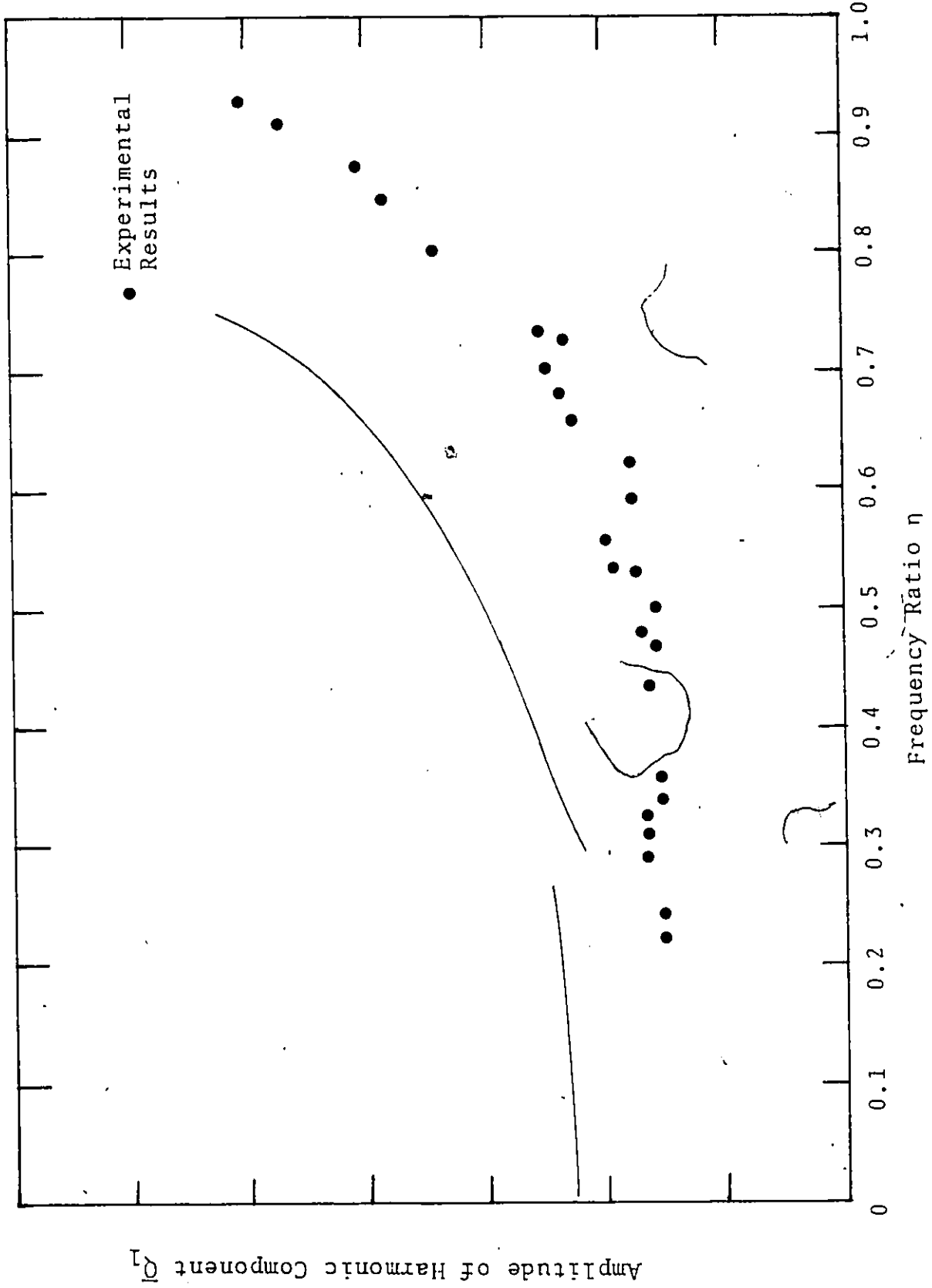


Figure 5.1.16 3rd Order Ultraharmonic Resonance Response for Asymmetrical System ($\bar{\theta}_1=0.05$) Disturbing Torque = $T \cos \omega t$ ($S=1.0$). Plot Q_1 Vs n .

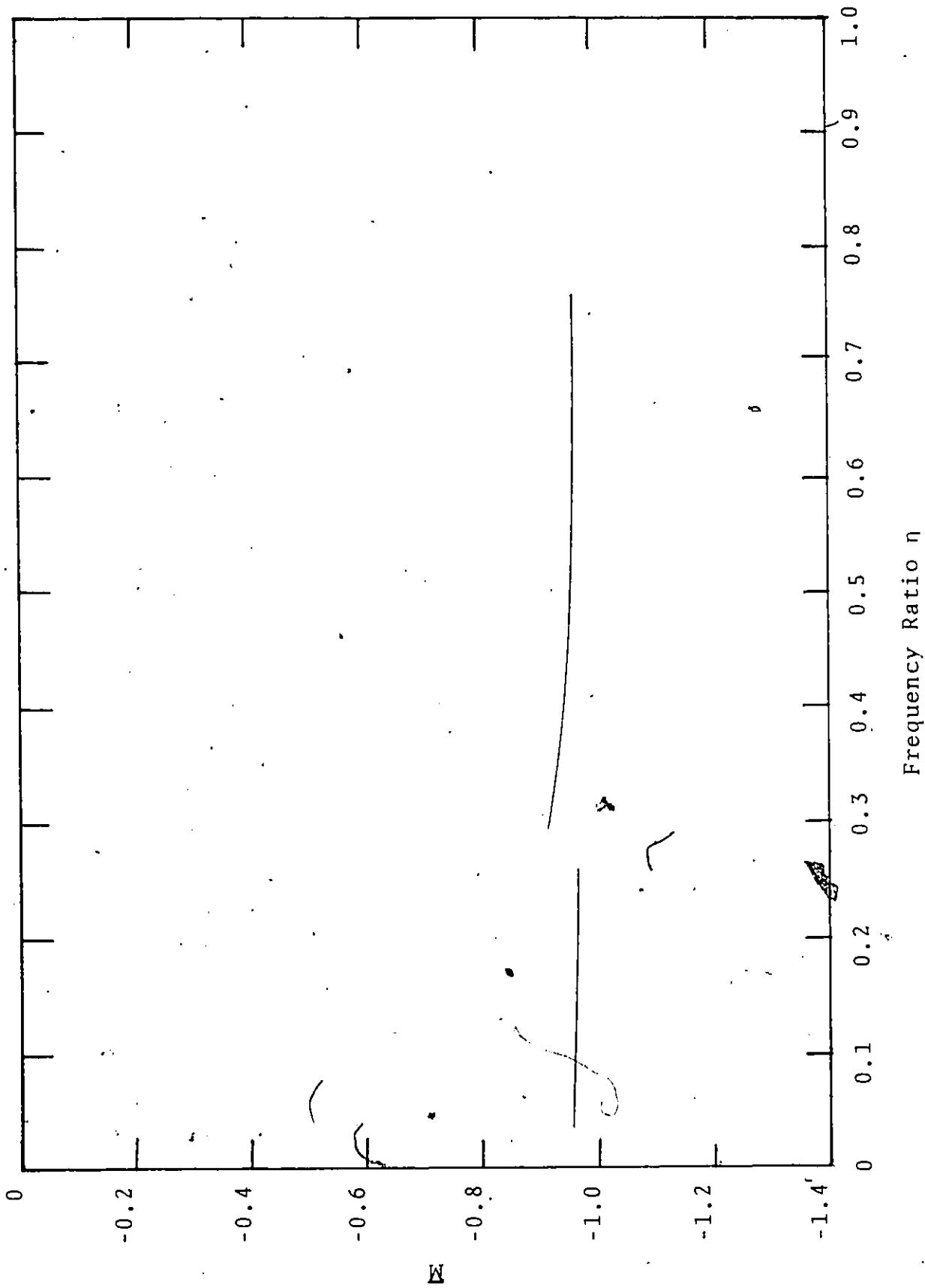


Figure 5.1.17 3rd Order Ultraharmonic Resonance Response for Asymmetrical System ($\sigma_1 = 0.05$)
Disturbing Torque = $T \cos \omega t$ ($\bar{S} = 1.0$). Plot \bar{M} Vs n .

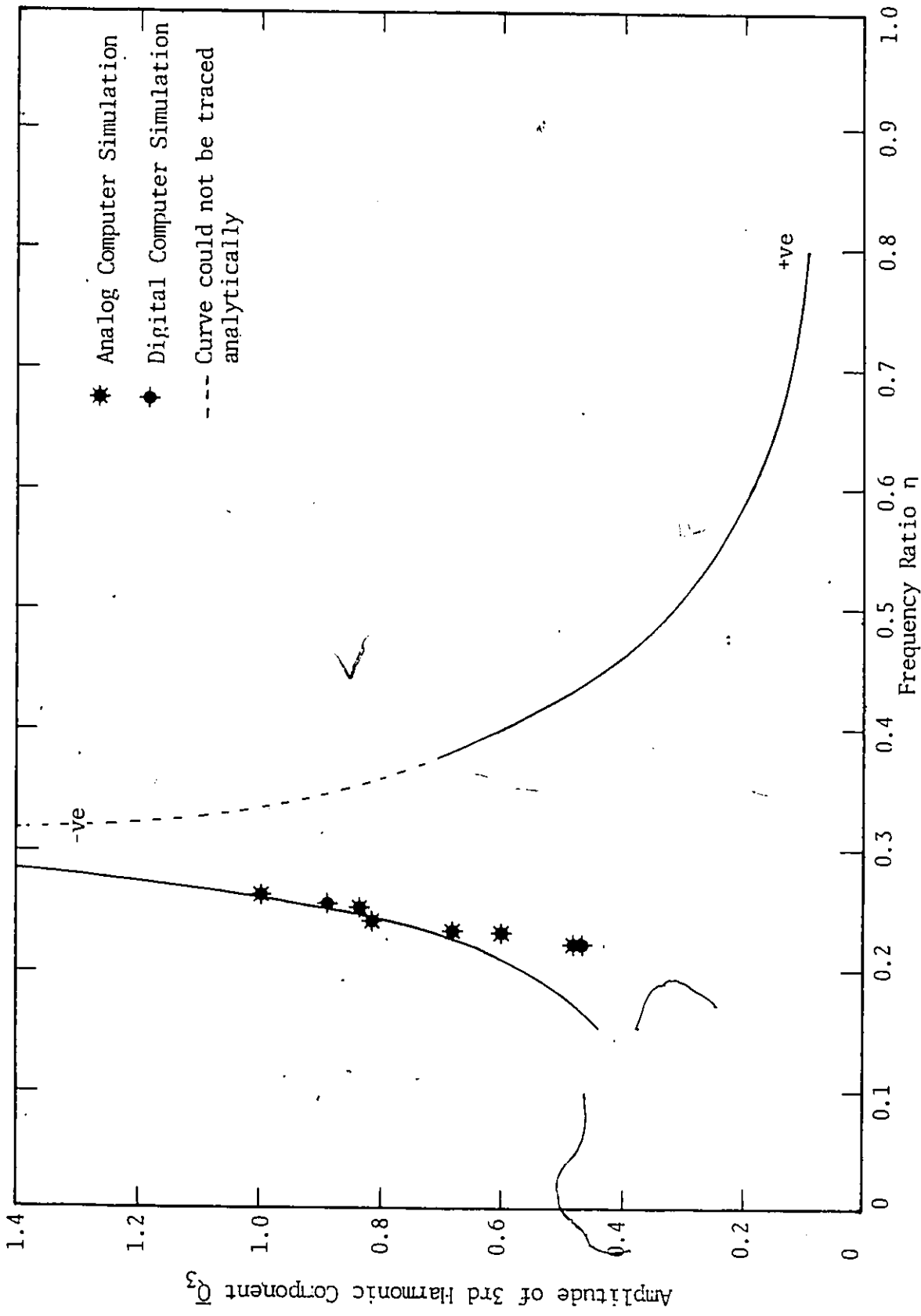


Figure 5.1.18 3rd Order Ultraharmonic Resonance Response for Symmetrical System Disturbing Torque = $C \omega^2 \cos \omega t$ ($Z' = 10.0$). Plot Q_3 Vs n .

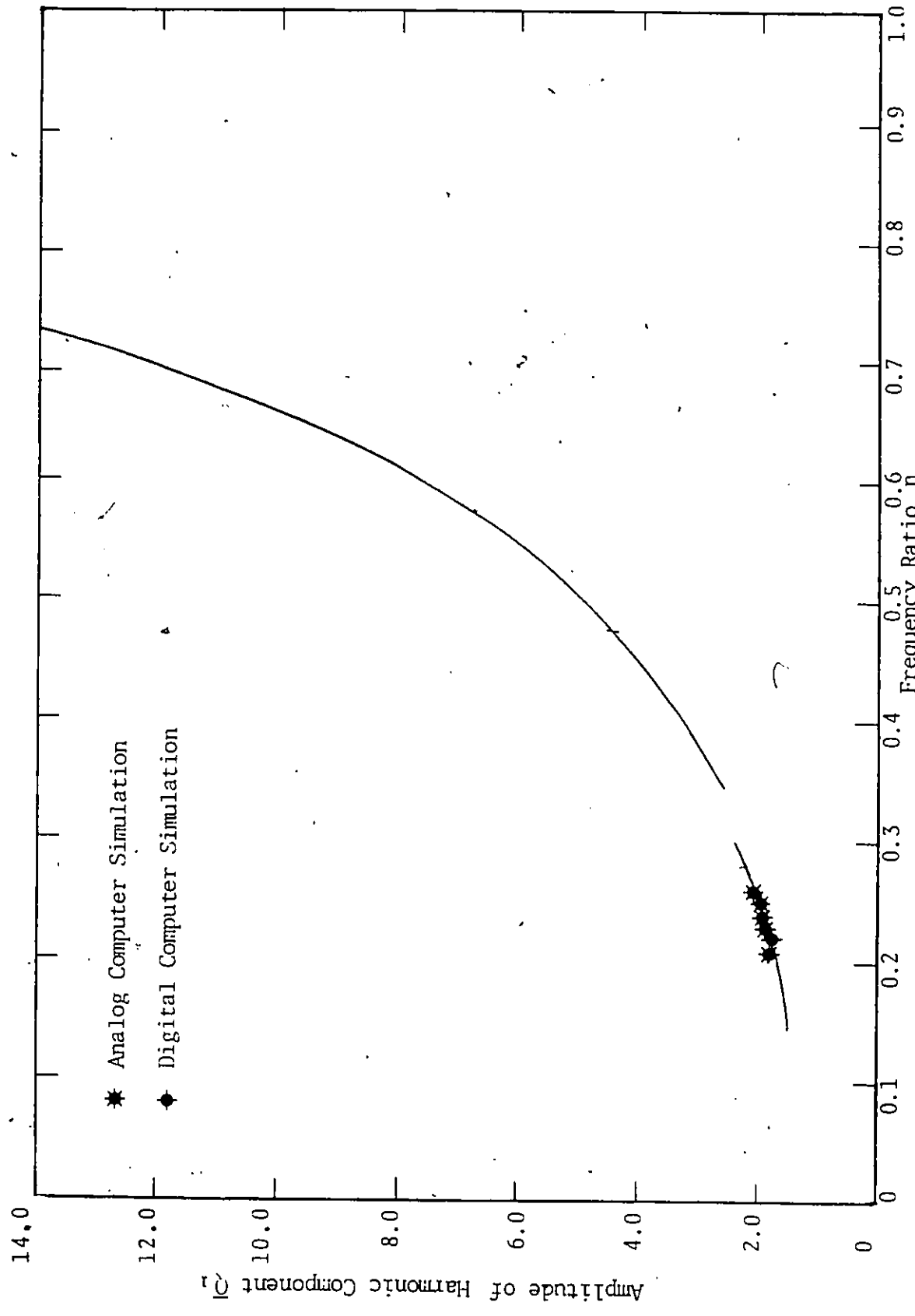


Figure 5.1.19 3rd Order Ultraharmonic Resonance Response for Symmetrical System
Disturbing Torque = $C \omega^2 \cos \omega t$ ($Z' = 10.0$). Plot Q_1 Vs η .

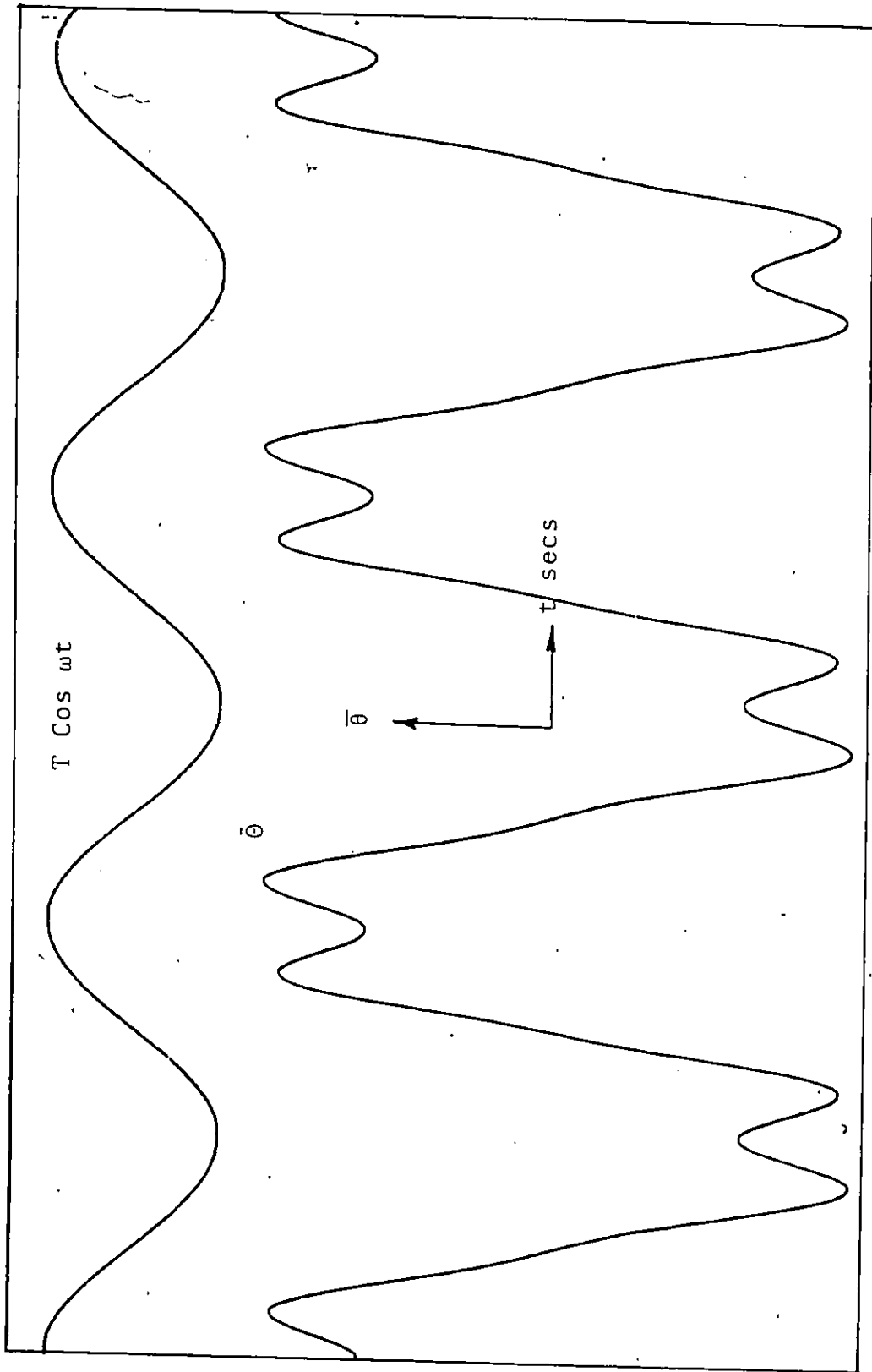


Figure 5.1.1.20 Analog Computer Output. 3rd Order Ultraharmonic Resonance
Response ($\eta = 0.24$)
Disturbing Torque = $T \cos \omega t$, $\hat{S} = 2.0$

e

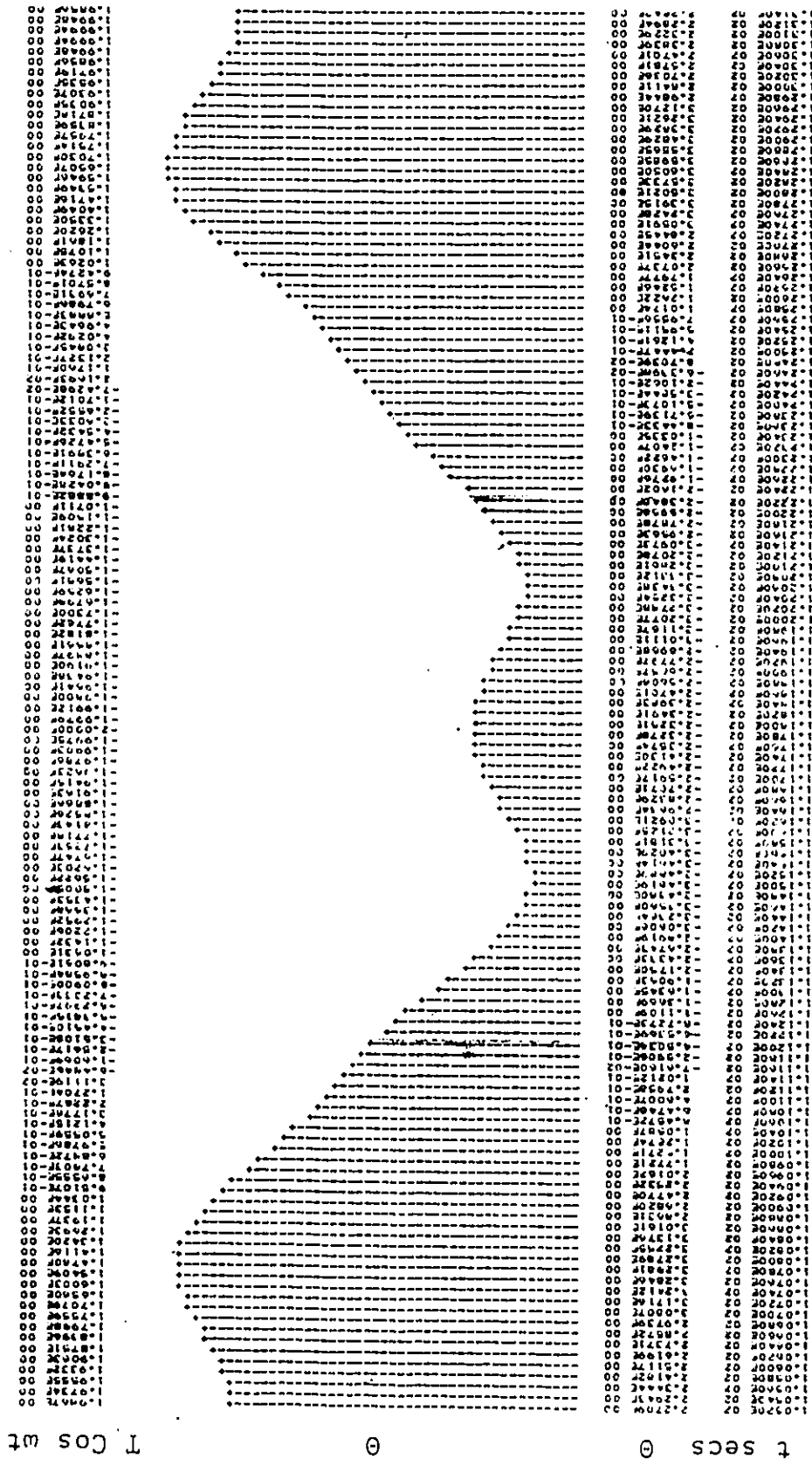


Figure 5.1.21 Digital Computer CSMP Output 3rd Order Ultraharmonic Resonance Response ($\eta = 0.24$) Disturbing Torque = $T \cos \omega t$ ($\bar{S} = 2.0$)

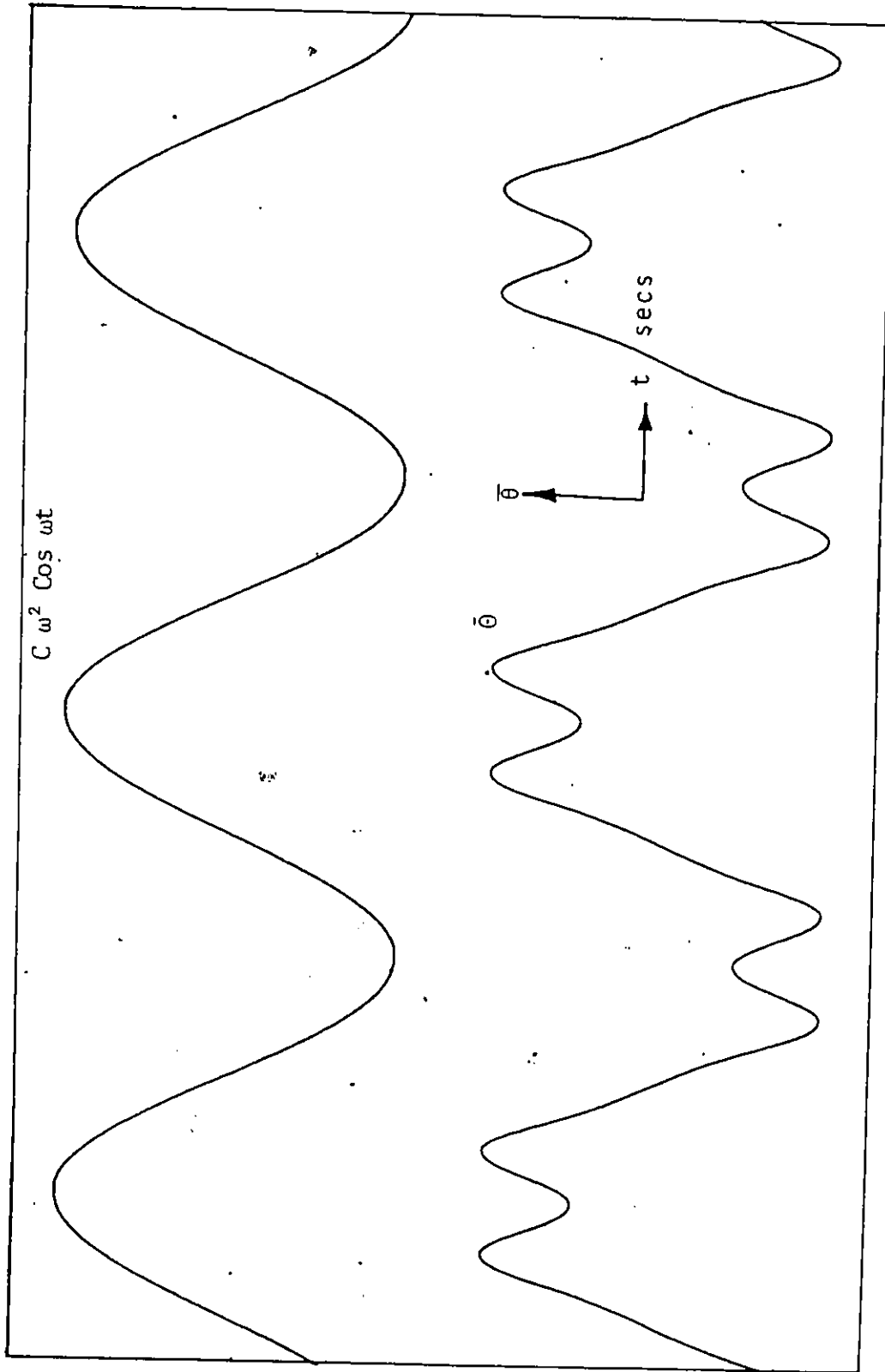


Figure 5.1.22 Analog Computer Output. 3rd Order Ultraharmonic Resonance
 Response for Symmetrical System ($\theta_1 = 0$, $\eta = 0.22$)
 Disturbing Torque = $C \omega^2 \text{Cos } \omega t$ ($Z' = 10.0$)

5

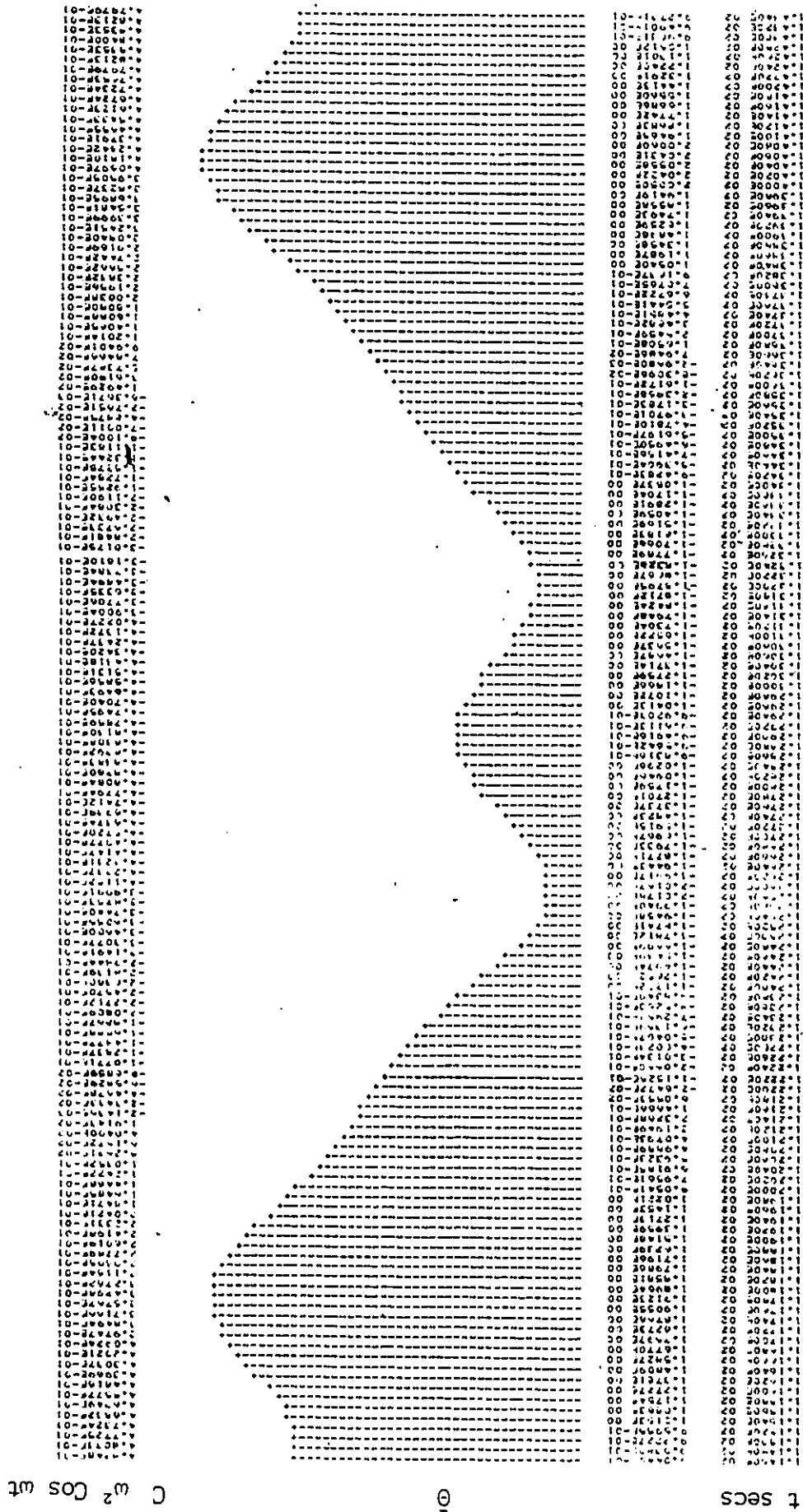


Figure 5.1.23 Digital Computer CSMP Output. 3rd Order Ultraharmonic Resonance Response for Symmetrical System ($\theta_1 = 0$, $\eta = 0.22$) Disturbing Torque = $C \omega^2 \cos \omega t$ ($Z' = 10.0$)

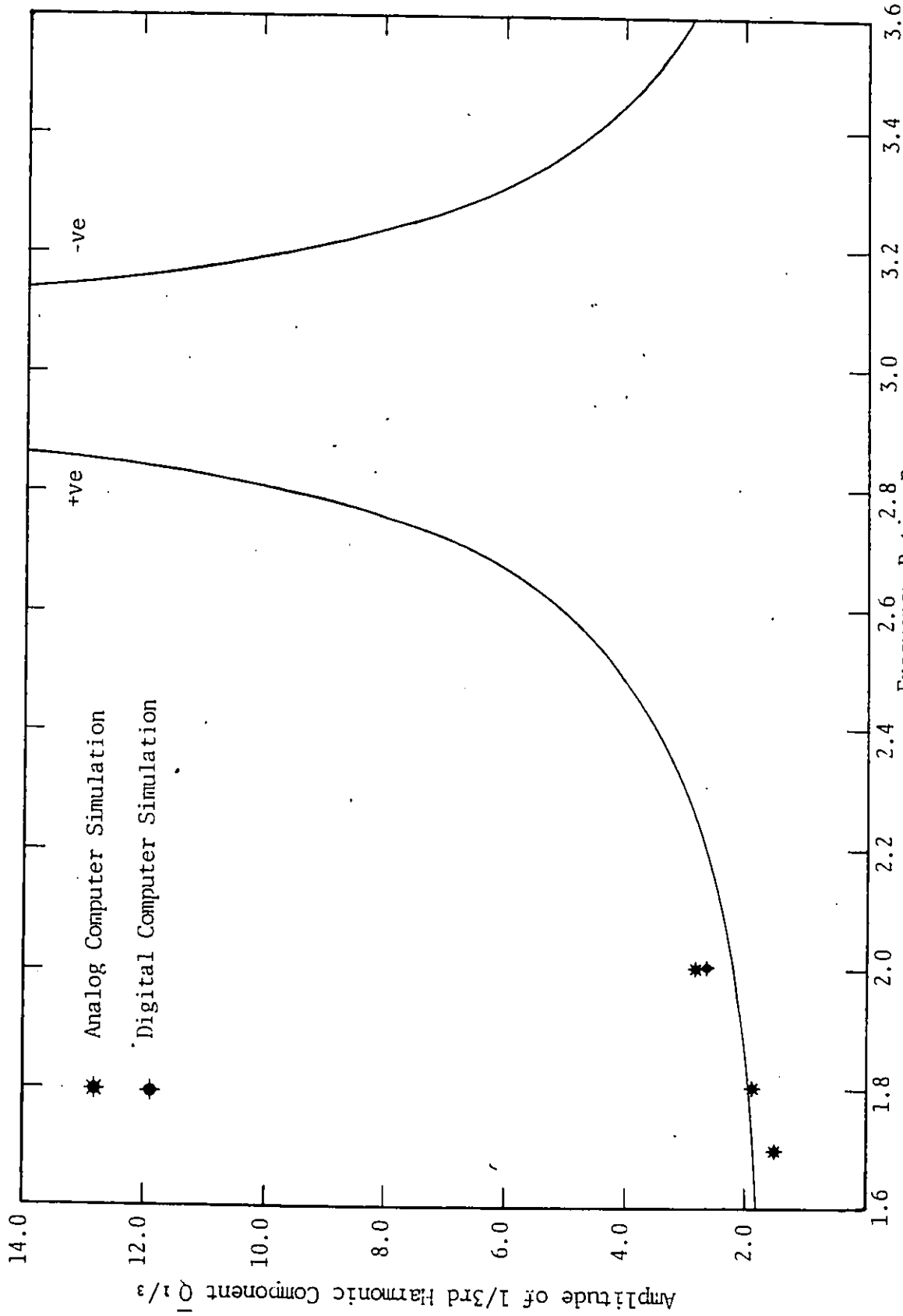


Figure 5.1.24 1/3rd Order Subharmonic Resonance Response for Symmetrical System ($\bar{\theta}_1=0, \bar{S}=2.0$)
Disturbing Torque = T Cos wt. Plot $Q_{1/3}$ Vs η .

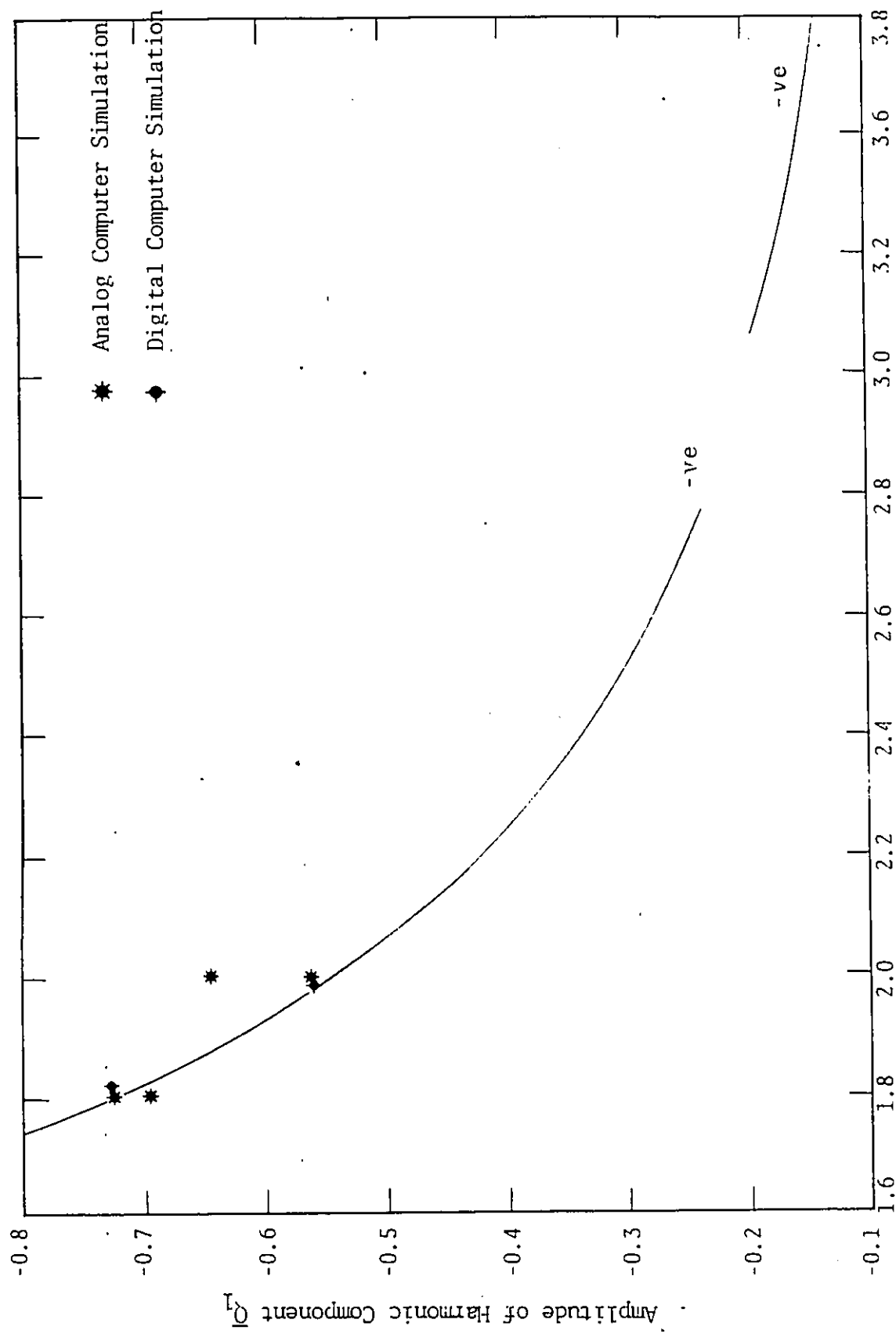


Figure 5.1.25 1/3rd Order Subharmonic Resonance Response for Symmetrical System ($\bar{\theta}_1 = 0, \bar{\gamma} = 2.0$)
Disturbing Torque = $T \cos \omega t$. Plot Q_1 Vs η .

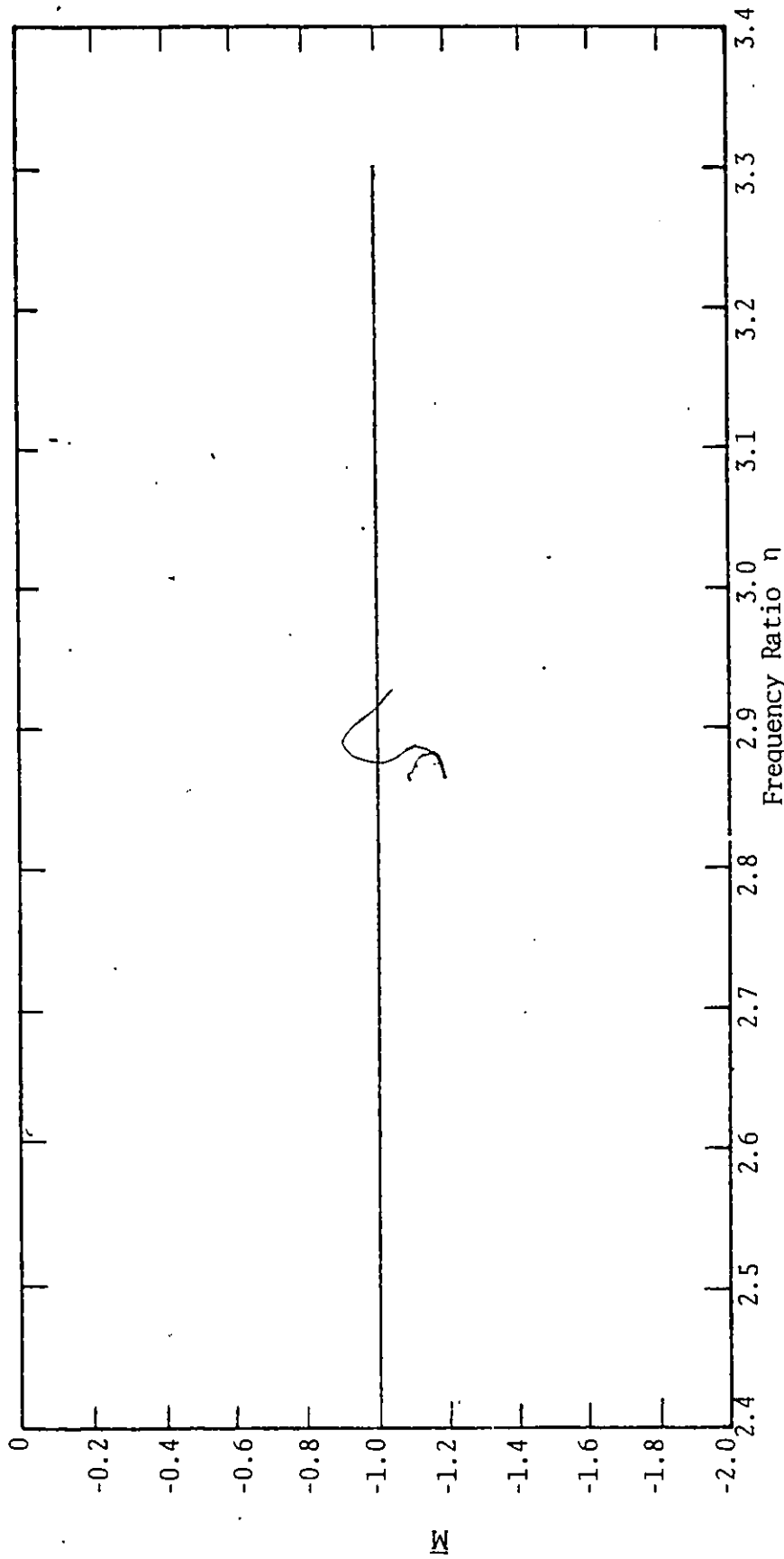


Figure 5.1.26 1/3rd Order Subharmonic Resonance Response for Symmetrical System ($\bar{\theta}_1 = 0$, $S = 2.0$). Disturbing Torque = $\bar{T} \cos \omega t$.

Plot \bar{M} Vs η .

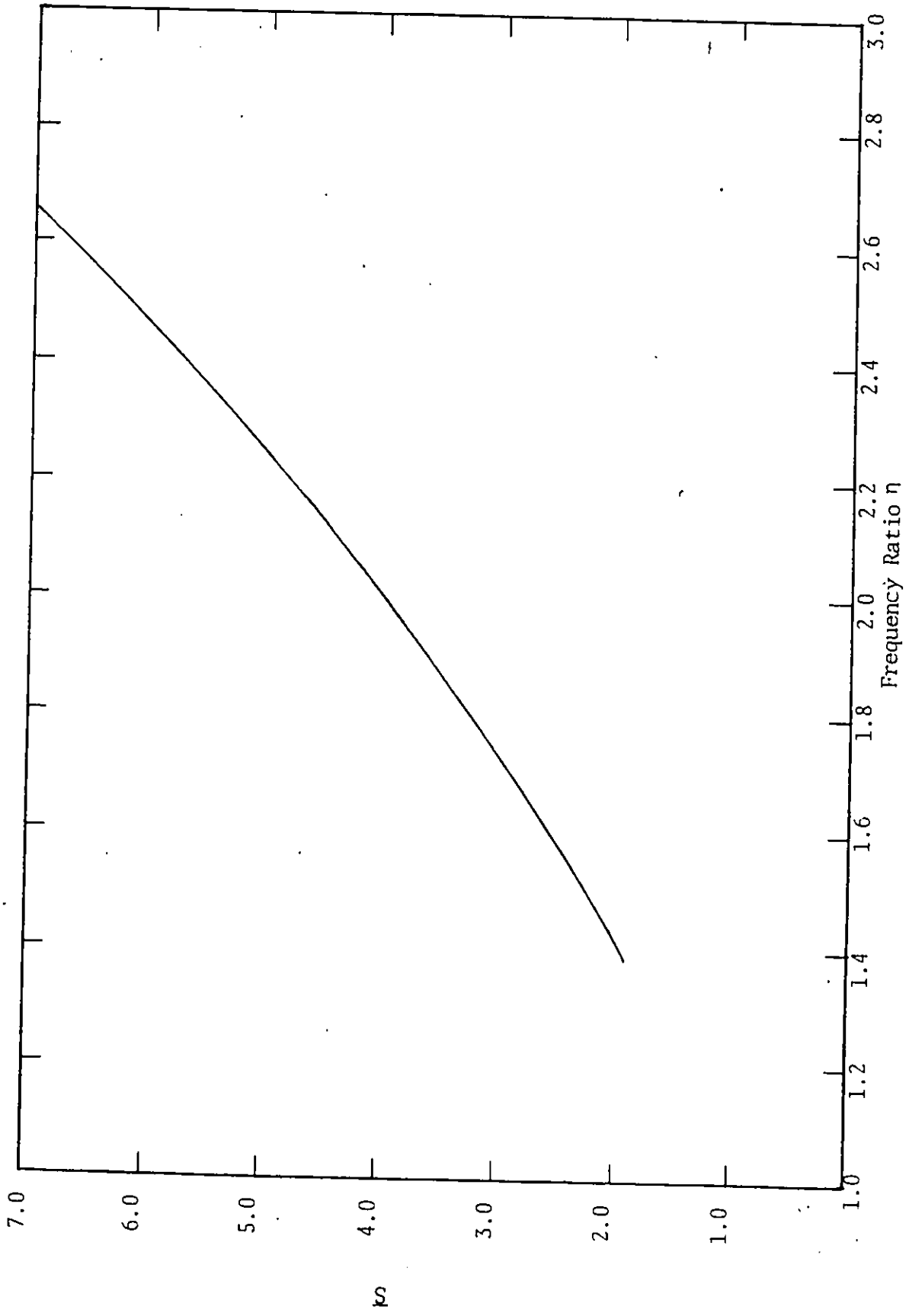


Figure 5.1.27 Locus of Cut Off Frequency, 1/3rd Order Subharmonic Resonance, Disturbing Torque = $T \cos \omega t$.

A

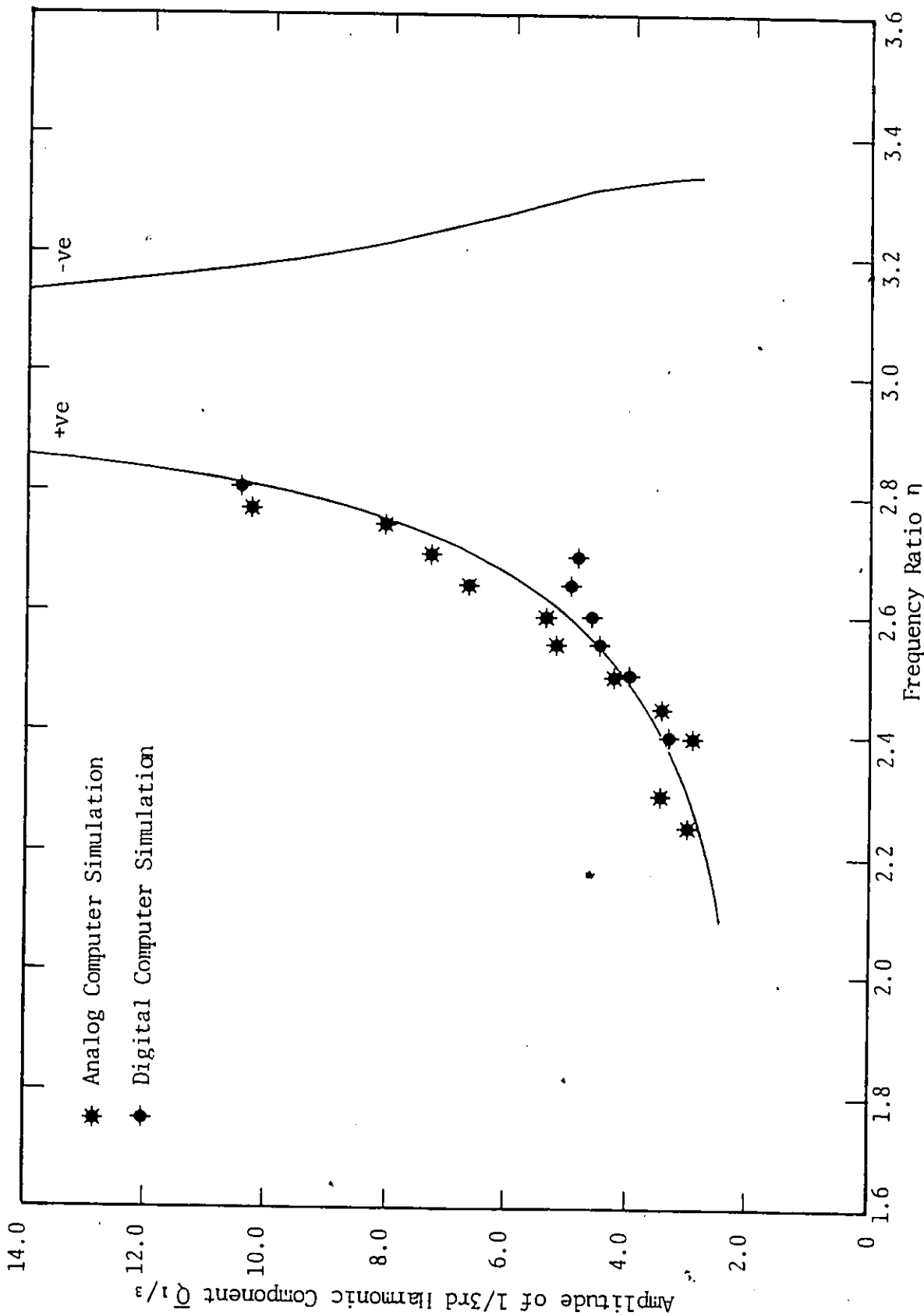


Figure 5.1.28 1/3rd Order Subharmonic Resonance Response for Symmetrical System. Disturbing Force = $C \omega^2 \cos \omega t$ ($Z' = 2.0$). Plot $Q_{1/3}$ Vs η .

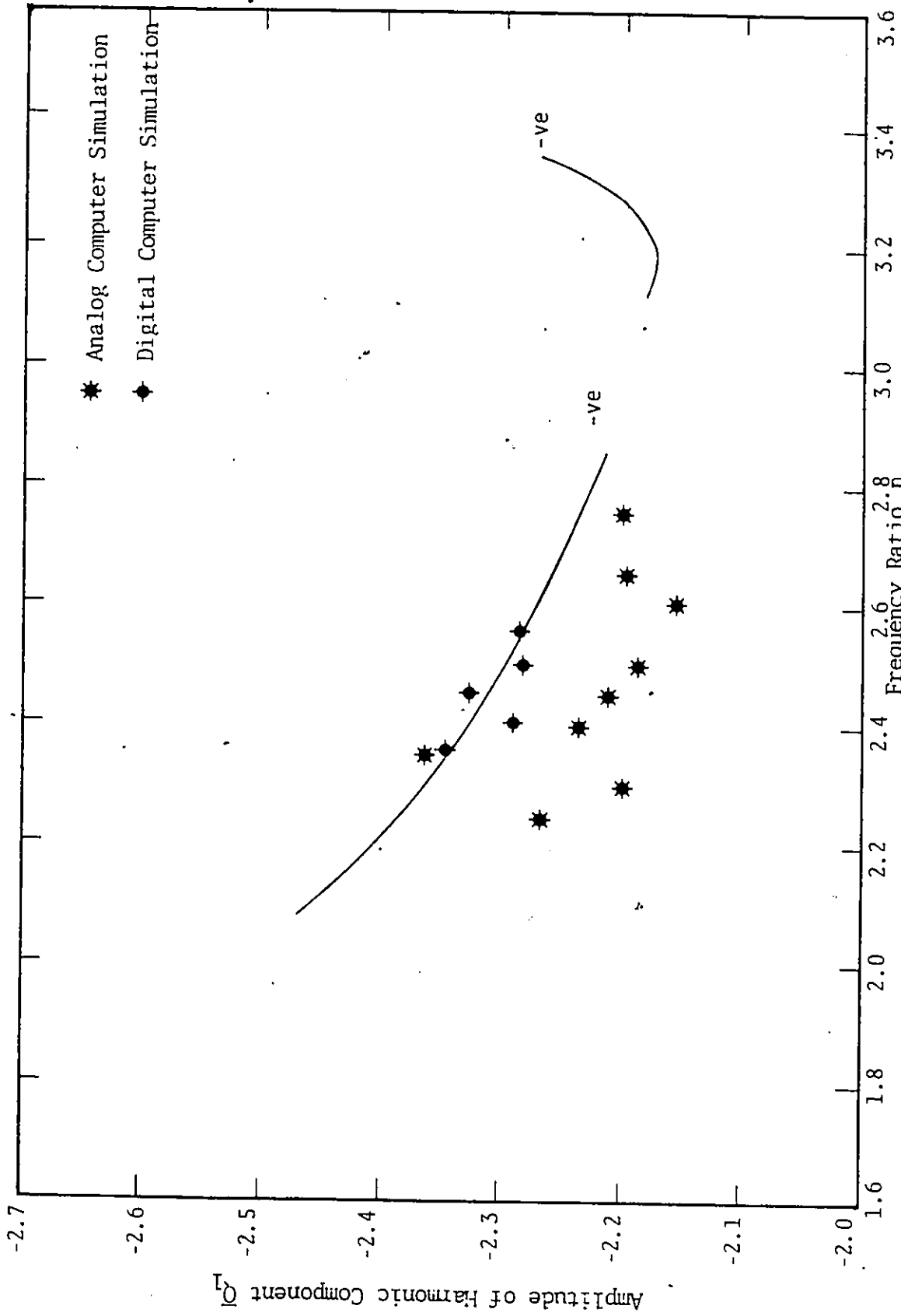


Figure 5.1.29 1/3rd Order Subharmonic Resonance Response for Symmetrical System Disturbing Torque = $C \omega^2 \cos \omega t$ ($Z' = 2.0$). Plot Q_1 Vs n .

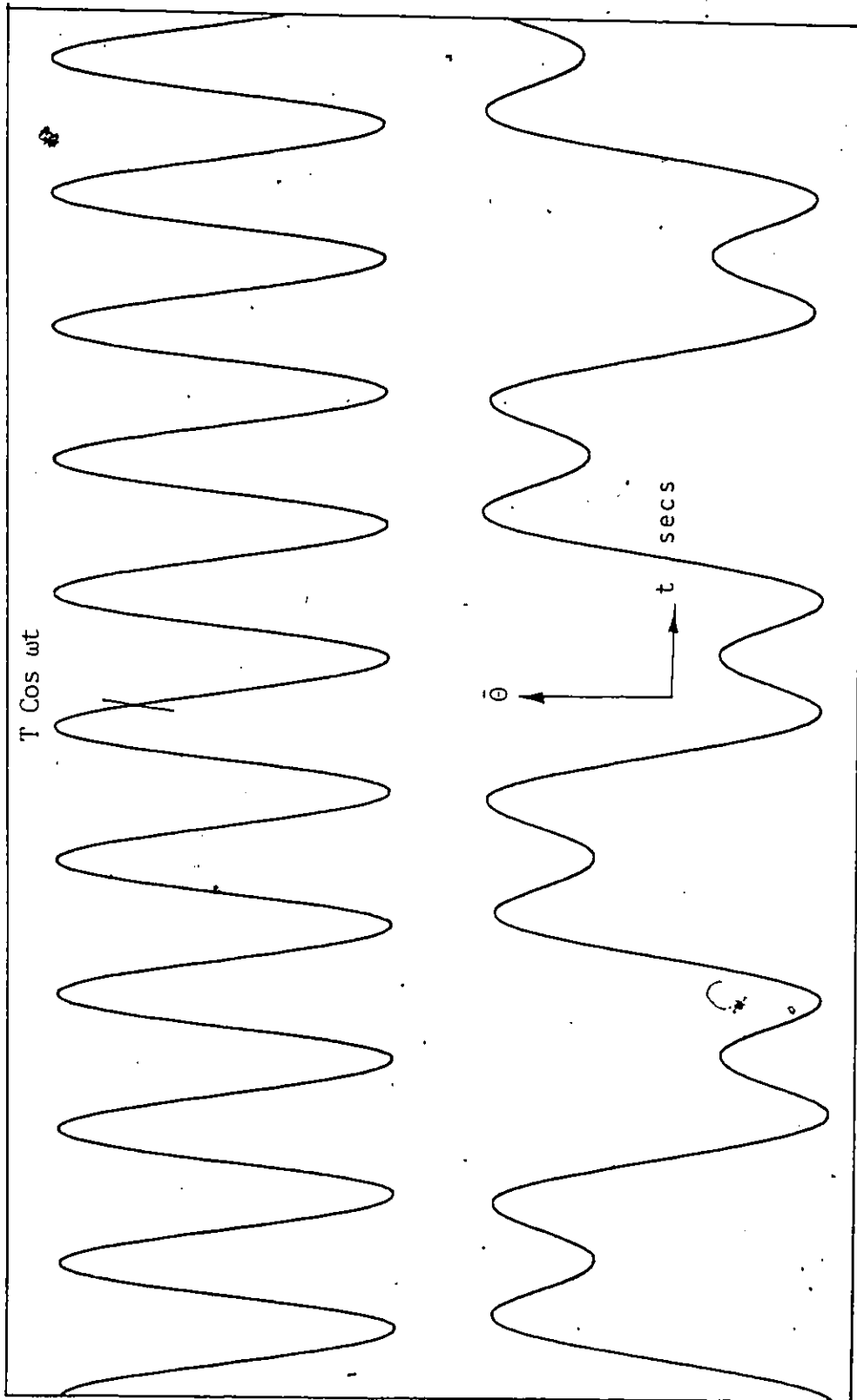


Figure 5.1.1.30 Analog Computer Output. 1/3rd Order Subharmonic Resonance Response for Symmetrical System ($\bar{\theta}_1 = 0, \eta = 1.6$) Disturbing Torque = $T \cos \omega t$ ($S = 2.0$)

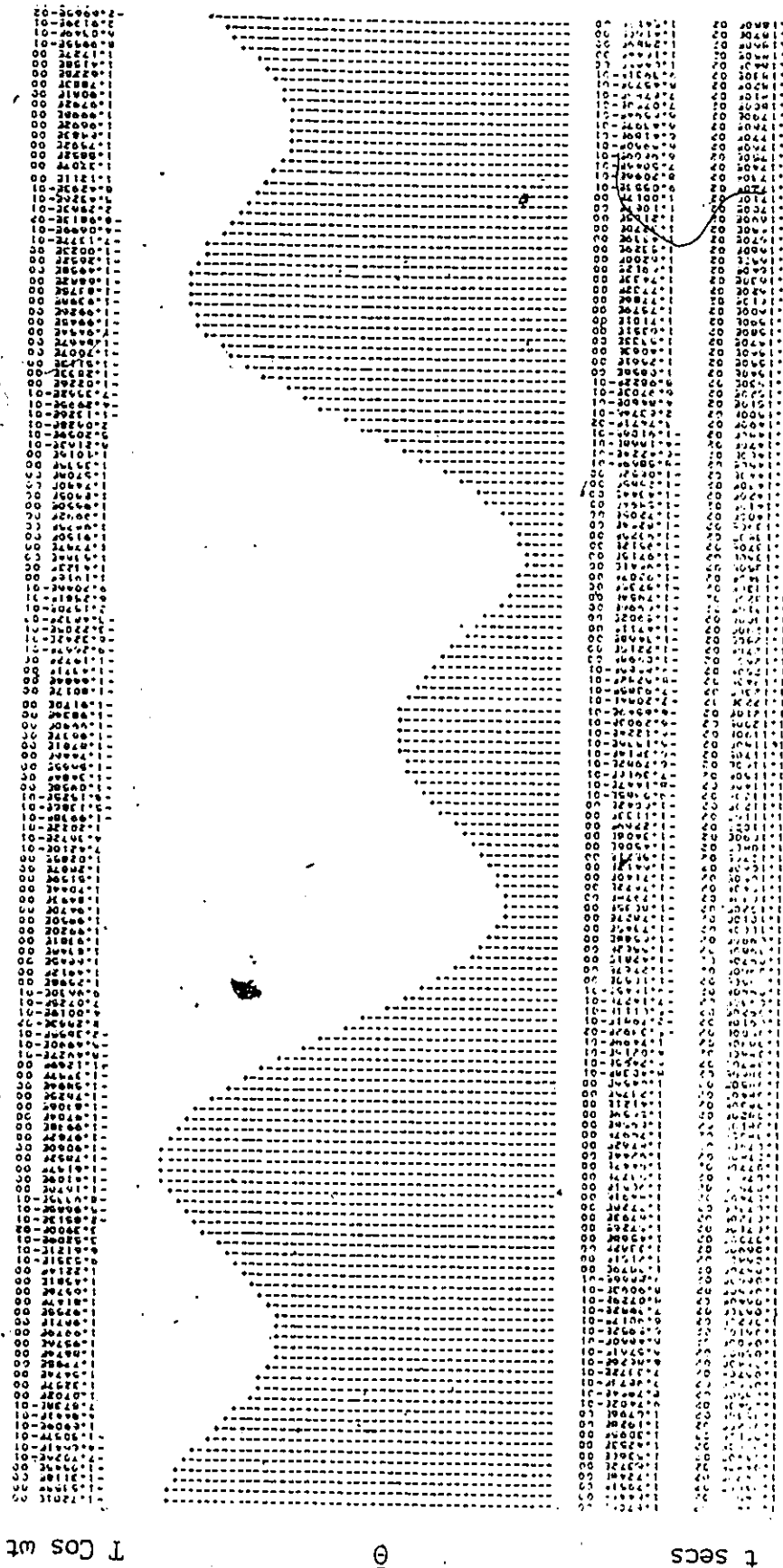


Figure 5.1.31 Digital Computer CSMP Output. 1/3rd Order Subharmonic Resonance
 Response for Symmetrical System ($\theta_1 = 0, \eta = 1.6$)
 Disturbing Torque = $T \cos \omega t$ ($\delta = 2.0$)

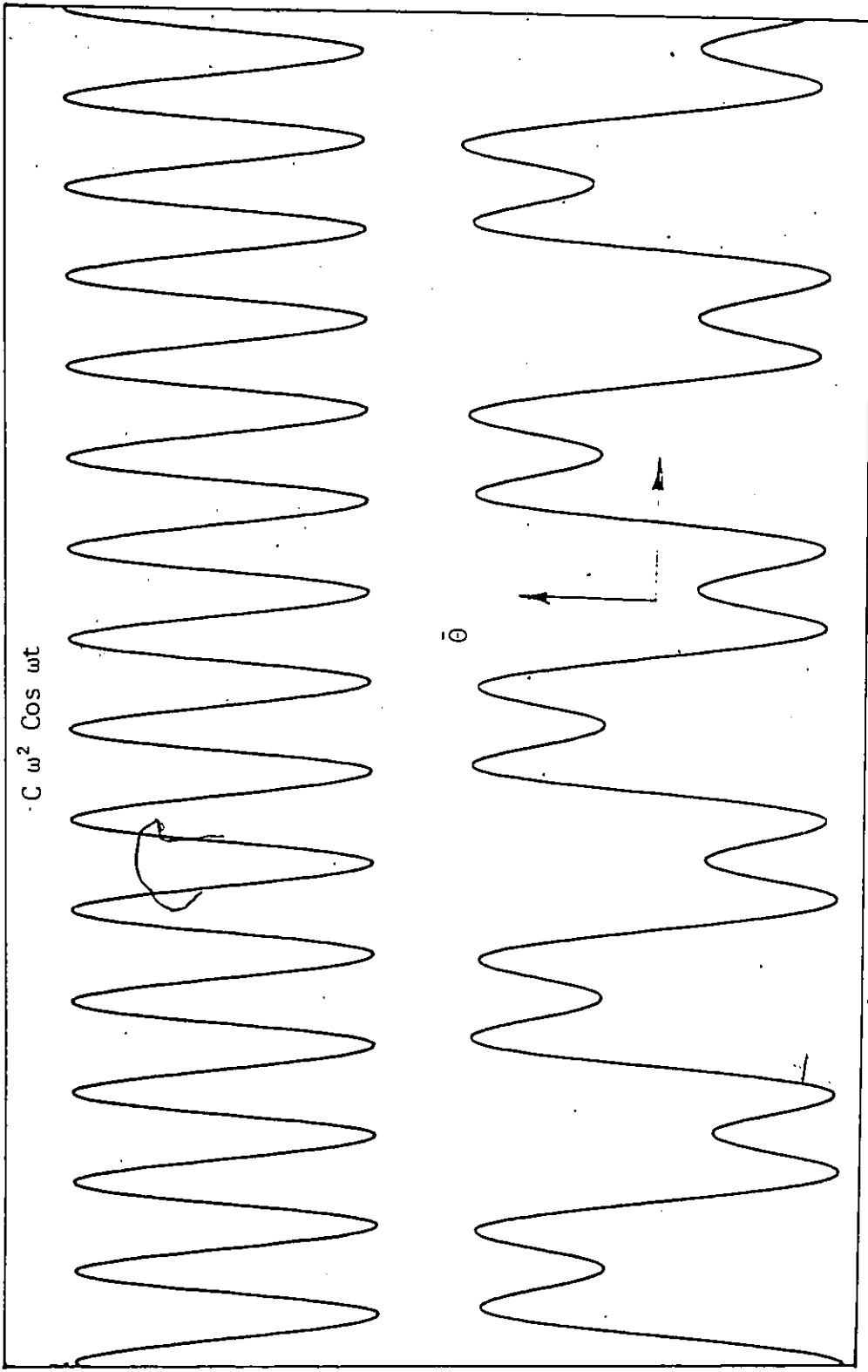


Figure 5.1.32 Analog Computer Output 1/3rd Order Subharmonic Resonance Response for Symmetrical System ($\bar{\theta}_1 = 0, \eta = 2.4$)
Disturbing Torque = $C \omega^2 \cos \omega t$ ($Z' = 2.0$)



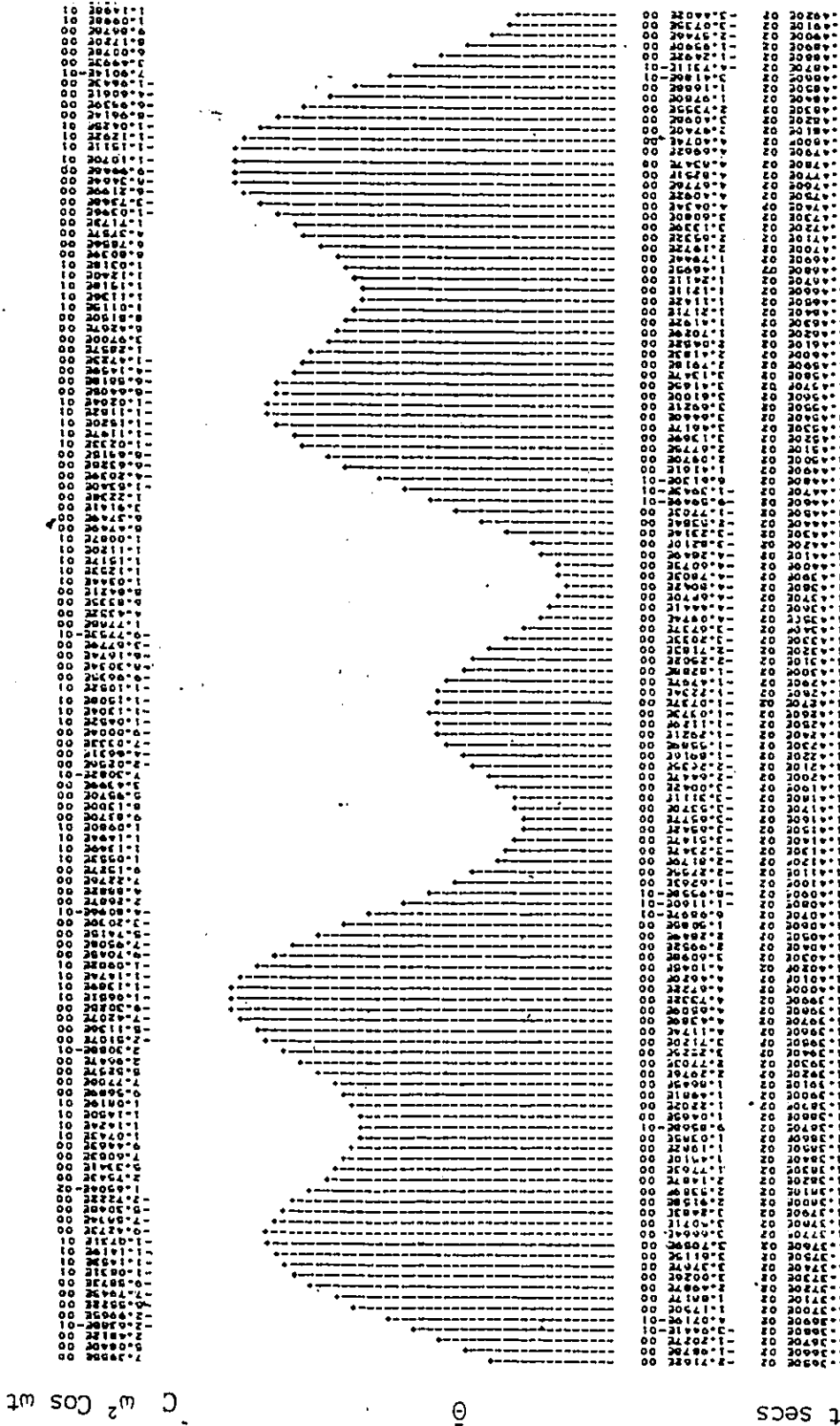


Figure 5.1.33 Digital Computer CSMP Output. 1/3rd Order Subharmonic Resonance Response for Symmetrical System ($\theta_1 = 0, \eta = 2.4$) Disturbing Torque = $C \omega^2 \text{Cos } \omega t$ ($Z' = 2.0$)

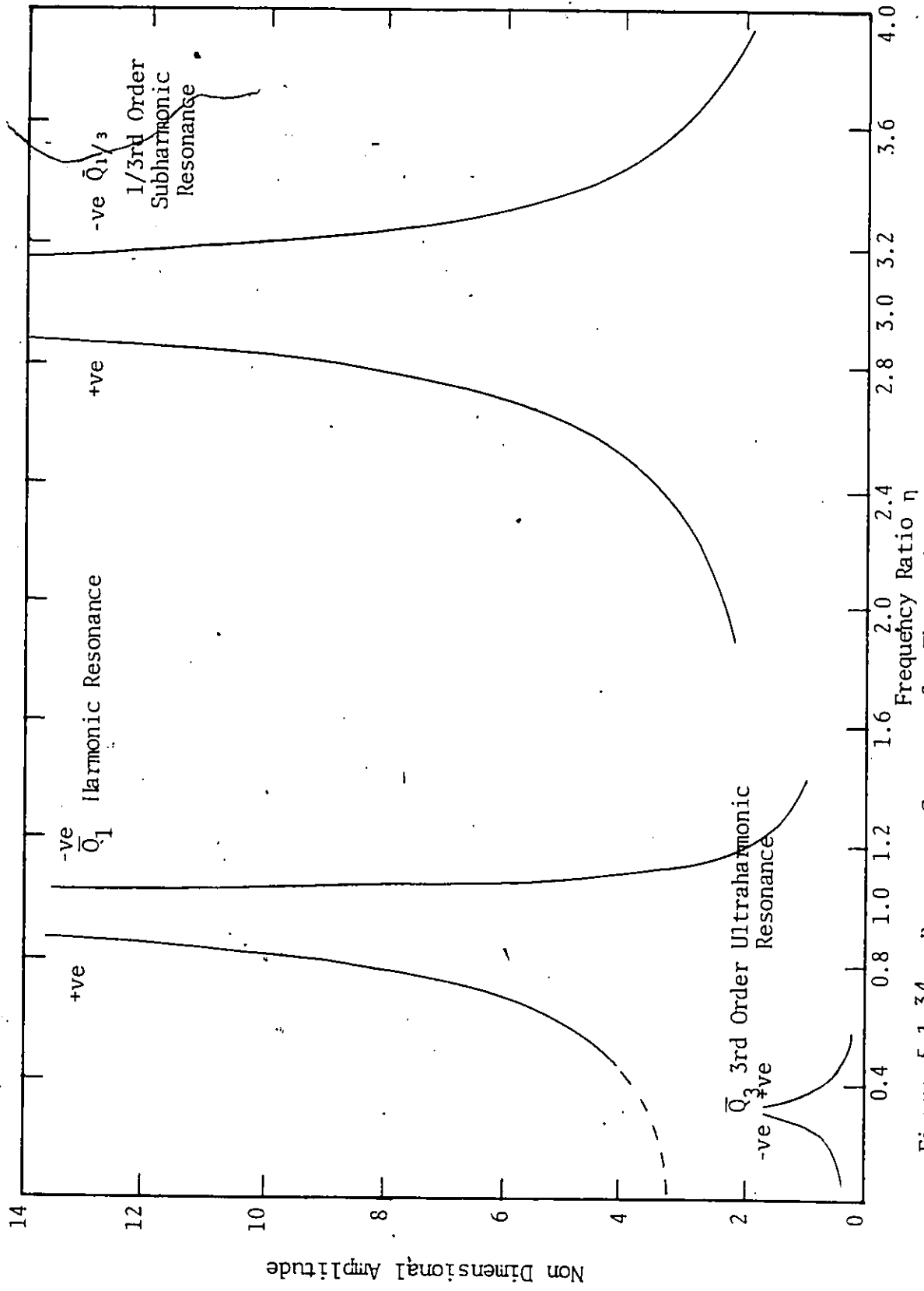


Figure 5.1.34 Resonance Spectrum for Theoretical Values of Main Components of Motion. Disturbing Torque = $T \cos \omega t$ ($S = 2.0$)

Shaker Pin
Displacement

Acceleration
Waveform at
Point 'P'

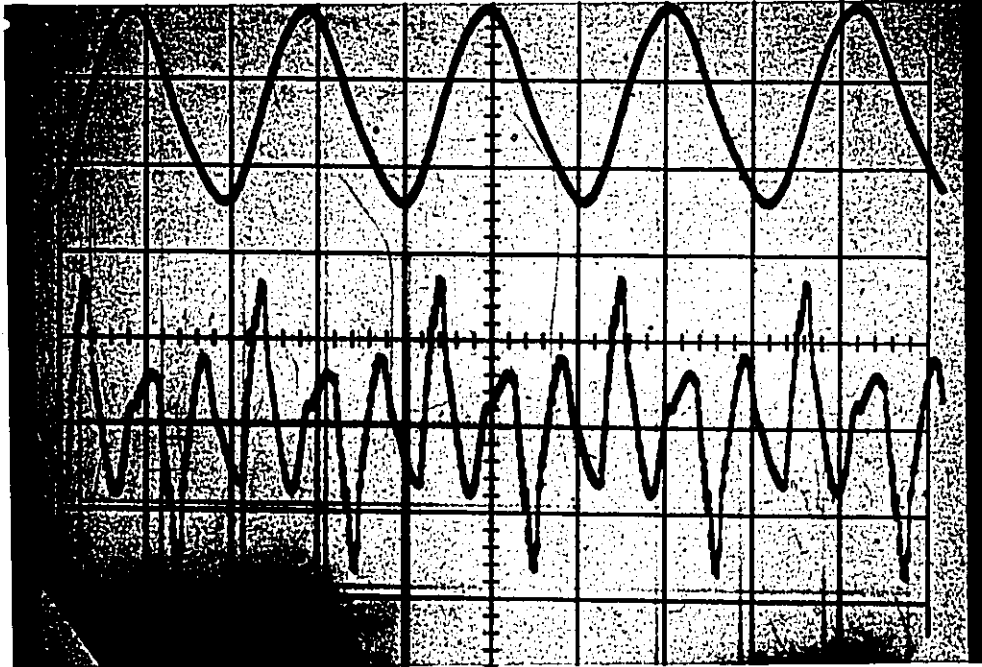


Figure 5.2.1 -Acceleration Waveform Display

$$f = 9.6 \text{ Hz}, p = 26.0 \text{ Hz},$$

$$\eta = 0.37, \bar{S} = 2.0$$

Shaker Pin
Displacement

Acceleration
Waveform at
Point 'P'

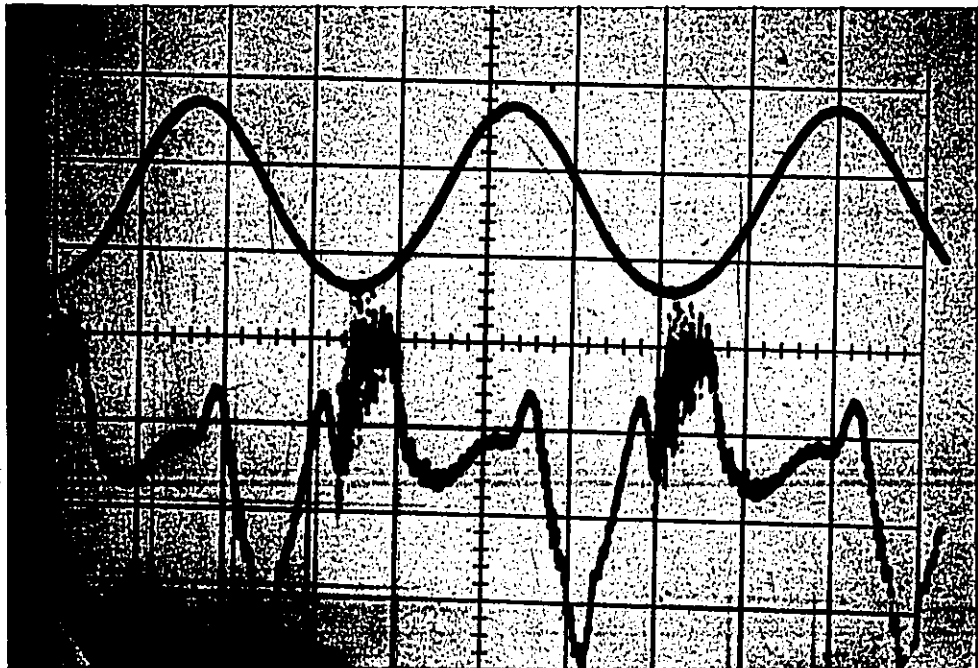


Figure 5.2.2 Acceleration Waveform Display

$$f = 13.8 \text{ Hz}, p = 26.0 \text{ Hz},$$

$$\eta = 0.53, \bar{S} = 2.0$$

Shaker pin
Displacement

Acceleration
Waveform at
Point 'P'

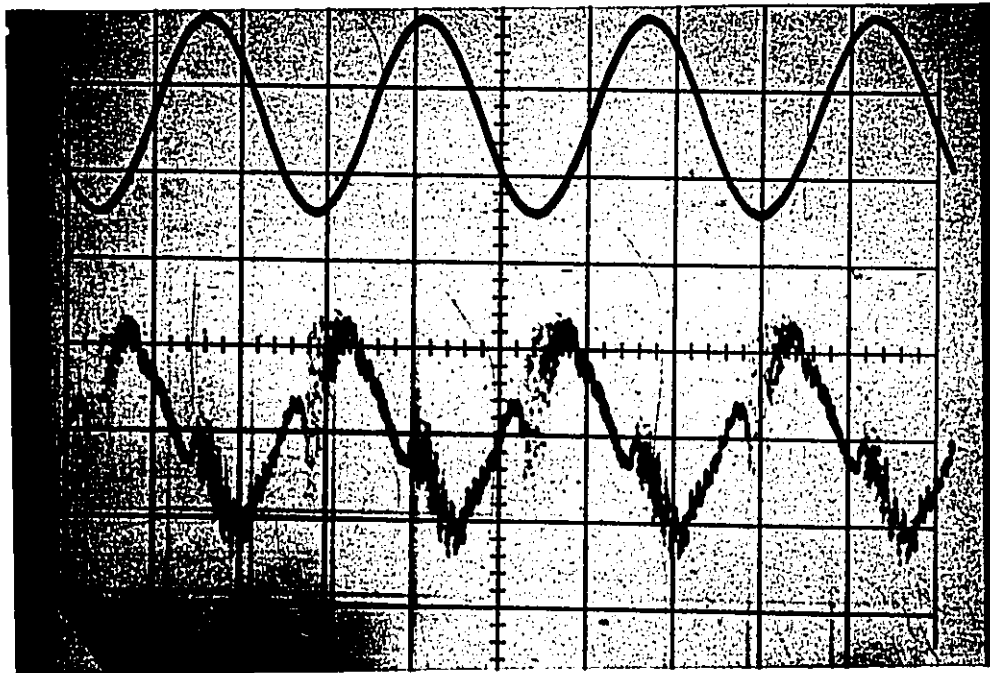


Figure 5.2.3 Acceleration Waveform Display

$$f = 19.9 \text{ Hz}, p = 26.0 \text{ Hz},$$

$$\eta = 0.76, \zeta = 2.0$$

Shaker Pin
Displacement

Acceleration
Waveform at
Point 'P'

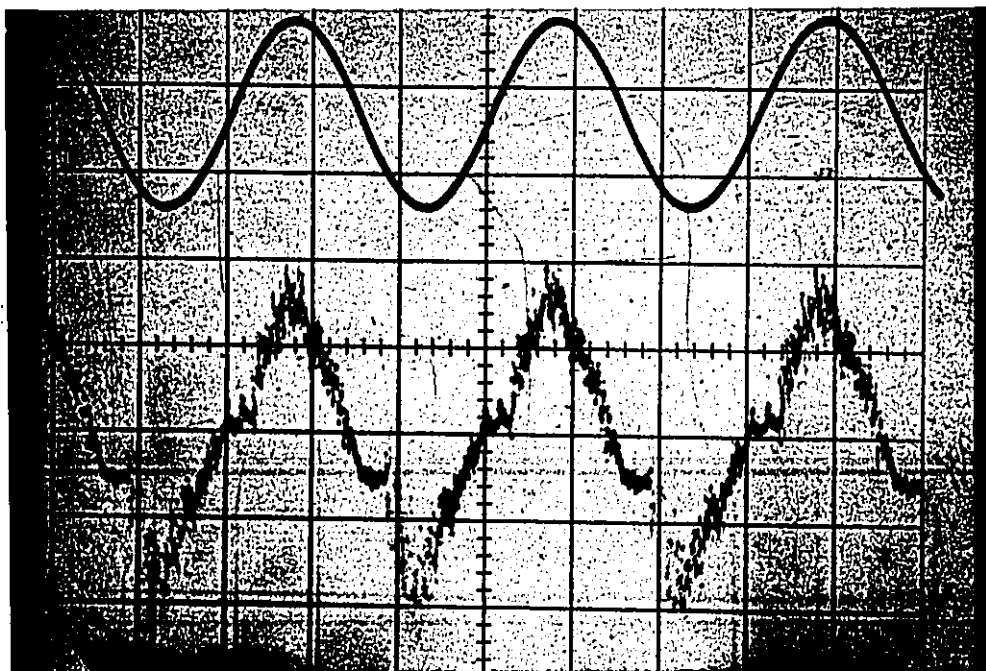


Figure 5.2.4 Acceleration Waveform Display

$$f = 33.3 \text{ Hz}, p = 26.0 \text{ Hz},$$

$$\eta = 1.28, \zeta = 2.0$$

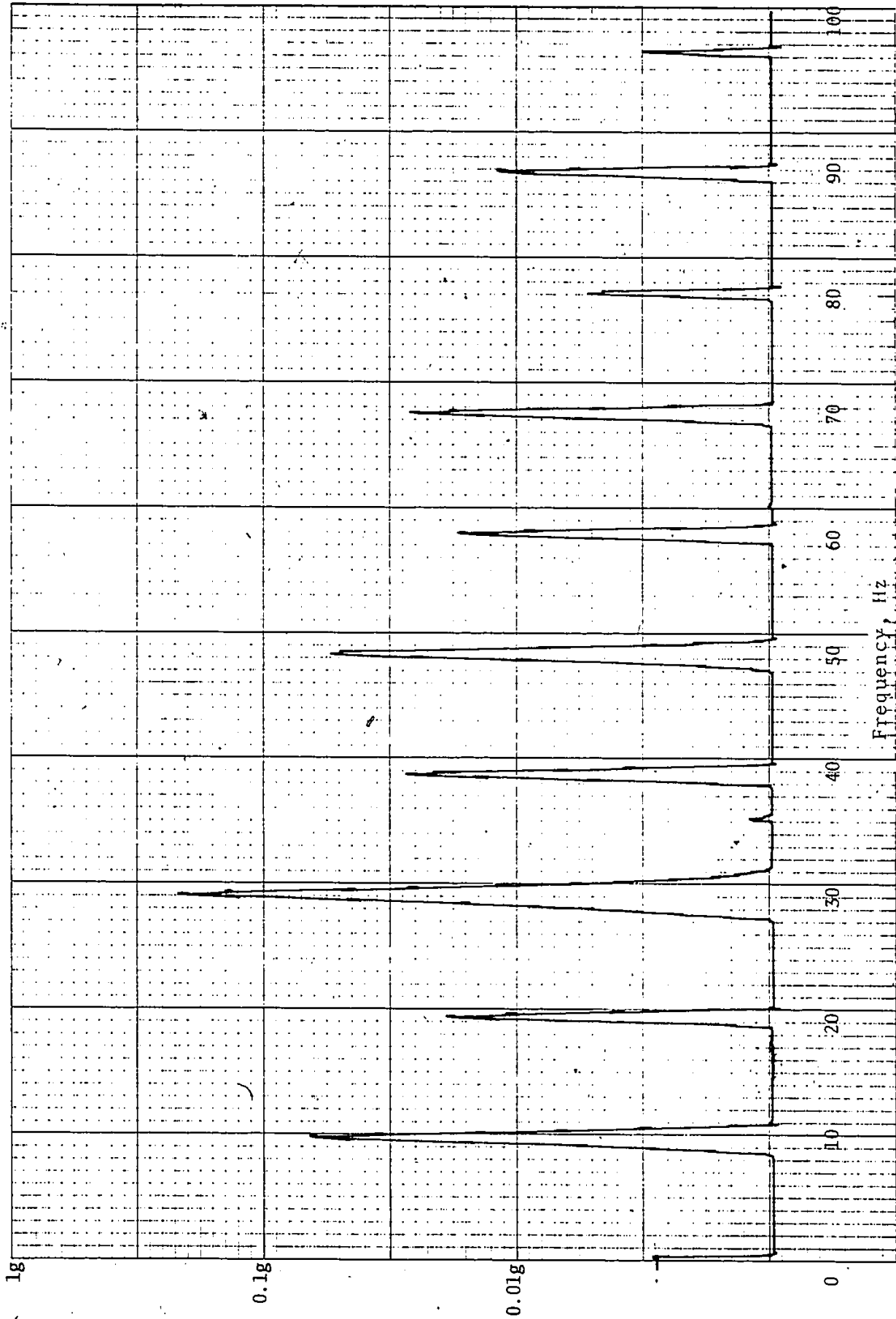


Figure 5.2.5 Frequency Spectrum of Acceleration At Point 'P' At $f = 9.6$ Hz, $\eta = 0.37$, $S_s = 2.0$

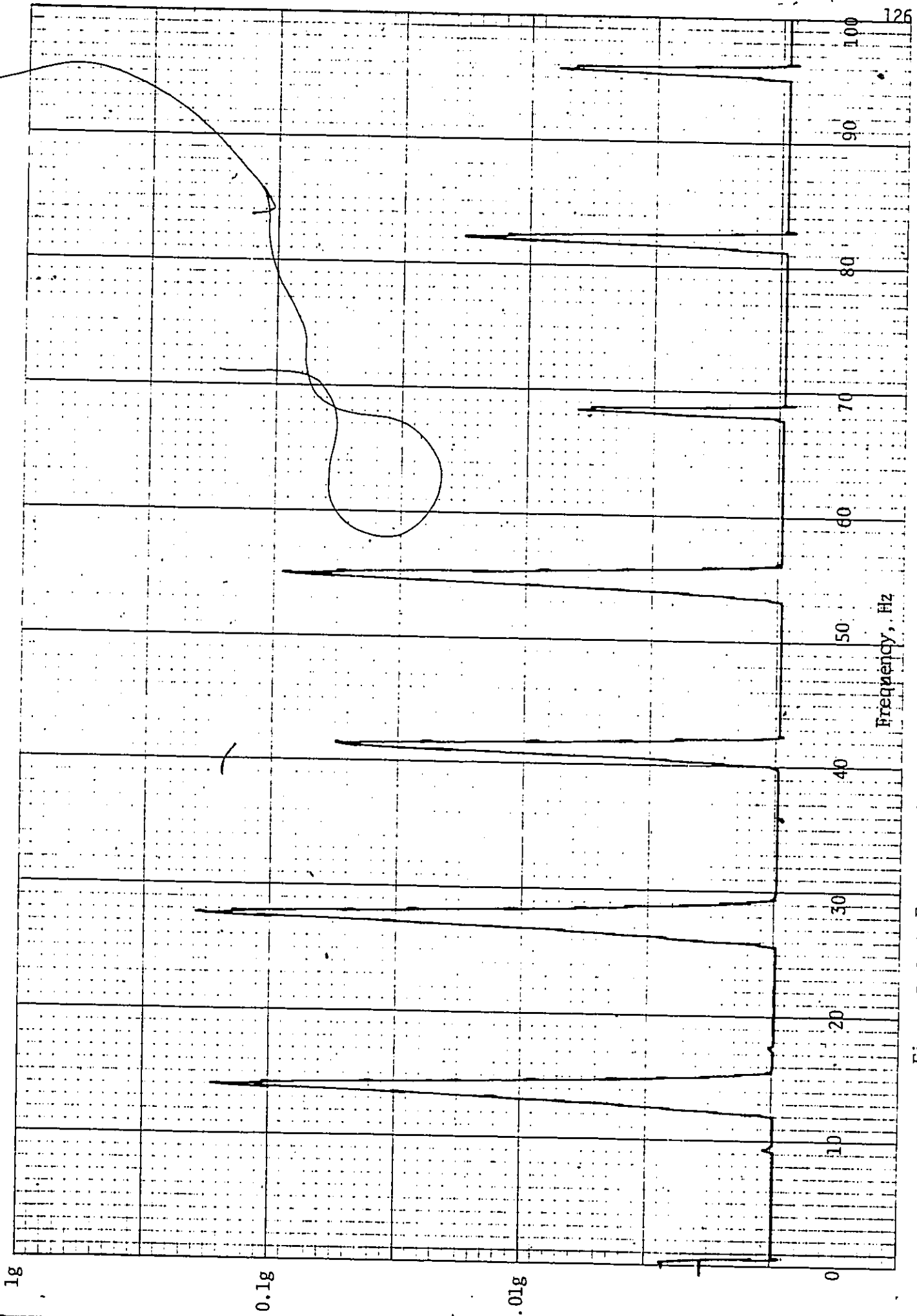


Figure 5.2.6 Frequency Spectrum of Acceleration At Point 'P' At $f = 13.8$ Hz, $\eta = 0.53$, $\bar{S} = 2.0$

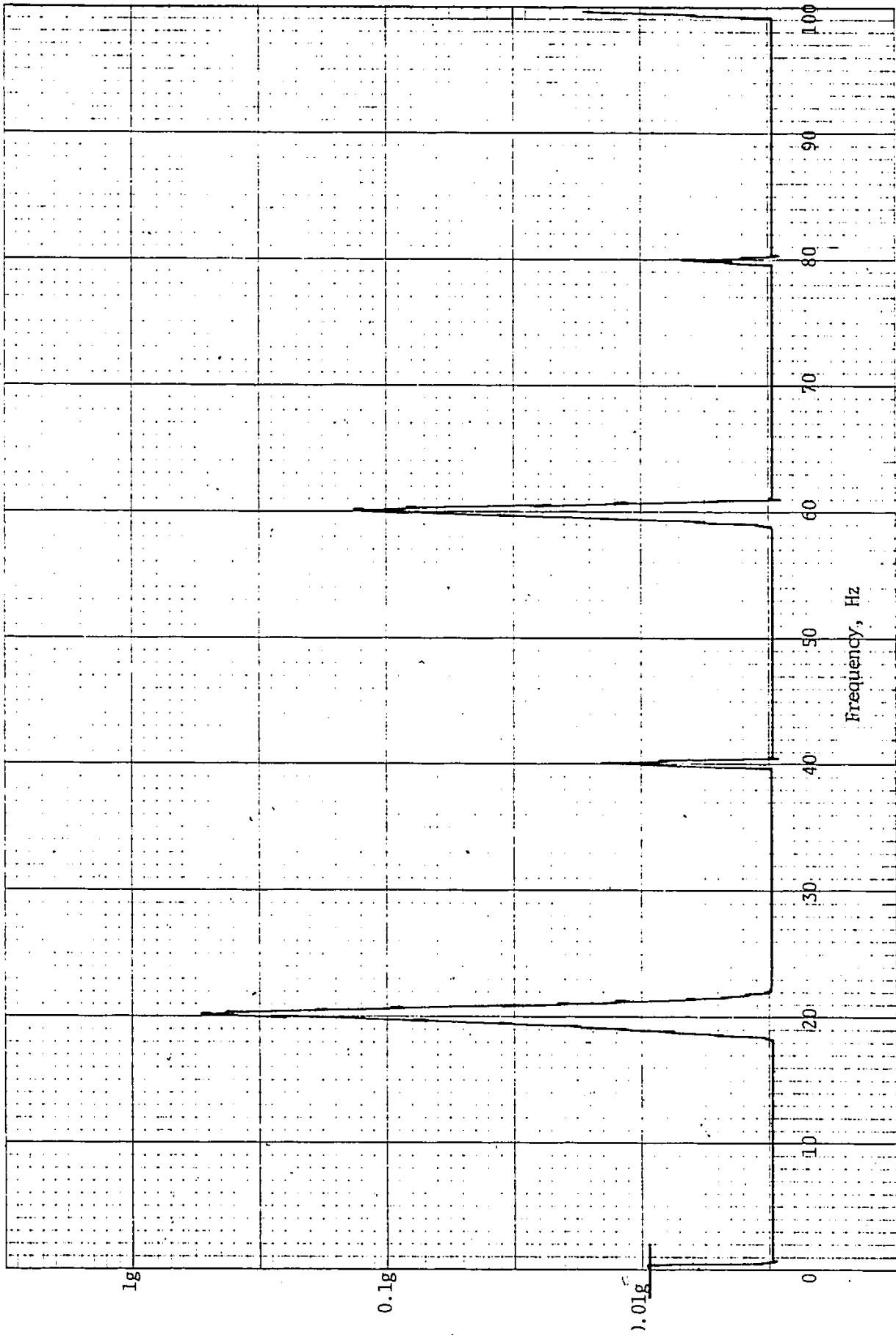


Figure 5.2.7 Frequency Spectrum of Acceleration At Point 'p' At $f = 19.9 \text{ Hz}$, $\eta = 0.76$, $\bar{S} = 2.0$

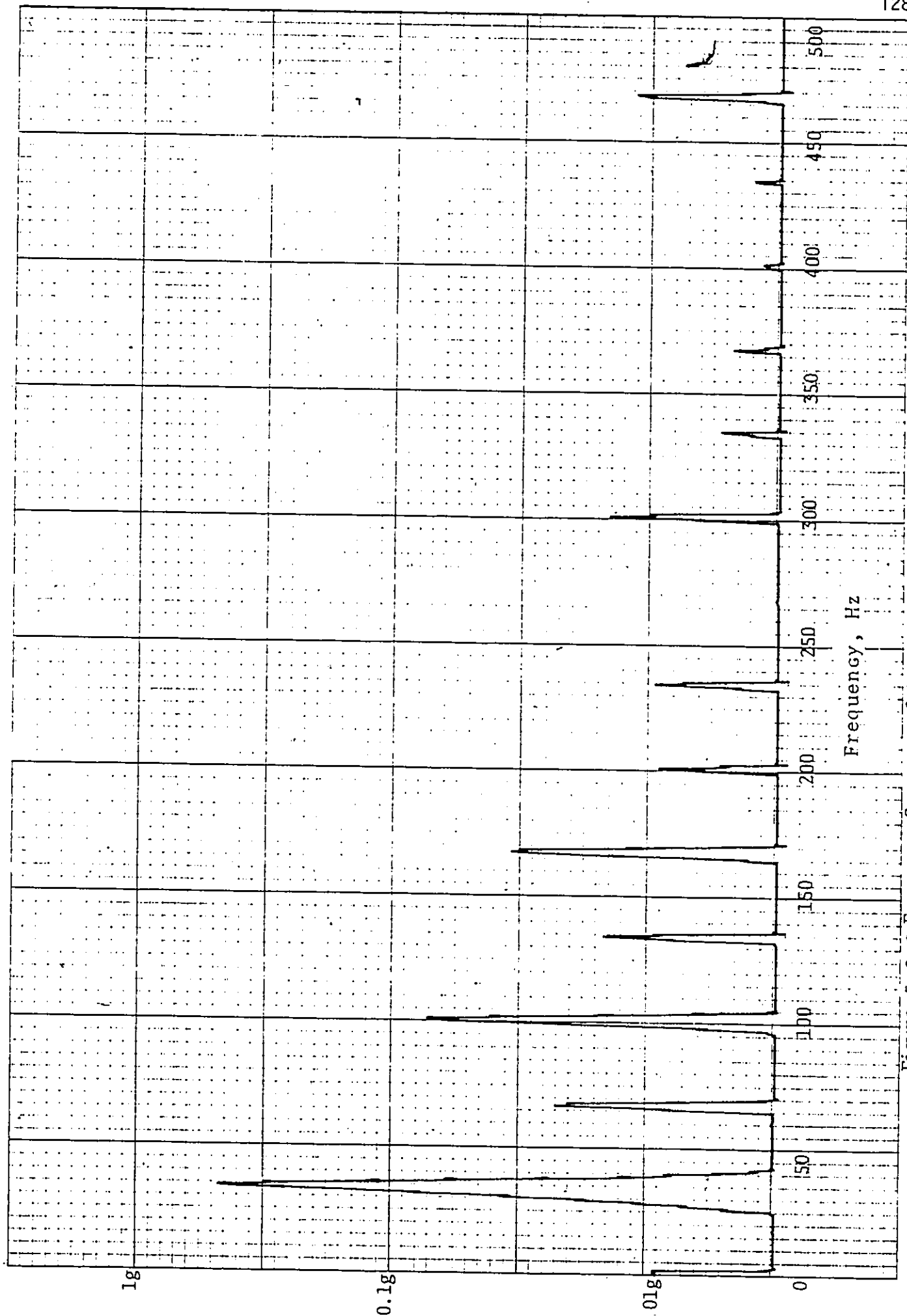


Figure 5.2.8 Frequency Spectrum of Acceleration At Point 'P' At $f = 33.3\text{Hz}$, $\eta = 1.28$, $S = 2.0$

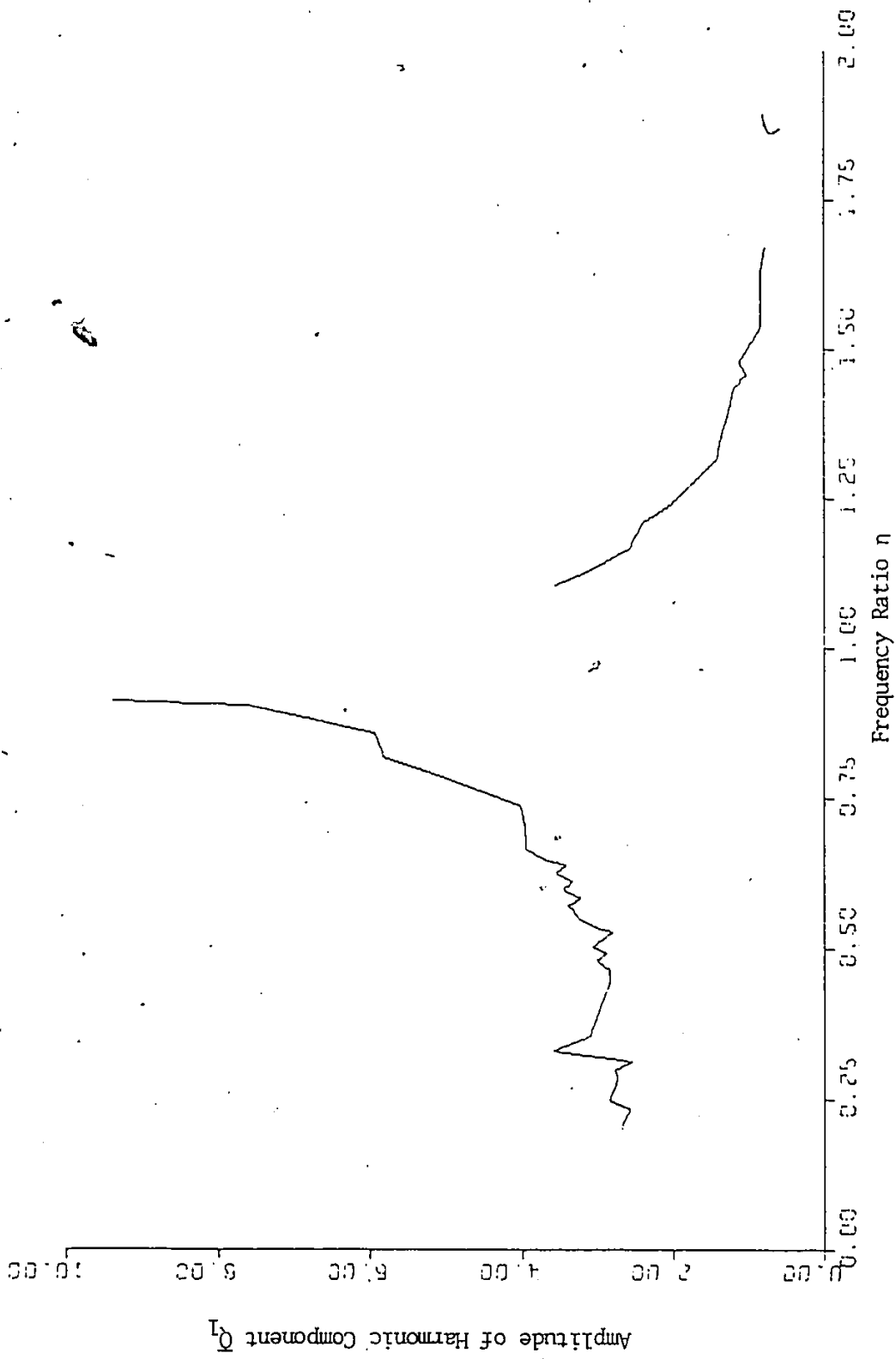


Figure 5.2.9 Experimental Results,
Plot \bar{Q}_1 Vs η , $S = 2.0$.

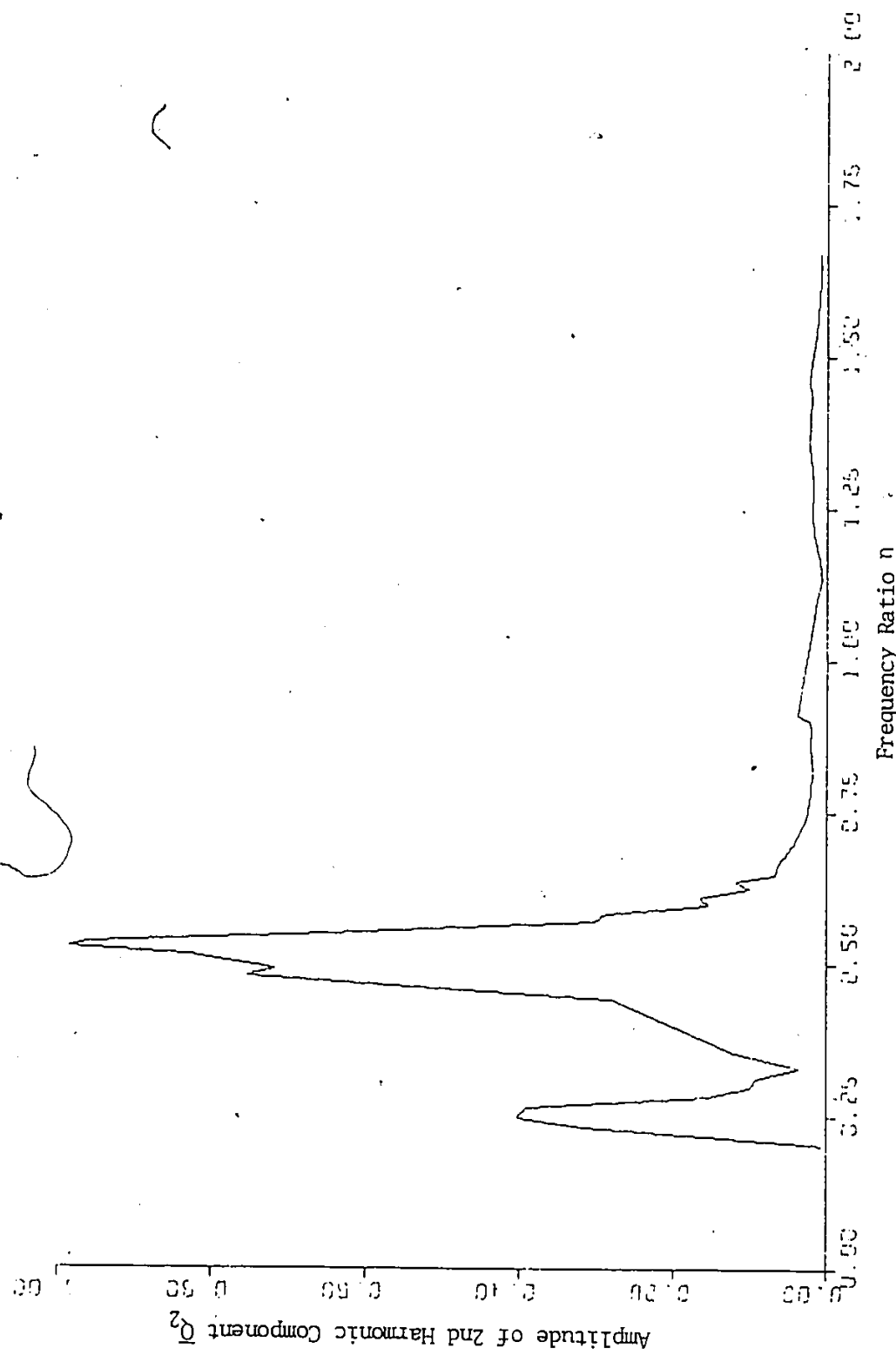


Figure 5.2.10 Experimental Results, Plot Q_2 Vs n , $\bar{S} = 2.0$

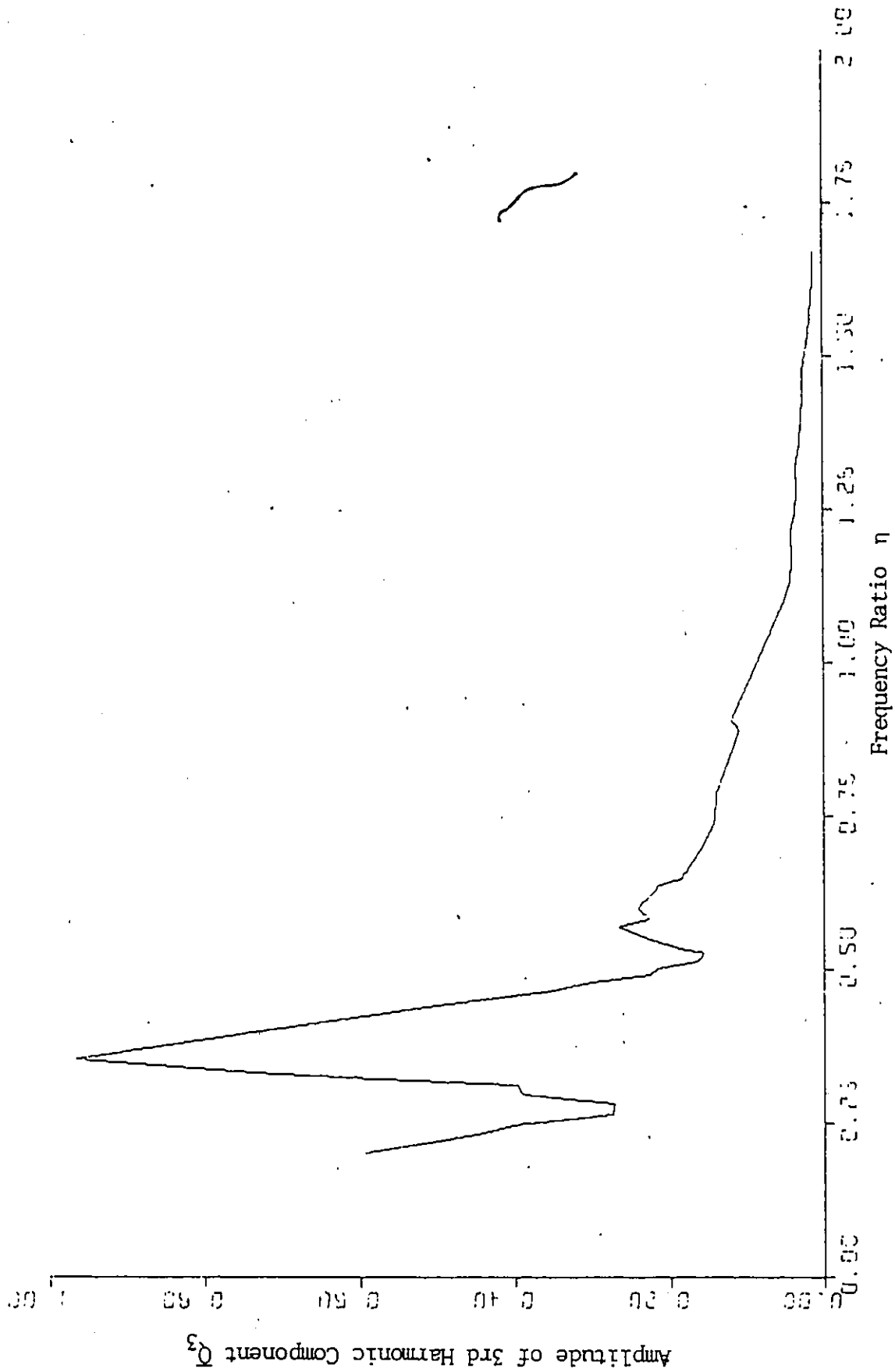


Figure 5.2.11 Experimental Results,
Plot Q_3 Vs η , $S = 2.0$.

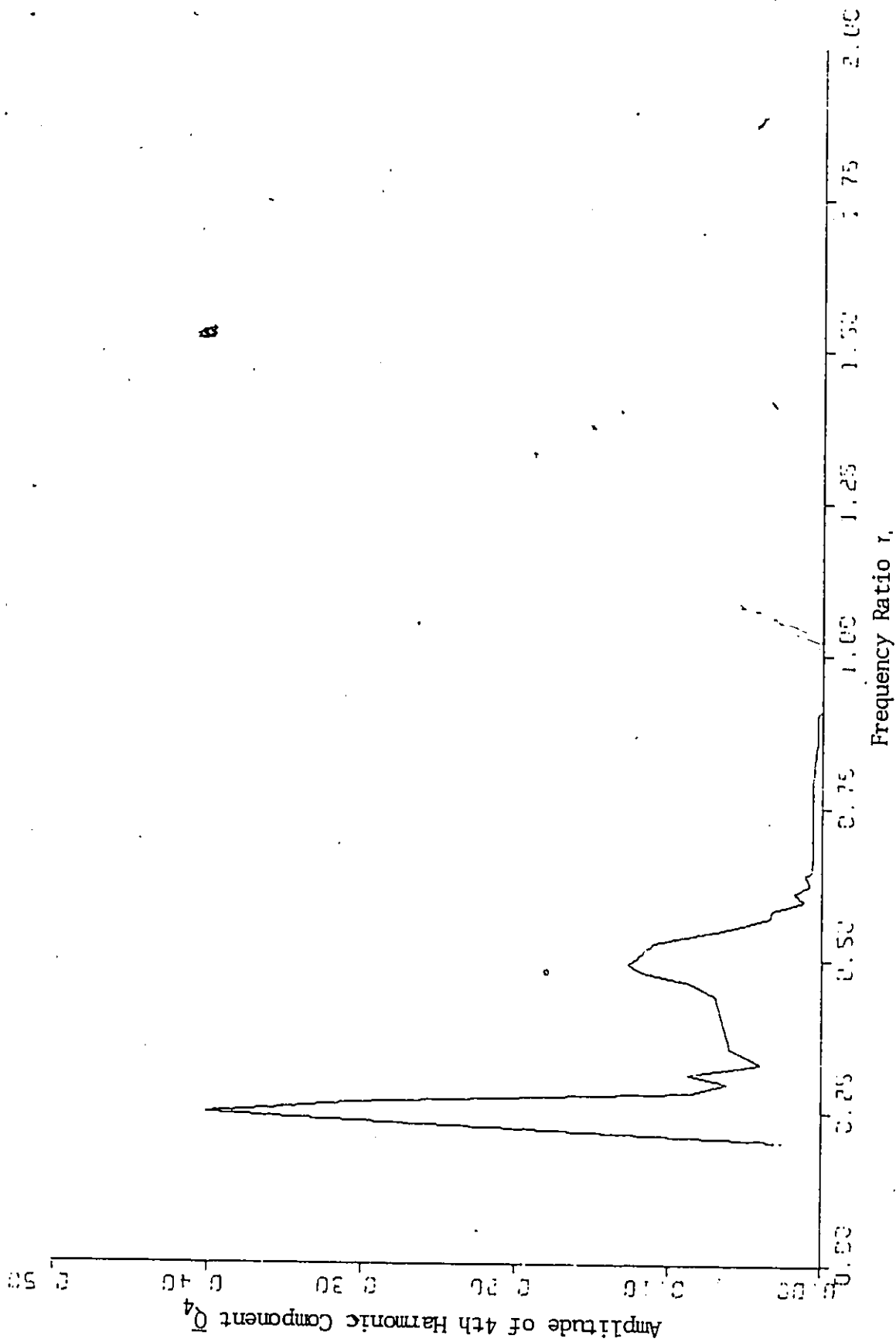


Figure 5.2.12. Experimental Results,
 Plot \bar{Q}_4 Vs η , $\bar{S} = 2.0$.

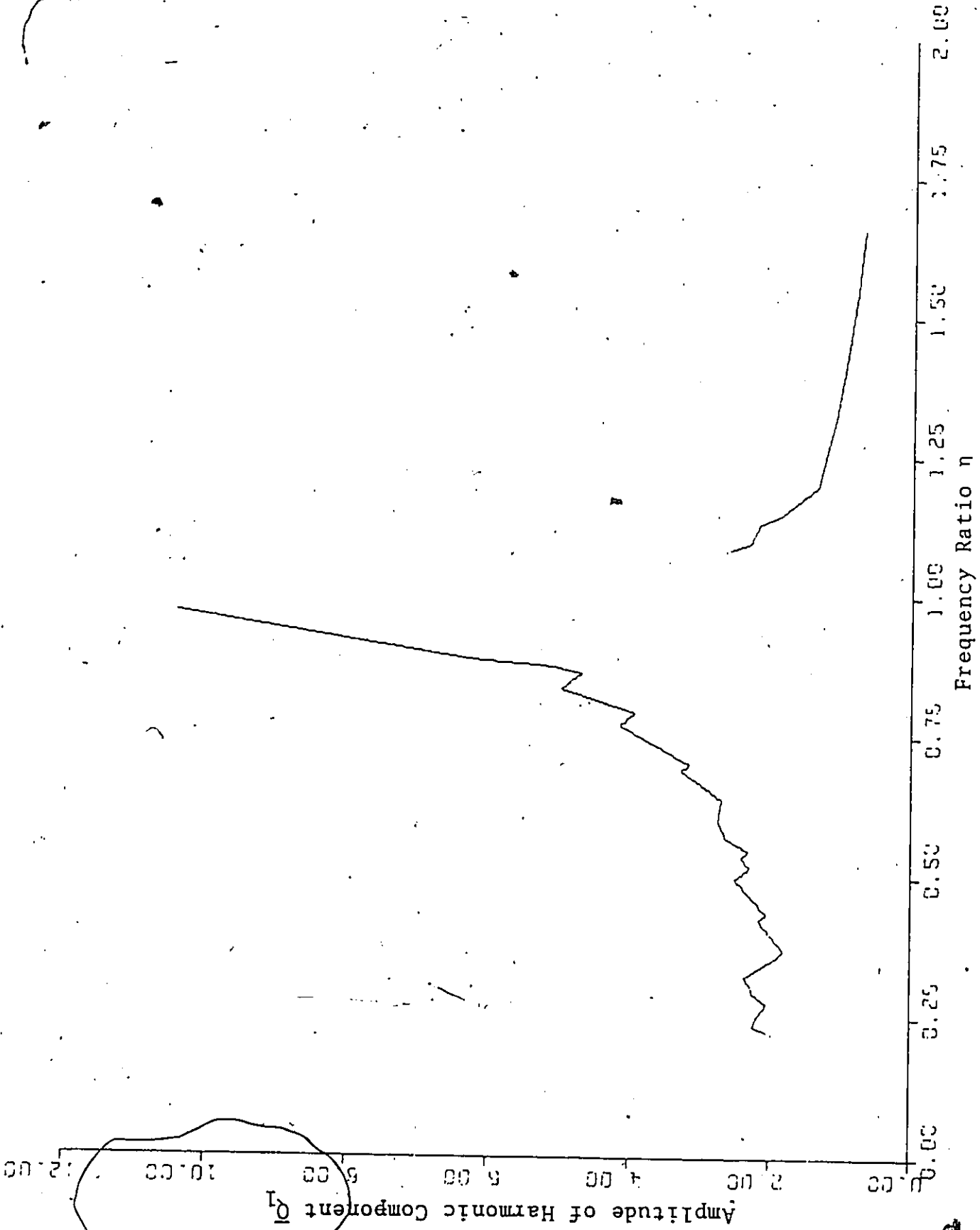


Figure 5.2.13 Experimental Results,
Plot Q_1 Vs η , $\bar{S} = 1.5$

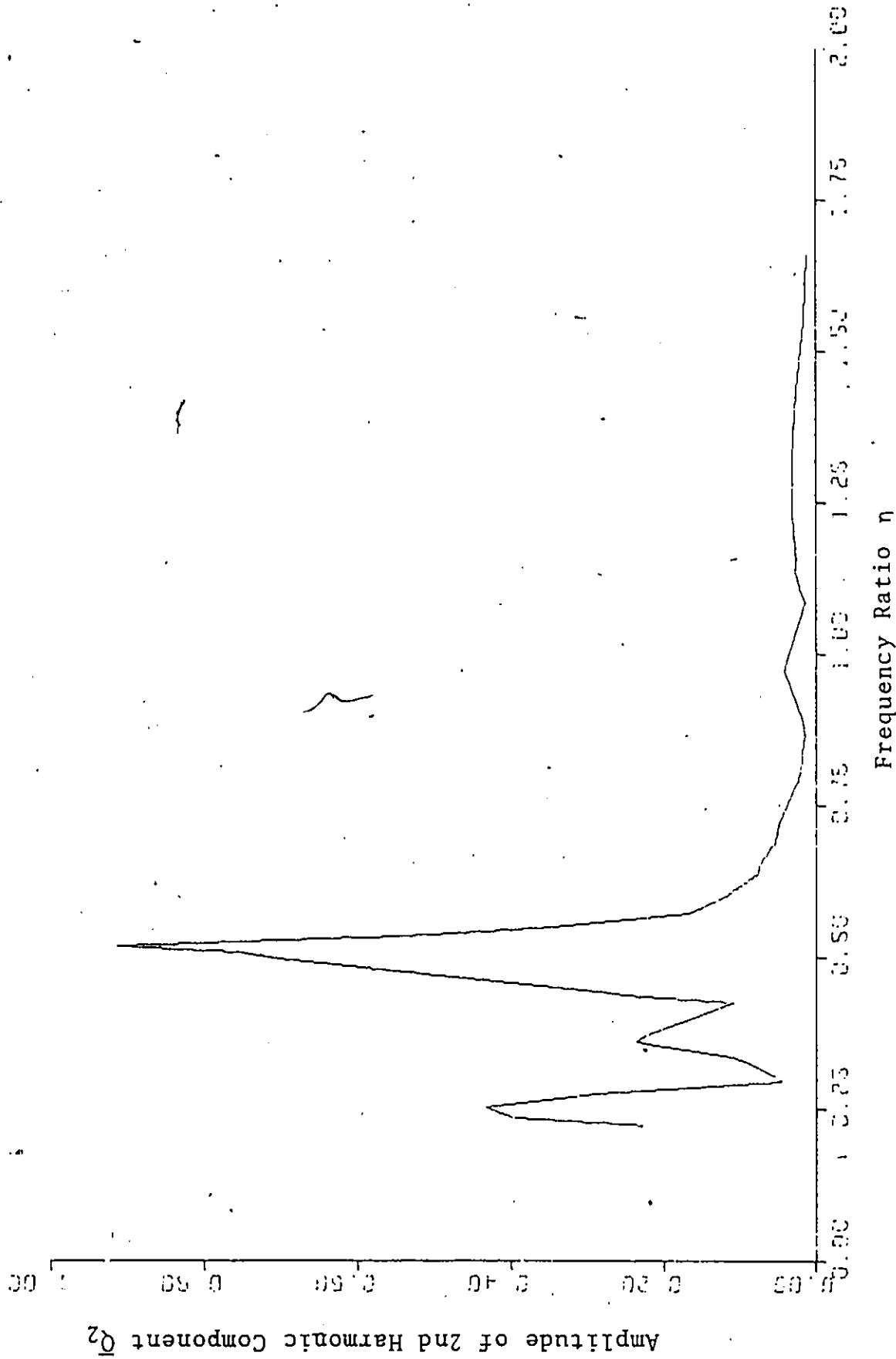


Figure 5.2.14 Experimental Results,
Plot \bar{Q}_2 Vs n , $\bar{S} = 1.5$

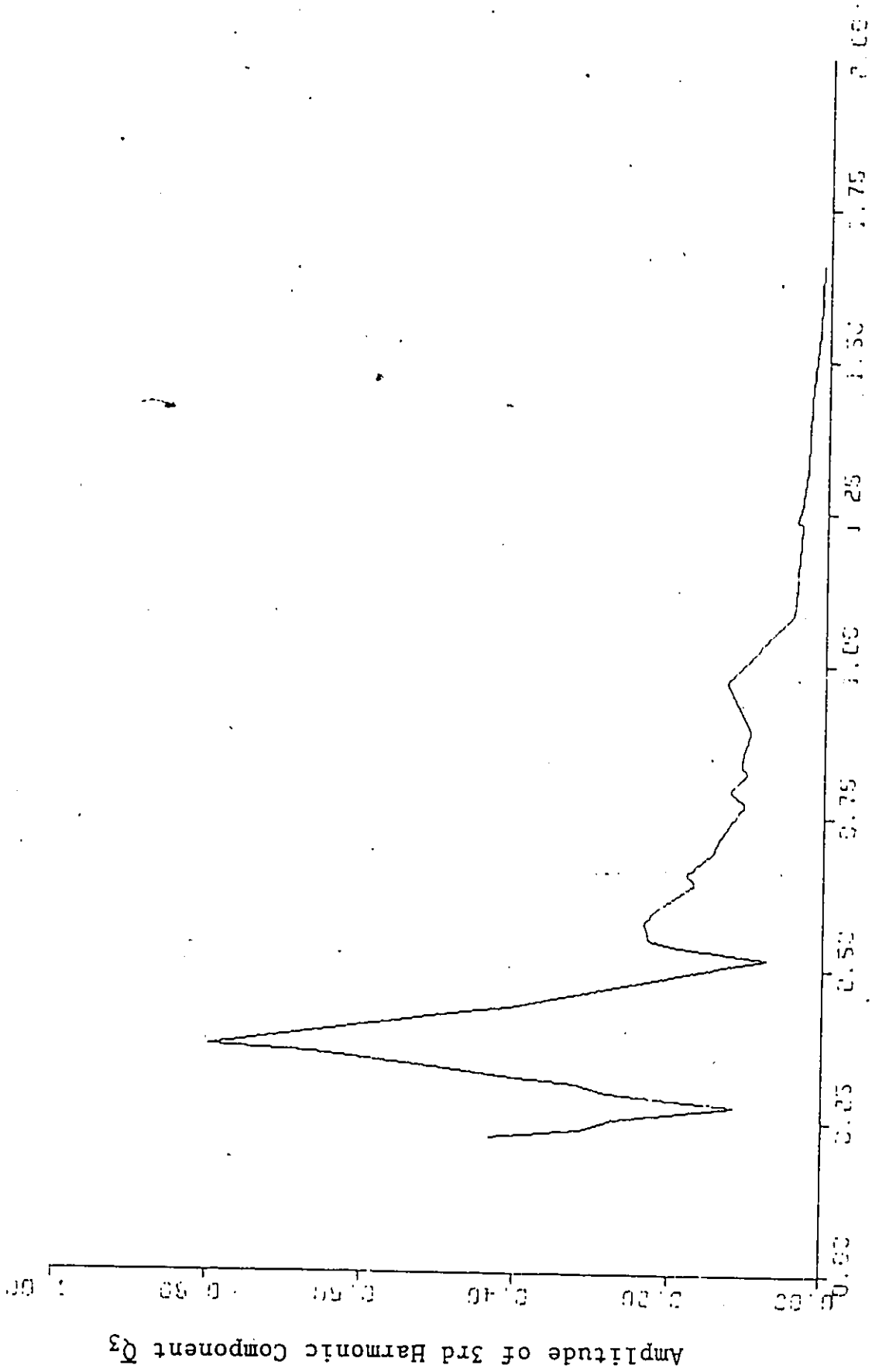


Figure 5.2.15 Experimental Results,
Plot Q_3 Vs n , $S = 1.5$

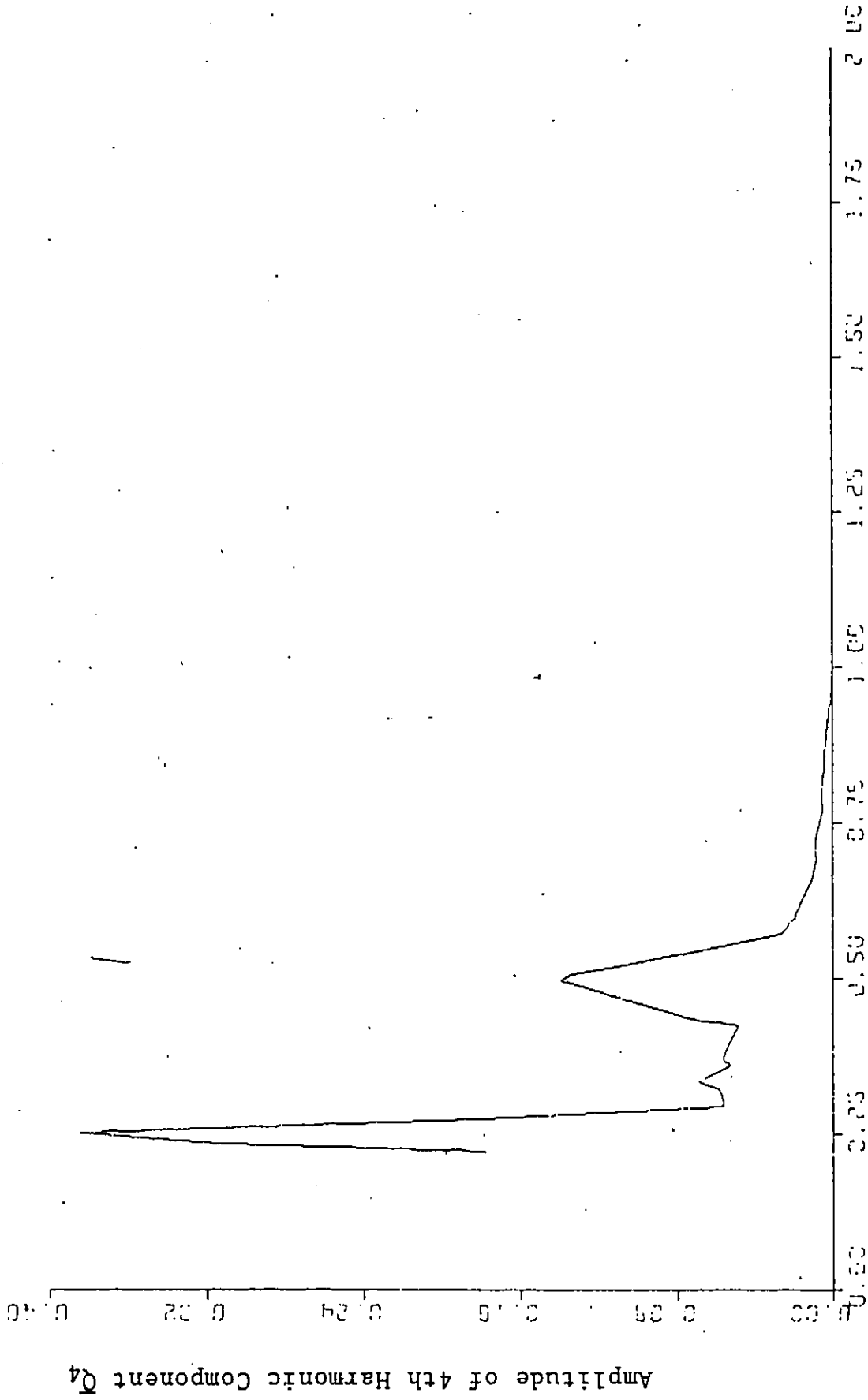


Figure 5.2.16 Experimental Results,
Plot \bar{Q}_4 Vs n , $\bar{S} = 1.5$.

Handwritten scribbles at the top of the page.

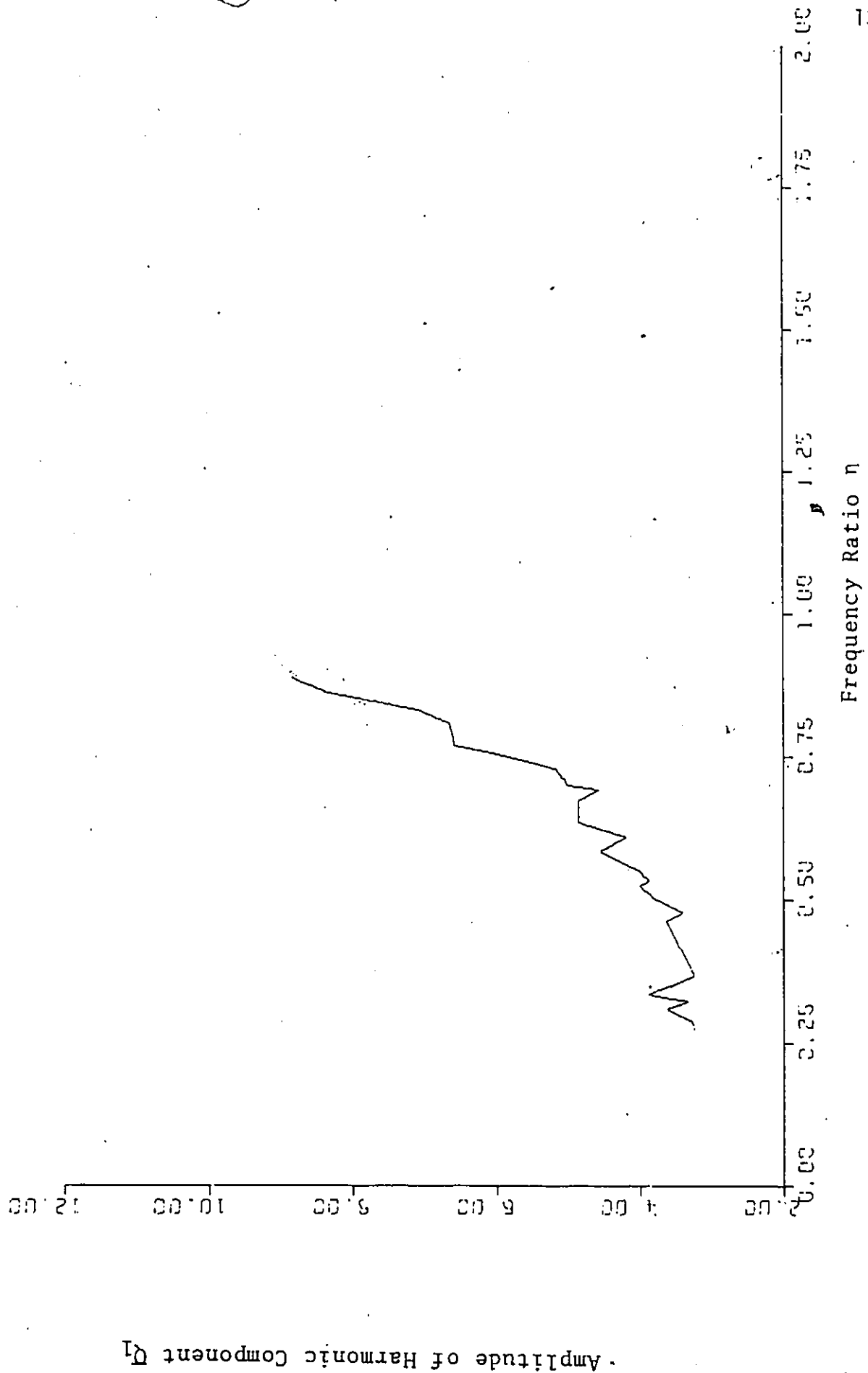


Figure 5.2.17 Experimental Results,
Plot Q_1 Vs n , $\bar{S} = 2.5$

Amplitude of Harmonic Component Q_1

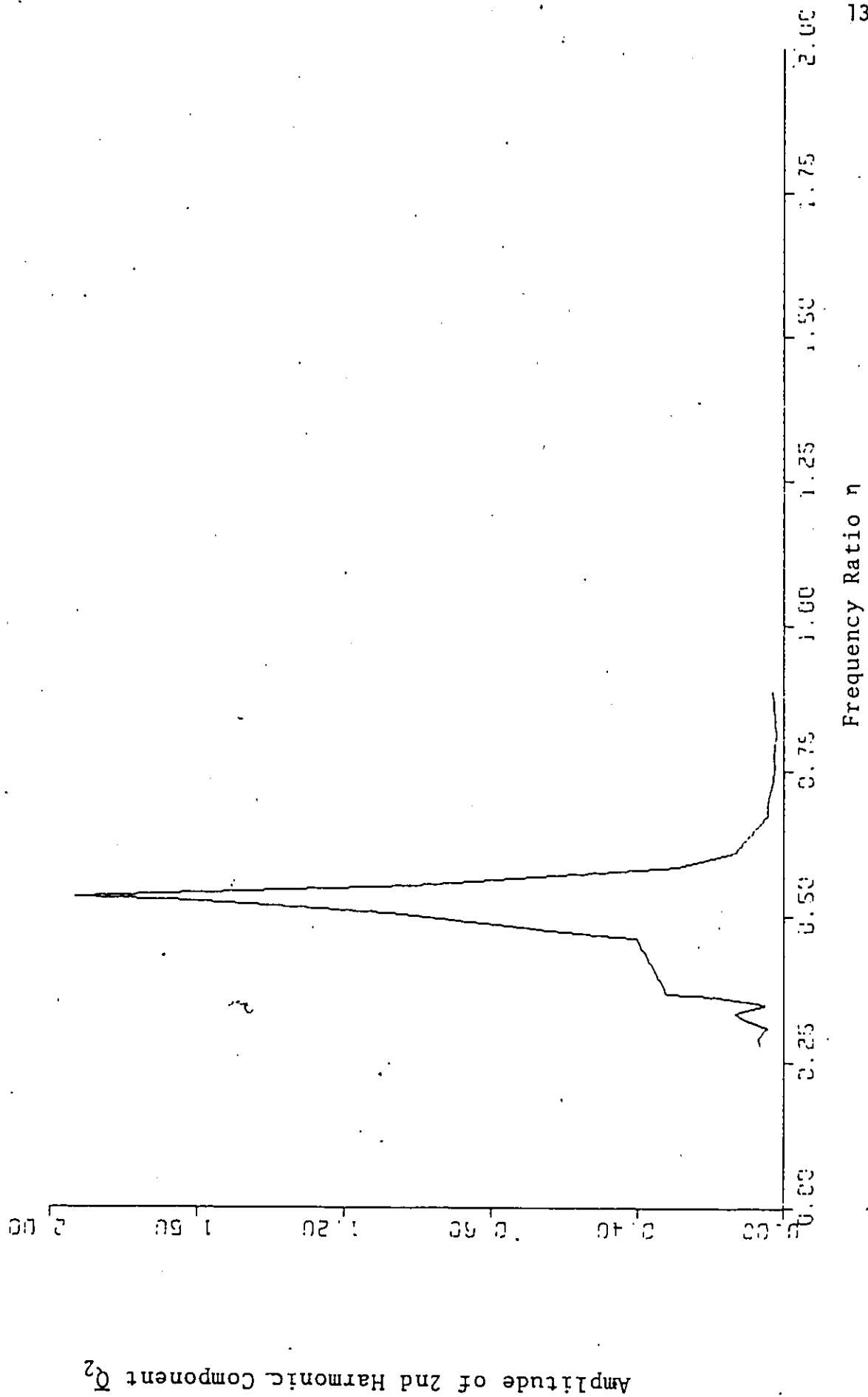


Figure 5.2.18 Experimental Results,
 Plot Q_2 Vs n , $\bar{S} = 2.5$

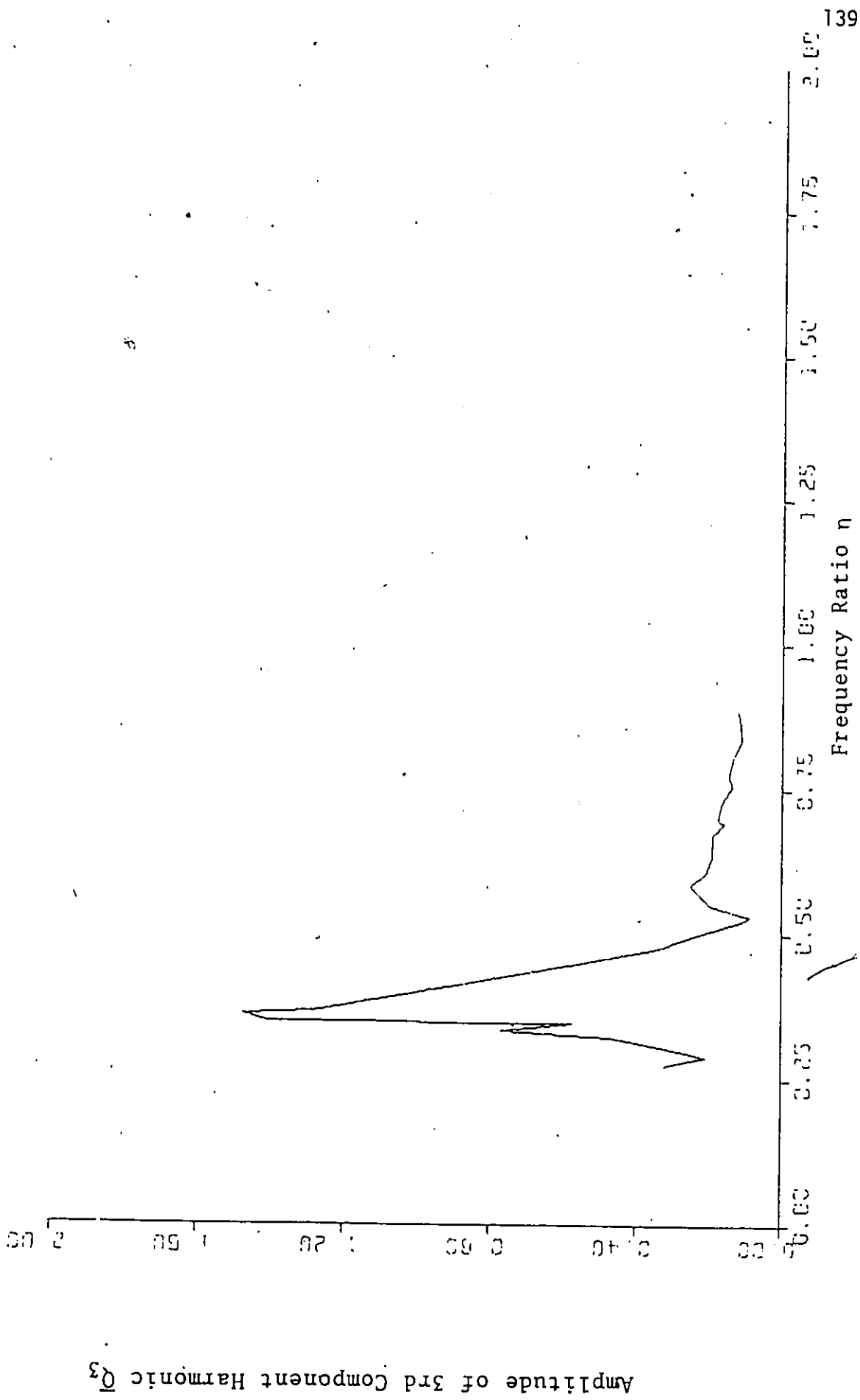


Figure 5.2.19 Experimental Results,
 Plot \bar{Q}_3 Vs n , $\bar{S} = 2.5$.

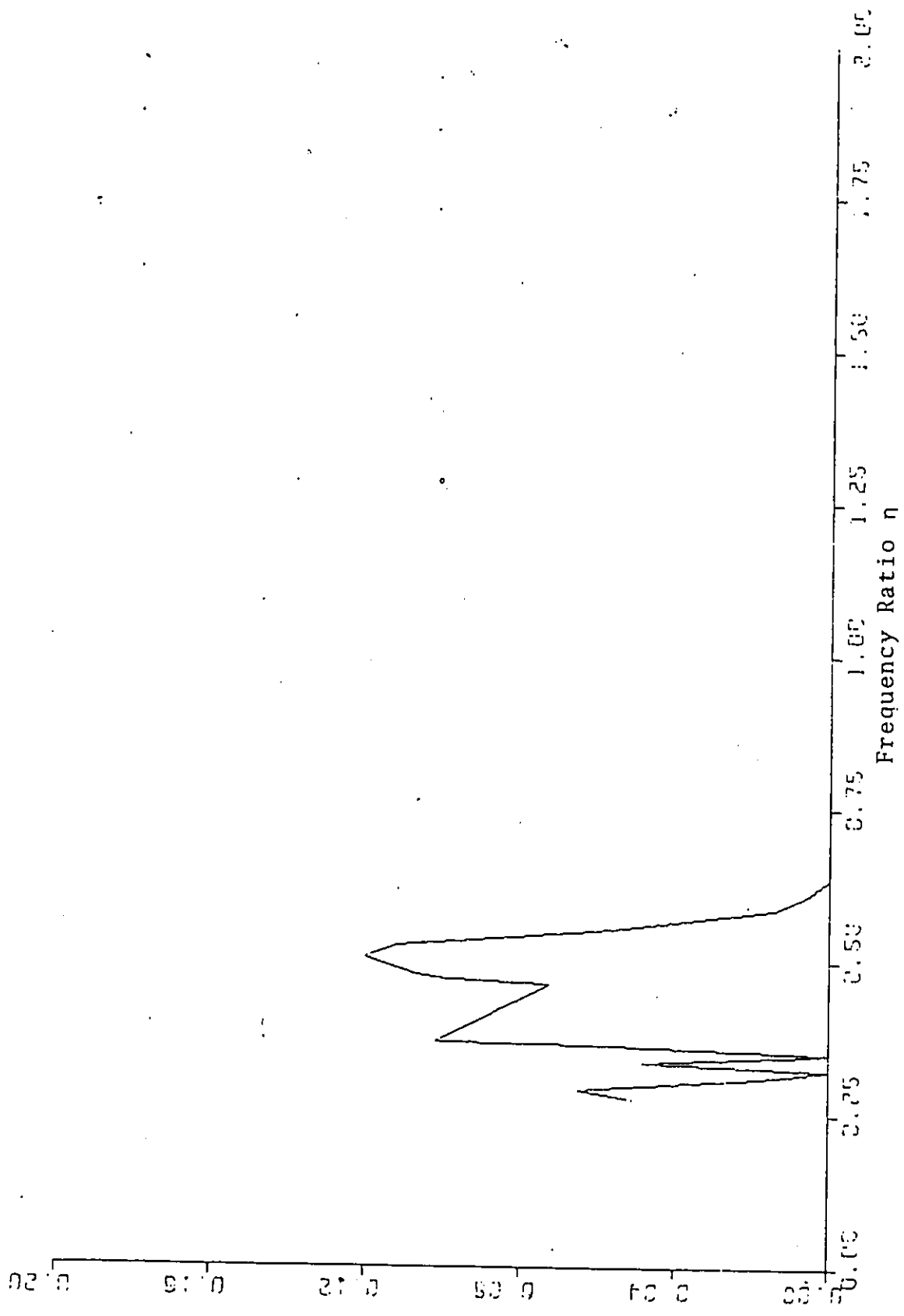


Figure 5.2.20 Experimental Results,
Plot Q_4 vs η , $\bar{S} = 2.5$.

Amplitude of 4th Harmonic Component Q_4

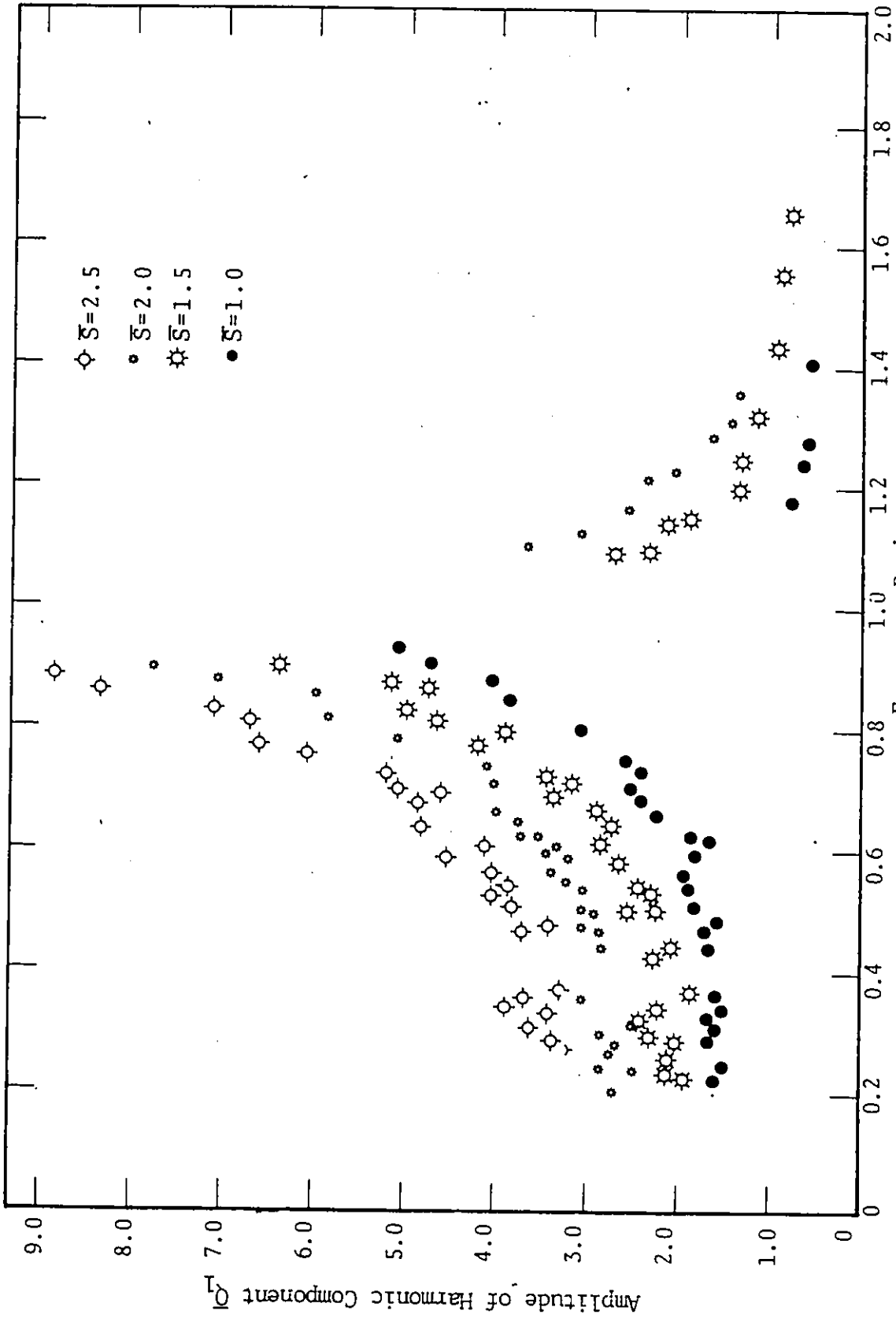


Figure 5.2.21 Experimental Results

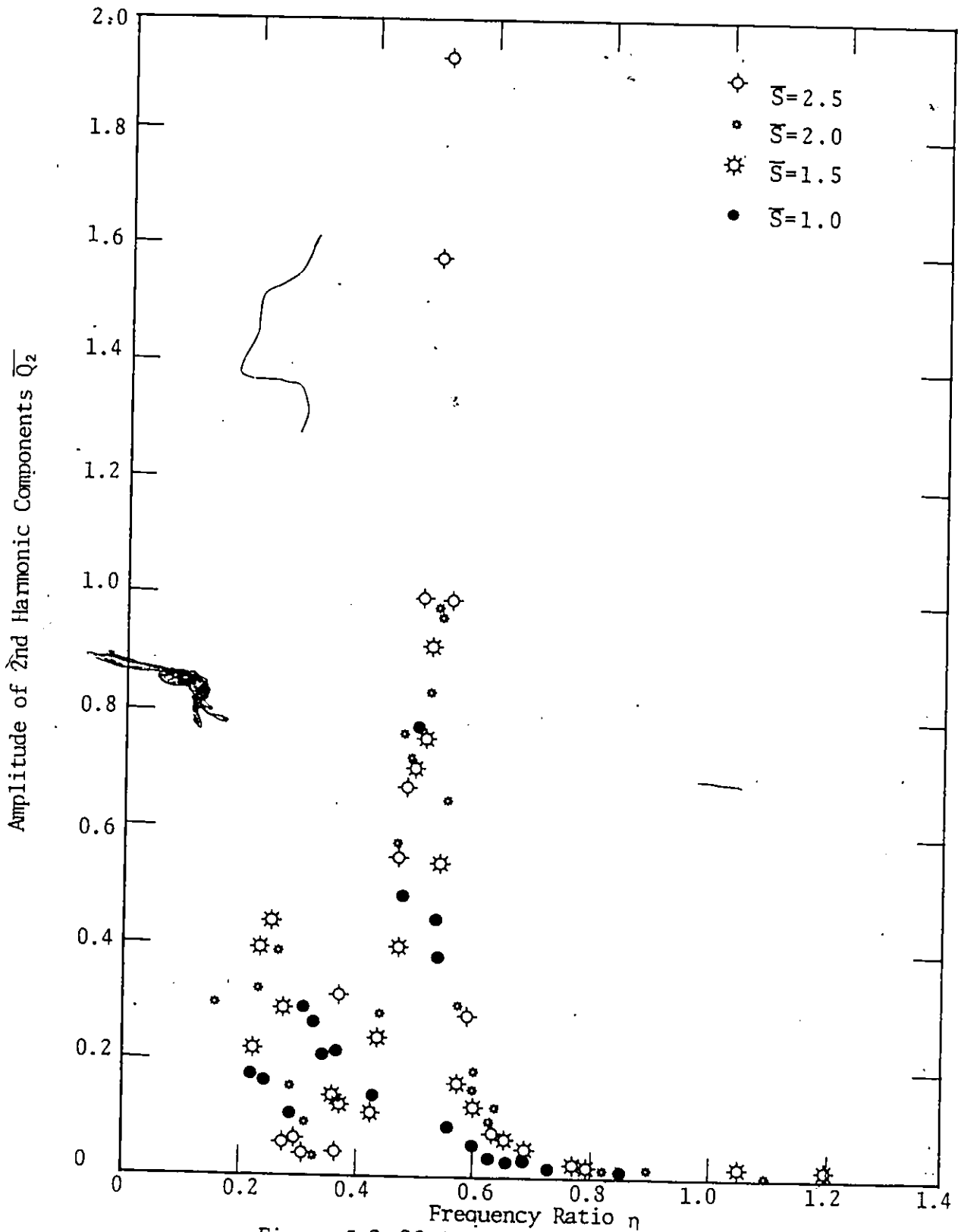


Figure 5.2.22 Experimental Results

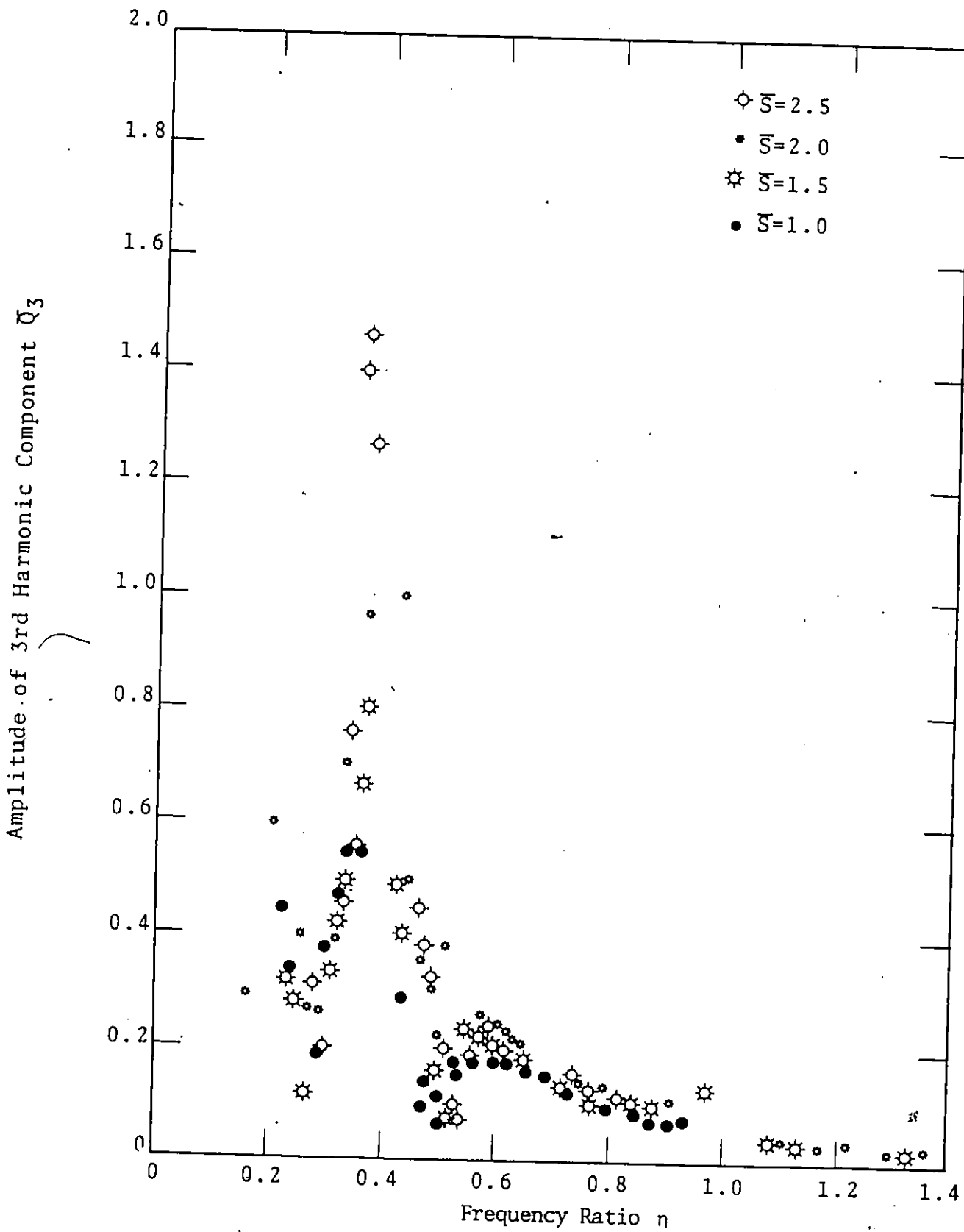


Figure 5.2.23 Experimental Results

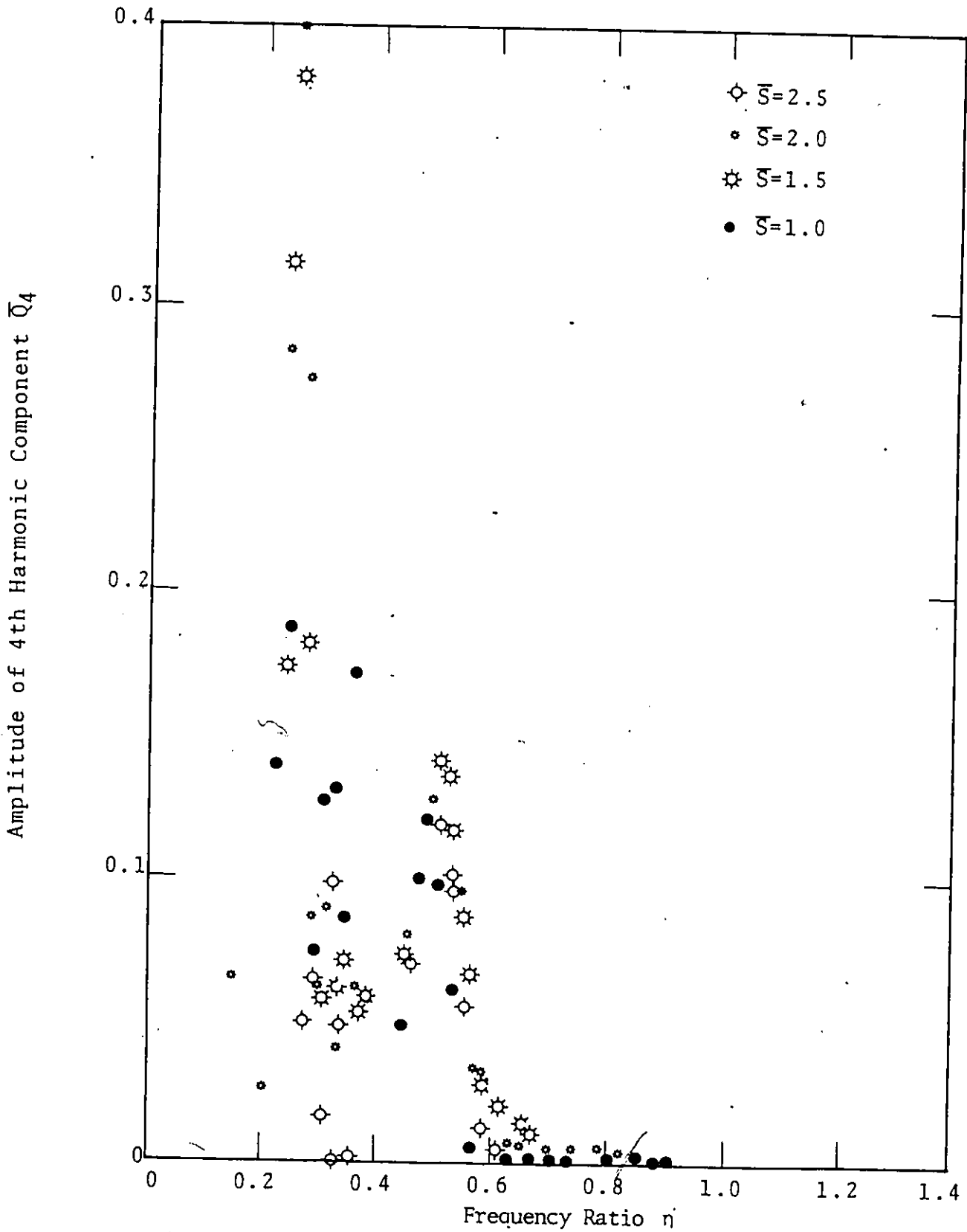


Figure 5.2.24 Experimental Results

APPENDIX I

ANALYTICAL SOLUTION DEVELOPMENT

I.1 SYSTEM RESPONSE TO A DISTURBING TORQUE OF TYPE

$T \cos \omega t$

General solutions for the asymmetrical case are derived here. These can be modified for the special case of a symmetrical system by omitting $\bar{\theta}_1$ from the solution.

I.1.1 HARMONIC RESONANCE:

Rewriting equations (3.1.A.1) through (3.1.A.3) in the following form:

$$\begin{aligned} E_1(\theta) &= J\ddot{\theta} + K\theta - T_0 - T \cos \omega t = 0 \\ E_2(\theta) &= J\ddot{\theta} - T_0 - T \cos \omega t = 0 \\ E_3(\theta) &= J\ddot{\theta} + K[\theta - \{ -(2\theta_0 + \theta_1) \}] - T_0 \lesssim T \cos \omega t = 0 \end{aligned} \quad (\text{I.1.1.1})$$

The simplest form of the solution, which can be assumed in this case is:

$$\tilde{\theta} = M + Q_1 \cos \omega t \quad (\text{I.1.1.2})$$

Substituting (I.1.1.2) for the approximate value of the displacement ($\tilde{\theta}$) in (I.1.1.1). The resulting equation is defined as $E(\tilde{\theta})$, in order to simplify the notation. Applying the Ritz averaging method, the following equations are obtained:

$$\begin{aligned} \int_0^{2\pi} E(\tilde{\theta}) d(\omega t) &= 0 \\ \int_0^{2\pi} E(\tilde{\theta}) \cos \omega t d(\omega t) &= 0 \end{aligned} \quad (\text{I.1.1.3})$$

In equation (I.1.1.3) $E(\tilde{\theta})$ is represented by $E_1(\tilde{\theta})$ between limits 0 to τ_1 , $E_2(\tilde{\theta})$ between τ_1 to τ_2 and $E_3(\tilde{\theta})$ between τ_2 and π . The $E_1(\tilde{\theta})$, $E_2(\tilde{\theta})$ and $E_3(\tilde{\theta})$ are expressed as:

$$E_1(\tilde{\theta}) = -J\omega^2 Q_1 \text{Cos } \omega t + K(M+Q_1 \text{Cos } \omega t) - T_0 - \bar{T} \text{Cos } \omega t = 0$$

$$E_2(\tilde{\theta}) = -J\omega^2 Q_1 \text{Cos } \omega t - T_0 - T \text{Cos } \omega t = 0$$

$$E_3(\tilde{\theta}) = -J\omega^2 Q_1 \text{Cos } \omega t + K(M+Q_1 \text{Cos } \omega t) + K(2\theta_0 + \theta_1) - T_0 - T \text{Cos } \omega t = 0$$

Referring to figure 3.1.1.2, equation (I.1.1.3) can be written in complete form as:

$$2 \int_0^{\tau_1} E_1(\tilde{\theta}) d(\omega t) + 2 \int_{\tau_1}^{\tau_2} E_2(\tilde{\theta}) d(\omega t) + 2 \int_{\tau_2}^{\pi} E_3(\tilde{\theta}) d(\omega t) = 0 \quad (\text{I.1.1.4})$$

$$2 \int_0^{\tau_1} E_1(\tilde{\theta}) \text{Cos } \omega t d(\omega t) + 2 \int_{\tau_1}^{\tau_2} E_2(\tilde{\theta}) \text{Cos } \omega t d(\omega t) + 2 \int_{\tau_2}^{\pi} E_3(\tilde{\theta}) \text{Cos } \omega t d(\omega t) = 0 \quad (\text{I.1.1.5})$$

Integration of expressions (I.1.1.4) and (I.1.1.5) yields two non-linear algebraic equations. From equation (I.1.1.4):

$$\bar{M} = \frac{\bar{Q}_1 (\text{Sin } \tau_2 - \text{Sin } \tau_1) - (2 + \bar{\theta}_1) (\pi - \tau_2) + \bar{\theta}_1 \pi}{(\pi + \tau_1 - \tau_2)} \quad (\text{I.1.1.6})$$

From equation (I.1.1.5)

$$\eta^2 = - \frac{5}{Q_1} + \left(\frac{2}{\pi}\right) \left(\frac{2}{\pi} + \frac{\tau_1}{2} - \frac{\tau_2}{2} + \frac{\text{Sin } 2\tau_1}{4} - \frac{\text{Sin } 2\tau_2}{4}\right) + \left(\frac{2}{\pi}\right) \left(\frac{\bar{M}}{Q_1}\right) (\text{Sin } \tau_1 - \text{Sin } \tau_2) - \left(\frac{2}{\pi Q_1}\right) (2 + \bar{\theta}_1) \text{Sin } \tau_2 \quad (\text{I.1.1.7})$$

From figure 3.1.1.2

$$\tilde{\theta} = -\theta_1 \quad \text{at } \omega t = \tau_1$$

and

$$\tilde{\theta} = -(2\theta_0 + \theta_1) \quad \text{at } \omega t = \tau_2$$

Applying these conditions to expression (I.1.1.2)

$$-\theta_1 = M + Q_1 \cos \tau_1$$

Dividing throughout by θ_0 and rewriting

$$-\bar{\theta}_1 = \bar{M} + \bar{Q}_1 \cos \tau_1$$

Therefore

$$\tau_1 = \cos^{-1} \left[\frac{-\bar{\theta}_1 - \bar{M}}{\bar{Q}_1} \right] \quad (\text{I.1.1.8})$$

Similarly,

$$-(2\theta_0 + \theta_1) = M + Q_1 \cos \tau_2$$

Dividing by θ_0 throughout and rewriting:

$$-(2 + \bar{\theta}_1) = \bar{M} + \bar{Q}_1 \cos \tau_2$$

Therefore

$$\tau_2 = \cos^{-1} \left[\frac{-2 - \bar{\theta}_1 - \bar{M}}{\bar{Q}_1} \right] \quad (\text{I.1.1.9})$$

I.1.2 3RD ORDER ULTRAHARMONIC RESONANCE:

The simplest form of the solution, which can be used in this case, consists of three terms, thus

$$\tilde{\theta} = \bar{M} + Q_1 \cos \omega t + Q_3 \cos 3\omega t \quad (\text{I.1.2.1})$$

Substituting (I.1.2.1) into (I.1.1.1) and redefining $E_1(\tilde{\theta})$, $E_2(\tilde{\theta})$ and $E_3(\tilde{\theta})$ as:

$$E_1(\tilde{\theta}) = -J\omega^2 Q_1 \cos \omega t - 9J\omega^2 Q_3 \cos 3\omega t + K(M + Q_1 \cos \omega t + Q_3 \cos 3\omega t) - T_0 - T \cos \omega t = 0$$

$$E_2(\tilde{\theta}) = -J\omega^2 Q_1 \cos \omega t - 9J\omega^2 Q_3 \cos 3\omega t - T_0 - T \cos \omega t = 0$$

$$E_3(\tilde{\theta}) = -J\omega^2 Q_1 \cos \omega t - 9J\omega^2 Q_3 \cos 3\omega t + K(M + Q_1 \cos \omega t + Q_3 \cos 3\omega t) + K(2\theta_0 + \theta_1) - T_0 - T \cos \omega t = 0$$

Applying the Ritz averaging method and referring to figure 3.1.2.1, the following equations are obtained:

$$2 \int_0^{\tau_1} E_1(\tilde{\theta}) d(\omega t) + 2 \int_{\tau_1}^{\tau_2} E_2(\tilde{\theta}) d(\omega t) + 2 \int_{\tau_2}^{\pi} E_3(\tilde{\theta}) d(\omega t) = 0 \quad (\text{I.1.2.2})$$

$$2 \int_0^{\tau_1} E_1(\tilde{\theta}) \cos \omega t d(\omega t) + 2 \int_{\tau_1}^{\tau_2} E_2(\tilde{\theta}) \cos \omega t d(\omega t) + 2 \int_{\tau_2}^{\pi} E_3(\tilde{\theta}) \cos \omega t d(\omega t) = 0 \quad (\text{I.1.2.3})$$

$$\text{and } 2 \int_0^{\tau_1} E_1(\tilde{\theta}) \cos 3\omega t d(\omega t) + 2 \int_{\tau_1}^{\tau_2} E_2(\tilde{\theta}) \cos 3\omega t d(\omega t) + 2 \int_{\tau_2}^{\pi} E_3(\tilde{\theta}) \cos 3\omega t d(\omega t) = 0 \quad (\text{I.1.2.4})$$

Integration of expressions (I.1.2.2) to (I.1.2.4) yields three non-linear algebraic equations.

From equation (I.1.2.2):

$$\bar{M} = \frac{\bar{Q}_1 (\sin \tau_2 - \sin \tau_1) + \bar{Q}_3 \frac{1}{3} (\sin 3\tau_2 - \sin 3\tau_1) - (2 + \bar{\theta}_1) (\pi - \tau_2) + \bar{\theta}_1 \pi}{(\pi + \tau_1 - \tau_2)} \quad (\text{I.1.2.5})$$

From equation (I.1.2.3):

$$\bar{Q}_1 = \frac{[(\bar{S})\pi - \bar{Q}_3 \{ \frac{1}{4} (\sin 4\tau_1 - \sin 4\tau_2) + \frac{1}{2} (\sin 2\tau_1 - \sin 2\tau_2) \}] - 2\bar{M} (\sin \tau_1 - \sin \tau_2) + 2(2 + \bar{\theta}_1) \sin \tau_2}{[(\pi + \tau_1 - \tau_2) + \frac{1}{2} (\sin 2\tau_1 - \sin 2\tau_2) - \pi \eta^2]} \quad (\text{I.1.2.6})$$

From equation (I.1.2.4):

$$\begin{aligned} \eta^2 = & \left(\frac{1}{9} \pi \right) \left(\frac{\bar{Q}_1}{\bar{Q}_3} \right) \left[\frac{1}{4} (\sin 4\tau_1 - \sin 4\tau_2) + \frac{1}{2} (\sin 2\tau_1 - \sin 2\tau_2) \right] \\ & + \left(\frac{1}{9} \pi \right) [\pi + (\tau_1 - \tau_2) + \frac{1}{6} (\sin 6\tau_1 - \sin 6\tau_2)] + \left(\frac{2}{27\pi} \right) \left(\frac{\bar{M}}{\bar{Q}_3} \right) \\ & (\sin 3\tau_1 - \sin 3\tau_2) - \left(\frac{2}{27\pi} \right) \left(\frac{1}{\bar{Q}_3} \right) (2 + \bar{\theta}_1) \sin 3\tau_2 \end{aligned} \quad (\text{I.1.2.7})$$

From figure 3.1.2.1

$$\tilde{\theta} = -\theta_1 \quad \text{at } \omega t = \tau_1$$

$$\tilde{\theta} = -(2\theta_0 + \theta_1) \quad \text{at } \omega t = \tau_2$$

Applying these conditions to expression (I.1.2.1)

$$-\theta_1 = \bar{M} + \bar{Q}_1 \cos \tau_1 + \bar{Q}_3 \cos 3\tau_1$$

Dividing throughout by θ_0 and rewriting

$$-\bar{\theta}_1 = \bar{M} + \bar{Q}_1 \cos \tau_1 + \bar{Q}_3 \cos 3\tau_1$$

Therefore,

$$\tau_1 = \cos^{-1} \left[\frac{-\bar{\theta}_1 - \bar{M} - \bar{Q}_3 \cos 3\tau_1}{\bar{Q}_1} \right] \quad (\text{I.1.2.8})$$

Similarly,

$$-(2\theta_0 + \theta_1) = M + Q_1 \cos \tau_2 + Q_3 \cos 3\tau_2$$

Dividing throughout by θ_0 and rewriting

$$-(2 + \bar{\theta}_1) = \bar{M} + \bar{Q}_1 \cos \tau_2 + \bar{Q}_3 \cos 3\tau_2$$

hence

$$\tau_2 = \cos^{-1} \left[\frac{-2 - \bar{\theta}_1 - \bar{M} - \bar{Q}_3 \cos 3\tau_2}{\bar{Q}_1} \right] \quad (\text{I.1.2.9})$$

I.1.3 1/3RD ORDER SUBHARMONIC RESONANCE:

The simplest form of the solution, which can be used in this case is:

$$\tilde{\theta} = M + Q_1 \cos \omega t + Q_{1/3} \cos \frac{\omega t}{3} \quad (\text{I.1.3.1})$$

Substituting (I.1.3.1) into (I.1.1.1) and redefining $E_1(\tilde{\theta})$, $E_2(\tilde{\theta})$ and $E_3(\tilde{\theta})$ as:

$$E_1(\tilde{\theta}) = -J\omega^2 Q_1 \cos \omega t - \frac{J\omega^2}{9} Q_{1/3} \cos \frac{\omega t}{3} + K(M + Q_1 \cos \omega t + Q_{1/3} \cos \frac{\omega t}{3}) - T_0 - T \cos \omega t = 0$$

$$E_2(\tilde{\theta}) = -J\omega^2 Q_1 \cos \omega t - \frac{J}{9} \omega^2 Q_{1/3} \cos \frac{\omega t}{3} - T_0 - T \cos \omega t = 0$$

$$E_3(\tilde{\theta}) = -J\omega^2 Q_1 \cos \omega t - \frac{J}{9} \omega^2 Q_{1/3} \cos \frac{\omega t}{3} + K(M + Q_1 \cos \omega t + Q_{1/3} \cos \frac{\omega t}{3}) + K(2\theta_0 + \theta_1) - T_0 - T \cos \omega t = 0$$

Applying the Ritz averaging method, and referring to figure 3.1.3.1, the following equations are obtained:

$$2 \int_0^{\tau_1} E_1(\tilde{\theta}) d(\omega t) + 2 \int_{\tau_1}^{\tau_2} E_2(\tilde{\theta}) d(\omega t) + 2 \int_{\tau_2}^{3\pi} E_3(\tilde{\theta}) d(\omega t) = 0$$

(I.1.3.2)

$$2 \int_0^{\tau_1} E_1(\tilde{\theta}) \cos \omega t d(\omega t) + 2 \int_{\tau_1}^{\tau_2} E_2(\tilde{\theta}) \cos \omega t d(\omega t) + 2 \int_{\tau_2}^{3\pi} E_3(\tilde{\theta}) \cos \omega t d(\omega t) = 0$$

(I.1.3.3)

and

$$2 \int_0^{\tau_1} E_1(\tilde{\theta}) \cos \frac{\omega t}{3} d(\omega t) + 2 \int_{\tau_1}^{\tau_2} E_2(\tilde{\theta}) \cos \frac{\omega t}{3} d(\omega t) + 2 \int_{\tau_2}^{3\pi} E_3(\tilde{\theta}) \cos \frac{\omega t}{3} d(\omega t) = 0$$

(I.1.3.4)

Integration of expressions (I.1.3.2) to (I.1.3.4) yields three non-linear algebraic equations.

From equation (I.1.3.2):

$$\bar{M} = \frac{\bar{Q}_1 (\sin \tau_2 - \sin \tau_1) - 3\bar{Q}_1/3 (\sin \frac{\tau_1}{3} - \sin \frac{\tau_2}{3}) - (2 + \bar{\theta}_1) (3\pi - \tau_2) + 3\pi \bar{\theta}_1}{(3\pi + \tau_1 - \tau_2)}$$

(I.1.3.5)

From equation (I.1.3.3):

$$\bar{Q}_1 = \frac{[3\pi \bar{S} - \bar{Q}_1/3 \{ \frac{3}{4} (\sin \frac{4\tau_1}{3} - \sin \frac{4\tau_2}{3}) + \frac{3}{2} (\sin \frac{2\tau_1}{3} - \sin \frac{2\tau_2}{3}) \} + 2\bar{M} (\sin \tau_1 - \sin \tau_2) - 2(2 + \bar{\theta}_1) \sin \tau_2]}{[3\pi + \tau_1 - \tau_2 + \frac{1}{2} (\sin 2\tau_1 - \sin 2\tau_2) - 3\pi \eta^2]}$$

(I.1.3.6)

From equation (I.1.3.4)

$$\begin{aligned} \eta^2 = & \left(\frac{6}{\pi}\right) \left(\frac{\bar{Q}_1}{\bar{Q}_{1/3}}\right) \left[\frac{3}{8} \left(\sin \frac{4\tau_1}{3} - \sin \frac{4\tau_2}{3}\right) + \frac{3}{4} \left(\sin \frac{2\tau_1}{3} - \sin \frac{2\tau_2}{3}\right)\right] \\ & + \left(\frac{6}{\pi}\right) \left[\frac{3\pi}{2} + \frac{1}{2} (\tau_1 - \tau_2) + \frac{3}{4} \left(\sin \frac{2\tau_1}{3} - \sin \frac{2\tau_2}{3}\right)\right] \\ & + \left(\frac{18}{\pi}\right) \left(\frac{\bar{M}}{\bar{Q}_{1/3}}\right) \left(\sin \frac{\tau_1}{3} - \sin \frac{\tau_2}{3}\right) - \left(\frac{18}{\pi \bar{Q}_{1/3}}\right) (2 + \bar{\theta}_1) \sin \frac{\tau_2}{3} \end{aligned} \quad (I.1.3.7)$$

From figure 3.1.3.1

$$\tilde{\theta} = -\theta_1 \quad \text{at} \quad \omega t = \tau_1$$

$$\tilde{\theta} = -(2\theta_0 + \theta_1) \quad \text{at} \quad \omega t = \tau_2$$

Applying these conditions to expression (I.1.3.1)

$$-\theta_1 = M + \bar{Q}_1 \cos \tau_1 + \bar{Q}_{1/3} \cos \frac{\tau_1}{3}$$

Dividing throughout by θ_0 and rewriting

$$-\bar{\theta}_1 = \bar{M} + \bar{Q}_1 \cos \tau_1 + \bar{Q}_{1/3} \cos \frac{\tau_1}{3}$$

Therefore,

$$\tau_1 = 3 \cos^{-1} \left[\frac{-\bar{\theta}_1 - \bar{M} - \bar{Q}_1 \cos \tau_1}{\bar{Q}_{1/3}} \right] \quad (I.1.3.8)$$

Similarly,

$$-(2\theta_0 + \theta_1) = \bar{M} + \bar{Q}_1 \cos \tau_2 + \bar{Q}_{1/3} \cos \frac{\tau_2}{3}$$

Dividing throughout by θ_0 and rewriting

$$-(2 + \bar{\theta}_1) = \bar{M} + \bar{Q}_1 \cos \tau_2 + \bar{Q}_{1/3} \cos \frac{\tau_2}{3}$$

hence

$$\tau_2 = 3 \cos^{-1} \left[\frac{-2 - \bar{\theta}_1 - \bar{M} - \bar{Q}_1 \cos \tau_2}{\bar{Q}_1/3} \right] \quad (\text{I.1.3.9})$$

I.2 SYSTEM RESPONSE TO A DISTURBING TORQUE OF TYPE C $\omega^2 \cos \omega t$

I.2.1 HARMONIC RESONANCE:

Rewriting equations (3.1.B.1) through (3.1.B.3) in the following form:

$$E_1(\theta) = \ddot{\theta} + p^2 (\theta - \theta_0) - Z \omega^2 \cos \omega t = 0$$

$$E_2(\theta) = \ddot{\theta} - Z \omega^2 \cos \omega t = 0$$

$$E_3(\theta) = \ddot{\theta} + p^2 [\theta - (-\theta_0)] - Z \omega^2 \cos \omega t = 0 \quad (\text{I.2.1.1})$$

The simplest form of the solution, which can be assumed in this case is:

$$\tilde{\theta} = Q_1 \cos \omega t \quad (\text{I.2.1.2})$$

Expression (I.2.1.2) for the approximate value of the displacement $\tilde{\theta}$ is substituted for θ in expression (I.2.1.1). The resulting equation is defined hereby as $E(\tilde{\theta})$. Applying the Ritz averaging method, the following equations are obtained:

$$\int_0^{2\pi} E(\tilde{\theta}) \cos \omega t \, d(\omega t) = 0 \quad (\text{I.2.1.3})$$

Because the characteristic is symmetrical with respect to the origin, the upper limit in equation (I.2.1.3) may be changed to $\pi/2$. In equation (I.2.1.3), $E(\tilde{\theta})$ is represented by $E_1(\tilde{\theta})$ between limits 0 to τ_1 , $E_2(\tilde{\theta})$ between τ_1 and $\pi/2$ with $\theta_0 = Q_1 \cos \tau_1$. The $E_1(\tilde{\theta})$ and $E_2(\tilde{\theta})$ are represented as:

$$E_1(\tilde{\theta}) = -\omega^2 Q_1 \cos \omega t + p^2 (Q_1 \cos \omega t - \theta_0) - Z \omega^2 \cos \omega t = 0$$

$$E_2(\tilde{\theta}) = -\omega^2 Q_1 \cos \omega t - Z \omega^2 \cos \omega t = 0$$

Thus, referring to figure 3.2.1.2, equation (I.2.1.3) may be written in the more complete form:

$$4 \int_0^{\tau_1} E_1(\tilde{\theta}) \cos \omega t \, d(\omega t) + 4 \int_{\tau_1}^{\pi/2} E_2(\tilde{\theta}) \cos \omega t \, d(\omega t) = 0 \quad (\text{I.2.1.4})$$

Integration of expression (I.2.1.4) yields:

$$(-\eta^2 \bar{Q}_1 - \frac{Z}{\theta_0} \eta^2) \pi + \bar{Q}_1 (2\tau_1 + \sin 2\tau_1) - 4 \sin \tau_1 = 0$$

or

$$\eta^2 = \frac{4 \sin \tau_1 - \bar{Q}_1 (2\tau_1 + \sin 2\tau_1)}{(-\bar{Q}_1 - Z') \pi} \quad (\text{I.2.1.5})$$

From figure 3.2.1.2

$$\tilde{\theta} = \theta_0 \quad \text{at} \quad \omega t = \tau_1$$

Applying this condition to expression (I.2.1.2)

$$\theta_0 = Q_1 \cos \tau_1$$

Dividing throughout by θ_0 and rewriting $1 = \bar{Q}_1 \cos \tau_1$

hence,

$$\tau_1 = \cos^{-1} \left[\frac{1}{\bar{Q}_1} \right] \quad (\text{I.2.1.6})$$

I.2.2 3RD ORDER ULTRAHARMONIC RESONANCE:

The simplest form of the solution, which can be used in this case, consists of two terms, thus

$$\tilde{\theta} = Q_1 \cos \omega t + Q_3 \cos 3\omega t \quad (\text{I.2.2.1})$$

Applying the Ritz averaging method, the following equations are obtained:

$$\int_0^{2\pi} E(\tilde{\theta}) \cos \omega t d(\omega t) = 0 \quad (\text{I.2.2.2})$$

$$\int_0^{2\pi} E(\tilde{\theta}) \cos 3\omega t d(\omega t) = 0$$

In equation (I.2.2.2), $E(\tilde{\theta})$ is represented by $E_1(\tilde{\theta})$ between limits 0 to τ_1 , $E_2(\tilde{\theta})$ between τ_1 to τ_2 and $E_3(\tilde{\theta})$ between τ_2 to π .

The $E_1(\tilde{\theta})$, $E_2(\tilde{\theta})$ and $E_3(\tilde{\theta})$ are expressed as:

$$E_1(\tilde{\theta}) = -\omega^2 Q_1 \cos \omega t - 9\omega^2 Q_3 \cos 3\omega t + p^2(Q_1 \cos \omega t + Q_3 \cos 3\omega t - \theta_0) - Z \omega^2 \cos \omega t = 0$$

$$E_2(\tilde{\theta}) = -\omega^2 Q_1 \cos \omega t - 9\omega^2 Q_3 \cos 3\omega t - Z \omega^2 \cos \omega t = 0$$

$$E_3(\tilde{\theta}) = -\omega^2 Q_1 \cos \omega t - 9\omega^2 Q_3 \cos 3\omega t + p^2(Q_1 \cos \omega t + Q_3 \cos 3\omega t + \theta_0) - Z \omega^2 \cos \omega t = 0$$

Referring to figure 3.2.2.1, equations (I.2.2.2) can be written in the complete form as:

$$2 \int_0^{\tau_1} E_1(\tilde{\theta}) \cos \omega t d(\omega t) + 2 \int_{\tau_1}^{\tau_2} E_2(\tilde{\theta}) \cos \omega t d(\omega t) + 2 \int_{\tau_2}^{\pi} E_3(\tilde{\theta}) \cos \omega t d(\omega t) = 0 \quad (\text{I.2.2.3})$$

$$\text{and } 2 \int_0^{\tau_1} E_1(\tilde{\theta}) \cos 3\omega t \, d(\omega t) + 2 \int_{\tau_1}^{\tau_2} E_2(\tilde{\theta}) \cos 3\omega t \, d(\omega t) \\ + 2 \int_{\tau_2}^{\pi} E_3(\tilde{\theta}) \cos 3\omega t \, d(\omega t) = 0 \quad (\text{I.2.2.4})$$

Integration of expressions (I.2.2.3) and (I.2.2.4) yields:

$$(-\eta^2 \bar{Q}_1 - \frac{Z}{\theta_0} \eta^2) \pi + \bar{Q}_1 (2\tau_1 + \sin 2\tau_1) + \bar{Q}_3 (\sin 2\tau_1 + 1/2 \\ \sin 4\tau_1) - 4\sin \tau_1 = 0 \quad (\text{I.2.2.5})$$

and,

$$-9\pi \eta^2 \bar{Q}_3 + \bar{Q}_1 (\sin 2\tau_1 + \frac{1}{2} \sin 4\tau_1) + \bar{Q}_3 (2\tau_1 + \frac{1}{3} \sin 6\tau_1) \\ - \frac{4}{3} \sin 3\tau_1 = 0 \quad (\text{I.2.2.6})$$

From expression (I.2.2.5):

$$\bar{Q}_1 = \frac{[4\sin \tau_1 - \bar{Q}_3 (\sin 2\tau_1 + \frac{1}{2} \sin 4\tau_1) + Z' \pi \eta^2]}{(2\tau_1 + \sin 2\tau_1 - \pi \eta^2)} \quad (\text{I.2.2.7})$$

From expression (I.2.2.6):

$$\eta^2 = \left(\frac{\bar{Q}_1}{9\pi \bar{Q}_3} \right) (\sin 2\tau_1 + \frac{1}{2} \sin 4\tau_1) + \left(\frac{1}{9\pi} \right) (2\tau_1 + \frac{1}{3} \sin 6\tau_1) \\ - \frac{4}{3} \left(\frac{1}{9\pi \bar{Q}_3} \right) \sin 3\tau_1 \quad (\text{I.2.2.8})$$

From figure 3.2.2.1

$$\tilde{\theta} = \theta_0 \quad \text{at} \quad \omega t = \tau_1$$

Applying this condition to expression (I.2.2.1)

$$\theta_0 = Q_1 \cos \tau_1 + Q_3 \cos 3\tau_1 \quad (\text{I.2.2.9})$$

Dividing throughout by θ_0 and rewriting

$$1 = \bar{Q}_1 \cos \tau_1 + \bar{Q}_3 \cos 3\tau_1$$

hence,

$$\tau_1 = \cos^{-1} \left[\frac{1 - \bar{Q}_3 \cos 3\tau_1}{\bar{Q}_1} \right]$$

I.2.3 1/3RD ORDER SUBHARMONIC RESONANCE:

The simplest form of the solution, which can be used in this case, consists of two terms, thus

$$\tilde{\theta} = Q_1 \cos \omega t + Q_{1/3} \cos \frac{\omega t}{3} \quad (\text{I.2.3.1})$$

Applying the Ritz averaging method, the following equations are obtained:

$$\int_0^{6\pi} E(\tilde{\theta}) \cos \omega t \, d(\omega t) = 0$$

and,

$$\int_0^{6\pi} E(\tilde{\theta}) \cos \frac{\omega t}{3} \, d(\omega t) = 0 \quad (\text{I.2.3.2})$$

In equation (I.2.3.2), $E_1(\tilde{\theta})$ is represented by $E_1(\tilde{\theta})$ between limits 0 to τ_1 , $E_2(\tilde{\theta})$ between τ_1 to τ_2 and $E_3(\tilde{\theta})$ between τ_2 to 3π .

The $E_1(\tilde{\theta})$, $E_2(\tilde{\theta})$ and $E_3(\tilde{\theta})$ are expressed as:

$$E_1(\tilde{\theta}) = -\omega^2 Q_1 \cos \omega t - \frac{\omega^2}{9} Q_{1/3} \cos \frac{\omega t}{3} + p^2 (Q_1 \cos \omega t + Q_{1/3} \cos \frac{\omega t}{3} - \theta_0) - Z \omega^2 \cos \omega t = 0$$

$$E_2(\tilde{\theta}) = -\omega^2 Q_1 \cos \omega t - \frac{\omega^2}{9} Q_{1/3} \cos \frac{\omega t}{3} - Z \omega^2 \cos \omega t = 0$$

$$E_3(\tilde{\theta}) = -\omega^2 Q_1 \cos \omega t - \frac{\omega^2}{9} Q_{1/3} \cos \frac{\omega t}{3} + p^2 (Q_1 \cos \omega t + Q_{1/3} \cos \frac{\omega t}{3} + \theta_0) - Z \omega^2 \cos \omega t = 0$$

Referring to figure 3.2.3.1, equations (I.2.3.2) can now be written as:

$$2 \int_0^{\tau_1} E_1(\tilde{\theta}) \cos \omega t d(\omega t) + 2 \int_{\tau_1}^{\tau_2} E_2(\tilde{\theta}) \cos \omega t d(\omega t) + 2 \int_{\tau_2}^{3\pi} E_3(\tilde{\theta}) \cos \omega t d(\omega t) = 0 \quad (\text{I.2.3.3})$$

$$2 \int_0^{\tau_1} E_1(\tilde{\theta}) \cos \frac{\omega t}{3} d(\omega t) + 2 \int_{\tau_1}^{\tau_2} E_2(\tilde{\theta}) \cos \frac{\omega t}{3} d(\omega t) + 2 \int_{\tau_2}^{3\pi} E_3(\tilde{\theta}) \cos \frac{\omega t}{3} d(\omega t) = 0 \quad (\text{I.2.3.4})$$

Integration of expressions (I.2.3.3) and (I.2.3.4) yields:

$$\left(-n^2 \bar{Q}_1 - \frac{Z}{\theta_0} n^2\right) \frac{3\pi}{2} + \bar{Q}_1 \left(\tau_1 + \frac{1}{2} \sin 2\tau_1\right) + \bar{Q}_{1/3} \left(\frac{3}{4} \sin \frac{4\tau_1}{3} + \frac{3}{2} \sin \frac{2\tau_1}{3}\right) - 2 \sin \tau_1 = 0 \quad (\text{I.2.3.5})$$

and,

$$\bar{Q}_1 \left[\frac{3}{4} \sin \frac{4\tau_1}{3} + \frac{3}{2} \sin \frac{2\tau_1}{3} \right] - \frac{3\pi}{2} \left(\frac{n^2}{9}\right) \bar{Q}_{1/3} + \bar{Q}_{1/3} \left(\tau_1 + \frac{3}{2} \sin \frac{2\tau_1}{3}\right) - 6 \sin \frac{\tau_1}{3} = 0 \quad (\text{I.2.3.6})$$

From expression (I.2.3.5)

$$\bar{Q}_1 = \frac{4\text{Sin } \tau_1 + 2 \cdot 3\pi \eta^2 - \bar{Q}_{1/3} \left(\frac{3}{2} \text{Sin } \frac{4\tau_1}{3} + 3\text{Sin } \frac{2\tau_1}{3} \right)}{(2\tau_1 + \text{Sin } 2\tau_1 - 3\pi \eta^2)} \quad (\text{I.2.3.7})$$

and from expression (I.2.3.6)

$$\eta^2 = \frac{\bar{Q}_1 \left(\frac{6}{\pi} \right) \left(\frac{3}{4} \text{Sin } \frac{4\tau_1}{3} + \frac{3}{2} \text{Sin } \frac{2\tau_1}{3} \right) + \left(\frac{6}{\pi} \right) \left(\tau_1 + \frac{3}{2} \text{Sin } \frac{2\tau_1}{3} \right) - \left(\frac{36}{\pi} \cdot \frac{1}{\bar{Q}_{1/3}} \right) \text{Sin } \frac{\tau_1}{3}}{\bar{Q}_{1/3}} \quad (\text{I.2.3.8})$$

From figure (3.2.3.1)

$$\tilde{\theta} = \theta_0 \quad \text{at} \quad \omega t = \tau_1$$

Applying this condition to expression (I.2.3.1):

$$\theta_0 = Q_1 \text{Cos } \tau_1 + Q_{1/3} \text{Cos } \frac{\tau_1}{3}$$

Dividing throughout by θ_0 and rewriting

$$1 = \bar{Q}_1 \text{Cos } \tau_1 + \bar{Q}_{1/3} \text{Cos } \frac{\tau_1}{3}$$

hence,

$$\tau_1 = 3\text{Cos}^{-1} \left[\frac{1 - \bar{Q}_1 \text{Cos } \tau_1}{\bar{Q}_{1/3}} \right] \quad (\text{I.2.3.9})$$



~

APPENDIX II

ITERATIVE PROCEDURE FOR THE SOLUTION OF SIMULTANEOUS EQUATIONS:

To illustrate the iterative procedure, simultaneous equations (I.1.1.6), (I.1.1.7), (I.1.1.8) and (I.1.1.9) will be solved using this technique.

$$\tau_1 = \text{Cos}^{-1} \left[\frac{-\bar{\theta}_1 - \bar{M}}{Q_1} \right] \quad (\text{I.1.1.8})$$

$$\tau_2 = \text{Cos}^{-1} \left[\frac{-2 - \bar{\theta}_1 - \bar{M}}{Q_1} \right] \quad (\text{I.1.1.9})$$

$$\bar{M} = \frac{Q_1 (\text{Sin } \tau_2 - \text{Sin } \tau_1) - (2 + \bar{\theta}_1) (\pi - \tau_2) + \bar{\theta}_1 \pi}{(\pi + \tau_1 - \tau_2)} \quad (\text{I.1.1.6})$$

$$\begin{aligned} n^2 = & - \left(\frac{\bar{S}}{Q_1} \right) + \left(\frac{2}{\pi} \right) \left[\frac{\pi}{2} + 1/2(\tau_1 - \tau_2) + 1/4(\text{Sin } 2\tau_1 - \text{Sin } 2\tau_2) \right] \\ & + \left(\frac{2}{\pi} \right) \left(\frac{\bar{M}}{Q_1} \right) (\text{Sin } \tau_1 - \text{Sin } \tau_2) - \left(\frac{2}{\pi Q_1} \right) (2 + \bar{\theta}_1) \text{Sin } \tau_2 \end{aligned} \quad (\text{I.1.1.7})$$

To initiate iteration, starting values are chosen for \bar{M} , τ_1 and τ_2 . New values of τ_1 and τ_2 are calculated by substituting the previously assumed starting values. Again, these new calculated values are taken as starting values and next new values are calculated. This procedure is continued until there is a sufficient convergence. The conditions for convergence are taken as --

$$\tau_1(I) - \tau_1(I-1) \leq \epsilon \quad \epsilon = 0.001 \text{ (error function)}$$

and

$$\tau_2(I) - \tau_2(I-1) \leq \epsilon$$

The iterated values of τ_1 and τ_2 are substituted into the expression for \bar{M} (I.1.1.6). The calculated value of \bar{M} is substituted into (I.1.1.7) to calculate η^2 .

The iterated values of τ_1 and τ_2 and calculated value of \bar{M} become starting values for the iterations of τ_1 and τ_2 . The new iterated values of τ_1 and τ_2 are used to calculate new values of \bar{M} and η^2 .

This procedure is continued until there is a sufficient convergence for \bar{M} and η^2 . The test of convergence is defined as --

$$\bar{M}(I) - \bar{M}(I-1) \leq \epsilon \quad \epsilon = 0.001 \text{ (error function)}$$

or

$$\eta^2(I) - \eta^2(I-1) \leq \epsilon$$

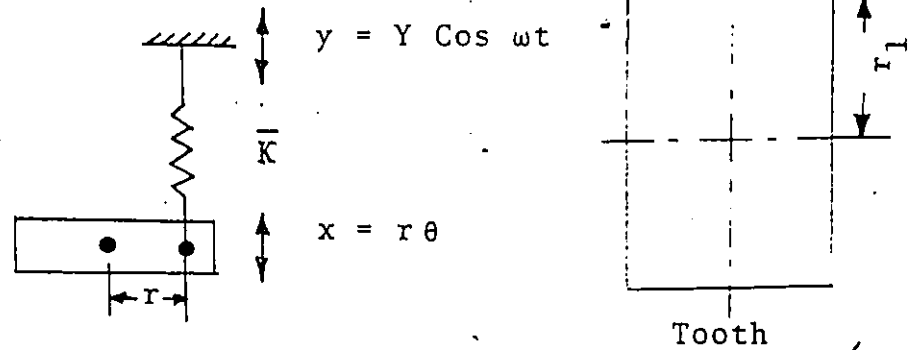
The computer program for the solution of the simultaneous equations using the iterative procedure is given on page 162.

```

1 1033  MATRY KXXXXXX
2 1034  MATHNOM COLUTION UNJASYMMETRICAL SYSTEM
3 1035  DIMENSION TAUI(1000),O,MBAR(1000),TAU2(1000),ETA(1000)
4 1036  REAL MBAR
5 1037  REAL MBAR
6 1038  REAL MBAR,EDS
7 1039  M=1+L*O
8 1040  TAU=1+L*O
9 1041  TAUI(1)=T*O*SI
10 1042  PI=3.141592653589793
11 1043  MBAR(1)=M*SI
12 1044  DO 40 K=1,11
13 1045  OMBAR(K)=O+O.05*(K-1)
14 1046  TAUI(K)=1+O.5*(J-1)
15 1047  MBAR(K)=O.04+O.04*(K-1)
16 1048  ETA(K)=O.04+O.04*(K-1)
17 1049  CALL TAUI,OX,OMBAR,O,X,O,MBAR,OX,MBAR,OX,ETA50,11X,TAUI,11X
18 1050  CALL TAUI,OX,OMBAR,OX,ETA
19 1051  M=1
20 1052  L=1
21 1053  DO 21 J=1,9
22 1054  TAUI(1)=ARCOS((-OMBAR(K)-MBAR(M-1))/OMBAR(J))
23 1055  IF(O) TAUI(1)=TAUI(1-1)*LEEPS GOTC 21
24 1056  IF(L) GOTO 21 TAUI(1)=TAUI(1)+TAUI(1)/2.0
25 1057  TAUI=TAUI(1)
26 1058  J=J+1
27 1059  GO TO 21
28 1060  L=L+1
29 1061  IF(L) TANCOS((-OMBAR(K)+2*OMBAR(M-1))/OMBAR(J))
30 1062  IF(L) TAUI(1)=TAUI(1-1)*LEEPS GOTC 20
31 1063  IF(L) GOTO 21 TAUI(1)=TAUI(1)+TAUI(1)/2.0
32 1064  TAUI=TAUI(1)
33 1065  GOTO 21
34 1066  TAUI(1)=OMBAR(J)*SIN(TAUI(1))-SIN(TAUI(1))-(2*OMBAR(K))*PI-
35 1067  TAUI(1)+OMBAR(J)*SIN(TAUI(1)) / (PI*TAUI(1)-TAUI(1))
36 1068  IF(O) TAUI(1)=OMBAR(J)*SIN(TAUI(1))+SIN(TAUI(1))-TAUI(1)+1/2.0
37 1069  IF(L) TAUI(1)=SIN(TAUI(1))-SIN(TAUI(1))+OMBAR(J)*SIN(TAUI(1))+SIN(TAUI(1))
38 1070  IF(L) TAUI(1)=SIN(TAUI(1))-SIN(TAUI(1))+OMBAR(J)*SIN(TAUI(1))+SIN(TAUI(1))
39 1071  PRINTA,TAUI(K)
40 1072  DO 40 J=1,11
41 1073  OMBAR(K)=O.04+O.04*(K-1)
42 1074  TAUI(K)=1+O.5*(J-1)
43 1075  MBAR(K)=O.04+O.04*(K-1)
44 1076  ETA(K)=O.04+O.04*(K-1)
45 1077  CALL TAUI,OX,OMBAR,O,X,O,MBAR,OX,MBAR,OX,ETA50,11X,TAUI,11X
46 1078  CALL TAUI,OX,OMBAR,OX,ETA
47 1079  M=1
48 1080  L=1
49 1081  DO 49 J=1,9
50 1082  TAUI(1)=ARCOS((-OMBAR(K)-MBAR(M-1))/OMBAR(J))
51 1083  IF(O) TAUI(1)=TAUI(1-1)*LEEPS GOTC 21
52 1084  IF(L) GOTO 21 TAUI(1)=TAUI(1)+TAUI(1)/2.0
53 1085  TAUI=TAUI(1)
54 1086  J=J+1
55 1087  GO TO 49
56 1088  L=L+1
57 1089  IF(L) TANCOS((-OMBAR(K)+2*OMBAR(M-1))/OMBAR(J))
58 1090  IF(L) TAUI(1)=TAUI(1-1)*LEEPS GOTC 20
59 1091  IF(L) GOTO 21 TAUI(1)=TAUI(1)+TAUI(1)/2.0
60 1092  TAUI=TAUI(1)
61 1093  GOTO 49
62 1094  TAUI(1)=OMBAR(J)*SIN(TAUI(1))-SIN(TAUI(1))-(2*OMBAR(K))*PI-
63 1095  TAUI(1)+OMBAR(J)*SIN(TAUI(1)) / (PI*TAUI(1)-TAUI(1))
64 1096  IF(O) TAUI(1)=OMBAR(J)*SIN(TAUI(1))+SIN(TAUI(1))-TAUI(1)+1/2.0
65 1097  IF(L) TAUI(1)=SIN(TAUI(1))-SIN(TAUI(1))+OMBAR(J)*SIN(TAUI(1))+SIN(TAUI(1))
66 1098  IF(L) TAUI(1)=SIN(TAUI(1))-SIN(TAUI(1))+OMBAR(J)*SIN(TAUI(1))+SIN(TAUI(1))
67 1099  PRINTA,TAUI(K)
68 1100  DO 40 J=1,11
69 1101  OMBAR(K)=O.04+O.04*(K-1)
70 1102  TAUI(K)=1+O.5*(J-1)
71 1103  MBAR(K)=O.04+O.04*(K-1)
72 1104  ETA(K)=O.04+O.04*(K-1)
73 1105  CALL TAUI,OX,OMBAR,O,X,O,MBAR,OX,MBAR,OX,ETA50,11X,TAUI,11X
74 1106  CALL TAUI,OX,OMBAR,OX,ETA
75 1107  M=1
76 1108  L=1
77 1109  DO 77 J=1,9
78 1110  TAUI(1)=ARCOS((-OMBAR(K)-MBAR(M-1))/OMBAR(J))
79 1111  IF(O) TAUI(1)=TAUI(1-1)*LEEPS GOTC 21
80 1112  IF(L) GOTO 21 TAUI(1)=TAUI(1)+TAUI(1)/2.0
81 1113  TAUI=TAUI(1)
82 1114  J=J+1
83 1115  GO TO 77
84 1116  L=L+1
85 1117  IF(L) TANCOS((-OMBAR(K)+2*OMBAR(M-1))/OMBAR(J))
86 1118  IF(L) TAUI(1)=TAUI(1-1)*LEEPS GOTC 20
87 1119  IF(L) GOTO 21 TAUI(1)=TAUI(1)+TAUI(1)/2.0
88 1120  TAUI=TAUI(1)
89 1121  GOTO 77
90 1122  TAUI(1)=OMBAR(J)*SIN(TAUI(1))-SIN(TAUI(1))-(2*OMBAR(K))*PI-
91 1123  TAUI(1)+OMBAR(J)*SIN(TAUI(1)) / (PI*TAUI(1)-TAUI(1))
92 1124  IF(O) TAUI(1)=OMBAR(J)*SIN(TAUI(1))+SIN(TAUI(1))-TAUI(1)+1/2.0
93 1125  IF(L) TAUI(1)=SIN(TAUI(1))-SIN(TAUI(1))+OMBAR(J)*SIN(TAUI(1))+SIN(TAUI(1))
94 1126  IF(L) TAUI(1)=SIN(TAUI(1))-SIN(TAUI(1))+OMBAR(J)*SIN(TAUI(1))+SIN(TAUI(1))
95 1127  PRINTA,TAUI(K)
96 1128  DO 40 J=1,11
97 1129  OMBAR(K)=O.04+O.04*(K-1)
98 1130  TAUI(K)=1+O.5*(J-1)
99 1131  MBAR(K)=O.04+O.04*(K-1)
100 1132  ETA(K)=O.04+O.04*(K-1)
101 1133  CALL TAUI,OX,OMBAR,O,X,O,MBAR,OX,MBAR,OX,ETA50,11X,TAUI,11X
102 1134  CALL TAUI,OX,OMBAR,OX,ETA
103 1135  M=1
104 1136  L=1
105 1137  DO 105 J=1,9
106 1138  TAUI(1)=ARCOS((-OMBAR(K)-MBAR(M-1))/OMBAR(J))
107 1139  IF(O) TAUI(1)=TAUI(1-1)*LEEPS GOTC 21
108 1140  IF(L) GOTO 21 TAUI(1)=TAUI(1)+TAUI(1)/2.0
109 1141  TAUI=TAUI(1)
110 1142  J=J+1
111 1143  GO TO 105
112 1144  L=L+1
113 1145  IF(L) TANCOS((-OMBAR(K)+2*OMBAR(M-1))/OMBAR(J))
114 1146  IF(L) TAUI(1)=TAUI(1-1)*LEEPS GOTC 20
115 1147  IF(L) GOTO 21 TAUI(1)=TAUI(1)+TAUI(1)/2.0
116 1148  TAUI=TAUI(1)
117 1149  GOTO 105
118 1150  TAUI(1)=OMBAR(J)*SIN(TAUI(1))-SIN(TAUI(1))-(2*OMBAR(K))*PI-
119 1151  TAUI(1)+OMBAR(J)*SIN(TAUI(1)) / (PI*TAUI(1)-TAUI(1))
120 1152  IF(O) TAUI(1)=OMBAR(J)*SIN(TAUI(1))+SIN(TAUI(1))-TAUI(1)+1/2.0
121 1153  IF(L) TAUI(1)=SIN(TAUI(1))-SIN(TAUI(1))+OMBAR(J)*SIN(TAUI(1))+SIN(TAUI(1))
122 1154  IF(L) TAUI(1)=SIN(TAUI(1))-SIN(TAUI(1))+OMBAR(J)*SIN(TAUI(1))+SIN(TAUI(1))
123 1155  PRINTA,TAUI(K)
124 1156  DO 40 J=1,11
125 1157  OMBAR(K)=O.04+O.04*(K-1)
126 1158  TAUI(K)=1+O.5*(J-1)
127 1159  MBAR(K)=O.04+O.04*(K-1)
128 1160  ETA(K)=O.04+O.04*(K-1)
129 1161  CALL TAUI,OX,OMBAR,O,X,O,MBAR,OX,MBAR,OX,ETA50,11X,TAUI,11X
130 1162  CALL TAUI,OX,OMBAR,OX,ETA
131 1163  M=1
132 1164  L=1
133 1165  DO 133 J=1,9
134 1166  TAUI(1)=ARCOS((-OMBAR(K)-MBAR(M-1))/OMBAR(J))
135 1167  IF(O) TAUI(1)=TAUI(1-1)*LEEPS GOTC 21
136 1168  IF(L) GOTO 21 TAUI(1)=TAUI(1)+TAUI(1)/2.0
137 1169  TAUI=TAUI(1)
138 1170  J=J+1
139 1171  GO TO 133
140 1172  L=L+1
141 1173  IF(L) TANCOS((-OMBAR(K)+2*OMBAR(M-1))/OMBAR(J))
142 1174  IF(L) TAUI(1)=TAUI(1-1)*LEEPS GOTC 20
143 1175  IF(L) GOTO 21 TAUI(1)=TAUI(1)+TAUI(1)/2.0
144 1176  TAUI=TAUI(1)
145 1177  GOTO 133
146 1178  TAUI(1)=OMBAR(J)*SIN(TAUI(1))-SIN(TAUI(1))-(2*OMBAR(K))*PI-
147 1179  TAUI(1)+OMBAR(J)*SIN(TAUI(1)) / (PI*TAUI(1)-TAUI(1))
148 1180  IF(O) TAUI(1)=OMBAR(J)*SIN(TAUI(1))+SIN(TAUI(1))-TAUI(1)+1/2.0
149 1181  IF(L) TAUI(1)=SIN(TAUI(1))-SIN(TAUI(1))+OMBAR(J)*SIN(TAUI(1))+SIN(TAUI(1))
150 1182  IF(L) TAUI(1)=SIN(TAUI(1))-SIN(TAUI(1))+OMBAR(J)*SIN(TAUI(1))+SIN(TAUI(1))
151 1183  PRINTA,TAUI(K)
152 1184  DO 40 J=1,11
153 1185  OMBAR(K)=O.04+O.04*(K-1)
154 1186  TAUI(K)=1+O.5*(J-1)
155 1187  MBAR(K)=O.04+O.04*(K-1)
156 1188  ETA(K)=O.04+O.04*(K-1)
157 1189  CALL TAUI,OX,OMBAR,O,X,O,MBAR,OX,MBAR,OX,ETA50,11X,TAUI,11X
158 1190  CALL TAUI,OX,OMBAR,OX,ETA
159 1191  M=1
160 1192  L=1
161 1193  DO 161 J=1,9
162 1194  TAUI(1)=ARCOS((-OMBAR(K)-MBAR(M-1))/OMBAR(J))
163 1195  IF(O) TAUI(1)=TAUI(1-1)*LEEPS GOTC 21
164 1196  IF(L) GOTO 21 TAUI(1)=TAUI(1)+TAUI(1)/2.0
165 1197  TAUI=TAUI(1)
166 1198  J=J+1
167 1199  GO TO 161
168 1200  L=L+1
169 1201  IF(L) TANCOS((-OMBAR(K)+2*OMBAR(M-1))/OMBAR(J))
170 1202  IF(L) TAUI(1)=TAUI(1-1)*LEEPS GOTC 20
171 1203  IF(L) GOTO 21 TAUI(1)=TAUI(1)+TAUI(1)/2.0
172 1204  TAUI=TAUI(1)
173 1205  GOTO 161
174 1206  TAUI(1)=OMBAR(J)*SIN(TAUI(1))-SIN(TAUI(1))-(2*OMBAR(K))*PI-
175 1207  TAUI(1)+OMBAR(J)*SIN(TAUI(1)) / (PI*TAUI(1)-TAUI(1))
176 1208  IF(O) TAUI(1)=OMBAR(J)*SIN(TAUI(1))+SIN(TAUI(1))-TAUI(1)+1/2.0
177 1209  IF(L) TAUI(1)=SIN(TAUI(1))-SIN(TAUI(1))+OMBAR(J)*SIN(TAUI(1))+SIN(TAUI(1))
178 1210  IF(L) TAUI(1)=SIN(TAUI(1))-SIN(TAUI(1))+OMBAR(J)*SIN(TAUI(1))+SIN(TAUI(1))
179 1211  PRINTA,TAUI(K)
180 1212  DO 40 J=1,11
181 1213  OMBAR(K)=O.04+O.04*(K-1)
182 1214  TAUI(K)=1+O.5*(J-1)
183 1215  MBAR(K)=O.04+O.04*(K-1)
184 1216  ETA(K)=O.04+O.04*(K-1)
185 1217  CALL TAUI,OX,OMBAR,O,X,O,MBAR,OX,MBAR,OX,ETA50,11X,TAUI,11X
186 1218  CALL TAUI,OX,OMBAR,OX,ETA
187 1219  M=1
188 1220  L=1
189 1221  DO 189 J=1,9
190 1222  TAUI(1)=ARCOS((-OMBAR(K)-MBAR(M-1))/OMBAR(J))
191 1223  IF(O) TAUI(1)=TAUI(1-1)*LEEPS GOTC 21
192 1224  IF(L) GOTO 21 TAUI(1)=TAUI(1)+TAUI(1)/2.0
193 1225  TAUI=TAUI(1)
194 1226  J=J+1
195 1227  GO TO 189
196 1228  L=L+1
197 1229  IF(L) TANCOS((-OMBAR(K)+2*OMBAR(M-1))/OMBAR(J))
198 1230  IF(L) TAUI(1)=TAUI(1-1)*LEEPS GOTC 20
199 1231  IF(L) GOTO 21 TAUI(1)=TAUI(1)+TAUI(1)/2.0
200 1232  TAUI=TAUI(1)
201 1233  GOTO 189
202 1234  TAUI(1)=OMBAR(J)*SIN(TAUI(1))-SIN(TAUI(1))-(2*OMBAR(K))*PI-
203 1235  TAUI(1)+OMBAR(J)*SIN(TAUI(1)) / (PI*TAUI(1)-TAUI(1))
204 1236  IF(O) TAUI(1)=OMBAR(J)*SIN(TAUI(1))+SIN(TAUI(1))-TAUI(1)+1/2.0
205 1237  IF(L) TAUI(1)=SIN(TAUI(1))-SIN(TAUI(1))+OMBAR(J)*SIN(TAUI(1))+SIN(TAUI(1))
206 1238  IF(L) TAUI(1)=SIN(TAUI(1))-SIN(TAUI(1))+OMBAR(J)*SIN(TAUI(1))+SIN(TAUI(1))
207 1239  PRINTA,TAUI(K)
208 1240  DO 40 J=1,11
209 1241  OMBAR(K)=O.04+O.04*(K-1)
210 1242  TAUI(K)=1+O.5*(J-1)
211 1243  MBAR(K)=O.04+O.04*(K-1)
212 1244  ETA(K)=O.04+O.04*(K-1)
213 1245  CALL TAUI,OX,OMBAR,O,X,O,MBAR,OX,MBAR,OX,ETA50,11X,TAUI,11X
214 1246  CALL TAUI,OX,OMBAR,OX,ETA
215 1247  M=1
216 1248  L=1
217 1249  DO 217 J=1,9
218 1250  TAUI(1)=ARCOS((-OMBAR(K)-MBAR(M-1))/OMBAR(J))
219 1251  IF(O) TAUI(1)=TAUI(1-1)*LEEPS GOTC 21
220 1252  IF(L) GOTO 21 TAUI(1)=TAUI(1)+TAUI(1)/2.0
221 1253  TAUI=TAUI(1)
222 1254  J=J+1
223 1255  GO TO 217
224 1256  L=L+1
225 1257  IF(L) TANCOS((-OMBAR(K)+2*OMBAR(M-1))/OMBAR(J))
226 1258  IF(L) TAUI(1)=TAUI(1-1)*LEEPS GOTC 20
227 1259  IF(L) GOTO 21 TAUI(1)=TAUI(1)+TAUI(1)/2.0
228 1260  TAUI=TAUI(1)
229 1261  GOTO 217
230 1262  TAUI(1)=OMBAR(J)*SIN(TAUI(1))-SIN(TAUI(1))-(2*OMBAR(K))*PI-
231 1263  TAUI(1)+OMBAR(J)*SIN(TAUI(1)) / (PI*TAUI(1)-TAUI(1))
232 1264  IF(O) TAUI(1)=OMBAR(J)*SIN(TAUI(1))+SIN(TAUI(1))-TAUI(1)+1/2.0
233 1265  IF(L) TAUI(1)=SIN(TAUI(1))-SIN(TAUI(1))+OMBAR(J)*SIN(TAUI(1))+SIN(TAUI(1))
234 1266  IF(L) TAUI(1)=SIN(TAUI(1))-SIN(TAUI(1))+OMBAR(J)*SIN(TAUI(1))+SIN(TAUI(1))
235 1267  PRINTA,TAUI(K)
236 1268  DO 40 J=1,11
237 1269  OMBAR(K)=O.04+O.04*(K-1)
238 1270  TAUI(K)=1+O.5*(J-1)
239 1271  MBAR(K)=O.04+O.04*(K-1)
240 1272  ETA(K)=O.04+O.04*(K-1)
241 1273  CALL TAUI,OX,OMBAR,O,X,O,MBAR,OX,MBAR,OX,ETA50,11X,TAUI,11X
242 1274  CALL TAUI,OX,OMBAR,OX,ETA
243 1275  M=1
244 1276  L=1
245 1277  DO 245 J=1,9
246 1278  TAUI(1)=ARCOS((-OMBAR(K)-MBAR(M-1))/OMBAR(J))
247 1279  IF(O) TAUI(1)=TAUI(1-1)*LEEPS GOTC 21
248 1280  IF(L) GOTO 21 TAUI(1)=TAUI(1)+TAUI(1)/2.0
249 1281  TAUI=TAUI(1)
250 1282  J=J+1
251 1283  GO TO 245
252 1284  L=L+1
253 1285  IF(L) TANCOS((-OMBAR(K)+2*OMBAR(M-1))/OMBAR(J))
254 1286  IF(L) TAUI(1)=TAUI(1-1)*LEEPS GOTC 20
255 1287  IF(L) GOTO 21 TAUI(1)=TAUI(1)+TAUI(1)/2.0
256 1288  TAUI=TAUI(1)
257 1289  GOTO 245
258 1290  TAUI(1)=OMBAR(J)*SIN(TAUI(1))-SIN(TAUI(1))-(2*OMBAR(K))*PI-
259 1291  TAUI(1)+OMBAR(J)*SIN(TAUI(1)) / (PI*TAUI(1)-TAUI(1))
260 1292  IF(O) TAUI(1)=OMBAR(J)*SIN(TAUI(1))+SIN(TAUI(1))-TAUI(1)+1/2.0
261 1293  IF(L) TAUI(1)=SIN(TAUI(1))-SIN(TAUI(1))+OMBAR(J)*SIN(TAUI(1))+SIN(TAUI(1))
262 1294  IF(L) TAUI(1)=SIN(TAUI(1))-SIN(TAUI(1))+OMBAR(J)*SIN(TAUI(1))+SIN(TAUI(1))
263 1295  PRINTA,TAUI(K)
264 1296  DO 40 J=1,11
265 1297  OMBAR(K)=O.04+O.04*(K-1)
266 1298  TAUI(K)=1+O.5*(J-1)
267 1299  MBAR(K)=O.04+O.04*(K-1)
268 1300  ETA(K)=O.04+O.04*(K-1)
269 1301  CALL TAUI,OX,OMBAR,O,X,O,MBAR,OX,MBAR,OX,ETA50,11X,TAUI,11X
270 1302  CALL TAUI,OX,OMBAR,OX,ETA
271 1303  M=1
272 1304  L=1
273 1305  DO 273 J=1,9
274 1306  TAUI(1)=ARCOS((-OMBAR(K)-MBAR(M-1))/OMBAR(J))
275 1307  IF(O) TAUI(1)=TAUI(1-1)*LEEPS GOTC 21
276 1308  IF(L) GOTO 21 TAUI(1)=TAUI(1)+TAUI(1)/2.0
277 1309  TAUI=TAUI(1)
278 1310  J=J+1
279 1311  GO TO 273
280 1312  L=L+1
281 1313  IF(L) TANCOS((-OMBAR(K)+2*OMBAR(M-1))/OMBAR(J))
282 1314  IF(L) TAUI(1)=TAUI(1-1)*LEEPS GOTC 20
283 1315  IF(L) GOTO 21 TAUI(1)=TAUI(1)+TAUI(1)/2.0
284 1316  TAUI=TAUI(1)
285 1317  GOTO 273
286 1318  TAUI(1)=OMBAR(J)*SIN(TAUI(1))-SIN(TAUI(1))-(2*OMBAR(K))*PI-
287 1319  TAUI(1)+OMBAR(J)*SIN(TAUI(1)) / (PI*TAUI(1)-TAUI(1))
288 1320  IF(O) TAUI(1)=OMBAR(J)*SIN(TAUI(1))+SIN(TAUI(1))-TAUI(1)+1/2.0
289 1321  IF(L) TAUI(1)=SIN(TAUI(1))-SIN(TAUI(1))+OMBAR(J)*SIN(TAUI(1))+SIN(TAUI(1))
290 1322  IF(L) TAUI(1)=SIN(TAUI(1))-SIN(TAUI(1))+OMBAR(J)*SIN(TAUI(1))+SIN(TAUI(1))
291 1323  PRINTA,TAUI(K)
292 1324  DO 40 J=1,11
293 1325  OMBAR(K)=O.04+O.04*(K-1)
294 1326  TAUI(K)=1+O.5*(J-1)
295 1327  MBAR(K)=O.04+O.04*(K-1)
296 1328  ETA(K)=O.04+O.04*(K-1)
297 1329  CALL TAUI,OX,OMBAR,O,X,O,MBAR,OX,MBAR,OX,ETA50,11X,TAUI,11X
298 1330  CALL TAUI,OX,OMBAR,OX,ETA
299 1331  M=1
300 1332  L=1
301 1333  DO 301 J=1,9
302 1334  TAUI(1)=ARCOS((-OMBAR(K)-MBAR(M-1))/OMBAR(J))
303 1335  IF(O) TAUI(1)=TAUI(1-1)*LEEPS GOTC 21
304 1336  IF(L) GOTO 21 TAUI(1)=TAUI(1)+TAUI(1)/2.0
305 1337  TAUI=TAUI(1)
306 1338  J=J+1
307 1339  GO TO 301
308 1340  L=L+1
309 1341  IF(L) TANCOS((-OMBAR(K)+2*OMBAR(M-1))/OMBAR(J))
310 1342  IF(L) TAUI(1)=TAUI(1-1)*LEEPS GOTC 20
311 1343  IF(L) GOTO 21 TAUI(1)=TAUI(1)+TAUI(1)/2.0
312 1344  TAUI=TAUI(1)
313 1345  GOTO 301
314 1346  TAUI(1)=OMBAR(J)*SIN(TAUI(1))-SIN(TAUI(1))-(2*OMBAR(K))*PI-
315 1347  TAUI(1)+OMBAR(J)*SIN(TAUI(1)) / (PI*TAUI(1)-TAUI(1))
316 1348  IF(O) TAUI(1)=OMBAR(J)*SIN(TAUI(1))+SIN(TAUI(1))-TAUI(1)+1/2.0
317 1349  IF(L) TAUI(1)=SIN(TAUI(1))-SIN(TAUI(1))+OMBAR(J)*SIN(TAUI(1))+SIN(TAUI(1))
318 1350  IF(L) TAUI(1)=SIN(TAUI(1))-SIN(TAUI(1))+OMBAR(J)*SIN(TAUI(1))+SIN(TAUI(1))
319 1351  PRINTA,TAUI(K)
320 1352  DO 40 J=1,11
321 1353  OMBAR(K)=O.04+O.04*(K-1)
322 1354  TAUI(K)=1+O.5*(J-1)
323 1355  MBAR(K)=O.04+O.04*(K-1)
324 1356  ETA(K)=O.04+O.04*(K-1)
325 1357  CALL TAUI,OX,OMBAR,O,X,O,MBAR,OX,MBAR,OX,ETA50,11X,TAUI,11X
326 1358  CALL TAUI,OX,OMBAR,OX,ETA
327 1359  M=1
328 1360  L=1
329 1361  DO 329 J=1,9
330 1362  TAUI(1)=ARCOS((-OMBAR(K)-MBAR(M-1))/OMBAR(J))
331 1363  IF(O) TAUI(1)=TAUI(1-1)*LEEPS GOTC 21
332 1364  IF(L) GOTO 21 TAUI(1)=TAUI(1)+TAUI(1)/2.0
333 1365  TAUI=TAUI(1)
334 1366  J=J+1
335 1367  GO TO 329
336 1368  L=L+1
337 1369  IF(L) TANCOS((-OMBAR(K)+2*OMBAR(M-1))/OMBAR(J))
338 1370  IF(L) TAUI(1)=TAUI(1-1)*LEEPS GOTC 20
339 1371  IF(L) GOTO 21 TAUI(1)=TAUI(1)+TAUI(1)/2.0
340 1372  TAUI=TAUI(1)
341 1373  GOTO 329
342 1374  TAUI(1)=OMBAR(J)*SIN(TAUI(1))-SIN(TAUI(1))-(2*OMBAR(K))*PI-
343 1375  TAUI(1)+OMBAR(J)*SIN(TAUI(1)) / (PI*TAUI(1)-TAUI(1))
344 1376  IF(O) TAUI(1)=OMBAR(J)*SIN(TAUI(1))+SIN(TAUI(1))-TAUI(1)+1/2.0
345 1377  IF(L) TAUI(1)=SIN(TAUI(1))-SIN(TAUI(1))+OMBAR(J)*SIN(TAUI(1))+SIN(TAUI(1))
346 1378  IF(L) TAUI(1)=SIN(TAUI(1))-SIN(TAUI(1))+OMBAR(J)*SIN(TAUI(1))+SIN(TAUI(1))
347 1379  PRINTA,TAUI(K)
348 1380  DO 40 J=1,11
349 1381  OMBAR(K)=O.04+O.04*(K-1)
350 1382  TAUI(K)=1+O.5*(J-1)
351 1383  MBAR(K)=O.04+O.04*(K-1)
352 1384  ETA(K)=O.04+O.04*(K-1)
353 1385  CALL TAUI,OX,OMBAR,O,X,O,MBAR,OX,MBAR,OX,ETA50,11X,TAUI,11X
354 1386  CALL TAUI,OX,OMBAR,OX,ETA
355 1387  M=1
356 1388  L=1
357 1389  DO 357 J=1,9
358 1390  TAUI(1)=ARCOS((-OMBAR(K)-MBAR(M-1))/OMBAR(J))
359 1391  IF(O) TAUI(1)=TAUI(1-1)*LEEPS GOTC 21
360 1392  IF(L) GOTO 21 TAUI(1)=TAUI(1)+TAUI(1)/2.0
361 1393  TAUI=TAUI(1)
362 1394  J=J+1
363 1395  GO TO 357
364 1396  L=L+1
365 1397  IF(L) TANCOS((-OMBAR(K)+2*OMBAR(M-1))/OMBAR(J))
366 1398  IF(L) TAUI(1)=TAUI(1-1)*LEEPS GOTC 20
367 1399  IF(L) GOTO 21 TAUI(1)=TAUI(1)+TAUI(1)/2.0
368 1400  TAUI=TAUI(1)
369 1401  GOTO 357
370 1402  TAUI(1)=OMBAR(J)*SIN(TAUI(1))-SIN(TAUI(1))-(2*OMBAR(K))*PI-
371 1403  TAUI(1)+OMBAR(J)*SIN(TAUI(1)) / (PI*TAUI(1)-TAUI(1))
372 1404  IF(O) TAUI(1)=OMBAR(J)*SIN(TAUI(1))+SIN(TAUI(1))-TAUI(1)+1/2.0
373 1405  IF(L) TAUI(1)=SIN(TAUI(1))-SIN(TAUI(1))+OMBAR(J)*SIN(TAUI(1))+SIN(TAUI(1))
374 1406  IF(L) TAUI(1)=SIN(TAUI(1))-SIN(TAUI(1))+OMBAR(J)*SIN(TAUI(1))+SIN(TAUI(1))
375 1407  PRINTA,TAUI(K)
376 1408  DO 40 J=1,11
377 1409  OMBAR(K)=O.04+O.04*(K-1)
378 1410  TAUI(K)=1+O.5*(J-1)
379 1411  MBAR(K)=O.04+O.04*(K-1)
380 1412  ETA(K)=O.04+O.04*(K-1)
381 1413  CALL TAUI,OX,OMBAR,O,X,O,MBAR,OX,MBAR,OX,ETA50,11X,TAUI,11X
382 1414  CALL TAUI,OX,OMBAR,OX,ETA
383 1415  M=1
384 1416  L=1
385 1417  DO 385 J=1,9
386 1418  TAUI(1)=ARCOS((-OMBAR(K)-MBAR(M-1))/OMBAR(J))
387 1419  IF(O) TAUI(1)=TAUI(1-1)*LEEPS GOTC 21
388 1420  IF(L) GOTO 21 TAUI(1)=TAUI(1)+TAUI(1)/2.0
389 1421  TAUI=TAUI(1)
390 1422  J=J+1
391 1423  GO TO 385
392 1424  L=L+1
393 1425  IF(L) TANCOS((-OMBAR(K)+2*OMBAR(M-1))/OMBAR(J))
394 1426  IF(L) TAUI(1)=TAUI(1-1)*LEEPS GOTC 20
395 1427  IF(L) GOTO 21 TAUI(1)=TAUI(1)+TAUI(1)/2.0
396 1428  TAUI=TAUI(1)
397 1429  GOTO 385
398 1430  TAUI(1)=OMBAR(J)*SIN(TAUI(1))-SIN(TAUI(1))-(2*OMBAR(K))*PI-
399 1431  TAUI(1)+OMBAR(J)*SIN(TAUI(1)) / (PI*TAUI(1)-TAUI(1))
400 1432  IF(O) TAUI(1)=OMBAR(J)*SIN(TAUI(1))+SIN(TAUI(1))-TAUI(1)+1/2.0
401 1433  IF(L) TAUI(1)=SIN(TAUI(1))-SIN(TAUI(1))+OMBAR(J)*SIN(TAUI(1))+SIN(TAUI(1))
402 1434  IF(L) TAUI(1)=SIN(TAUI(1))-SIN(TAUI(1))+OMBAR(J)*SIN(TAUI(1))+SIN(TAUI(1))
403 1435  PRINTA,TAUI(K)
404 1436  DO 40 J=1,11
405 1437  OMBAR(K)=O.04+O.04*(K-1)
406 1438  TAUI(K)=1+O.5*(J-1)
407 1439  MBAR(K)=O.04+O.04*(K-1)
408 1440  ETA(K)=O.04+O.04*(K-1)
409 1441  CALL TAUI,OX,OMBAR,O,X,O,MBAR,OX,MBAR,OX,ETA50,11X,TAUI,11X
410 1442  CALL TAUI,OX,OMBAR,OX,ETA
411 1443  M=1
412 1444  L=1
413 1445  DO 413 J=1,9
414 1446  TAUI(1)=ARCOS((-OMBAR(K)-MBAR(M-1))/OMBAR(J))
415 1447  IF(O) TAUI(1)=TAUI(1-1)*LEEPS GOTC 21
416 1448  IF(L) GOTO 21 TAUI(1)=TAUI(1)+TAUI(1)/2.0
417 1449  TAUI=TAUI(1)
418 1450  J=J+1
419 1451  GO TO 413
420 1452  L=L+1
421 1453  IF(L) TANCOS((-OMBAR(K)+2*OMBAR(M-1))/OMBAR(J))
422 1454  IF(L) TAUI(1)=TAUI(1-1)*LEEPS GOTC 20
423 1455  IF(L) GOTO 21 TAUI(1)=TAUI(1)+TAUI(1)/2.0
424 1456  TAUI=TAUI(1)
425 1457  GOTO 413
426 1458  TAUI(1)=OMBAR(J)*SIN(TAUI(1))-SIN(TAUI(1))-(2*OMBAR(K))*PI-
427 1459  TAUI(1)+OMBAR(J)*SIN(TAUI(1)) / (PI*TAUI(1)-TAUI(1))
428 1460  IF(O) TAUI(1)=OMBAR(J)*SIN(TAUI(1))+SIN(TAUI(1))-TAUI(1)+1/2.0
429 1461  IF(L) TAUI(1)=SIN(TAUI(1))-SIN(TAUI(1))+OMBAR(J)*SIN(TAUI(1))+SIN(TAUI(1))
430 1462  IF(L) TAUI(1)=SIN(TAUI(1))-SIN(TAUI(1))+OMBAR(J)*SIN(TAUI(1))+SIN(TAUI(1))
431 1463  PRINTA,TAUI(K)
432 1464  DO 40 J=1,11
433 1465  OMBAR(K)=O.04+O.04*(K-1)
434 1466  TAUI(K)=1+O.5*(J-1)
435 1467  MBAR(K)=O.04+O.04*(K-1)
436 1468  ETA(K)=O.04+O.04*(K-1)
437 1469  CALL TAUI,OX,OMBAR,O,X,O,MBAR,OX,MBAR,OX,ETA50,11X,TAUI,11X
438 1470  CALL TAUI,OX,OMBAR,OX,ETA
439 1471  M=1
440 1472  L=1
441 1473  DO 4
```

APPENDIX III

III.1 RELATIONSHIP BETWEEN SHAKER PIN MOTION AND INPUT TORQUE TO THE SHAFT:



Equation of motion is given by:

$$EM = J\ddot{\theta}$$

$$J\ddot{\theta} + K\theta + \bar{K}(x-y)r = 0$$

Where K = shaft torsional stiffness

$$J\ddot{\theta} + (K + \bar{K}r^2)\theta = \bar{K}y r$$

\bar{K} = spring constant

$$J\ddot{\theta} + K'\theta = \bar{K}Y r \cos \omega t$$

$$K' = K + \bar{K}r^2$$

$$\ddot{\theta} + p^2 \theta = \frac{\bar{K}}{J} Y r \cos \omega t$$

$$p^2 = \frac{K'}{J}$$

$$\ddot{\theta} + p^2 \theta = \frac{T}{J} \cos \omega t$$

$$T = \bar{K}Y r$$

Since

$$p^2 = \frac{K'}{J} = \frac{(K + \bar{K}r^2)}{J}$$

$$\text{or } K + \bar{K}r^2 = Jp^2 \quad (1)$$

For the vibrating arm and the counter weight

$$J = 0.179 \text{ lb in}^2 \text{ sec}^2$$

For the shaft

$$K = \frac{\pi d^4 G}{32L}$$

$$d = 5/8'' \quad L = 32''$$

$$K = 5617.60 \text{ lb in/rad}$$

From the experiment $p = 29.3$ c/s

From equation (1) --

$$K + \bar{K}r^2 = Jp^2$$

$$5617.60 + \bar{K}(3.5)^2 = 0.179 (2\pi \times 29.3)^2$$

$$\bar{K} = 34.5 \text{ lb/in}$$

Since

$$T = \bar{K} Yr$$

$$\therefore Y = \frac{T}{\bar{K}r}$$

And

$$\bar{S} = \frac{T}{K\theta_o}$$

Therefore

$$\bar{S} = \frac{\bar{K} Yr}{K\theta_o}$$

$$Y = \frac{\bar{S} K \theta_o}{\bar{K} r} \text{ inches}$$

$$K = 5617.60, \theta_o = \frac{0.0015}{r_1} = 2.0$$

$$\bar{K} = 34.5 \quad r = 3.5, r_1 = 2.0$$

$$Y = 0.175'' \text{ peak-peak}$$

$$\text{for } \bar{S} = 2.5$$

$$Y = 0.140'' \text{ peak-peak}$$

$$\bar{S} = 2.0$$

$$Y = 0.105'' \text{ peak-peak}$$

$$\bar{S} = 1.5$$

$$Y = 0.070'' \text{ peak-peak}$$

$$\bar{S} = 1.0$$

$$Y = 0.056'' \text{ peak-peak}$$

$$\bar{S} = 0.8$$

III.2. CALCULATION OF THE NON-DIMENSIONAL AMPLITUDES OF MOTION.

Let G_1, G_2, G_3 & G_4 be the amplitudes of the 1st, 2nd, 3rd and 4th harmonic components of acceleration at a certain forcing frequency.

Since $a = \ddot{\theta}$, and $\theta = Q_1 \cos \omega t$

$$\therefore G_1 = -\omega^2 Q_1 \cos \omega t$$

$$\therefore |G_1| = \omega^2 Q_1 \quad \text{III.2.1}$$

and $G_2 = -4\omega^2 Q_2 \cos 2\omega t$, since $\theta = Q_2 \cos 2\omega t$

or $|G_2| = 4\omega^2 Q_2$

Similarly $|G_3| = 9\omega^2 Q_3$

and $|G_4| = 16\omega^2 Q_4$

From III.2.1. $Q_1 = \frac{G_1}{\omega^2}$
 $= \frac{n_1 \times 386.4}{(2\pi/t)^2}$ inches where $n_1 =$ magnitude of acceleration in 'g' and $t =$ periodic time.

$$Q_1 (\text{Angular}) = \left(\frac{1}{r}\right) \cdot \frac{n_1 \times 386.4}{(2\pi/t)^2} \text{ rad.}$$

$$\theta_0 (\text{clearance}) = 0.0015 \text{ inches}$$

$$\theta_0 (\text{Angular clearance}) = \frac{\theta_0}{r_1} \text{ rad. } \&$$

$$\begin{aligned} \bar{Q}_1 &= -\frac{Q_1}{\theta_0} = \left(\frac{1}{r}\right) \frac{n_1 \times 386.4}{(2\pi/t)^2} / \left(\frac{\theta_0}{r_1}\right) \\ &= \left(\frac{r_1}{r}\right) \frac{n_1 \times 386.4}{(2\pi/t)^2} \times \frac{1}{\theta_0} \quad \text{III.2.2} \end{aligned}$$

Similarly $\bar{Q}_2 = \left(\frac{r_1}{r}\right) \frac{n_2 \times 386.4}{4(2\pi/t)^2} \times \frac{1}{\theta_0}$ III.2.3

$$\bar{Q}_3 = \left(\frac{r_1}{r}\right) \frac{n_3 \times 386.4}{9(2\pi/t)^2} \times \frac{1}{\theta_0} \quad \text{III.2.4}$$

and $\bar{Q}_4 = \left(\frac{r_1}{r}\right) \frac{n_4 \times 386.4}{16(2\pi/t)^2} \times \frac{1}{\theta_0}$ III.2.5

n_2, n_3, n_4 are the magnitudes of acceleration in 'g's.

5

APPENDIX IV

LIMITING CONDITIONS FOR THE GENERATION OF THE
HIGHER ORDER RESONANCES IN SYMMETRICAL SYSTEM

For a certain value of a forcing amplitude \bar{S} , after passing through the harmonic resonance, the amplitude of motion decreases with the increase of n . If the first subharmonic resonance is not initiated before the tooth loses contact with the restrainer walls, the restoring force and the system become linear and subharmonic resonances cannot be generated. The value of n at which the tooth loses contact is called the cut-off frequency, which can be used as a critical value for defining the limit of the subharmonic generation capacity. Hence, the term "cut-off" frequency means the frequency above which a forcing function of a given amplitude cannot excite the subharmonic resonance.

The relationships between the forcing amplitude \bar{S} and the corresponding cut off frequency n for the two types of disturbing torques are derived below.

a. Disturbing torque = $T \cos \omega t$

The equation of motion within the clearance is given by

$$J\ddot{\theta} = T \cos \omega t$$

or
$$\ddot{\theta} = \frac{T}{J} \cos \omega t \quad (\text{IV.1})$$

Substituting the approximation for displacement, which is valid within the range of the harmonic resonance,

$$\tilde{\theta} = Q_1 \cos \omega t$$

into (IV.1) we have

$$-\omega^2 Q_1 \cos \omega t = \frac{T}{J} \cos \omega t$$

or $|Q_1| = \frac{T}{J\omega^2}$

Since $\bar{Q}_1 = \frac{Q_1}{\theta_0}$ and $\eta = \frac{p}{p'}$

hence $|\bar{Q}_1| = \frac{T}{J p^2 \eta^2 \theta_0}$

But

$$\bar{S} = \frac{T}{K\theta_0} \quad \text{and} \quad p^2 = \frac{K}{J}$$

therefore $|\bar{Q}_1| = \frac{TJ}{JK\theta_0 \eta^2} = \frac{\bar{S}}{\eta^2}$

The condition for loss of tooth contact and hence for the limiting angular amplitude below which non-linear conditions do not exist is given by $|\bar{Q}_1| = 1$. Therefore,

$$\eta^2 = \bar{S}$$

or

$$\eta = \sqrt{\bar{S}}$$

i.e. "cut-off" frequency.

Thus if the conditions for the initiation of the sub-harmonic resonance at a specific value of \bar{S} occur at a frequency above $\eta = \sqrt{\bar{S}}$, then this resonance will not take place. The graph of \bar{S} vs "cut off" η is shown in figure 5.1.27.

b. Disturbing torque = $C \omega^2 \text{Cos } \omega t$

The equation of motion, within the clearance is given by

$$J\ddot{\theta} = C \omega^2 \text{Cos } \omega t$$

or
$$\ddot{\theta} = Z \omega^2 \text{Cos } \omega t \quad (\text{IV.2})$$

where
$$Z = \frac{C}{J}$$

Assuming the simplest solution which is valid near harmonic resonance $\tilde{\theta} = Q_1 \text{Cos } \omega t$ and substituting into (IV.2) yields:

$$-\omega^2 Q_1 \text{Cos } \omega t = Z \omega^2 \text{Cos } \omega t$$

or

$$|Q_1| = Z$$

or

$$|\bar{Q}_1| = Z'$$

The limiting value of Z' for the "cut-off" frequency below which non-linear conditions do not exist, is given by:

$$Z' = |\bar{Q}_1| = 1$$

Therefore it is only possible to excite the subharmonic resonance at values $Z' > 1$.

APPENDIX V

EXPERIMENTAL ERROR ANALYSIS

The textbook (36) and reference (43) & (86) describe a method to estimate the uncertainty in the calculated result on the basis of the uncertainties in the primary measurements. The result R is given as a function of the independent variables x_1, x_2, \dots, x_n . Thus

$$R = R(x_1, x_2, x_3, \dots, x_n)$$

Let W_r be the uncertainty in the result and W_1, W_2, \dots, W_n be the uncertainties in the independent variables. If the uncertainties in the measurement of independent variables are all given with the same odds, then the uncertainty in the result having these odds is given as

$$W_r = \left[\left(\frac{\partial R}{\partial x_1} \cdot W_1 \right)^2 + \left(\frac{\partial R}{\partial x_2} \cdot W_2 \right)^2 + \dots + \left(\frac{\partial R}{\partial x_n} \cdot W_n \right)^2 \right]^{1/2}$$

...V.1

Estimation of Errors in Measurements of the Amplitude of Motion:

From equation III.2.2

$$\begin{aligned} \bar{Q}_1 &= \left(\frac{r_1}{r} \right) \cdot \frac{n_1 \times 386.4}{(2\pi/t)^2} \cdot \frac{1}{\theta_0} \\ &= f(r_1, r, n_1, t, \theta_0) \end{aligned}$$

Using equation V.1

$$W_R = \left[\left(\frac{\partial \bar{Q}_1}{\partial r_1} \cdot W_{r_1} \right)^2 + \left(\frac{\partial \bar{Q}_1}{\partial r} \cdot W_r \right)^2 + \left(\frac{\partial \bar{Q}_1}{\partial n_1} \cdot W_{n_1} \right)^2 + \left(\frac{\partial \bar{Q}_1}{\partial t} \cdot W_t \right)^2 + \left(\frac{\partial \bar{Q}_1}{\partial \theta_0} \cdot W_{\theta_0} \right)^2 \right]^{1/2}$$

where W_{r_1} , W_r , W_{n_1} , W_t and W_{θ_0} are uncertainties in measurements of radial distances r_1 & r , acceleration components, time period t and the gap clearance θ_0 . The uncertainties W_{r_1} and W_r are of the order of $\pm 0.1\%$. The uncertainty W_T is of the order $\pm 0.1\%$, since the period was measured in milli seconds employing a digital counter. The uncertainty W_{θ_0} is of the order of $\pm 0.1\%$.

Hence neglecting W_{r_1} , W_r , W_t and W_{θ_0} in the above relationship yields

$$W_R = \left(\frac{\partial \bar{Q}_1}{\partial n_1} \cdot W_{n_1} \right)$$

$$\text{or } W_R = \left(\frac{r_1}{r} \right) \frac{386.4}{(2\pi/t)^2} \cdot \left(\frac{1}{\theta_0} \cdot W_{n_1} \right) \dots V.2$$

The above expression V.2 shows that uncertainties of measurements of the amplitudes of motion is proportional to the uncertainties involved in acceleration measurements. When using the real time spectrum analyser, the amplitude of the acceleration component can be read within ± 1 dB or 12.23% accuracy. The error of the accelerometer and the associated instrumentation is well within 3%. Hence the uncertainty of the calculated values of the amplitude of motion are within 15.23%.

Similarly for higher harmonics Q_3, Q_3, Q_4 , etc.

From equation III.2.3

$$\bar{Q}_2 = \left(\frac{r_1}{r}\right) \cdot \frac{386.4}{4(2\pi/t)^2} \cdot \frac{1}{\theta_0} \quad \dots V.3$$

From equation V.2

$$W_R = \left(\frac{r_1}{r}\right) \frac{386.4}{4(2\pi/t)^2} \cdot \frac{1}{\theta_0} \cdot W_{n_2}$$

Similarly uncertainty involved in Q_3 is given by

$$W_R = \left(\frac{r_1}{r}\right) \frac{386.4}{9(2\pi/t)^2} \cdot \frac{1}{\theta_0} \cdot W_{n_3} \quad \dots V.4$$

From the above expressions it is evident that uncertainties involved in higher order amplitudes of motion are 1/4, 1/9 & 1/16 of the uncertainties of measurements of fundamental component.

VITA

- 1942 Born in Multan, W. Pakistan
- 1965 Received the degree of Bachelor of Science in Mechanical Engineering, Ranchi University, Bihar, India.
- 1965-1969 Worked as a Mechanical Engineer for several companies in India.
- 1970 Received M.Sc. Degree in Applied Dynamics and Mechanical Vibrations, University of Surrey, Surrey, England.
- 1974-1975 Worked for Zinder Engineering Inc., Ann Arbor, Michigan as an Acoustic Engineer.
- 1976-1977 Worked for Schwitzer Engineered Components, Indianapolis, Indiana as a Project Engineer.
- 1977- Presently employed by Ford Motor Co., Dearborn, Michigan as a Research Engineer.
- A candidate for the degree of Doctor of Philosophy in Mechanical Engineering, University of Windsor, Windsor, Ontario, Canada.